A MODEL FOR THE DEVELOPMENT OF A LOBATE ALPINE ROCK GLACIER IN SOUTHWEST COLORADO, USA: IMPLICATIONS FOR WATER ON MARS

A Dissertation

by

JOHN JEROME DEGENHARDT

Submitted to the Office of Graduate Studies of
Texas A&M University
in partial fulfillment of the requirements for the degree of

DOCTOR OF PHILOSOPHY

August 2002

Major Subject: Geography

A MODEL FOR THE DEVELOPMENT OF A LOBATE ALPINE ROCK GLACIER IN SOUTHWEST COLORADO, USA: IMPLICATIONS FOR WATER ON MARS

A Dissertation

by

JOHN JEROME DEGENHARDT

Submitted to Texas A&M University
in partial fulfillment of the requirements
for the degree of

DOCTOR OF PHILOSOPHY

Approved as to style and content by:

John R. Giardino (Chair of Committee)	Vatche P. Tchakerian (Member)
David B.Prior (Member)	Mark Everett (Member)
Douglas Sherman (Head of Department)	

August 2002

Major Subject: Geography

ABSTRACT

A Model for the Development of a Lobate Alpine Rock Glacier in Southwest Colorado, USA: Implications for Water on Mars. (August 2002)

John Jerome Degenhardt, B.S., Texas A&M University;

M.S., University of Houston

Chair of Advisory Committee: Dr. John R. Giardino

Rock glaciers play a significant role in the alpine debris transport system. For practical and engineering considerations, identifying the internal structure and its relationship to surface characteristics is significant in terms of how rock glaciers settle during periods of melting, and how they deform. A better understanding of these factors is important for engineers, engineering geologists and geomorphologists who must make prudent evaluations of rock glaciers as potential sites for human development and uses. It is equally important for evaluating potential stores for water on other planets such as Mars.

Ground penetrating radar (GPR) shows that the internal structure of a lobate rock glacier located in the San Juan Mountains of southwest Colorado consists of continuous to semi-continuous horizontal layers of ice-supersaturated sediments and coarse blocky rockslide debris which likely formed through catastrophic episodes of rockfall from the cirque headwall. Folds in the uppermost layers correspond to the surface expression of ridges and furrows, indicating that compressive stresses originating in the steep accumulation zone are transmitted downslope through the rock glacier. The rock glacier is a composite feature formed by the development and overlap of discrete flow lobes that have overridden older glacial moraine and protalus rampart materials. The latter materials have been incorporated into the present flow structure of the rock glacier.

The discovery of rock glacier-like features on Mars suggests the presence of flowing, or once-flowing ice-rock mixtures. These landforms, which include lobate debris aprons,

concentric crater fill and lineated valley fill, hold significant promise as reservoirs of stored water ice that could be used as fuel sources for human exploration of Mars and provide a frozen record of the climatic history of the planet. To this end, the Colorado rock glacier was used as a surrogate for similar Martian landforms. Liquid water, found to be abundant in this rock glacier, occurs within a network of interconnected channels that permeate throughout the landform. In terms of water storage within Martian analogs, consideration must include the possibility that some water ice may be stored as lenses and vein networks supplied by seasonal frost accumulation and/or water influx from below.

DEDICATION

I dedicate this dissertation to my Mother and to my Dad, John J. Degenhardt, Sr., who passed away prior to its completion.

> *God is able to make all grace abound to you, so that in all things at all times, having all that you need, you will abound in every good work.*
>
> - II Corinthians 9:8 NIV

ACKNOWLEDGEMENTS

I thank Dr. John R. Giardino for his support and enthusiasm through the development of my small contribution to the understanding of rock glaciers. Only the energy and philosophy he shares with his students, which provided strong motivation for me through all of the challenging aspects of the dissertation, outweighs his significant contributions to the science. I am grateful to Drs. Vatche P. Tchakerian, David B. Prior, Mark Everett, and Thomas DeWitt for serving on my committee and to Chris Mathewson for serving on the defense committee. Their reviews and comments on the dissertation were invaluable.

Thanks also to the USDA Forest Service, particularly to James Free, District Ranger, for granting permission to conduct the research in the Uncompaghre National Forest. Maureen McCormack and Ron Trujillo of the Ouray Ranger District Office in Colorado also provided valuable assistance and made Texas A&M feel welcome during the field stays.

A great deal of appreciation goes to M. Brian Junck, Michael Quintana, Chris Neel, Michael Neel, and Carl Pierce for their assistance (i.e., hard work) in the field. Without them, the challenging task of data collection in the harsh alpine environment would not have been possible.

Finally, I owe a debt of gratitude to Wilfred Haeberli, Jack Vitek, Dick Marston, Jack Shroder, Joe Nicholas, Noel Potter, Jr., Francisco Pèrez, Harry Jol, and Mark Everett for taking time out of their busy schedules to provide outside reviews of the chapters that have been submitted for publication. Their comments were of great value and their insights certainly improved the quality of the research.

This work was made possible by a grant from the NASA Mission to Mars Program, and NASA grants NAG9-807 and 47710 to John R. Giardino.

TABLE OF CONTENTS

Page

ABSTRACT iii

DEDICATION v

ACKNOWLEDGEMENTS vi

TABLE OF CONTENTS vii

LIST OF FIGURES ix

LIST OF TABLES xiii

CHAPTER

I INTRODUCTION 1

Introduction 1
Statement of Problem 2
Objectives 3
Literature Review 3
Justification 11
Organization of the Dissertation 12

II ENGINEERING GEOMORPHOLOGY OF ROCK GLACIERS 14

Overview 14
Introduction 15
The Rock Glacier Look 17
Rock Glacier Occurrence and Formation 21
Rock Glacier Classification 31
Rock Glacier Make-up 32
Active or Inactive Status 33
Stratigraphy 34
Engineering Considerations 44
Hydrology 56
Water Discharge Characteristics 61
Closing Remarks 64

III GPR SURVEY OF A LOBATE ROCK GLACIER IN YANKEE BOY BASIN, CO, USA 67

Overview 67

CHAPTER Page

Introduction 67
Significance and Occurrence of Rock Glaciers 68
Formation of Rock Glaciers 69
Geologic Setting 70
Application of Ground Penetrating Radar (GPR) 73
Results 77
Discussion 84
Conclusions 92

IV SUBSURFACE INVESTIGATION OF A ROCK GLACIER USING GROUND PENETRATING RADAR (GPR): IMPLICATIONS FOR LOCATING STORED WATER ON MARS 94

Overview 94
Introduction 95
Similar Features on Mars 97
Convergence of Investigative Approaches 101
Results – Implications for Landforms on Mars 119
Summary and Conclusions 129

V INTERPRETATION OF A BLOCK STREAM IN TOM MAYS CANYON, FRANKLIN MOUNTAINS, TX 131

Overview 131
Introduction 131
Morphology of the Tom Mays Block Stream 133
Fabric Analysis 146
Discussion 152
Conclusions 159

VI SUMMARY 160

Introduction 160
Engineering Aspects: Rock Glacier Geomorphology 160
Model Based on Yankee Boy Rock Glacier 162
A Surrogate for Landforms on Mars 162
Convergence of Landform Morphology 164
Closing Remarks and Future Research 164

REFERENCES 167
VITA 187

LIST OF FIGURES

FIGURE Page

1.1 Front view of Yankee Boy Basin rock glacier..... 7

1.2 Lobate mass-wasting features on Earth and Mars 8

2.1 California Peak rock glacier, located in the Sangre de Cristo Mountains of southern Colorado, U.S.A. 16

2.2 Talus rock glaciers, Lower Grizzly Creek..... 18

2.3 A view of California Peak rock glacier showing its proximity to the valley below..... 20

2.4 Mercator projection map of major rock glacier study sites 24

2.5 Models of rock glacier formation..... 25

2.6 Diagram illustrating the alpine landscape continuum 27

2.7 Multiple process diagram illustrating possible processes for formation of rock glaciers. 30

2.8 Progression of rock glacier development postulated by Vick (1987) 35

2.9 Platy fabric typical of the outer layer of a rock glacier 40

2.10 Grain size distribution for the interior of a typical rock glacier 41

2.11 Development of groundwater in sediments beneath a rock glacier (Haeberli, 1985). 58

2.12 A model of water flow through a rock glacier..... 59

2.13 Cascading system for a rock glacier hydrologic cycle (Giardino et al., 1992) 60

3.1 Yankee Boy Basin rock glacier..... 71

3.2 Geographic location of the Yankee Boy Basin study site 72

FIGURE Page

3.3 United States Department of Agriculture (USDA) 1:20,000 scale vertical aerial photo of Yankee Boy rock glacier taken in 1979 76

3.4 Common mid point (CMP) surveys 78

3.5 Topographically corrected longitudinal profile collected at f = 25 MHz (velocity = 0.12 m/ns) 81

3.6 Topographically corrected 50 MHz GPR profile B-B' 83

3.7 Topographically corrected 50 MHz GPR profile C-C' 85

3.8 Intersection of profiles B-B' and C-C' 86

3.9 Migrated longitudinal profile from Fig. 3.5 88

3.10 Correlation between the main depositional units 90

3.11 Model for rock glacier formation 91

4.1 Lobate viscous flow features on Earth and Mars 98

4.2 Mars Orbiter Camera (MOC) image of a lobate debris apron 100

4.3 Viscous flow features located in the East and Northeast regions of the Hellas impact basin (27.5˚-42.5˚S, 260˚-275˚W) 102

4.4 Components of the Yankee Boy Basin rock glacier 105

4.5 Aerial photograph of the Yankee Boy rock glacier taken in 1979 107

4.6 Longitudinal profile collected using 25 MHz antennae (uncorrected for topography) 108

4.7 Topolographically corrected 25 MHz longitudinal profile 109

4.8 Diagram illustrating the concept of collecting a common midpoint profile (CMP) for velocity determinations 111

4.9 Common midpoint profile (CMP) used for determination of the radarwave velocity through the rock glacier medium 112

FIGURE Page

4.10 Variations corresponding to phase differences throughout the rock glacier....114

4.11 Topographically corrected GPR profile trending southwest to northeast along transect line B-B' shown in Fig. 4.5....116

4.12 Topographically corrected GPR profile trending west to east along transect line C-C' 118

4.13 Diagram illustrating the alpine landscape continuum....120

4.14 Snow-covered rock glacier at Yankee Boy Basin....123

4.15 Diagrams illustrating water storage and flow through a terrestrial rock glacier and a conceptual Martian rock glacier based upon information obtained from terrestrial rock glaciers. 127

5.1 General geology of the Franklin Mountains, West Texas....134

5.2 Area map of the Franklin Mountains State Park....135

5.3a 1-m resolution digital orthophoto quarter quadrangle (DOQQ) image (Canutillo SE quadrangle) of Tom Mays Canyon....136

5.3b Geologic map of the area around Tom Mays Park 137

5.4a Enlarged aerial photograph of the Tom Mays block stream 138

5.4b Downvalley view atop the block stream illustrating the character of individual blocks....139

5.5 Topographic cross-sections made at five positions along the block stream illustrating the lack of symmetry in cross-canyon directions 140

5.6 The volumetric dependence of effective travel distance (L) and mean drop gradient (H/L) among sturzstroms on Earth....142

5.7 Longitudinal profile covering 290 m of the 378 m-long Tom Mays block stream 143

FIGURE Page

5.8 Slope-angle line graph (a) using 1-m unit-length measurements on the Tom Mays block stream, and corresponding sequence of ground-surface roughness indices (b) 144

5.9 Slope-angle line graph (a) using 4-m averaged lengths on the Tom Mays block stream and corresponding sequence of ground-surface roughness indices (b) showing elimination of trend in roughness at 4-m resolution.....145

5.10 Fabric data for several positions along six transects across the Tom Mays block stream 148

5.11 Graph of normalized eigenvalues plotted on a two-axis ratio diagram showing fabric shape 150

5.12 Partial ternary plot of normalized eigenvalue data for the Tom Mays block stream 153

LIST OF TABLES

TABLE Page

2.1 Assessing rock glacier status (after Giardino and Vick, 1987; Imhof, 1996). 19

2.2 Characteristics of rock glaciers 22

2.3 Rock glacier classification criteria criteria (after Corte, 1987a) 28

2.4 Internal structure of rock glaciers 36

2.5 Grain size of rock glacier layers 42

2.6 Rock glacier investigation methods 49

2.7 Rock glacier water quality 63

5.1 Eigenvalues for the Tom Mays block stream with ratios used in the two-axis ratio diagram (Fig. 5.11) 151

5.2 List of observed clast direction (V_1) compared to the directional tendency of the surface (expected trend) 154

5.3 The null hypothesis used for the chi-squared test 155

CHAPTER I

INTRODUCTION

INTRODUCTION

Movement and deformation of lobate or tongue-shaped bodies composed of mixtures of poorly sorted, angular, blocky rock debris and ice are controlled by basic laws of physics. These terrestrial landforms, which are called rock glaciers (Giardino et al., 1987; Giardino, 1983), move by slip, flow and/or creep deformation (Giardino and Vitek, 1988b) and have distinctive surface morphologies, including ridges and furrows perpendicular to flow direction. Serious study of rock glaciers began with the seminal work by Wahrhaftig and Cox (1959), who put forth the idea that rock glaciers represent a landform continuum in the alpine environment. Barsch (1977) and Giardino (1979) later addressed the role of rock glaciers in terms of debris transport within alpine systems and found that rock glaciers account for approximately 60% of all mass transport in the alpine environment. Our current understanding of rock glacier deformation as outlined in the works of Haeberli (1985), Giardino et al. (1987), and Barsch (1996), is based on models of creep flow adopted from studies of glaciers and limited physical data from rock glaciers around the world (Burger et al., 1999; Konrad and Humphrey, 2000).

Interest in rock glaciers continues to expand as illustrated by recent work in the engineering aspects of rock glaciers (Burger et al., 1999), the role of rock glaciers in alpine landscape ecology (Parker et al., 1999), process and landform morphology (Fitzgerald et al., 1993; Fitzgerald, 1994; Barsch, 1996; Giardino et al., 1999), prediction of rock glacier occurrence (Sloane and Dyke 1998), and hydrology (Burger et al., 1997). Rock glaciers are now being considered from a planetary perspective as well. Similar morphological features are being discovered on Mars (Squyres, 1978; Lucchitta, 1993;

This dissertation follows the style and format of Geomorphology.

Degenhardt and Giardino, 1999a; Degenhardt and Giardino, 1999b) and on Callisto, one of the moons of Jupiter (Chuang, et al., 1999). Viking Orbiter and Mars Orbiter Camera (MOC) images of the northern plains on Mars reveal lobate flow bodies with wrinkled surfaces associated with rift valleys and the peripheral margins of splash-form craters. Based on their morphologic similarity to terrestrial rock glaciers, these landforms have been postulated to contain significant volumes of the planet's frozen water (Lucchitta, 1986; Carr, 1987).

STATEMENT OF PROBLEM

We are beginning to appreciate that rock glaciers are ubiquitous throughout the solar system. Although the geomorphology of lobate landforms with surficial ridges and furrows perpendicular to flow direction is well documented, our current knowledge of their movement mechanics and flow behavior is based on limited data obtained exclusively from terrestrial rock glaciers. Knowledge of the internal composition and fabric of a rock glacier is necessary to understand the flow dynamics responsible for its deformation, but the difficulty and cost associated with direct observation of the internal characteristics make acquisition of these data problematic. For example, direct rheological measurements (i.e., flow direction, flow velocity, and stress fields) are time dependent and lengthy because rock glacier flow is not observable at human time-scales.

To fully understand the movement and deformation patterns within rock glaciers, a fundamental (i.e., generic) description of their development is required. However, before the mechanics of motion can be understood, internal structure must be accurately identified. Identifying the internal structure makes it possible to describe the deformation processes that contribute to the mechanics of motion. This can be achieved using a non-intrusive technique such as ground penetrating radar (GPR).

This dissertation attempts to refine our understanding of the formation and deformation of periglacial rock glaciers through the application of GPR, an effective, non-invasive method. It marks the beginning of a long-term effort to characterize the

different types of rock glaciers (i.e., lobate, tongue-shaped, valley-side, ice-saturated, and ice-cored) in many different locations on Earth, and on planets such as Mars.

OBJECTIVES

The objectives of the dissertation were directed at determining whether folding is the primary mode of deformation within the rock glacier (Fitzgerald, 1994) and bolstering or refuting the concept of kinematic wave theory as an explanation for the mechanics of motion and associated ridge and furrow morphology. In general, the objectives involved gathering information about the internal structure of an active rock glacier using remote sensing means, and using the internal structural data to provide an appropriate description of alpine rock glacier formation. Information gained from the rock glacier in Colorado was then used to develop a model for the development and storage of water within analogous landforms on Mars.

The following objectives were accomplished:

(1) identified the internal structure of an active lobate rock glacier with characteristic ridge and furrow surface structure using GPR, a non-intrusive method;

(2) analyzed rock glacier surface morphology in relation to its subsurface characteristics;

(3) developed a model that describes the movement mechanics and development of the rock glacier; and

(4) applied the model to Martian analogues using the terrestrial rock glacier as a surrogate. The model was developed for the purpose of evaluating Martian landforms for potential stores of water.

LITERATURE REVIEW

Rock Glacier Occurrence and Formation

Rock glaciers are distinctive landforms whose wide distribution, occurrence, and significance often go unnoticed. During the last century, they have been identified in almost all of the major mountain ranges of the world (Schweizer, 1968; Giardino, 1979; Höllerman, 1983). Rock glaciers generally occur in dry, continental areas rather than

humid regions, perhaps because thin to absent snow cover favors their persistence (Humlum, 1997a). Ages range from incipient rock glaciers on Pico de Orizaba volcano (Palacios and Vazquezselem, 1996) through 500-year old forms associated with the Little Ice Age (Humlum, 1996), to features several thousand years old (e.g., Kaeaeb et al., 1997; Calkin et al., 1998). Relict rock glaciers that formed at the end of the last Ice Age about 10,000 years ago have also been documented (Sandeman and Ballantyne, 1996; Humlum, 1998). The occurrence of past or present glaciers is not necessarily a prerequisite to the formation of rock glaciers because these landforms exist in both glacial and non-glacial areas (Giardino, 1979, 1983; Johnson, 1983; Haeberli, 1985).

Three types of geomorphic systems are known to produce rock glaciers as a physical response. These systems include glacial, periglacial (Items 1 and 2 as diagrammed by Johnson, 1984), and talus (as illustrated by Shakesby et al., 1987). The pioneering work of Wahrhaftig and Cox (1959) suggested that rock glaciers formed by permafrost processes to create a frozen mixture of rock debris and ice within talus or morainal debris. These findings have been affirmed and expanded by subsequent studies with the advent of new technology and the global interest in recognizing and studying rock glaciers. A few studies provide evidence of thick massive ice in the rock glacier interior and suggest that these forms are actually debris-covered glaciers (Potter, 1972; Whalley, 1974; Clark et al., 1994; Whalley et al., 1994).

The formation of an ice-saturated rock glacier begins with accumulation of ice in the upper reaches of the landform. The ice flows downslope, where it ablates slowly within or beneath the debris of the rock glacier. General conditions for the formation of rock glaciers have been reviewed by Corte (1987a):

(1) relatively young mountain ranges having bedrock with rock mass properties (e.g., joint spacing, weathering characteristics, etc.) favoring the formation of blocky debris;
(2) microclimate conducive to daily freeze-thaw cycles or frost weathering, sufficient ground moisture for periglacial processes, low to moderate snowfall sufficient for production of debris and avalanche, and low insulating snow cover;

(3) a combination of geographic position (e.g., latitude, elevation) and climate conditions (e.g., temperature, aspect) that promote periglacial processes and sustained subzero ground temperatures; and

(4) Talus supply promoted by steep, rough terrain, perhaps by debris from a previous glaciation, frequent freeze/thaw cycles, and rock mass properties.

Rock glaciers are generally situated at the base of massive, homogeneous and fractured cliffs and are rarely found where debris is finely crushed or where headwall fractures are excessively large (Wahrhaftig and Cox, 1959; Evin, 1987).

Morphology and Kinematic Properties

Stratigraphic mapping by Johnson (1992) and fabric analysis by Giardino (1979) and Giardino and Vitek (1988) demonstrated that ridges exhibit fold characteristics. Many researchers, including Haeberli (1985) and Giardino (1979), have reported that ridge and furrow development is most pronounced at sites of increased compression (i.e., slope decline). Fitzgerald (1994) later suggested that ridges and furrows originate as small irregularities on the surface and develop into large ridges at the lower sections of rock glaciers, where slope decline results in increased compressive stresses. This type of behavior lends itself to description in terms of kinematic wave development.

Kinematic properties have long been used to describe a variety of geomorphic systems including pool and riffle development, ice glacier surge, distributed stream flow, and slow mass movement (Langbien and Leopold, 1968; Gerber and Scheidegger, 1979). Kinematic wave theory, as applied to glaciers (Lighthill and Whitman, 1955) and rock glaciers (Olyphant, 1987), requires that a wave of increased discharge (kinematic wave) travels down the rock glacier at a speed greater than the mean velocity of the surface (Nye, 1960). The existence of the kinematic wave depends upon a functional relationship between the flow or flux and the concentration of material comprising the medium. In terms of rock glacier development, the propagation of a kinematic wave can explain the discrepencies observed in rock glacier movement (rate and distance) as compared to talus supply rate (Birkeland, 1973; Miller, 1973; White, 1987). Thus, kinematic wave theory allows for disproportionally higher rates of movement in the

snout of a rock glacier to be realized with little or no increase in talus supply rate at the head.

Distinctive surface geometry (Fig. 1.1) suggests that ridges and furrows may form as folds while the rock glacier moves. The surface of a rock glacier will deform into sequences of folds when: (1) compression develops parallel to the flow direction and (2) viscosity decreases downward from the surface of the rock glacier to the interior of the mass. Where valley walls diverge and the slope flattens, flow becomes less confined and the development of surficial ridges and furrows is consistent with decreased flow rate in the toe. Ridge and furrow structures, therefore, represent 'buckling' of the material to compensate for decreased flow velocity downvalley (i.e., conservation of mass) with a corresponding increase in force provided by faster flowing material upvalley. The morphologic response to this movement is increased thickness in the toe, which has been documented in a number of terrestrial and Martian landforms (Squyres, 1978, Lucchitta, 1993).

Morphologic Indicators on Mars

Martian analogues to terrestrial rock glaciers (Fig. 1.2) are postulated to contain significant volumes of the planet’s frozen water (Lucchitta, 1986; Lucchitta, 1993). Viking images of the northern plains on Mars reveal lobate flow bodies with wrinkled surfaces associated with rift valleys and the peripheral margins of splash-form craters. Lobate aprons have also been interpreted as possible viscous ice-flow features (e.g., Lucchitta, 1993; Carr, 1987) derived from materials loosened from their original locations. The material appears to have been transported generally down gradient by mass-wasting processes followed by accumulation and subsequent creeping flow (Squyres, 1978).

Lobate debris aprons are thick, topographically convex accumulations of debris at the base of escarpments. The surface of a debris apron slopes gently away from its source (e.g., the escarpment), and then steepens to form a distinct flow terminous analogous to the toe of a rock glacier. This morphology is a reliable indicator that deformation and flow have taken place throughout a significant thickness of the deposit.

In terrestrial rock glaciers, a well-developed toe indicates that the landform is currently active or was active in the recent past (Giardino et al., 1987). Some lobate debris aprons exhibit distinctive surface lineations that are both parallel and transverse to flow. These bear striking resemblance to terrestrial rock glacier counterparts.

Fig. 1.1. Front view of Yankee Boy Basin rock glacier. Note the over-steepened toe (front) and transverse ridges and furrows (arrows). Transverse ridges can be seen at left center. Wright's Lake is in the foreground; jeep trail provides scale.

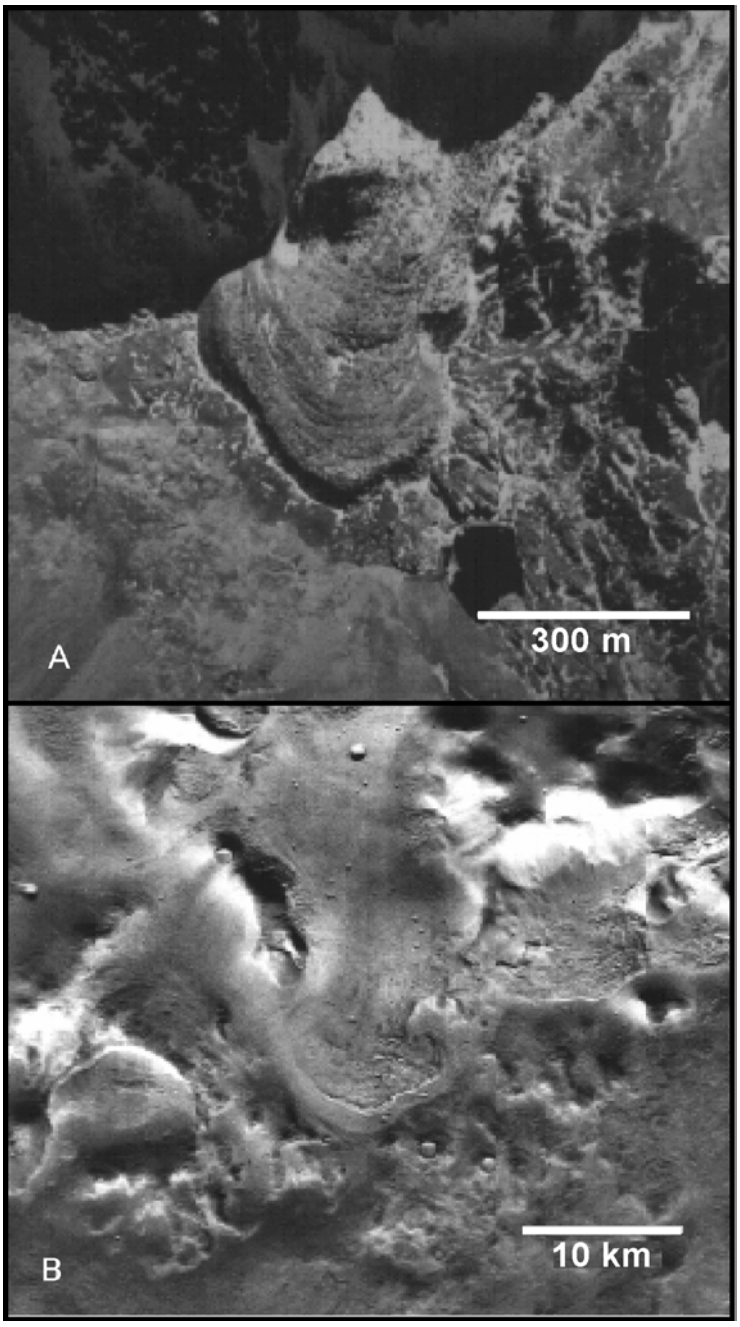

Fig. 1.2. Lobate mass-wasting features on Earth and Mars. (a) Rock glacier located in the San Juan Mountains of Southwest Colorado, USA; (b) A landform on Mars resembling terrestrial rock glaciers. This feature is located in the northeast portion of the Hellas Impact Basin (Viking Orbiter Image 585-B09, courtesy of LPI).

To fully understand movement and deformation patterns within rock glaciers a fundamental description of their development is required. At present, however, studies of rock glaciers on Earth have contributed minimally to our knowledge of their subsurface character (Burger et al., 1999). Because movement processes for such landforms cannot be observed directly, formation mechanisms must be treated with uncertainty, and the model must account for similar forms produced from diverse physical settings.

Previous Methods of Investigation

Rock glacier researchers have used both direct and indirect methods in their investigations of rock glacier structure. Until recently, direct investigative methods included tunnels through rock glaciers (e.g., Brown, 1925), visual inspection of exposures, and shallow pits (e.g., Wahrhaftig and Cox, 1959; among others). Potter (1972) successfully used shovel and bulldozer excavations to investigate Galena Creek rock glacier. Giardino (1979) used bulldozer excavations to study the structure of rock glaciers on Mount Mestas, Colorado.

Coring methods must negotiate the difficult surface debris as well as interior heterogeneity. Mechanically operated drills have proven to be effective in penetrating both rock and ice by changing drill bits to meet encountered conditions (e.g., Haeberli et al. 1988). Clark et al. (1996) used a light-weight, hand-operated auger for studies of Galena Creek rock glacier (i.e., massive ice); the coarse outer layer had to be removed before augering. The tool was useful at this locality because the volcanic source rock breaks down into small clasts, making hand excavation of the debris feasible. During the summer of 1997, Giardino and Degenhardt were able to extract ice cores from the Yankee Boy rock glacier in the San Juan Mountains of Colorado. Such coring may no longer be possible in this area, however, because of increased government restrictions on sampling, equipment use, and the addition of new areas designated as national parkland. Most of the techniques outlined above are also impractical for many localities where investigation is restricted by resources and accessibility. Large clast sizes and thick debris covers on rock glaciers challenge many investigations.

Indirect methods of investigation include geophysical surveys, such as seismic refraction, gravimetry, resistivity, radio-echo surveys, and ground penetrating radar. In contrast to the labor- and time-intensive direct methods, geophysical methods allow relatively rapid and inexpensive acquisition of three-dimensional data for the rock glacier. Seismic refraction and resistivity surveys are the most commonly applied geophysical techniques. According to Haeberli and Vonder Müehll (1996), surface layer seismic velocities, typically ranging from 300 to 1,000 m/s, contrast sharply with velocities from the top of ice-bearing layers. This contrast roughly parallels the surface of the rock glacier, can be traced along its length, and is readily interpreted as the refractor representing the top of frozen sediment. Ice-supersaturated frozen material has an average seismic velocity of 3,500 m/s and a seismic velocity range of 2,000 to 4,000 m/s (indicating a degree of heterogeneity).

Electrical resistivity of frozen sediments ranges from 1 to 10,000 kΩm and resistivity magnitude is related to ice content and type (Haeberli and Vonder Müehll, 1996). Ice at marginal permafrost conditions has low resistivity (5-500 kΩm); massive ice has much higher resistivity (1,000-2,000 kΩm). Recent gravimetry applications at the much studied Murtèl-Corvatsch rock glacier (Swiss Alps) were successful, but required an intense modeling effort to correct for surrounding topography and utilized significant existing data to develop the model (Vonder Müehll and Klingelé, 1994). Few results from the use of geophysical methods mentioned above have been tested by drilling or other methods to determine “ground truth,” and few results except the depth of the boundary between an unfrozen surface layer and frozen material below are unequivocal. General limitations of these geophysical techniques sometimes include complex modeling efforts that can produce non-unique models and may require additional ground-truthing data collection.

Based on the above limitations, a more practical method of subsurface remote sensing is needed for rock glaciers. Ground penetrating radar now provides a low-cost, accurate alternative to standard seismic techniques, without noise and disturbance to the ground. It is the method used in this study.

Ground Penetrating Radar Method

Ground penetrating radar (GPR) is a relatively recent development (Morey, 1974; Annan and Davis, 1976; Ulriksen, 1982), having reached user practicality in the mid-1980's. This technique offers the sophistication of other geophysical techniques combined with portability and ease of use. It is ideally suited to applications in the alpine, where logistics and expense are usually prohibitive. GPR has been used effectively in a variety of geologic and geomorphologic environments including karst, glacial, periglacial, fluvial, and wetlands (e.g., McMechan et al., 1998; Murray et al., 1997; Horvath, 1998; Roberts et al., 1997; Jol and Smith, 1995). To date, however, little research involving the application of GPR to rock glaciers has been carried out (e.g., Isaksen et al., 2000).

Digital GPR profiles are generated using transient electromagnetic energy reflections and are similar in appearance to standard seismic profiles. High frequency (10-1,000 MHz) EM energy is transmitted into the ground in the form of short pulses. Subsurface stratigraphy is inferred from the radar return signals as a portion of the transmitted energy is reflected back to the surface. Reflections are generated by changes in bulk electrical properties of the underlying materials (Smith and Jol, 1997). Such changes in electrical properties can be attributed to sedimentological variation (i.e., changing grain size), facies changes, differences in state of materials (i.e., water-rock or water-ice contacts), mineralogy, and density. Resolution of GPR at 100 MHz (assuming a velocity of 0.1 m/ns) is approximately 0.25-0.50 m, which is about 10 times greater than conventional high-resolution shallow seismic sounding (Jol, 1995).

JUSTIFICATION

This work is an important step toward understanding the fundamental development process for rock glaciers. The flow dynamics of rock glaciers and similar landforms can be understood only with knowledge of internal structure and composition. However, the difficulty and cost associated with direct observation of the internal characteristics make acquisition of these data problematic. Measurements of rheologic data (e.g., flow

direction, flow velocity, and stress fields) are not possible because flow is not observable at human time-scales. Consequently, observable data (e.g., site conditions, composition and morphology) must be used to analyze rock glaciers and Martian landforms. Subsurface data obtained by the proposed means will provide validity for any model of motion mechanics applied to rock glaciers and similar landforms.

ORGANIZATION OF THE DISSERTATION

This dissertation represents a compilation of manuscripts, which in combination address the overall objectives of the study. Each manuscript has been submitted to notable journal publishers with the author's intent that the knowledge gained through the application of GPR to rock glaciers is provided in the broadest forum. Following the introduction, problem statement, objectives, literature review, and justification sections of the first chapter are five additional chapters. Because the manuscripts have been incorporated in their original peer-reviewed forms, some of the introductory and background information has been restated in Chapter I of this dissertation, as deemed appropriate by the author.

In Chapter II, the engineering aspects of rock glaciers are covered in a published manuscript entitled "Engineering Geomorphology of Rock Glaciers" (Burger et al., 1999). It focuses on the human development considerations and our current state of knowledge regarding rock glaciers.

Chapter III discusses the application of GPR to a rock glacier in Yankee Boy Basin, southwest Colorado. The underlying GPR work is presented and a model for the formation of composite ice-cemented rock glaciers is presented.

In Chapter IV, the Yankee Boy rock glacier is treated as a surrogate for similar landforms on Mars. The model for rock glacier development discussed in Chapter III is used to evaluate the potential for locating water on Mars.

Chapter V addresses the problem of interpreting the origin of a landform having morphological features that are similar to those that are diagnostic of rock glaciers. The subject is a block stream located near El Paso, Texas for which a satisfactory

interpretation has been lacking. This study offers a refined interpretation based on new fabric and morphological data. The analytical approach used is one that has been effective for rock glaciers and a number of other landforms such as alpine tills, lowland glacial tills, landslides, and certain talus flows.

A discussion and summary of results are provided in Chapter VI. It is a compilation of conclusions that were drawn from the individual works presented in Chapters II through V.

CHAPTER II

ENGINEERING GEOMORPHOLOGY OF ROCK GLACIERS*

OVERVIEW

A partnership between geomorphology and engineering is facilitating human development in harsh alpine environments where rock glaciers are common. Rock glaciers provide locations for urban water sources, construction borrow sources, drill sites, shaft and tunnel portals, ski tower supports, and dam abutments. Rock glaciers, as dynamic landforms, necessitate proper identification in the field. Placing structures on, in, or adjacent to rock glaciers requires an appreciation and understanding of their temporal stability. Internal and surface characteristics provide important clues to the development and deformation of rock glaciers.

Rock glaciers play a significant role in the alpine debris transport system. Active movement and mass wasting are perhaps the most obvious geologic hazards affecting engineered works. The structure of the rock glacier is conducive to the production of a steady, continuous supply of meltwater during summer months. Thus, rock glaciers do serve as alpine aquifers. Consideration of rock glaciers as potential aquifer sources requires caution because of the long-term impact of climate change on the temporal nature of the landform. From the rock glaciers that we have monitored for water quality characteristics, it appears that they provide quality potable water.

This paper provides a foundation for appreciation and understanding of rock glaciers from an engineering geomorphologic point of view. The approach taken in this paper provides practical, important information to aid the engineer and engineering geologist in prudent evaluations of rock glaciers as potential sites for human development and uses. The bottom line is: *rock glaciers must be avoided for essentially all structures.*

---

*Reprinted with permission from "Engineering Geomorphology of Rock Glaciers" by Burger, K. C., Degenhardt, J. J. Jr., Giardino, J. R., 1999. *Geomorphology*, 31, 93-132.

INTRODUCTION

Human development of the alpine environment has been facilitated through a partnership between geomorphology, which is providing an increased understanding of the various geomorphic processes operating in this harsh environment, and innovative engineering. As a result of increasing leisure time and a greater number of individuals wanting to live in mountain areas, human development in alpine areas has created increased pressures on this environment. The alpine, an unforgiving environment dominated by high relief, steep slopes, mass wasting, tectonic activity, and extreme micro-climates, is composed of numerous landform assemblages. The landforms operate in concert to make up these assemblages and to serve as pathways to move both energy and material from higher to lower elevations. One of the major energy and material transporters in this landform assemblage is the rock glacier (Barsch, 1977; Giardino, 1979).

Rock glaciers, one form in the landscape continuum, have been mistakenly confused with other landforms (e.g., rock streams, talus flows, rubble streams). The question of what constitutes a rock glacier has been addressed by every researcher who has ever studied rock glaciers or has undertaken a review of the literature on rock glaciers, including Wahrhaftig and Cox (1959), Schweizer (1968), Corte (1976a), White (1976), Höllerman (1983), Haeberli (1985), Giardino and others (1987), and Martin and Whalley (1987). Rock glaciers are perhaps best defined as lobate- or tongue-shaped bodies of frozen debris that are separated from the surrounding terrain by a steep front and side slopes and that have a surface expression of furrows, and ridges which are generally perpendicular to the direction of flow (Giardino et al., 1987) (Fig. 2.1). The "wrinkled" pattern of the ridges and furrows influenced Capps (1910) to coin the term “rock glacier.” Flow velocity of most rock glaciers has been estimated to be between a few centimeters and decimeters per year. Most findings indicate that movement is the result of plastic deformation of ice contained within the structure (Haeberli, 1985; Barsch, 1988; Clark, 1988). Many forms of underground ice are contained within rock glaciers including, ice from freezing meteoric and ground water, ice transformed from snow, and

ice deformed by rock glacier movement (Haeberli and Vonder Müehll, 1996), and perhaps dead glacial ice.

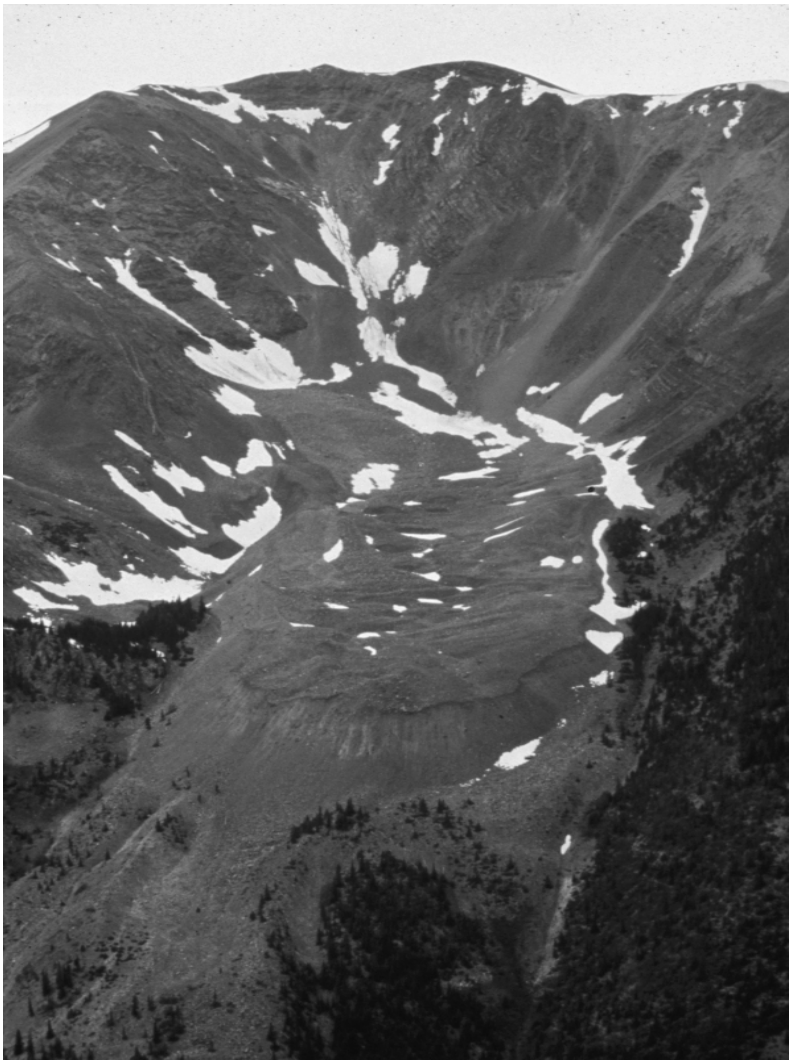

Fig. 2.1. California Peak rock glacier, located in the Sangre de Cristo Mountains of southern Colorado, U.S.A. Note the characteristic 'wrinkled' look provided by ridges and furrows. The toe of the rock glacier is unstable, as indicated by its steep face.

Rock glaciers provide backdrops for residential and commercial developments, such as urban water sources, construction borrow sources, drill sites, shaft and tunnel portals, ski tower supports, and dam abutments (Giardino and Vick, 1987). It is the interaction between humans and these diverse, dynamic landforms that mandates a well-grounded comprehension of the geomorphic processes operating in the alpine environment. We are gaining a better understanding of how these varied features form and behave under dynamic conditions. However, rock glaciers are poorly understood not only by the engineer, but also by the engineering geologist. Many engineers and engineering geologists treat rock glaciers as static landforms; rock glaciers are, in fact, dynamic landforms. Thus, this paper provides a discussion of the formation and dynamic aspects of rock glaciers as well as guidelines for engineering geomorphic evaluation and use of rock glaciers. The purpose of this paper is to discuss how rock glaciers look, how they form, the mechanics of their formation and movement, their physical properties, and engineering considerations.

THE ROCK GLACIER LOOK

Rock glaciers have a distinct surface look (Fig. 2.1). Significant variability in surface morphology from location to location occurs in response to both lithologic and topographic variables. Nonetheless, rock glaciers have a unique, characteristic appearance. Rock glaciers have been defined as a deposit of poorly-sorted, angular or blocky to tabular debris that is held together by massive ice or a matrix of ice-cemented fine clastics (Giardino, 1979; Giardino and Vitek, 1988b). Ordinarily, rock glaciers are characterized by a slope angle midway between those of the adjoining rock face above the valley floor, a surface of coarse fragments, little or no surface vegetation, concave-upward slope profiles in the upper parts (Figs. 2.2 and 2.3a) and strongly convex fronts (Fig. 2.3b). The “look” of a rock glacier can provide a reference point to quickly evaluate the status of the rock glacier (Table 2.1).

The distinct wrinkled surface of ridges and furrows (Fig. 2.2), the most characteristic feature of rock glacier morphology mentioned by observers, can be used to identify rock

glaciers both in the field and on aerial photographs. Analogous to forms associated with lava flows, mudflows, and molasses (Giardino and Vick, 1987), these microrelief forms are interpreted to be related to flow characteristics. The flow-like structures are defined by sets of parallel, curved ridges separated by long V-shaped furrows. At ground level, the furrows occur as irregular lines of elliptical depressions (Wahrhaftig and Cox, 1959). Ridges and furrows occur both parallel (longitudinal) and perpendicular (transverse or arcuate) to the direction of motion. Transverse features are bowed downvalley and may

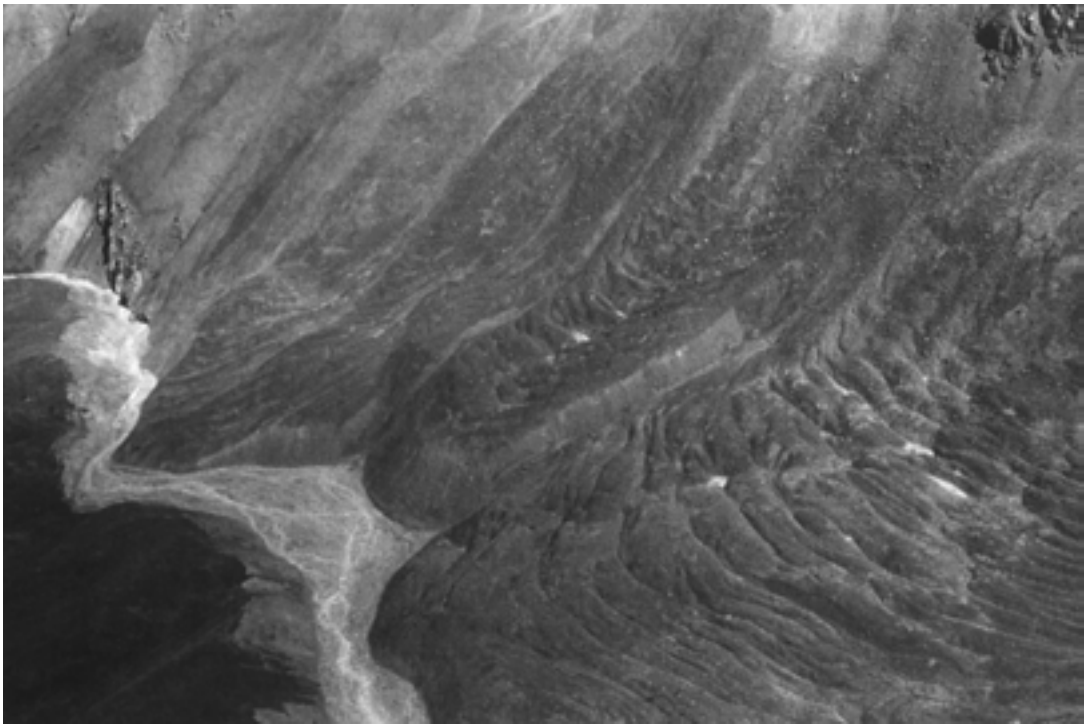

Fig. 2.2. Talus rock glaciers, lower Grizzly Creek. Ridges and furrows provide the distinct surface appearance which is common on active rock glaciers. The active rock glacier in this photo is located in the center, and is distinguishable by its steep terminus (photo courtesy of Peter Johnson).

Table 2.1. Assessing rock glacier status (after Giardino and Vick, 1987; Imhof, 1996).

Characteristic	Active	Inactive
Front Slope	•At angle of repose; •Sharp angle with upper surface; •Steep •Microform evidence of recent movement	•Rises at ~20 to 35°; rounded, gentle transition to top surface
Lichen and/or Vegetation on Toe	•Devoid of lichen or vegetation; •Noticeable lighter tone on aerial photographs	•Lichen and vegetation present
Shifting Position of Toe	•Changing distances between toe and fixed points	•Distances between toe and fixed points do not change
Surface Debris	•Freshly broken rock fragments; •Overturned fragments with lichens on underside and iron staining on upper side	•Weathered rock fragments •Rock fragments covered with lichen
Stability of Boulders on Surface	•Several ton boulders often can be moved slightly by shifting the weight of the person standing on them	•Several ton boulders cannot be moved by shifting the weight of the person standing on them
Trees	•Tilted trees on surface and below toe •Scarred trees below deposit toe	•Upright trees on surface and below toe
Push Lobes at Base of Toe	•Active basal sliding	•Not present or relict
Calculated Basal Shear[1]	•1.0 to 2.0 bars	•< 1.0 bar
Collapsed Meandering Furrow	•Sometimes, with ice exposed inside	•Present; interior ice has melted causing collapse of surface
Head Detached from Cirque or Valley-Side Wall	•Non-diagnostic: rock glacier could be moving faster than debris supply	•Non-diagnostic: Debris supply has discontinued or rock glacier is moving faster than debris supply
Temperature of Springs Emanating from Rock Glacier	•Even in summer should be ≤ 0ºC, or only slightly warmer	•Likely to be > 0ºC during summer months

[1]Empirical correlation developed for Alaskan rock glaciers by Wahrhaftig and Cox (1959) and tested elsewhere.

be an extension or compressive flow or a result of changes in the rate of debris added to the rock glacier. The ridges and furrows that comprise the characteristic microrelief found on most rock glaciers can be attributed to rate of talus supply (i.e., rock debris supplied by the headwall), or to the rate and frequency of movement of the rock glacier itself. Another form that develops on the rock glacier surface is the meandering furrow. These features were identified and described by Wahrhaftig and Cox (1959) as tightly meandering incised trenches extending lengthwise down the rock glacier.

Many studies of active, inactive, and relict rock glaciers describe enclosed depressions, large pits, and linear depressions that are thought to be associated with ice melt, seasonal sediment removal, and freeze/thaw processes. Geomorphic studies of relict rock glaciers that suggest several meters of subsidence have occurred as a result of ice melt and consolidation (e.g., Humlum, 1998).

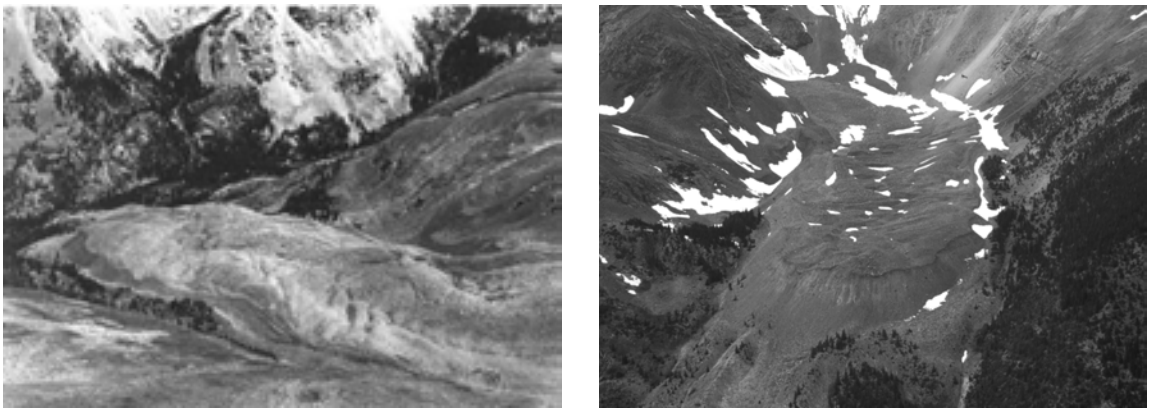

Fig. 2.3. A view of California Peak rock glacier showing its proximity to the valley below. The surface slope of the rock glacier grades from steep walls around the head to a flatter slope in the valley (a). Elevation of California Peak is 4221m and the elevation of the rock glacier toe is 3413m. (b) Lower portion of the California Peak rock glacier showing the strong convex front at the toe. Concave-upward profiles begin above the abrupt break in slope between the top and sides of the rock glacier; this indicates slope instability.

ROCK GLACIER OCCURRENCE AND FORMATION

Rock glaciers are distinctive landforms whose wide distribution, occurrence, and significance often go unnoticed. During the last century, rock glaciers have been identified in almost all of the major mountain ranges of the world (Table 2.2; Fig. 2.4) (Schweizer, 1968; Giardino, 1979; Höllerman, 1983). These features generally occur in dry, continental areas rather than humid regions, perhaps because thin to absent snow cover favors their persistence (Humlum, 1997a). Ages of rock glaciers range from incipient forms on Pico de Orizaba volcano (e.g., Palacios and Vazquezselem, 1996) to 500-year old forms associated with the Little Ice Age (e.g., Humlum, 1996), to features several thousand years old (e.g., Kaeaeb et al., 1997; Calkin et al., 1998). Relict rock glaciers that formed at the end of the last Ice Age about 10,000 years ago have also been documented (e.g., Sandeman and Ballantyne, 1996; Humlum, 1998). The occurrence of past or present glaciers is not necessarily a prelude to the formation of rock glaciers because these landforms exist in both glacial and non-glacial areas (Giardino, 1979, 1983; Johnson, 1983; Haeberli, 1985).

Rock glaciers are a response to three types of geomorphic processes: (1) glacial, (2) periglacial (Items 1 and 2 as diagrammed by Johnson, 1984; Fig. 2.5), or (3) talus (as illustrated by Shakesby and others, 1987). The pioneering work of Wahrhaftig and Cox (1959) suggested that rock glaciers formed by permafrost processes to create a frozen mixture of rock debris and ice within talus or morainal debris. These findings have been affirmed and expanded by subsequent studies with the advent of new technology and the global interest in recognizing and studying rock glaciers. A few studies provide evidence of thick massive ice in the rock glacier interior and suggest that these forms are actually debris-covered glaciers (Potter, 1972; Whalley, 1974; Clark et al., 1994; Whalley et al., 1994). However, these studies have yet to provide definitive evidence of glacial ice.

Table 2.2. Characteristics of rock glaciers.

Name/Location	Position	Shape	Bedrock	Status	Length (m)	Width (m)	Thickness/ Terminus Height (m)	Elevation/ Latitude (mmsl)	Rate of Front Advance* ($cm \cdot yr^{-1}$)	Ref.
Prins Karls Forland, Western Svalbard	Valley wall	Lobate	Quartzite	A		500	--/ 30-60	--/ 78°50′N	5.2-13.8	1
Mullemfjörd, Disko Island, Greenland	Cirque	Tongue	Basalt	A	1700	500	--/ 90	100-200/ 69°15′N	10	2
Central Brooks Range, Alaska USA	Valley wall	Lobate	Sedimentary	A & I	10-210		15-75/ 15-70	900-2000/ 67°37′ - 68°N	40	3
	Cirque	Tongue		A & I	≤3500		50-100/ 15-70	1100-1800/ 67°37′ - 68°N	10	
Kigluaik Mountains, Alaska, USA	Valley floor	Tongue	Metamorphic; granite	A	350-800			500-930/ 65°N		4
Alaska Range, USA	Valley wall	Lobate	Metamorphic; volcanic	A & I	60-1080	90-3085	20-50	865-1850/ 63°15′ - 64°N	48-72	5
	Cirque	Tongue		A & I	150-1540	60-775	10-125			
Slims River, Yukon Territory, Canada	Valley floor	Lobate	Greenstone, granite	A	1700	55-180		784-1250/ 61°N	6.7	6
Grizzly Creek, Yukon Territory, Canada	Cirque	Lobate	Metamorphosed sediments; intrusive volcanics	A & I	430-1430	200-1000		1650-2000/ 61°N		7
Valais Region, Switzerland	Valley floor	Lobate Elongate		A	600			2650-3000/ 46°N	20	8
Murtèl/Corvatsch, Swiss Alps	Cirque	Tongue	Granodiorite	A	400	200	50/ 20	2620-2850/ --		9
Laurichard, French Alps		Tongue	Granite	A	400	40-200		2500/ 45°N	30	10
Galena Creek, Absaroka Mountains, USA	Cirque	Tongue	Volcanic	A	1600	240-300	70-120/ 50	2680-3110/ 44°38′30" N	3-14	11
Lombardy, Italian Alps	45% Cirque	Lobate	76% Metamorphic	A&I	535	326		2110-2540		12

Table 2.2 (Continued).

Name/Location	Position	Shape	Bedrock	Status	Length (m)	Width (m)	Thickness/ Terminus Height (m)	Elevation/ Latitude (mmsl)	Rate of Front Advance* (cm•yr^{-1})	Ref.
Mount Emilius, Valle d'Aosta, Italy	Valley wall	Lobate	Gneiss, calc-schists, greenstones	A	190	200		2815/ --		13
				I	140	150		2550/ --		
	Cirque	Lobate		I	470	240		2310/ --		
				A	470	270		3000/ --		
	Valley floor	Tongue		A	1800			2600/ --		
SW Alps, France & Italy		Lobate	Metamorphic; Limestone	A&I	200-300			1500-2850/ 44°N	8	14
Ürümqi River, Tianshan Mountains	Valley side	Lobate	Gneiss	A	30-60	100-150	--/ 20-40	3900/ 43°04′-43°08′N	11-75	15
Northern Tien Shan & Djungar Ala Tau, Kazakhstan	River basin	Tongue	Granite	82%A	750-2000	350-980	20-75/ --	2100-3500/ 42°30′-45°30′N	60-93	16
Albanian Alps		Tongue	Carbonates, flysch, magmatic	I	200-1000	75-325		1690-2200/ 42°27′-42°33′N		17
		Lobate			120-200	100-130				
Colorado Front Range, USA	Cirque	Lobate Tongue	Granite	A	405-640	170-215	21 - >37/ 13-40	3320-3710/ 40°01′-40°16′N	5-20	18
Mosquito Range, Colorado, USA	Valley wall	Lobate	Granodiorite	I	90-275	180-600		3330-3975/ 39°10′-39°17′N		19
La Sal Mountains, Utah, USA		Lobate Tongue	Igneous; sedimentary	A < I	400-1000	150-800	15-40			20

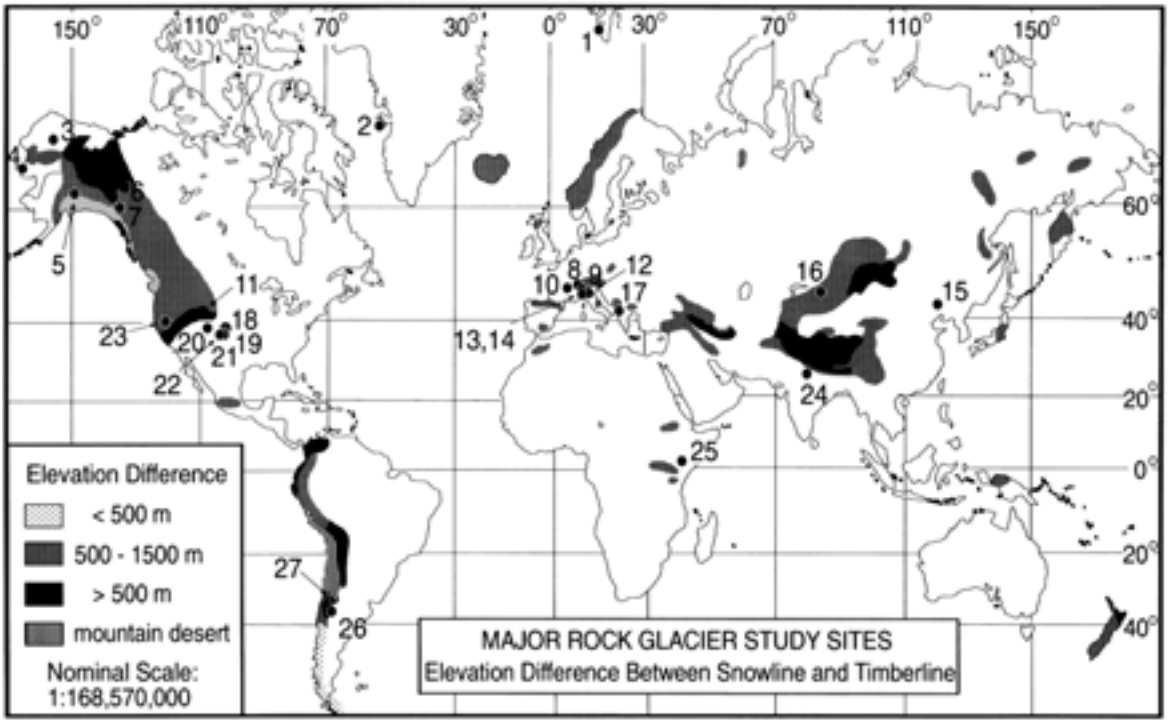

Fig. 2.4. Mercator projection map of major rock glacier study sites. Areas of elevation difference between snowline and timberline are shown (adapted from Hermes, 1955). Numbered points indicate locations of major rock glacier study sites in Table 2.2.

Rock glacier formation begins with accumulation of ice in the upper reaches of the rock glacier. The ice flows downslope, where it ablates slowly within or beneath the debris of the rock glacier. General requirements for the formation of rock glaciers include (after Corte, 1987a):

(1) relatively young mountain ranges having bedrock with rock mass properties (e.g., joint spacing, weathering characteristics) favoring the formation of blocky debris;

(2) Microclimate conducive to daily freeze-thaw cycles or frost weathering, sufficient ground moisture for periglacial processes, low to moderate snowfall sufficient for production of debris and avalanche, and low insulating snow cover;

(3) A combination of geographic position (e.g., latitude, elevation) and climate conditions (e.g., temperature, aspect) that allow periglacial processes and sustained subzero ground temperatures; and

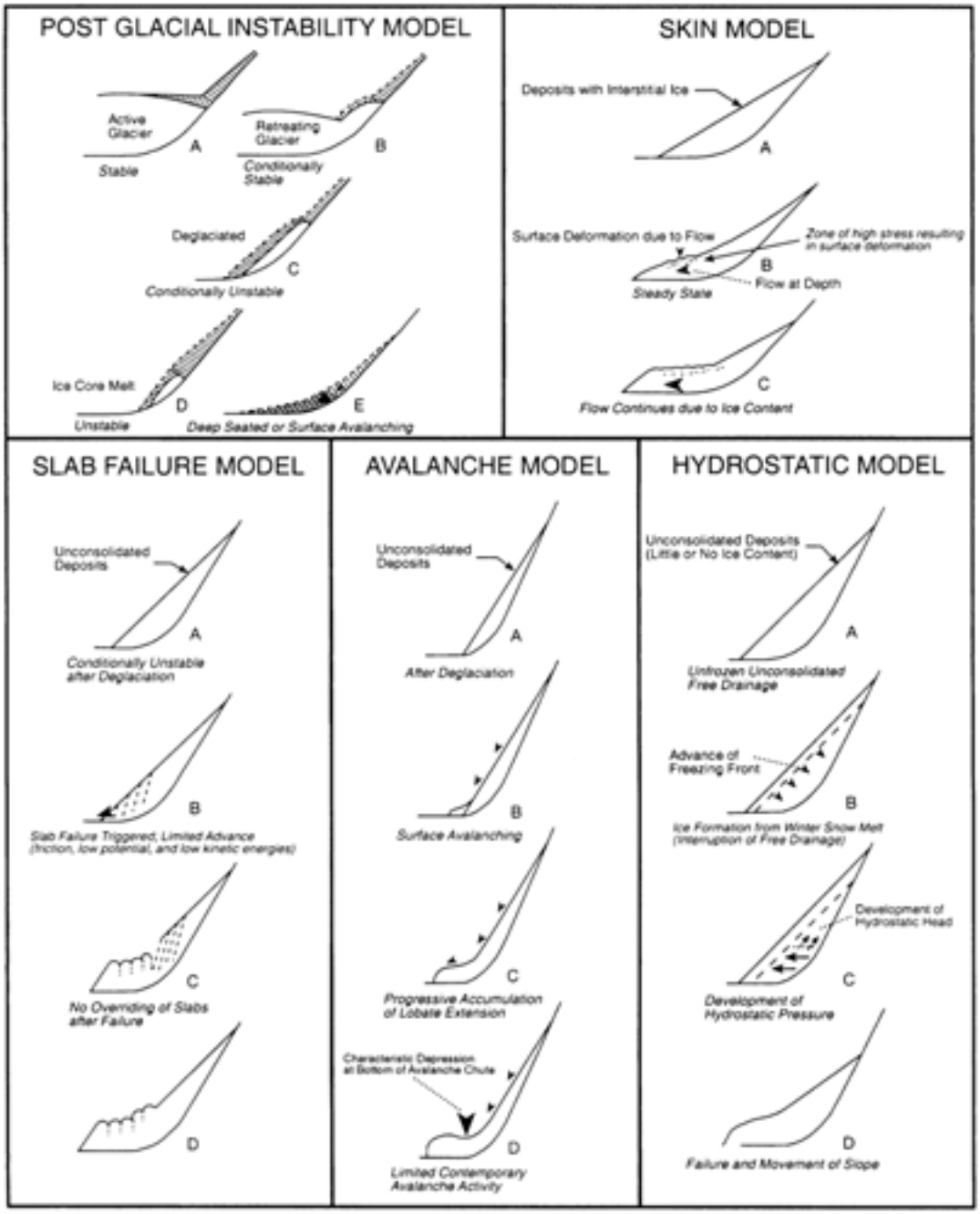

Fig. 2.5. Models of rock glacier formation. Included are glacial, periglacial and talus types of geomorphic processes. Post-glacial Instability Model and Skin Model were developed by Johnson (1984); Slab Failure Model and Avalanche Model by Whalley et al. (1983); Hydrostatic Model by Giardino (1983).

(4) Talus supply promoted by steep, rough terrain, perhaps by debris from previous glaciation, frequent freeze/thaw cycles, and rock mass properties.

Rock glaciers are generally situated at the base of massive, homogeneous and fractured cliffs and are rarely found where debris is finely crushed or where headwall fractures are excessively large (Wahrhaftig and Cox, 1959; Evin, 1987).

Rock Glaciers in the Landscape Continuum

As with other natural sloping landforms, rock glaciers represent a component of a continuous landscape, grading into and out of other landforms. Although some portions of rock glaciers exhibit distinct morphology, other portions definitely merge into talus slopes, debris flows, avalanche deposits, or glacial moraines, thus making identification as discrete landforms difficult. The idea that rock glaciers represent a landform continuum, originally put forth by Wahrhaftig and Cox (1959), has been expanded by subsequent continuum-based (Fig. 2.6; Giardino and Vitek, 1988b), dynamics-based (Johnson, 1978; Johnson, 1983), and form-based (Table 2.3; Corte, 1987a) classification schemes.

From a continuum perspective, rock glaciers can be viewed as temporally transitional forms of glacial or periglacial processes (Fig. 2.7; Giardino and Vitek, 1988b). The multiplicity of processes means that a variety of scenarios can lead to the formation of a rock glacier. Debris or slope failure may provide talus cover to a retreating glacier or remnant glacier core. The moisture balance and climatic conditions of the site may support formation of ice in the interstices of a talus body. Ice within a rock glacier may melt during warming climatic conditions, leaving a deposit that may easily be mistaken for till. As these examples illustrate, distinctly different processes are capable of generating the same fundamental morphologic form. Thus, what preceded the present form and what this form will be in the future depend upon the active processes. Although it is not within the scope of this paper to discuss the link between climate change and rock glaciers, it is important that the engineer and engineering geologist always consider that the environment is dynamic when contemplating engineering

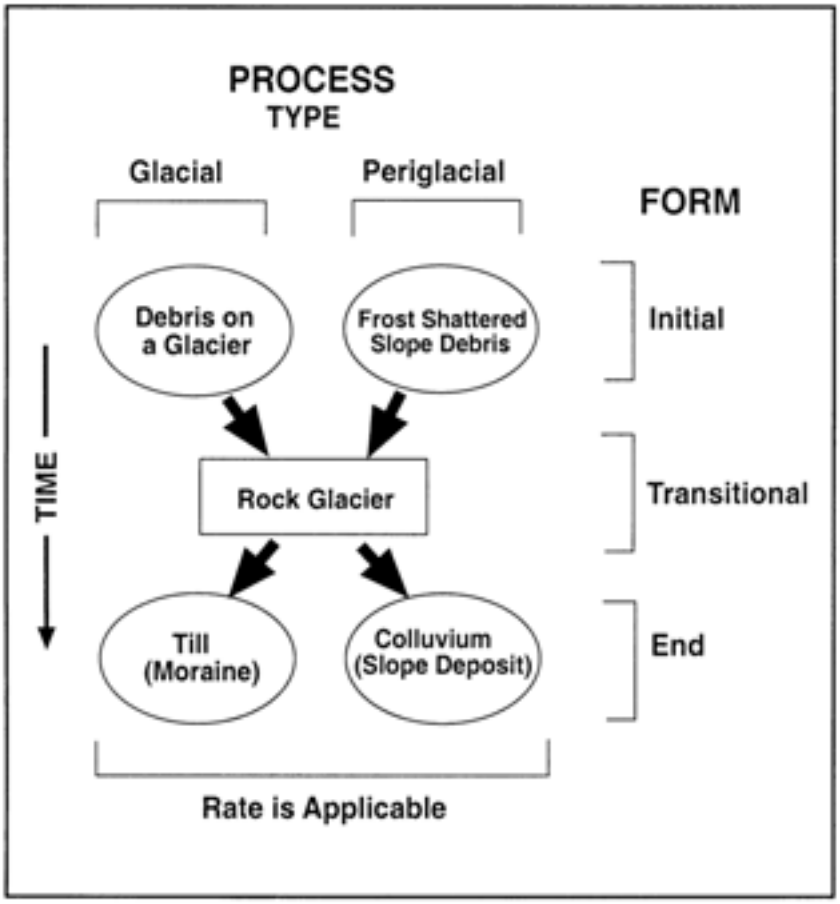

Fig. 2.6. Diagram illustrating the alpine landscape continuum. Rock glaciers are transitional forms that can develop from two distinct processes and can progress to two distinct end-members. Rate of movement is related to process, not form (modified from Giardino and Vitek, 1988b).

Table 2.3. Rock glacier classification criteria (after Corte, 1987a).

Source of Material
- Talus
- Morainic Debris

Location
- Talus Rock Glacier
  - Valley head, including cirques
  - Valley side walls
  - Footslope below cliff
- Debris Rock Glacier
  - Glacier terminus
  - Side of glacier

Connection to Source Area
- Direct
- None
  - Relation between flow of rock glacier and talus production
  - Melting of glacier
  - Outflow of rock glacier

Surface Relief
- Very well developed
- Subdued to well developed
- No furrows and ridges

Form
- Singular
- Complex (several units)

Shape
- Lobate (W≥L) Young landform
- Tongue (L>W) Mature landform
- Spatulate (L>W) Mature landform

Size
- Small ($<10^4$ m^2)
- Medium (10^4 - 10^5 m^2)
- Large ($>10^5$ m^2)

Note: Criteria listed in order of significance (Corte, 1987a); W = width; L = length

solutions in the alpine environment. Temperature is an important regulator in alpine areas. Because ice in a rock glacier is insulated with a mantle of rubble, the rock glacier response to climate warming or cooling has a longer lag time than a glacier. The insulated core provides the opportunity for an ice record to accumulate and be preserved for a long period of time. This ice record can provide a detailed description of past climate change. Unfortunately, extracting ice cores from rock glaciers is more difficult than extracting an ice core from glaciers. Thus, few successful attempts to obtain cores from rock glaciers have been made (e.g., Barsch et al., 1979; Haeberli et al., 1988; Clark et al., 1996; among a few others). *The fundamental point to remember is that rock glacier stability is partially temperature-driven.* A rock glacier that appears to be stable today could experience substantial surface deformation and slope instability as a result of climatic change or disturbance of the insulative debris mantle, causing damage to structures built on or adjacent to the rock glaciers.

Debris Transport System

The role of rock glaciers in debris transport in an alpine system is often neglected. Barsch (1977) and Giardino (1979) recognized that rock glaciers play a significant role in the alpine debris transport system. Active rock glaciers transport the surplus debris from talus slopes and glaciers down valley or down slope to other transport systems. As such, rock glaciers are of great importance to the geomorphic periglacial transport systems of high mountains. For example, 40 to 60% of the debris being transported in the Sangre de Cristo Mountains of Colorado can currently be described as rock glaciers (Giardino et al., 1987). Barsch and others (1979) estimated that 15 to 20% of periglacial mass transport in the Swiss Alps is incorporated in active rock glaciers.

Rock glacier movement, not to mention long-term rock glacier survival, requires a continuous talus supply. Rock glaciers tend to form from blocky-weathered bedrock. Blocky weathering results from a three-dimensional network of discontinuities. Talus supply thus depends upon the fracture pattern and linear fracture density (Evin, 1983; 1987) as well as the influence of weathering and ice and water activity (Haeberli et al., 1979; Giardino, 1983). In order for a rock glacier to maintain contact with its source

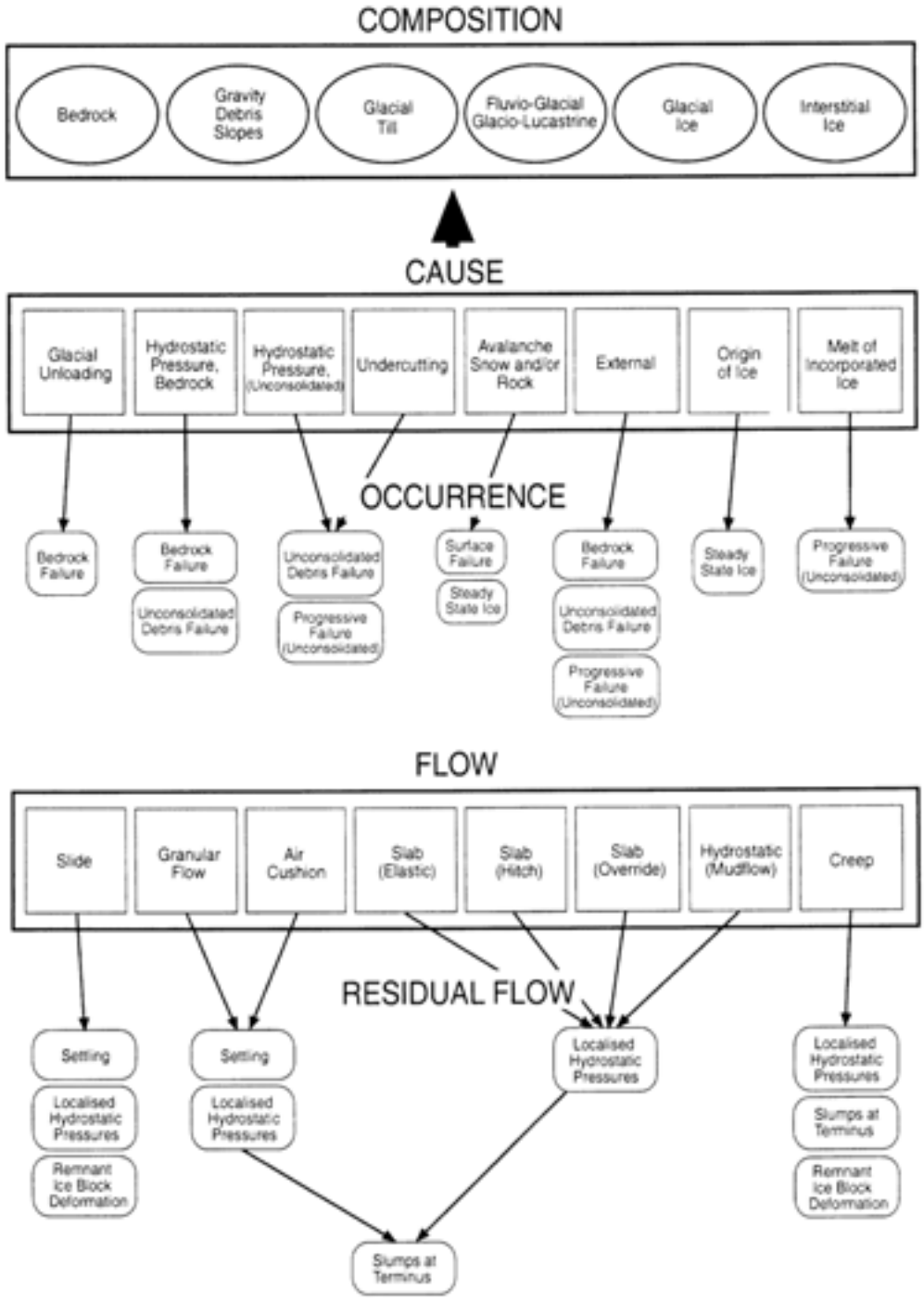

Fig. 2.7. Multiple process diagram illustrating possible processes for formation of rock glaciers. Diagram is based on flow and trigger mechanisms adapted from Johnson (1987).

area, a talus slope must exist below the rockwall to serve as temporary debris storage. Also, the rock glacier must advance slowly in order to overcome periods of low talus production. Increased flow velocity resulting from increasing slope angle is likely responsible for the loss of contact with the source cliffs observed in some rock glaciers. The variables of rock glacier flow and talus production are normally very stable, therefore it may be that rockwall height, talus production rate, rock glacier size, and flow velocity represent a slow-moving dynamic system that maintains equilibrium over a period of thousands of years.

The debris incorporated in rock glaciers of a given area can be used to calculate talus production in the rock glacier source area. Headwall retreat rates range from 0.3 to 0.7 $mm \bullet y^{-1}$ for an arid mountain system (Gorbunov, 1983) to 1.7 to 3.4 mm/yr for the Loch Lomond stadial (Ballantyne and Kirkbride, 1987). Schrott (1996) estimated a headwall retreat rate of 1 mm/yr for the Agua Negra catchment near San Juan, Argentina. Alternatively, the required size of a rock glacier source area can be calculated. Given an average velocity of 0.1 to 0.3 m/yr and an average debris content of 40 to 50%, Clark (1988) estimated that a rock glacier having a 30-m average thickness and situated below a 50 to 100 m wide talus slope must transport 60 to 450 m^3/yr If the source area is three times as wide as the rock glacier and the source area talus production rate is 1 to 2 mm/yr (as proposed for the Alps during the Holocene), then the rockwalls above the rock glacier must have a length of between 400 to 1000 m and a height of 350 to 800 m (assuming a slope angle of 50 to 60^o).

ROCK GLACIER CLASSIFICATION

Rock glaciers display a variety of origins, shapes, geomorphic positions, ice content, and other characteristics (Table 2.2). This complexity has led to the development of several classification schemes, recently reviewed by Hamilton and Whalley (1995), in efforts to better understand these features. Genetic classifications identify debris-covered glaciers, ice-cored rock glaciers, and ice-cemented rock glaciers (Martin and Whalley, 1987). Geometric/topographic classifications identify rock glacier types based on length

to width ratios and landscape position (Wahrhaftig and Cox, 1959; Outcalt and Benedict, 1965). Rock glaciers have also been classified using the landscape continuum concept developed by Giardino and Vitek (1988b) and Johnson (1983). It appears that the tiered classification criteria outlined by Corte (1987a) (Table 2.3) is the most readily applicable for engineering geomorphic purposes. These criteria incorporate elements of earlier classification approaches.

ROCK GLACIER MAKE-UP

Internal characteristics provide important clues to the development and deformation of rock glaciers. This information is crucial to anyone who must plan or carry out construction in areas that are potentially affected by rock glacier movement. Two categories of rock glaciers have been identified *based on internal structure near the landform surface and margins*:

(1) predominantly interstitial ice: rock glaciers comprised of an accumulation of clasts ranging in size from boulders to fines that is saturated with interstitial ice. Many investigators, most notably Barsch (1977) and Haeberli (1985) refer to ice-cemented rock glaciers as “permafrost” bodies having periglacial ice because of their perennially-frozen state. The interstitial ice is derived from two primary sources: (a) rain or meltwater percolating through the rock glacier matrix during warm periods; and/or (b) snow accumulations in winter. Ground water has also been documented as contributing to ice build-up in rock glaciers (Haeberli and Vonder Müehll, 1996).

(2) predominantly massive ice: rock glaciers containing plugs of ice that are covered by ice-saturated talus or landslide rock debris. Such plugs may represent the remnants of glacier ice (controversial) or moraines that became covered and preserved upon glacial retreat. Ice-cored rock glaciers may also have formed as accumulations of snowfall in cirques. The snow is compacted, converted to ice, and subsequently covered by boulder avalanches, rock slides, and rockfall events. In fact, recent coring of the entire thickness of a rock glacier revealed a highly complex mixture of both massive and interstitial ice (Haeberli et al., 1988). Several geophysical studies conducted during

the 1990s also suggest highly heterogeneous and complex ice distribution indicating the inadequacy of a simple two-endmember model to describe these features.

From an engineering perspective, the internal structure of a rock glacier is significant for two reasons: (1) how the rock glacier settles during periods of melting (e.g., climate change or disturbance of the debris mantle); and (2) mode of deformation. Greater and perhaps more catastrophic settlement of the rock glacier surface would occur in predominantly massive-ice versus ice-cemented rock glaciers. For ice-cemented types, rock glaciers with more blocky weathering source areas (e.g., massive rock such as granite, gneiss, limestone, etc.) will settle more than more platy-weathering source areas because platy-weathering rocks will have more support from the finer interstitial matrix. Given the heterogeneity in ice content and/or type within rock glaciers, it follows that movement mechanisms are also highly complex (Haeberli et al., 1998). Furthermore, individual layers within the landform move with different viscosity and under different horizontal/vertical strain rates (Haeberli et al., 1998). Because any observed change in surficial form represents responses to external stresses and internal resistances, use of surface measurements as an indicator of overall mode and rate of deformation can be misleading on some rock glaciers.

It is difficult to settle upon any of the suggested flow laws to accurately describe the overall deformational properties of a rock glacier because the conditions under which deformation occurs vary with ice content and type as well as strain conditions. In general, predominantly ice-cemented rock glaciers tend to deform at slower rates than predominantly massive-ice forms.

ACTIVE OR INACTIVE STATUS

An important consideration for the engineering geologist is whether the rock glacier is active or inactive (Giardino, 1979, 1983; Giardino and Vick, 1987). Active movement requires a constant supply of debris at the head of the deposit, a characteristic that distinguishes rock glaciers from other slope-creep features. Any observed movement, whether in the range of less than 1 cm/yr or greater than 150 cm/yr, has been used to

indicate an active status. Where movement rates have not been assessed, geomorphologists use geomorphic characteristics and other criteria to interpret movement status (Table 2.1). Apparently, more rock glaciers are inactive than active at this time (Giardino and Vick, 1987). More than half of the 200 rock glaciers in the Alaska Range studied by Wahrhaftig and Cox (1959) were inactive. In a 100 km^2 area in the Colorado Mosquito Range, 18 of 23 rock glaciers identified were inactive (Vick, 1981). This observation holds true even where rock glaciers coexist with true ice glaciers.

Because the relationships between material and movement mechanisms are not fully understood, lack of movement has been incorrectly equated with inactive status (Giardino and Vick, 1987). The transition from active to inactive is a slow temporal process in which inactivity is merely a state of temporary equilibrium. Thus, rates of movement can only indicate the current status of the process. Activity resulting in loading of the surface, removing material from the toe or sides, or tunneling into or through the rock glacier might result in a change from active to inactive state.

Active and inactive states should be considered as states of a movement continuum (Fig. 2.8) and should not be equated with the end-member status ultimately attained by a landform. Because a variety of processes can eventually transform a rock glacier into some other landform or sedimentary deposit, a rock glacier should be considered to be a transitional form rather than an end-member form (Fig. 2.6).

STRATIGRAPHY

Advancing technology has allowed progressively sophisticated methods for assessing the internal structure of rock glaciers (Table 2.4). Structural studies have progressed from shallow excavations and exposed cuts (e.g., Capps, 1910; Brown, 1925; Domaradzki, 1951, Wahrhaftig and Cox, 1959; White, 1971) to geophysical methods (e.g., Potter, 1972; Barsch et al., 1979; Corte, 1987b; Cui and Zhu, 1989; Francou and Reynaud, 1992; Guglielmin et al., 1994; Wagner, 1996) and, more recently, core drilling of these features (e.g., Haeberli et al., 1988; Clark et al., 1996). Other researchers have

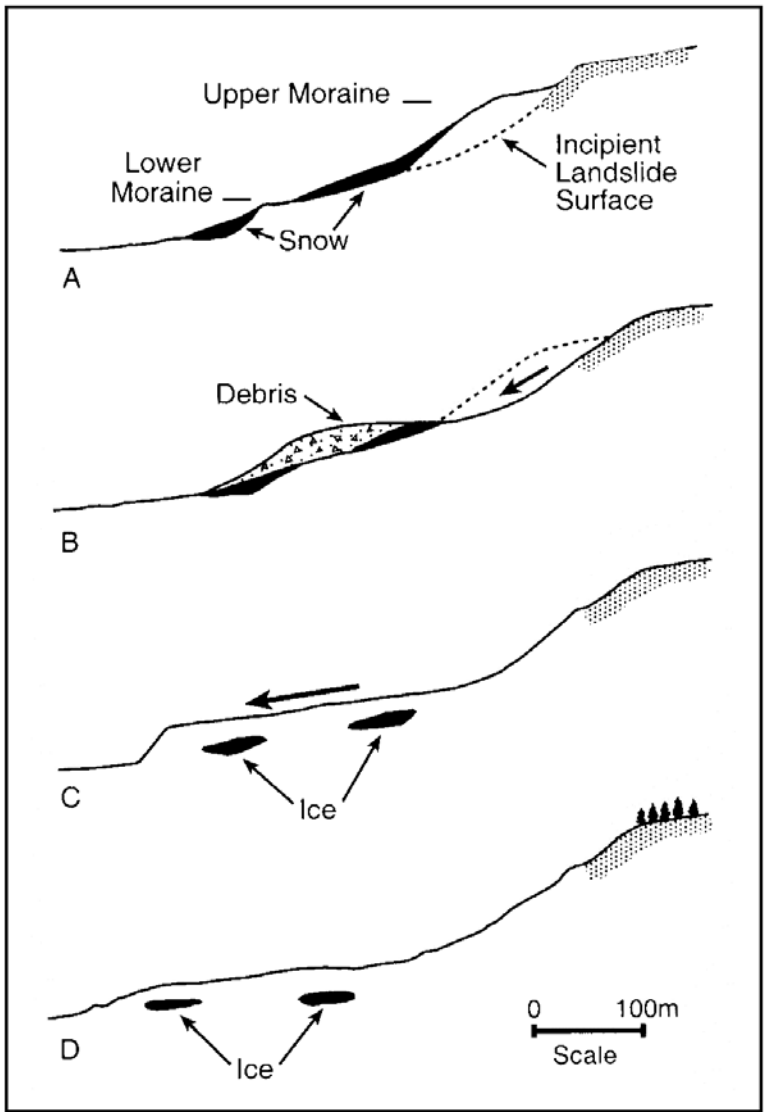

Fig. 2.8. Progression of rock glacier development postulated by Vick (1987). (a) Initial conditions following recession of an ice glacier; (b) Landslide in upper moraine and debris loading on lower frozen moraine; (c) Movement by active creep; (d) inactive.

Table 2.4. Internal structure of rock glaciers.

Location	Investigation Method	Interior Layers	Ref.
Alaska	Shallow excavations	Layer 1: Loose, angular blocks; <1 m thick Layer 2: Ice-cemented debris	1
Hurricane Basin, Colorado	Mine tunnel	Layer 1: Loose, angular blocks; ~1 m thick Layer 2: Ice-bound rock; variable ice content and clast size Layer 3: Clear ice Layer 4: Bedrock	2
Switzerland	Shallow excavations	Layer 1: Loose, angular blocks; 1-2 m thick Layer 2: Ice masses 2-3 m thick	3
Alaska Range, U.S.A.	Exposed by streamcuts, landslide scars, and in rock glacier head areas; shallow excavation	Layer 1: Loose, angular blocks; <1 m thick Layer 2: Boulders with sandy debris-filled pores cemented with clear ice	4
Arapaho Rock Glacier, Colorado Front Range	Blasted pit	Layer 1: Coarse outer mantle Layer 2: Frozen muddy sand cemented with 1-2 cm long ice granules	5
Gruben Rock Glacier, Swiss Alps	Drill coring	Layer 1: Active layer; 2-3 m thick; 4-28 kΩm Layer 2: Frozen debris; 70-110 m thick; 500-600 kΩm	6
Vallecitos, Cordón del Plata, Mendoza, Argentina	Electrical and magnetotelluric soundings	Layer 1: Active layer; 15-20 m thick Layer 2: Permafrost; 68-70 m thick Layer 3: Aquifer sub-permafrost; 63 m thick Layer 4: Bedrock	7
Ürümqi River, Tianshan Mountains	Pits and DC resistivity soundings	Layer 1: Active layer; 1.5 m thick; 1.4-1.9 m depth to top; 2.5 kΩm Layer 2: Frozen sand and gravel with ice; 32-37 kΩm	8
Laurichard, French Alps	Geoelectrical soundings	Layer 1: Active layer; 4-5 m thick Layer 2: Permafrost layer; 30-40m thick; 800 kΩm	9
Livigno area, Sondrio, northern Italy	Geoelectrical surveys	<u>Regional Scenarios</u> Type A: Thin permafrost layer; 0.7-2.5 m thick; 20-40 kΩm Type B: Single permafrost layer immediately below active layer; 1.9-18 m thick Type C: Single permafrost layer at or below 5 m depth; 6-10.5 m thick Type D: Two permafrost layers separated by unfrozen ground; one at surface, one below 20 m depth <u>Permafrost Bodies</u> Active Layers: 2-4.7 m thick Top Permafrost: 8-21.1 m depth Resistivity: 18-560 kΩm	10
Grizzly Creek, Yukon Territory, Canada	Resistivity soundings	Layer 1: Active layer; 1-2.5 m Layer 2: Frozen layer with low to moderate ice content; 10-30 m thick; 60-250 kΩm; occasional massive ice lenses; Layer 3: Metasedimentary bedrock?; 6.5 kΩm	11
Sainte-Anne, Queyras Area, Southern Alps, France	Electrical soundings	Layer 1: A few meters of ice-free sediments; 1.5-8m thick; 1-17 kΩm Layer 2: Complex layer with massive & interstitial ice, unfrozen tongue, ice-cemented active terminal lobe; about 20-50 m thick; 3-400 kΩm Layer 3: 2.5-500 kΩm	12

Table 2.4. (Continued).

Location	Investigation Method	Interior Layers	Ref.
Prins Karls Forland, Western Svalbard	Geoelectrical soundings	Layer 1: Active layer; 0.1-25 kΩm; Layer 2: Permafrost; 30-500 kΩm Layer 3: Sub-rock glacier; 0.1-13 kΩm	13
Northwestern Svalbard	DC resistivity & seismic refraction soundings	<u>BrÌggerhalvÌya, Ny-èlesund area</u> Layer 1: Active layer; 1-3 m thick; 2-8 kΩm Layer 2: Frozen layer with variable ice content; 20-50 m thick; 20-90 kΩm; 3.4-4.5 km/s Layer 3: Active layer; 0.5-1 m thick Bedrock: 5.2-6.1 km/s <u>Stuphallet 1 (Active)</u> Layer 1: Active layer; 1.3-2.2 m thick 0.2-0.3 kΩm; <1.9 km/s Layer 2: Frozen layer; 20 m thick; 3.1-4.8 kΩm; 4.0 km/s <u>Stuphallet 2 (Somewhat Active)</u> Layer 1: Active layer; 2-4 m thick; 11-35 kΩm Layer 2: Frozen layer; 15-20 m thick; 200-900 kΩm; 4.0 km/s Layer 3: Active layer; 2-6 kΩm <u>Stuphallet 3 (Inactive)</u> Layer 1: Active layer; 2 m thick; 4.6-5.5 kΩm Layer 2: Frozen layer; 20 m thick; 300-1500 kΩm; 3.8-4.5 km/s	14
Murtèl-Corvatsch, Upper Engadin, Swiss Alps	Core drilling	Layer 1: Active layer; 2-4 m thick Layer 2: Very pure ice; 9-11 m thick Layer 3: Interlayered frozen to highly supersaturated silt, sand, and gravel and thick ice lenses; 4 m thick Layer 4: Coarse, saturated frozen rock debris with layers of vertically-continuous frozen sand; 18 m thick Layer 5: Highly fissured, permeable granodiorite bedrock; 4 m thick	15
Galena Creek Absaroka Mountains, U.S.A.	Coring	Layer 1: Rock debris; 1 m thick Layer 2: Continuous ice with regularly-spaced silty-sand layers; >9.5 m	16

1) Capps (1910)
2) Brown (1925)
3) Domaradzki (1951)
4) Wahrhaftig and Cox (1959)
5) White (1971)
6) Barsch et al. (1979); Haeberli et al. (1979); King et al. (1987)
7) Corte (1987b)
8) Cui and Zhu (1989)
9) Francou and Reynaud (1992)
10) Guglielmin et al. (1994)
11) Evin et al. (1997)
12) Assier et al. (1996)
13) Berthling et al. (1998)
14) Wagner (1996)
15) Haeberli et al. (1988)
16) Clark et al. (1996)

used hydrologic characteristics and isotopic studies to predict the internal characteristics of rock glaciers (e.g., Johnson, 1981; Blumstengel, 1988; Giardino et al., 1992). Rock glaciers can typically be considered as an outer (upper) unfrozen layer (generally <1 to 5 m thick) and a less understood inner (lower) layer (generally 20 to 50 m thick. The boundary between the two layers fluctuates in position and thickness seasonally 1 to 5 m (see Table 2.4). The active layer is analogous to active layers of other periglacial landforms.

Outer Layer

The outer layer typically consists of angular, talus-like rock fragments with open interstices (Fig. 2.9). Sand and silt size fractions are rare; clay size particles are generally absent (Table 2.5). Fragment diameter commonly ranges from about 0.5 to 1.5 m (Table 5) and fragment lengths up to 6 m long have been reported (Wahrhaftig and Cox, 1959). The size of rock fragments on a given rock glacier is a function of the bedrock source material (e.g., Wahrhaftig and Cox, (1959) data in Table 2.5) and the fracture spacing of the rock material (Evin, 1987). Shroder (1987) found no correlation between fragment size and position in rock glaciers in the La Sal Mountains. Vick (1981) used excavation and stripping of coarse surface material to demonstrate the formation of the coarse outer layer. Subsequent thawing of the matrix led to erosion of gravel-size and finer particles by percolating waters, leaving behind a layer enriched in coarse rock fragments. Large open voids develop between the fragments and result in an edge-supported (“house-of-cards”) arrangement. These voids create a loose, unstable, and compressible consistency with low shear strength (Ives, 1940).

Inner Layer

Limited data are available on the interior characteristics of rock glaciers. The interior of active ice-cemented rock glaciers generally contains a matrix of silt, sand and gravel supporting larger fragments as well as ice cement, lenses, and/or layers (Tables 2.4 and 2.5). The grain size distribution for a typical rock glacier interior is shown in Fig. 2.10. Direct evidence of internal properties was obtained by coring the upper 10 m of the Galena Creek rock glacier (Clark et al., 1996) and Murtèl-Corvatsch rock glacier

(Haeberli et al., 1988). The structure of Murtèl-Corvatsch rock glacier appears to be substantially more complex (Table 2.4). Haeberli et al. (1988) divided the inner layer of this rock glacier into four layers (in order of increasing depth): 9 to 11 m of very pure ice; 4 m of interlayered frozen to highly supersaturated matrix and ice lenses; 18 m of coarse, saturated frozen rock debris; and 4 m of highly fissured permeable bedrock. Several geophysical surveys of other rock glaciers have also suggested complex, heterogeneous interior layers. For example, rock glaciers in the Livigno area of northern Italy (Guglielmin et al., 1994) have been divided into four possible types based on the number and position of interpreted permafrost layers (Table 2.4). The rock glacier interior may contain one or more frozen layers separated by unfrozen and water-bearing layers. Both Haeberli (1985) and Corte (1987b) report subpermafrost aquifers beneath the frozen sediments.

Ice Content

Ice has been documented in active as well as many inactive rock glaciers. Ice occurs interstitially, as isolated granules, or as nearly continuous (massive) fill. The ice in some rock glaciers is thought to originate from: (a) interstitial freezing of percolating meteoric and melt waters (Wahrhaftig and Cox, 1959; White, 1976; Barsch, 1988; among others); (b) buried snow avalanches (Outcalt and Benedict, 1965); or (c) combinations of these sources. New or dead glacial ice is also a source considered for areas where rock glaciers are clearly transitioning from glaciers in the landscape continuum (Potter, 1972; Whalley, 1974, 1983; Calkin et al., 1987; among others). Clear ice layers of considerable thickness also can develop when accumulation of snow on the rock glacier surface is later buried by talus or other debris. Vick (1981) attributed an ice layer behind the front of an inactive rock glacier to this source. Elconin and LaChapelle (1997) describe a rock glacier in the Wrangell Mountains, Alaska, whose front was “blown away” by a flood. The whole front was exposed for a short while in cross-section, interestingly showing both clean ice and debris-rich ice. In many cases the actual origin of the ice is still under debate.

Fig. 2.9. Platy fabric typical of the outer layer of a rock glacier. The angular, platy shapes of the rock fragments are the result of weathering. Photo taken at Mt. Mestas, Colorado (Giardino and Vitek, 1988a).

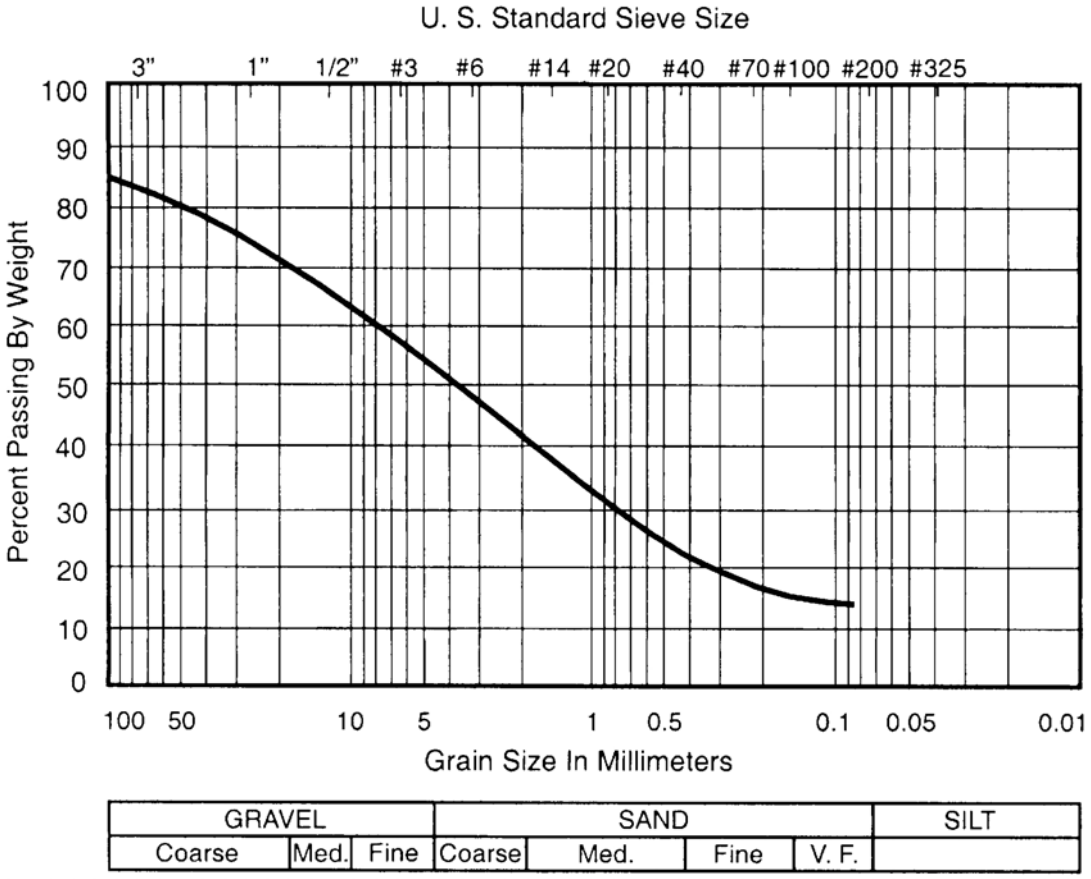

Fig. 2.10. Grain size distribution for the interior of a typical rock glacier. The distribution excludes the 150 mm fraction (adapted from Giardino and Vitek, 1987).

Table 2.5. Grain size of rock glacier layers.

Layer	USCS Classification	Grain Size	Source Rock	Reference
Upper	GW	Mean: 5.9 - 22.2 mm	Greenstone, granite	Blumstengel (1988)
Upper	0-25 cm: GP 25-120 cm: GW	•Ranges from 8 to 64 cm; •Increased sand content with depth; •Little or no silt and clay	Volcanic	Potter (1972)
Upper	GW	•Mean: 0.3-1.5 m long •Max: 1.5 to 6 m long	Granodiorite, greenstone, metavolcanic schist, stretched conglomerate, latite	Wahrhaftig and Cox (1959)
		Mean: 15 cm long	Biotite-cordierite hornfels	
		Mean: 2.5-5 cm long	Phyllite, slate	
Upper		0.1-3 m diameter	Granodiorite, quartz monzonite	Clark et al. (1994)
Upper		•0.1-0.5 m diameter •Large cobbles to small boulders common	Igneous, sedimentary	Shroder (1987)
Upper		•up to 0.6 m	Granodiorite	Vick (1987)
Lower		•23-43% fine sand •15% gravel •1-2% clay •50-70% of samples classified as sand		Barsch et al. (1979)
Lower	SW (matrix only)	<u>Matrix Only</u> •85-98% sand size •0.2-1.6 mm •Rare/absent clay	Metamorphics, limestone	Evin (1987)

Rock glaciers of periglacial origin are generally considered to have an ice content of 50 to 70% (Barsch, 1977; Giardino, 1979). Barsch and others (1979) visually estimated the ice content of Gruben rock glacier to be about 60% by volume, an estimate confirmed by gamma-gamma (density) and neutron-neutron (porosity) borehole measurements. Borehole geophysics data also showed an asymptotic decrease in ice content from nearly 100% by volume near the permafrost table (~2 m deep) to 50 to 70% several meters below the rock glacier surface. The ice content of Murtèl-Corvatsch rock glacier was determined to be 90% by volume near the surface of the frozen material

(Layer 2; Table 2.4), decreasing to 30 to 60% with depth (Layers 3 and 4; Table 2.4) (Haeberli, 1985; Haeberli et al., 1988; Vonder Müehll and Klingelé, 1994). Thus, some rock glaciers long considered to be of periglacial origin have been shown to contain clear ice cores or clear ice layers of significant thickness. Interestingly, the age of ice in the upper 20 m of the Murtèl-Corvatsch rock glacier has been estimated via several independent techniques to be several thousand years old (Haeberli and Vonder Müehll, 1996).

As described in the previous paragraph, studies of the Murtèl-Corvatsch rock glacier found significant thicknesses of massive ice in addition to the expected interstitial ice (Haeberli et al., 1988; Vonder Müehll and Klingelé, 1994; Haeberli et al., 1998). Relic plugs of clear (massive) ice have been found in rock glaciers thought to be derived from remnant glaciers (Potter, 1972; Outcalt and Benedict, 1965; Brown, 1925) as well as rock glaciers known to be of periglacial origin. Brown (1925) described a zone of internal ice that was 30 m wide near the head of a rock glacier. Recent studies by Clark and others (1994) and Whalley and others (1994) found greater than 90% ice in cores recovered from Galena Creek rock glacier. Further study of the cores by Clark and others (1996) found the ice to be clean, with cm-thick, regularly-spaced silty-sandy layers.

Haeberli and Vonder Müehll (1996) grouped rock glacier ice into three categories based on resistivity soundings: (1) extremely high resistivity (>10,000 kΩm); (2) high resistivity massive ice (1,000-2,000 kΩm); and (3) low resistivity ice at marginal permafrost conditions (20 kΩm). Types 1 and 2 are thought to form from freezing meteoric waters. The extremely high resistivity of Type 1 ice is characteristic of glacial ice and is rarely encountered in rock glaciers (personal communication, Haeberli, 1998). The greater ionic content of Type 3 ice suggests that this ice is of ground-water origin. Resistivity soundings along longitudinal transects generally show a disappearance of Types 1 and 2 ice and the appearance of Type 3 ice as one moves from the upper to lower reaches of a rock glacier. Haeberli and Vonder Müehll (1996) emphasize that the

range of resistivities detected in the rock glacier is evidence of significant heterogeneity and anisotropy in the internal layer and of multiple origins of ice in the rock glacier.

ENGINEERING CONSIDERATIONS

Movement Rheology

Current consensus of rock glacier movement mechanisms generally includes: creep of massive ice; creep of interstitial ice; landsliding; and/or basal shear facilitated by elevated pore pressure (Giardino, 1979; Giardino, 1983; Giardino and Vick, 1987). The relative importance of these mechanisms is not clearly understood. Movement of a given rock glacier may operate via one or more mechanisms and dominance of a given mechanism may change with time. To-date, no systematic subsurface exploration or *in situ* instrumentation has been implemented to document movement characteristics.

Creep Processes

Rock glaciers can be considered long-term, secondary creep phenomena where ice-rich permafrost is deformed under nearly constant stresses, strain rates and temperatures (Haeberli, 1985). The plastic deformation of the ice in an active rock glacier is a function of the amount of mineral component present, grain size of the minerals, pressure, temperature, orientation of the ice crystals, air content, degree of overall consolidation of materials making up the rock glacier, and slope angle (Barsch, 1988). Although not directly analogous to rock glaciers, deformation of frozen soils is attributed to (Sayles and Haynes, 1974): (1) pressure melting of ice at soil grain contacts; (2) migration of unfrozen water to lower stress regions; (3) structural breakdown of the ice and detachment from soil grains; (4) plastic deformation of pore ice, and (5) readjustment in the particle arrangement. Using an shearbox apparatus, Nickling and Bennett (1984) found that the shear strength of ice-rock mixtures changes with increasing ice content. They attributed changes in shear strength directly to changes in internal friction and the cohesive effects of the pore ice. The creep process involves strengthening resulting from packing of soil particles which counteracts weakening caused by reduction in cohesion and increasing amounts of unfrozen water in the frozen material. Strength and

deformation characteristics of frozen soils, therefore, are dictated by soil type, structure, density, ice content, mineralogy, temperature, and the magnitude and sense of loading.

Proponents of ice-cored rock glaciers often cite ice-core creep as a fundamental transport mechanism for active rock glaciers. Whalley (1974) believed that ice-core creep was essential because computed shear strengths for ice-debris mixtures were too great to allow flow of thinner rock glaciers without invoking an ice core. Haeberli (1985) provides borehole geophysical evidence for movement of an ice-cemented rock glacier known to be actively moving. Barsch (1969), White (1976), and Barsch and others (1979) concluded that movement of ice-cemented rock glaciers results from mass loading on the upper reaches of the glacier and a consequent creep of interstitial ice. A minimum level of internal shear stress must exist to initiate and maintain creep movement within the frozen material. This shear stress is most likely generated by a continuous source of debris to the head area. If a rock glacier has a high ice content (> 60%), the deformation stress in the debris-ice mixture is concentrated at the interface between the ice and mineral particles. However, if the rock glacier has a lower ice content (< 60%), then deformation stress is concentrated at particle-particle contacts. In a debris-ice mixture, the deformation stress is concentrated at the interface between the ice and the mineral particles. Localized melting of the ice at the interface may be caused by pressure, and the meltwater may flow to areas under less stress and refreeze. This model is still highly speculative as researchers have had limited opportunity to gain direct access to the interior of rock glaciers.

Landsliding

Early rock glacier researchers hypothesized that rock glaciers must result from large, sudden rockfall avalanches (e.g., Howe, 1909). Chaix (1919, 1923, 1943) suggested that slow landslide movement of rock glaciers was a result of high fines content, freeze/thaw cycles, and internal erosion. Bell and Rahn (1972) thought that debris sliding on top of stagnant glacial ice might contribute to rock glacier movement. Landsliding as a dominant movement mechanism has generally been abandoned. After conducting a stability analysis of two rock glaciers in the Colorado Mosquito Range, Vick (1981)

concluded that interstitial ice creep was dominant movement mechanism even though landsliding of moraine deposits supplied debris to form the rock glaciers.

Shroder (1987) concluded that rock glaciers and other similar boulder deposits of mixed origin in the High Plateaus and La Sal Mountains are polygenetic, with complex mechanisms involving both ice and landslip dynamics. Steep fronts at the angle of repose seem to occur where basal-shear resistance is sufficient to produce oversteepening characteristic of rock glaciers (Wahrhaftig and Cox, 1959). In cases where landslip (basal slip) is more active, basal push lobes and fronts of gentle slope develop. The observed norm for rock glacier activity in the above regions involves movement or massive failure of the igneous and underlying unstable sedimentary rock as a unit, rather than creep deformation of internal ice. A zone of interstitial ice is developed in the associated rock rubble, which likely provides an impermeable barrier to the upward migration of groundwater, aiding further the movement of these features. Landslip-generated shear failure and basal slip is likely facilitated by water through freezing and addition to permafrost, and by increased load. The primary activation, however, is supplied by hydrostatic or pore-water pressure beneath impermeable permafrost lenses.

Basal Shear and Pore Pressures

Certain features of rock glaciers may be explained by related theories of movement associated with basal shear and internal pore pressure (Giardino, 1979, 1983; Giardino and Vick, 1987). A study of internal fabric of rock glaciers in the Sangre de Cristo Range of Colorado showed movement over a basal slip plane rather than via creep mechanisms (Giardino, 1979; Giardino and Vitek, 1985). Pressure from pore water trapped between frozen sediments may also contribute to basal shear movement (Giardino, 1979, 1983). The relationship between slippage and ground water in rock glaciers was also reported by Haeberli et al. (1979). Johnson (1981) noted the association of water and impervious planar beds in rock glacier movement in southwest Yukon Territory, Canada. Studies of rock glaciers on the high plateaus of Utah suggested that massive bedrock failure at rock glacier heads pointed to the significance

of basal shear in rock glacier formation (Shroder, 1973a). The importance of pore-water pressure in one rock glacier was suggested by century-spanning tree-ring analyses that indicated direct correlation between movement and periods of high summer precipitation (Shroder, 1978).

It is fundamental to understand that it is the change in pore-water pressure and volume resulting from state change from liquid water to ice that provide the driving forces for movement (Terzaghi and Peck, 1948). Water *can* provide an environment conducive for the growth of moss and algae, which create a slick surface. Thus, water flowing into the rock glacier can transport the moss and algae at depth, thus creating a slick surface which could facilitate sliding along an internal shear plane.

Rate of Movement

Movement velocities of selected rock glaciers are summarized in Table 2.2. Velocities of rock glaciers are orders of magnitude smaller than glacier advance rates. The main problem with directly measuring rock glacier advance is defining the exact position of the rock glacier front. Movement rates are typically monitored by establishing survey lines (e.g., Francou and Reynaud, 1992) or through photogrammetrical analysis (e.g., Gorbunov et al., 1992; Haeberli and Schmid, 1988; Kaeaeb et al., 1997). Both observation and creep theory suggest that the velocity distribution varies with depth according to a parabolic function, with the rock glacier surface moving faster than the base (Wahrhaftig and Cox 1959). A recent synopsis of research on the Murtèl-Corvatsch rock glacier (Haeberli et al., 1998) emphasized two points related to this velocity distribution: (1) the occurrence of an ice-saturated, thick stiff layer at the base of the deforming permafrost layer (supersaturated with ice); and (2) the causal relationship between heterogeneous ice content and subsequent deformation.

Slope, ice content, and thickness are the principal controls over the movement of an active rock glacier (Barsch, 1988). Sudden increases in inclination of the slope over which a rock glacier flows may result in relatively high flow velocities. Movement velocities of up to 5 m/yr have been measured for portions of the active rock glacier Obergurgl, near Innsbruck, Austria (Vietoris, 1972). Characterizing the overall advance

of rock glaciers, Haeberli (1985) pointed out that movement is faster at the surface than at positions within the body of the rock glacier. The rate of rock glacier advance, therefore, cannot be determined simply by measuring surface velocity. In general, if basal sliding is negligible and slope-parallel velocity varies linearly with depth, then the rate of advance of the rock glacier is approximately 50% of the surface speed.

Long-term studies of the Gorodetsky rock glacier showed that rock glacier advance averaged 0.9 m/yr between 1923 and 1946, 0.8 m/yr between 1946 and 1977, and dropped to 0.6 m/yr after 1980 (Gorbunov, 1983; Titkov, 1988; Gorbunov et al., 1992). Other long-term studies in the northern Tien Shan and Kazakhstan have also indicated variable movement rates for discrete rock glacier bodies (Gorbunov et al., 1992). A 25-year photogrammetric study of Gruben rock glacier indicated an average advance rate of 0.1 m/yr (Kaeaeb et al., 1997). This study also indicated a lowering of rock glacier surface elevation at a rate of 5 cm/yr.

Investigation Methods

Rock glacier researchers have used both direct and indirect methods in their investigations of rock glacier structure. Table 2.6 summarizes some of the more sophisticated of these techniques. Until recently, direct investigation methods included tunnels through rock glaciers (e.g., Brown, 1925), visual inspection of exposures, and shallow pits (e.g., Wahrhaftig and Cox, 1959; among others). Potter (1972) successfully used shovel and bulldozer excavations to investigate Galena Creek rock glacier. Giardino (1979) used bulldozer excavations to study the structure of rock glaciers in Mount Mestas, Colorado. However, these techniques can prove impractical for some localities where investigation is restricted by resources and accessibility. Large clast sizes and thick debris covers on rock glaciers challenge many investigations. White (1971) used explosives to blast a pit in Arapaho rock glacier. Coring methods must negotiate the difficult surface debris as well as interior heterogeneity. Mechanically operated drills have proven to be effective in penetrating both rock and ice by changing drill bits to meet encountered conditions (e.g., Haeberli et al. 1988; Table 2.6). Clark et

Table 2.6. Rock glacier investigation methods.

Technique	Suggested Application	Description	Limitations	References
Age-Dating Methods				
Lichenometry	Relative age dating of rock glaciers	•Uses concept that lichens increase in size with time •Must develop lichen growth curve for locality	•Must know age of substrate on which lichen occur •Affected by environmental factors such as snow kill and talus disintegration •Useful for age range: 2 to 3000 years	Nicholas and Butler (1996)
Schmidt Hammer		•Uses rebound value of hammer to infer relative age •Fast, simple technique	•Use cautiously, generally indicates fresh v. weathered materials •May not correlate with other age indicators for a given locality •Assumes rock hardness changes in a unidirectional manner •Affected by position relative to edges and surface roughness	
Weathering Rind Thickness		•Increased thickness for older materials •Usually see consistent trend within given study area	•Depending on age of rock glaciers, may not be useful	
Movement Surveys				
Surveying	Monitoring rates of movement	•Establish painted block survey lines transversely and longitudinally across rock glacier •Tie lines to bedrock •Survey points periodically	•Must mark large, deeply-implanted blocks on rock glaciers as monitoring points	Francou and Reynaud (1992)
Photogrammetry	Assessing long-term rates of movement	•Orthophotomaps of common scale produced from aerial photographs •Plan control extension via automated stereocomparator •Block-type analytical phototriangulation of compilation survey •Estimate movement via changes in coordinates of control points	•Photograph availability	Gorbunov et al. (1992) Clark et al. (1994)

Table 2.6 (Continued).

Technique	Suggested Application	Description	Limitations	References
Movement Surveys (Continued)				
Advanced Photogrammetry	Three-dimensional determination of surface displacement	•Aerophotogrammetric determination of digital terrain models (DTMs) using monotemporal stereo models •Monotemporal stereomodels composed of 2 or more overlapping photographs taken from different places •Computer-aided photogrammetric compilation system •Comparison of multitemporal DTMs having same grid (25 m squares)	•Photographic coverage •Time intensive •Error of 8 cm/yr •Accuracy of photogrammetry	Kaeaeb et al. (1997)
Direct Methods				
Hand-operated auger	Sampling in ice-cored rock glacier	•Light-weight auger recovered continuous core at 1-m intervals in clear ice to a depth of 9.5 m	•Coring began after clearing surface debris from ice surface •Volcanic source material for test locality readily breaks down to small clasts •Freezing of coring chips limited borehole depth to 9.5 m	Clark et al. (1996)
Mechanized drilling	Sampling permafrost interior rock glacier	•Surface debris to base of active layer cased off with 6-m casing emplaced with Odex system •Heavy hydraulic rotational core drill with triple core-tube system used to obtain samples •Hard metal bit used in ice and ice-rich zones; diamond crown bit used in ice-containing rock •Air cooling and core-tube systems used to minimize thermal disturbance and recover uncontaminated cores •Instrumentation installed through 0.84-m diameter plastic tubes grouted to bedrock; annular-seal of introduced water which froze	•Problems with unstable borehole walls increased with depth •Attempts to stabilize by injecting grout failed because of high permeability zones below permafrost layer •Recovered ice samples heavily broken as a result of stress release •Time intensive; coring effort spanned late April into early July; continuity of effort not known	Haeberli et al. (1988)

Table 2.6 (Continued).

Technique	Suggested Application	Description	Limitations	References
Indirect Methods				
Seismic Refraction	Investigating internal characteristics	•24-channel device, recording signal by vertically-spaced, one-component geophones with resonance frequency of 10 Hz. •Fast-burning explosive dynamite. •Interpret with intercept method and ray tracing	•Seismic velocity contrasts between layers cannot always be achieved because of layer thickness or rock type	Wagner (1996)
Gravimetry	Detecting presence of ground ice; estimating thickness of ice	•Conduct gravimeter surveys across rock glacier •Correct data for latitude, elevation, earth tide, topography of surrounding terrain •Model data to determine shape and density of body producing gravity anomaly	•Can require intense modeling effort to correct for surrounding topography and topography can limit resolution of gravity anomaly due to density variation of material (i.e., ice content) •Requires additional data to support data modeling efforts (e.g., γ-γ logs, refraction data, borehole logs) •Problems when ice content increases continuously along profile	Vonder Müehll and Klingelé (1994)
Geoelectrical/ DC Resistivity	Distinguishing between glacial ice and ice-cemented sediments	•Conduct soundings using asymmetrical Schlumberger or Hummel configuration •Verify results using same configuration at a different location on rock glacier or additional measurements at same site with another layout •Wagner (1996) used 3 current electrodes (iron stick and salt-water soaked sponges) and 2 potential electrodes (clay pots filled with copper sulfate) •Model soundings as 3 or 4 layers as outlined by Vonder Müehll (1993) •Begin with simple model efforts that illustrate fundamental character of subsurface conditions then develop more complex models	•Coarse surface of rock glacier may require salt-water soaked sponges to achieve ground contact •Lateral effects causing oversteepened sounding graphs result from soundings on long, narrow bodes •Minimum thickness of permafrost required for detection •Cannot distinguish between permafrost near freezing point and unfrozen ground •Several multi-layer models may produce same sounding graph	King et al. (1987); Wagner (1996)
Radio-Echo	Rough estimates of permafrost thickness; identify ice type	•Survey with USGS monopulse ice radar •Signal attenuation in frozen sediment is much higher than in glacier ice	•Unfrozen water causes absorption and scattering effects •Penetration depth limitations	King et al. (1987)

al. (1996) used a light-weight, hand-operated auger for studies of Galena Creek rock glacier (massive ice); the coarse outer layer had to be removed before augering. The tool was useful at this locality because the volcanic source rock breaks down into small clasts, making hand excavation of the debris feasible. During the summer of 1997, Giardino and Degenhardt were able to extract ice cores from the Yankee Boy rock glacier in the San Juan Mountains of Colorado.

Indirect methods of investigation include geophysical surveys, such as seismic refraction, gravimetry, resistivity, and radio-echo surveys. In contrast to the labor- and time-intensive direct methods, geophysical methods allow relatively rapid and inexpensive acquisition of three-dimensional data for the rock glacier. Seismic refraction and resistivity surveys are the most commonly applied geophysical techniques. According to Haeberli and Vonder Müehll (1996), surface layer seismic velocities, typically ranging from 300 to 1,000 m/s, contrast sharply with the top of ice-bearing layers. The refractor representing the top of frozen sediment roughly parallels the surface of the rock glacier and can be traced along its length. Ice-supersaturated frozen material has an average seismic velocity of 3,500 m/s and a seismic velocity range of 2,000 to 4,000 m/s (indicating degree of heterogeneity). Electrical resistivity of frozen sediments ranges from 1 to 10,000 kΩm and resistivity magnitude is related to ice content and type (Haeberli and Vonder Müehll, 1996). Ice at marginal permafrost conditions has low resistivity (5-500 kΩm); massive ice has much higher resistivity (1,000-2,000 kΩm). Recent gravimetry applications at the much studied Murtèl-Corvatsch rock glacier were successful, but required an intense modeling effort to correct for surrounding topography and utilized significant existing data to develop the model (Vonder Müehll and Klingelé, 1994). Few results from the use of geophysical methods have been tested by drilling or other methods to determine “ground truth,” and few results except the depth of the boundary between an unfrozen surface layer and frozen material below are unequivocal. General limitations of geophysical techniques often include complex modeling efforts that can produce non-unique models and that can require additional ground-truth data collection.

Geologic Hazards

Active movement and mass wasting are perhaps the most obvious geologic hazards affecting engineered works (Giardino and Vick, 1987). Shear stresses generated by differential movement of the coarse mantle surface and between the coarse mantle and underlying frozen layer generally preclude long-term engineered structures in contact with rock glaciers. Structures that contact or penetrate the rock glacier, or contact both the active rock glacier and stable ground, have the greatest potential for differential movement. Given that mass wasting is an inherent component in rock glacier formation and movement, simple proximity to a rock glacier is hazardous. Boulders from the surface of the coarse mantle have been observed to cascade down the toe and sides of rock glaciers. Boulders have been observed rolling from an active rock glacier in Alaska at a rate of one every other minute (Foster and Holmes, 1965). Giardino and Vick (1987) reported boulders rolling up to 26 m from an “inactive” rock glacier in Colorado and 81 m down valley from a rock glacier in the La Sal Mountains of Utah.

Aside from active movement, other deformation processes affecting both active and inactive rock glaciers include subsidence, induced creep, and surface layer compression. The potential for subsidence beneath structures completed on the landform remains high because: (1) melting ice can be initiated by even minor changes in thermal equilibrium; and (2) internal erosion of fines along preferential water pathways occurs seasonally. A rock glacier can be expected to experience predominantly lowering of the surface on the order of cm/yr in response to: sediment accumulation and removal; three-dimensional effects of extensional and compressional deformation; and freeze/thaw processes (Kaeaeb et al., 1997). Induced creep has been observed where cuts or excavations have been made into the rock glacier or where the thermal regime has been disturbed. Evaluation of a 1963 Colorado State Department of Highway excavation into the toe of a rock glacier resulted in surface creep as much as 100 m behind the cut during the next six years (Giardino et al., 1984). Surface compression, a short-term phenomenon related to the loose particle arrangement and high compressibility of the coarse mantle, could cause excessive foundation settlement during or after structural loading.

High pore water pressures building up within the rock glacier pose another geologic hazard (Giardino, 1983). Although unusual, “blowout” type failures resulting in a sudden release of water and debris could endanger structures. A climbing expedition in Afghanistan observed: “Gallons of stored water forced open the screes with a roar that echoed about the crags above. Boulder stones and mud hurtled into the air and avalanched downhill” (Scott and Cheverst, 1968; p. 29).

The growing number of mountain subdivisions constructed in alpine regions necessitates studies of potential hazards that are created as a result of the interaction of humans with geologic processes. These potential hazards must be recognized and mapped using standard mapping schemes that quickly and accurately integrate various engineering site characteristics. Fitzgerald and others (1988) used GIS to study hazard potential in a project site representing numerous mountain subdivisions and resort centers in the Sangre de Cristo mountains of Colorado. U.S. Geological Survey topographic maps (1:24000), geologic maps, aerial photographs, and field data for various geologic attributes of the site were digitized into the system. GIS was then used to produce maps of bearing strength, erosion rates, and permeability. These data allowed implementation of an engineering-based geological evaluation of the site. Potential hazards were identified prior to construction, resulting in a much higher degree of safety for the development.

Siting and Design Recommendations

Rock glaciers cause three primary types of damage to engineered works (Giardino and Vick, 1985):

(1) damage from gross active movement;
(2) damage from other deformation processes (see previous section); and
(3) damage from sloughing material.

The primary recommendation for negotiating the hazards associated with rock glaciers is *prudent siting and/or design measures*. In many cases, avoidance is the best approach!

General recommendations for building include:

(1) Select locations where clear ice layers do not directly underlie structures.
(2) Design structures to accommodate settlement and support characteristics of the loose outer mantle.
(3) Do not induce accelerated thawing by stripping or excavating of the coarse surface layer.
(4) Allow for periodic jacking and re-leveling of settlement- and alignment-sensitive structures.
(5) Avoid projects that require excavation to minimize potential for triggering thermal instability or inducing creep.

The impact of rock glaciers on structures and consequent design measures are a function of the structure type, acceptable risk, and failure consequences (Giardino and Vick, 1985). Light structures such as mine buildings, utility towers, ski lift towers, and communication towers have been built on rock glaciers (Haeberli and Keusen, 1983). Siting of transportation alignments across active rock glaciers requires continuous maintenance and realignment. For larger structures, few design measures can mitigate the effects of differential movement and settlement as well as other deformation processes on a structure. Differential settlement of the compressible outer mantle can be reduced by rigid mat-type foundations or pre-loading during construction (Giardino and Vick, 1985). Thaw-induced settlement can be mitigated using slab insulation, ventilation, or pile foundations and other geotechnical principles for development of foundations on permafrost (Andersland and Anderson, 1978).

The narrow valleys occupied by some rock glaciers are tempting sites for dam construction. The rock glacier landform is often misidentified as rockslide debris, thus the rock glacier hazard is unrecognized. Primary considerations for dam construction tied to rock glaciers are to (Giardino and Vick, 1985): ensure that the rock glacier is inactive through baseline field survey data; avoid clear ice and design to minimize thermal disturbance; select designs that are deformation-tolerant and control cracking such as earth or rockfill dams; and select well-graded, erosion-resistant core material.

Mining activities in alpine areas are frequently observed to intersect active and inactive rock glaciers. Shafts and tunnels in active rock glaciers experience substantial deformation. Griffiths (1976) attributed the collapse of an adit and raise in the Camp Bird Mine near Ouray, Colorado, to deformation-induced movement of an active rock glacier. Given the easily-disturbed metastable structure and thermal conditions of rock glaciers, the most prudent design is to locate portals and entries away from these features (Giardino and Vick, 1985). Where intersection is unavoidable, the shafts and tunnels must be designed to withstand considerable deformation and to accommodate the effects of thawing.

Rock Glaciers as Borrow Sources

Rock glaciers are tempting sources of borrow material in the alpine environment having limited alternative materials. However, once the coarse outer material is removed, the frozen till-like material in the rock glacier core is difficult and costly to rip or shoot. Simply allowing the finer material to thaw naturally is not feasible because of the 0.5 to 1 m/yr recession rate of the thawing front. In the time needed to thaw a given thickness, much of the fines may have migrated downward. The high costs and slow thaw rate of borrow materials from a rock glacier forced the Colorado State Highway Department to locate an alternative borrow source for construction of the La Veta Pass road in 1963 after encountering these conditions. Excavation of an active rock glacier to provide fill for the Grande Dixence dam in Switzerland also produced unsatisfactory results because of a slow thaw rate and shallow frozen layer (Fisch et al., 1977).

HYDROLOGY

Despite over 100 years of study beginning with Steepstrup (1883), the hydrologic significance of rock glaciers has only recently been realized (Corte, 1976a,b; Johnson, 1981; Evin, 1983, 1984; Haeberli, 1985; Gardner and Bajewsky, 1987; Bajewsky and Gardner, 1989; Vonder Müehll and Haeberli, 1990; Giardino et al., 1992; Schrott, 1996). The matrix of angular rocks, fine sediments, and ice comprise a “porous” medium that functions as an aquifer having recharge, discharge, through-flow characteristics, and

storage. The aquifer potential of these features is demonstrated by streams flowing from frontal slopes of many alpine rock glaciers (Giardino et al., 1992, among others). The hydrologic balance of a rock glacier includes inputs from direct precipitation, runoff from adjacent slopes, avalanche, and ground water and outputs via surface runoff, subsurface discharge, subsurface seepage, sublimation, evaporation, and ice storage (Giardino et al., 1992). Rock glaciers store significant volumes of water for extended periods of time (Fig. 2.11; Johnson, 1981; Haeberli, 1985; Gardner and Bajewsky, 1987; Bajewsky and Gardner, 1989; Giardino et al., 1992; Haeberli and Vonder Müehll, 1996; Schrott, 1996). Several researchers describe water in liquid and solid states in storage within and upon rock glacier surfaces (e.g., Potter, 1972; Corte, 1978; Barsch, 1977; Giardino, 1983; Giardino et al., 1992; Schrott, 1996; Elconin and Lachapelle, 1997). The net change in water storage within a rock glacier is a function of the microclimates that maintain periglacial conditions as well as the regional climate that drives the hydrologic cycle (Johnson, 1981), but because of the insulative debris mantle, those changes are usually slow. This point becomes very important when one considers changing water storage conditions in light of long-term climate change.

The hydrology of a rock glacier is highly complex given: various possible inputs and outputs; phase changes and movement of water associated with the active layer; irregular distribution of frozen matrix that allows convoluted pathways for water flow; and deep crevices into which water disappears, among other complicating factors. A model of water flow through rock glaciers (Fig. 2.12) was developed by Giardino and others (1992) based on suggestions in Haeberli (1985) and other observations of water movement relative to rock glaciers. This model considers water flow via near subsurface flow above the permafrost (suprapermafrost) and deep subsurface flow (subpermafrost). Initiation and maintenance of the two flow paths requires persistence of an impermeable (probably frozen) layer within the rock glacier. Giardino and others (1992) suggested that the rock glacier hydrologic cycle be viewed as a cascading system in order to define the manner in which water moves through the landform (Fig. 2.13). The cascading

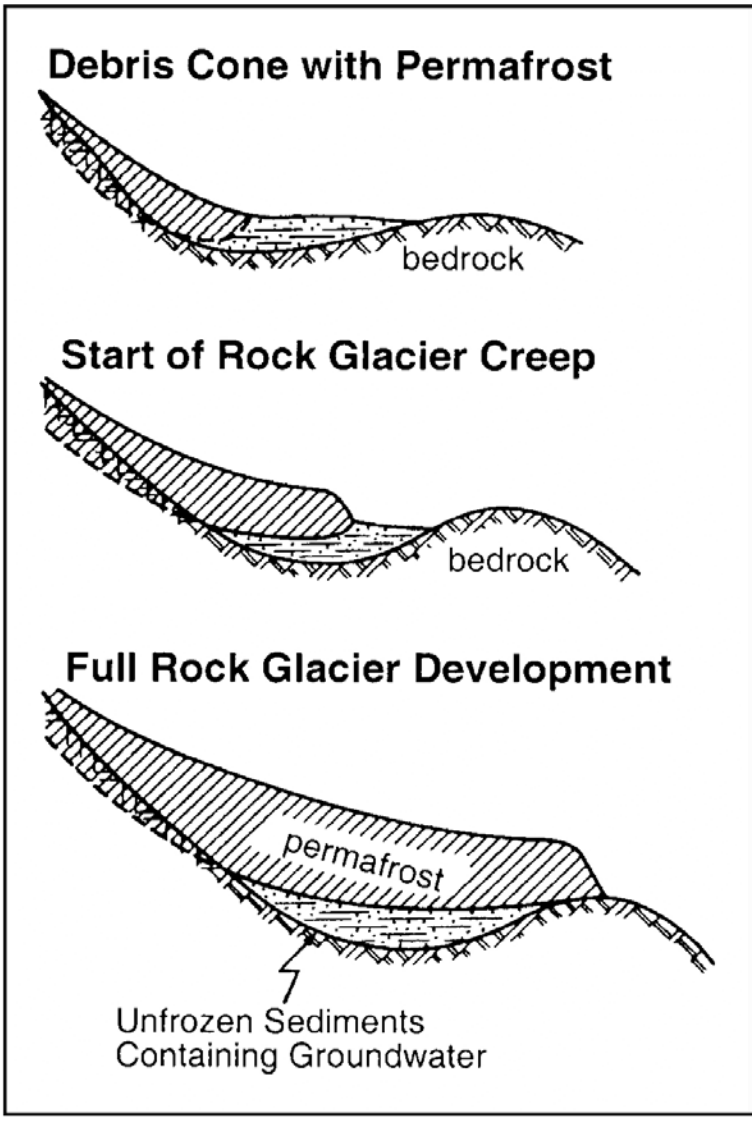

Fig. 2.11. Development of groundwater in sediments beneath a rock glacier (Haeberli, 1985).

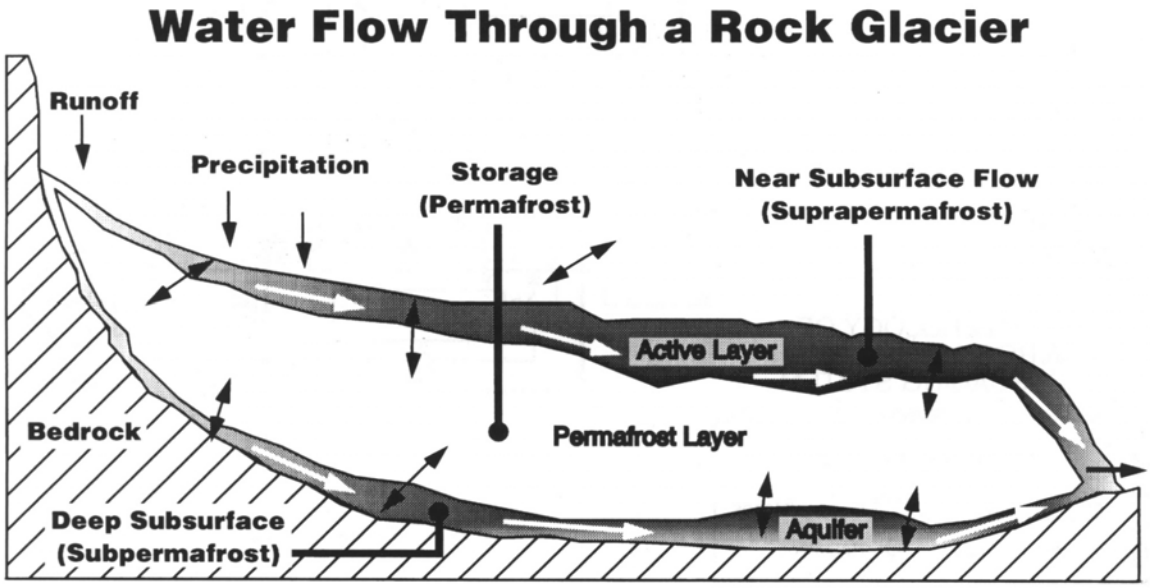

Fig. 2.12. A model of water flow through a rock glacier. Figure after Giardino et al. (1992) and Haeberli (1985).

system is comprised of four interrelated subsystems: cliff and talus; surface; subsurface; and ground water. The output from one subsystem provides input to another subsystem.

The amount of water and rate at which it moves through a rock glacier is a function of input, storage, output, and pathway. Johnson (1981) used dye tracers to demonstrate the rapid response of Grizzly Creek Rock Glacier to precipitation and melting events. Dye travel times through the rock glacier were on the order of 0.7-0.9 hours and 1.6-2.1 hours. This study observed that surface flow on the rock glacier usually dissipated after 12-15 hours of a precipitation event.

The hydrologic cycle of rock glaciers varies slowly with long-term climatic changes and more rapidly with seasonal fluctuations in ambient temperatures (Johnson, 1981). Seasonal characteristics of the hydrologic cycle include (Burger et al., 1997):

Late winter: Water within the active layer is frozen and discharge originates entirely from ground-water flow systems at the base of the glacier.

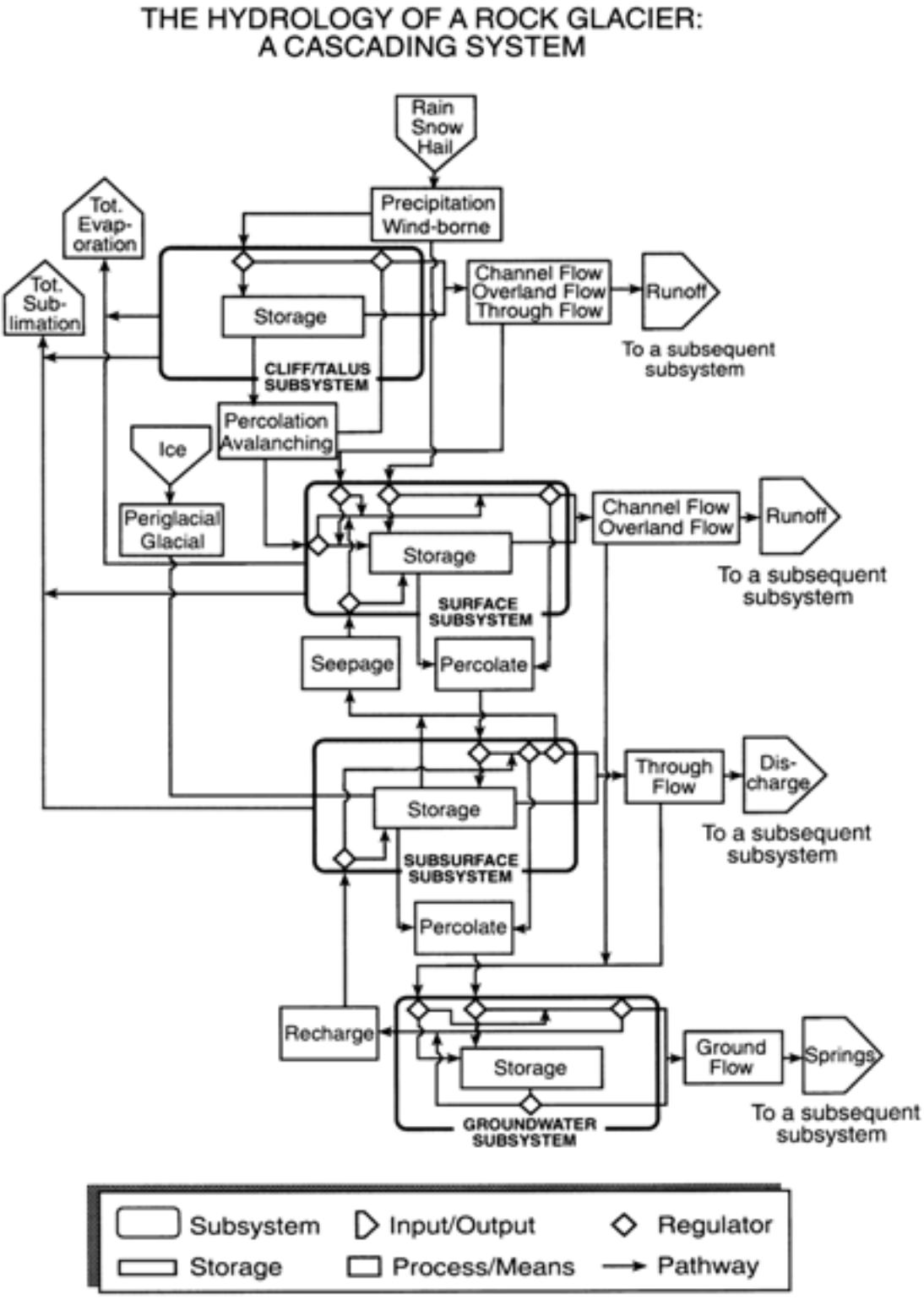

Fig. 2.13. Cascading system for a rock glacier hydrologic cycle (Giardino et al., 1992).

Late spring/early summer: The thawing front moves downward toward the top of the perennial permafrost; melting snow and ice recharges the upper portion of the glacier creating a seasonal aquifer perched on top of the frozen core.

Summer: Free water within the upper portion of the rock glacier has discharged and discharge again originates from the base of the rock glacier. Melt water from snow patches in depressions on the surface continues to melt through the summer.

Late summer/early fall: Falling temperatures create freezing fronts that move upward from the perennial permafrost and downward from the rock glacier surface, squeezing together the remaining water in the central portion of the active layer. Seasonal thunderstorms replenish free water in the active layer.

WATER DISCHARGE CHARACTERISTICS

Discharge from rock glaciers varies from a few liters per minute to several hundred liters per minute (Domaradzki, 1951; Schweizer, 1968; Jackson and MacDonald, 1980; Haeberli, 1985; Bajewsky and Gardner, 1989). Rock glacier discharge is generally more consistent than discharge from glaciers (Potter, 1972; Corte, 1987b). This discharge may originate from a single source or be a mixture of several sources. Possible sources include releases from the rock glacier itself, ground-water discharge at the toe of the rock glacier, precipitation events, and through-flowing glacier meltwaters upstream of the rock glacier (for example, Grizzly Creek Rock Glacier, Yukon Territory; Johnson, 1981). Relative contributions of these sources can often be distinguished through water isotopic signatures and chemistry. Blumstengel (1988) used $^{18}O_{water}$ and conductivity data to demonstrate a largely real-time meteoric source of discharge from the Slims River rock glacier. The analyses showed a link between thawing of the active layer, rainfall inputs, and discharge.

Relative to glacier-fed streams, discharge from rock glaciers generally contains lower suspended sediment load and higher total dissolved solids (TDS) (Johnson, 1981; Giardino et al., 1992). A water quality study of three rock glaciers in the Blanca Massif,

Colorado demonstrated low TDS (1.5 to 32 mg/L; Table 7) (Giardino et al., 1992) consistent with alpine stream concentrations measured by Vitek and others (1981) for the same study area. The highest TDS concentrations coincided with the rock glacier having the lowest volumetric discharge (California Rock Glacier); mineralogy and flow through a moraine were interpreted to be additional factors in the higher TDS. In contrast to input waters with pH ranging between 6.4 and 7.0, outflow from the rock glaciers had pH ranging between 7.3 and 8.4. The pH increase between influent and effluent reflects the incongruent dissolution of cation-rich silicate minerals during water contact with the rock glacier. Outflow from the rock glaciers was also more oxygenated as a result of turbulent flow through the rock glacier.

The ion concentrations determined by the Colorado study are generally lower than those measured by other studies (Table 2.7). For example, total hardness of Colorado rock glacier effluent (23 to 50 mg/L) is about 50% of the total hardness measured for Hilda Rock Glacier (Gardner and Bajewsky, 1987), 17% of the total hardness measured for rock glaciers in the Andes (Corte, 1978), and 11% of the total hardness measured for Grizzly Creek Rock Glacier (Johnson, 1981). These water quality differences are interpreted to reflect lithologic differences between study areas (Giardino et al., 1992). The Blanca Massif area is primarily composed of amphibolites, granite diorites, hornblende gneisses, and quartzites, accounting for the majority of ions detected (e.g., Ca^{2+}, Mg^{2+}, SiO_2, CO_3^{2-}). Other studies reporting water quality data from rock glaciers were conducted in areas of soft rock, such as limestones and sandstones, volcanic rocks, and areas influenced by discharge from glaciers (e.g., Johnson, 1981).

Thus, the low TDS and nearly constant discharge emanating from rock glaciers makes these landforms potential water supplies. Some rock glaciers are already contributing to municipal water supplies. The city of Boulder, Colorado obtains its water supply from a watershed containing the Arapaho rock glacier. Although most of the flow is maintained by meltwater from snowpack, water from the rock glacier appears to contribute a continuous low-volume input. Developments planning to use rock glaciers as their primary water source must consider the implications of climate change. Climatic

Table 2.7. Rock glacier water quality.

Location	Position on Rock Glacier	Distance from Cirque Wall (m)	T ℃	TDS Mg/L	pH	O_2 Mg/L	Conductivity Sc/m	SiO_2 mgL^{-1}	Alkalinity Mg/L $CaCO_3$	Total Hard. Mg/L $CaCO_3$	References
California Rock Glacier, Blanca Massif, Colorado	Influent	0	0.0	1.5	6.4	6.1	2.0	<0.1	1.3	0.0	Giardino et al. (1992)
	Effluent	1155	4.5	32.0	8.4	8.2	80.0	5.0	44.4	50.1	
Lost Lake Rock Glacier, Blanca Massif, Colorado	Influent	0	0.0	2.0	6.7	5.9	3.0	<0.1	2.0	0.0	
	Effluent	241	0.0	29.0	7.3	9.0	44.0	6.0	21.5	23.1	
Dutch Creek Rock Glacier, Blanca Massif, Colorado	Influent	0	0.0	3.7	6.9	6.6	5.7	<0.1	2.2	0.0	
	Effluent	1152	0.6	29.9	7.9	9.2	44.5	2.1	20.6	24.1	
Rock Glaciers in the Andes Mountains	Effluent									204 - 208	Corte (1978)
Grizzly Creek Rock Glacier, Yukon Territory	Effluent				6.5 -6.8		171 -164			~320	Johnson (1981)
Slims Creek Rock Glacier, Yukon Territory	Effluent				~8.0		650 - 1050				Blumstengel (1988)
Hilda Rock Glacier, Canadian Rocky Mountains	Effluent									60 - 80	Gardner and Bajewsky (1987)

warming will deplete the rock glacier ice and thus the rock glacier recharge. Continued climatic change will cause rock glacier-fed streams to dry up. During this process, the hydrographs of these streams will progress from a relatively constant discharge to a higher discharge of short duration associated with spring melt.

CLOSING REMARKS

Human development in the alpine environment has occurred because of an understanding of geomorphology and creative engineering. Rock glaciers, which are distinctive landforms occurring in alpine environments, provide locations for urban water sources, construction borrow sources, drill sites, shaft and tunnel portals, ski tower supports, and dam abutments. The growing number of mountain subdivisions constructed in alpine regions necessitates an understanding of potential hazards that are created because of the interplay between humans and rock glaciers and the geologic processes associated with their formation and movement.

Rock glaciers are dynamic landforms. Unfortunately, many engineers and engineering geologists regard them as static forms. To address this serious lack of knowledge and understanding of the important role rock glaciers play in alpine environments, this paper attempts to provide a discussion of the formation and dynamic aspects. In addition, a discussion and guidelines for engineering and geomorphic evaluation and use of rock glaciers have been developed. The coupling of this approach with the development of practical tables should help engineers and engineering geologists to deal competently with rock glaciers.

The most significant issue associated with rock glaciers is lack of recognition. No rational human development that will be built on or adjacent to a rock glacier can proceed without geologists and engineers being aware of and understanding the formation and dynamics of this feature. The unique morphology of rock glaciers makes them easy to identify. However, identification is only the first step. It is important thatthe current status (i.e., active or inactive) of the rock glacier be determined. This important step will determine engineering approaches that can be employed. Placing structures on,

in, or adjacent to rock glaciers requires an appreciation and understanding of the temporal stability of these forms. From an engineering perspective, the internal structure of a rock glacier is significant because it provides important evidence on how the rock glacier deforms as well as how the rock glacier settles during periods of melting.

Rock glaciers cause three primary types of damage to engineered works: damage from gross active movement; damage from other deformational processes; and damage from settlement and sloughing. Although we have worked with engineers in the siting of ski towers on rock glaciers, the placement of these features has required extensive engineering at a considerable cost. Even the most slow-moving active rock glacier will damage or destroy structures built directly on or through it. When inactive rock glaciers are considered, the consequences of structural failure and the availability of alternative sites are the primary considerations. Although we address the potential problems that must be considered and overcome to build on a rock glacier, the bottom line to this paper is: *rock glaciers must be avoided for essentially all structures*.

Rock glaciers play a significant role in the alpine debris transport system. Active movement and mass wasting are perhaps the most obvious geologic hazards affecting engineered works. Rock glaciers represent a component of the continuous landscape, grading into and out of other landforms. From a continuum perspective, rock glaciers are temporary transitional forms from glacial or periglacial processes to current processes.

In addition to their role as debris transport phenomena, rock glaciers also serve as sources of stream flow. As alpine aquifers they have limited spatial extent, however, the structure of the rock glacier is conducive to the production of a steady, continuous supply of meltwater during the summer months. This structure provides an insulating layer of debris over an ice matrix or ice core. The interior ice body is generally of sufficient mass and slower to melt than ice and snow that accumulates in adjacent talus slopes. Thus, the hydrology of rock glaciers is highly complex as the result of various inputs and outputs, phase changes and movement of water. An important consideration is the fact that the hydrologic cycle of rock glaciers is influenced slowly by long-term climate change. The engineer who would consider rock glaciers as potential aquifer

sources is cautioned to consider carefully the long-term impact of climate change on the temporal nature of the rock glacier. And, because rock glaciers serve as sources of potable water for human consumption through stream flow and as aquifers, water quality characteristics are of fundamental importance. From the rock glaciers that have been monitored for water quality characteristics, it appears that they provide quality potable water.

This paper provides a foundation for appreciation and understanding of rock glaciers from an engineering geomorphologic point of view. The approach taken in this paper provides practical, important information in tabular form to aid the engineer and engineering geologist in prudent evaluations of rock glaciers as potential sites for human development and uses.

CHAPTER III

GPR SURVEY OF A LOBATE ROCK GLACIER IN YANKEE BOY BASIN, CO, USA

OVERVIEW

The internal structure of a lobate rock glacier located in the San Juan Mountains of southwest Colorado was investigated using ground penetrating radar (GPR). A 440 m longitudinal profile (f = 25 MHz) oriented along the central axis of the rock glacier shows continuous to discontinuous reflection horizons or layers that can be recognized clearly down to 30-35 m depth. The layers are interpreted to represent ice-supersaturated sediments and coarse blocky rockslide debris. Profiles collected at f = 50 MHz indicate that in the upper 20 m of the rock glacier many of these layers are laterally continuous. The total depth of penetration (~40 m at f = 25 MHz) was sufficient to identify the rock glacier-cirque floor interface and up to 5 meters of underlying moraine. Several prominent reflection events, which subdivide the profile into broad layers 10-15 m thick, represent contacts between major depositional units. We interpret this rock glacier to be a composite feature that formed by a process involving the development and overlap of discrete flow lobes that have overridden older glacial moraine and protalus rampart materials. The latter materials have been incorporated into the present flow structure of the rock glacier.

INTRODUCTION

Rock glaciers are lobate or tongue-shaped landforms composed of mixtures of poorly sorted angular, blocky rock debris and ice. Although they are located in cirques and valleys of many mountain ranges throughout the world, rock glaciers remain poorly understood constituents of alpine debris systems. Active (flowing) rock glaciers transport the surplus debris from talus slopes and glaciers down valley or down slope to

other debris systems. Barsch (1977) and Giardino (1979) addressed the role of rock glaciers in terms of debris systems and found that rock glaciers account for approximately 60% of all mass transport in alpine environments where they occur. As such, they are of great importance to the geomorphic periglacial transport systems in high mountains. For example, 40-60% of the debris being transported in the Sangre de Cristo Mountains of Colorado can currently be described as rock glaciers (Giardino et al., 1987). Barsch et al. (1979) estimated that 15-20% of periglacial mass transport in the Swiss Alps is incorporated in active rock glaciers. Thus, rock glaciers constitute an important component of a cascading system in which stream water, groundwater and rock materials move from mountain headwalls and talus slopes to environments downvalley (Giardino and Vitek, 1988b).

SIGNIFICANCE AND OCCURRENCE OF ROCK GLACIERS

Within the alpine environment, rock glaciers are the visible expression of mountain permafrost, making them principal geoecological indicators within alpine geosystems. As stores for ice and permafrost, they are valuable surrogates for information on past atmospheric and water compositions (i.e. dissolved solids, heavy metals, pollutants, and oxygen isotope ratios) and are useful for monitoring global change (i.e. predicted global warming) (Steig et al., 1998). Rock glaciers occupy the heads of many of the watersheds that supply communities with water throughout western North America and other parts of the world. They act as long-term (centuries to millennia) reservoirs for water, releasing a steady flow over the course of a year. Rock glaciers are also being considered from a planetary perspective. Similar morphological features have been discovered on Mars (Squyres, 1978; Lucchitta, 1993; Degenhardt and Giardino, 1999b) and Callisto, one of the moons of Jupiter (Chuang et al., 1999). Based on their morphologic similarity to rock glaciers, these landforms have been postulated to contain significant volumes of frozen water.

Although distinctive and widely distributed, the occurrence and significance of rock glaciers often goes unnoticed. They generally occur in dry, continental areas rather than

humid regions, perhaps because thin to absent snow cover favors their persistence (Humlum, 1997). Ages of rock glaciers range from incipient rock glaciers on Pico de Orizaba volcano (Palacios and Vazquezselem, 1996) to 500-year old forms associated with the Little Ice Age (Humlum, 1996), and features several thousand years old (e.g., Kaeaeb et al., 1997; Calkin et al., 1998). Relict rock glaciers that formed at the end of the last Ice Age about 10,000 years ago have also been documented (Sandeman and Ballantyne, 1996; Humlum, 1998). The occurrence of past or present glaciers is not necessarily a prelude to the formation of rock glaciers because these landforms exist in both glacial and non-glacial areas.

FORMATION OF ROCK GLACIERS

Rock glaciers are a physical response to three types of geomorphic processes: (1) glacial, (2) periglacial (Items 1 and 2 as diagrammed by Johnson, 1984, fig. 5), and (3) talus (as illustrated by Shakesby et al., 1987). The pioneering work of Wahrhaftig and Cox (1959) suggested that rock glaciers formed by permafrost processes to create a frozen mixture of rock debris and ice within talus or moraine materials. These findings have been affirmed and expanded by subsequent studies (see Haeberli, 1985; Barsch, 1996) with the advent of new technology and the global interest in recognizing and studying rock glaciers. A few studies also provide evidence of thick massive ice in the rock glacier interior and suggest that some forms are actually debris-covered glaciers (e.g., Potter, 1972; Clark et al., 1994).

Rock glacier formation begins with accumulation of ice in the upper reaches of the rock glacier. The ice flows downslope, where it ablates slowly within or beneath the debris of the rock glacier. General requirements for the formation of rock glaciers have been reviewed by Corte (1987). Rock glaciers are generally situated at the base of massive, homogeneous and fractured cliffs and are rarely found where debris is finely crushed or where headwall fractures are excessively large (Wahrhaftig and Cox, 1959; Evin, 1987).

Although the morphology of rock glaciers and other lobate landforms with surficial ridges and furrows is well documented (Giardino et al., 1987), it is also necessary to understand the flow dynamics responsible for generating these characteristic features. Information about the internal composition and fabric of a rock glacier is required to understand the flow dynamics (Potter et al., 1998), but the difficulty and costs associated with direct observation of the internal characteristics make acquisition of these data problematic. For example, direct rheological measurements (i.e., flow direction, flow velocity, and stress fields) are time dependent and lengthy because the flow of rock glaciers ranges from millimeters to decimeters per year.

Without detailed internal evidence of stresses and strain rates, temperatures, ice-rock mixtures, and bedrock characteristics, discussion of the process or processes that form rock glaciers is premature. On this basis, the study of rock glaciers has evolved toward the development of field methods for characterizing ice/debris ratios and rheological models. Current understanding of the movement of a rock glacier, outlined in the work of Haeberli (1985) and Barsch (1996), is based on models of creep flow adopted from studies of glaciers and limited physical data from rock glaciers around the world (e.g., Burger et al., 1999; Konrad and Humphrey, 2000).

The movement of rock glaciers has been related to many topographic, lithologic and climatic variables. Equations for mass transport in confined valleys, locations where rock glaciers commonly form, suggest that the thickness of a rock glacier should increase downslope. Kinematic wave theory (Gerber and Scheidegger, 1979) dictates that the geometry of valley and cirque walls control mass transport resulting from gravity. Ridge and furrow structures, therefore, represent 'buckling' of the material to compensate for decreased velocity of flow downvalley with a corresponding increase in force provided by faster flowing material upvalley (Fink, 1980).

GEOLOGIC SETTING

Yankee Boy Basin, located in the San Juan Mountains of southwest Colorado, was chosen as the study site because of the abundance of rock glaciers having ridges and

furrows (Fig. 3.1). The site is in close proximity to a variety of rock glacier types (Figs. 3.2a and 3.2b) that include lobate, valley side, and tongue-shaped morphologies

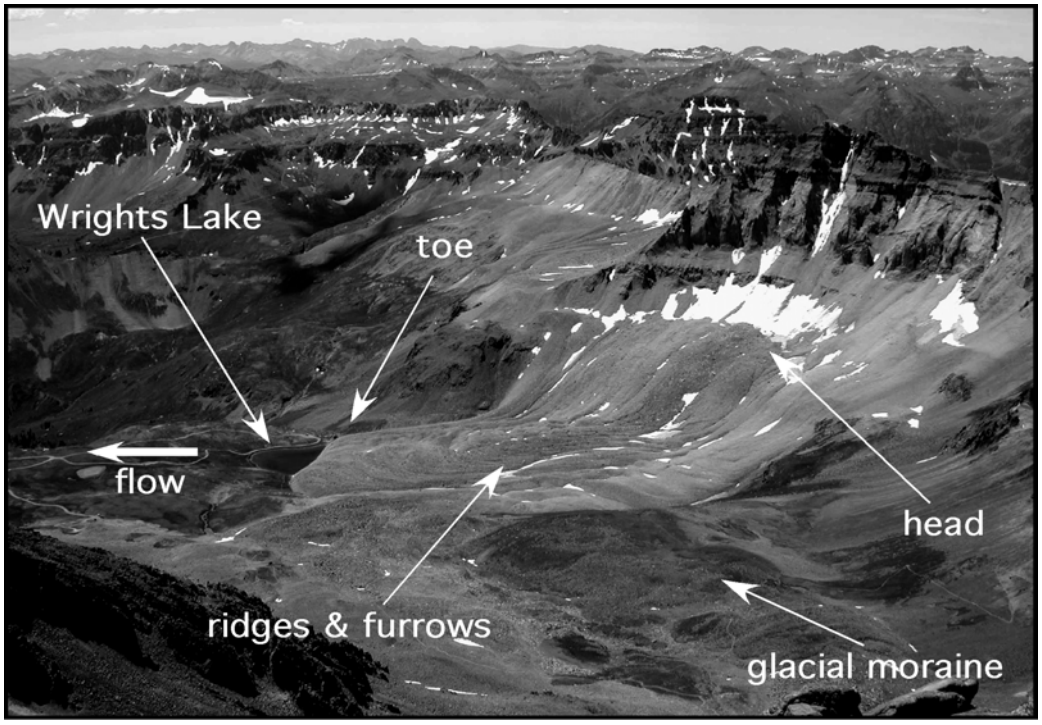

Fig. 3.1. Yankee Boy Basin rock glacier. The basin is located in the San Juan Mountains of southwest Colorado. Photo was taken from atop nearby Mount Sneffels, a 4,328 m (14,200 ft) peak. The rock glacier is approximately 500 m (1,640 ft) long from the snowline to the toe at Wright's Lake, and 300 m (984 ft) wide at the middle.

(Wahrhaftig and Cox, 1959; Burger et al., 1999). Exposed rocks in Yankee Boy Basin are almost exclusively comprised of Tertiary volcanics, which are underlain by a block of Precambrian quartzite (Luedke and Burbank, 1976). Mountain peaks that flank the basin are composed of San Juan volcanics, including Gilpin Peak tephra deposits, the Picayune Formation and the San Juan Formation. The Picayune Formation consists of a series of flows, breccias and tephra layers of intermediate composition and the San Juan Formation is mainly bedded tephra deposits of felsic composition. In the area of Mt. Sneffels, and along the northern edge of the basin, the mountains also include cores composed of older granodiorite and gabbro stock containing Precambrian quartzite

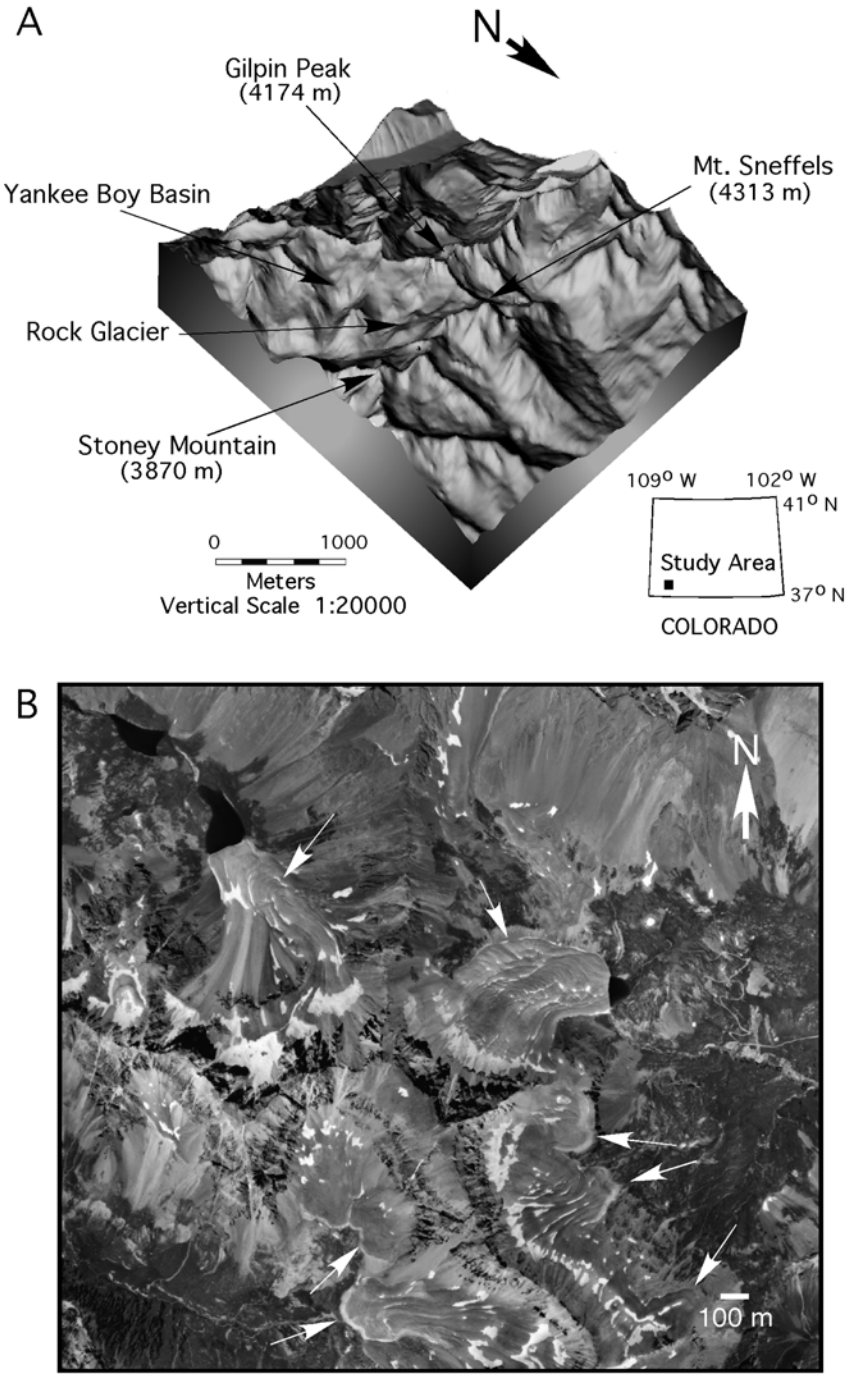

Fig. 3.2. Geographic location of the Yankee Boy Basin study site. (a) Hillslope shaded relief map illustrating the mountainous setting within the San Juan Mountain Range of southwest Colorado. (b) United States Department of Agriculture (USDA) 1:20,000 scale vertical aerial photo of Yankee Boy rock glacier and surrounding area taken in 1965. White arrows point to lobate, tongue-shaped, and valley side rock glaciers in the vicinity of Yankee Boy rock glacier (center and right).

inclusions. Quaternary deposits consisting mainly of the San Juan Formation cover most of the basin floor with limited exposure of the granodiorite and gabbro stock. The easily eroded bedrock supplies the parent material for deposits such as rock glaciers, alluvium, glacial drift, and landslide deposits. Holocene talus deposits cover much of the valley walls and rock glaciers typically occupy cirques and cirque valleys.

APPLICATION OF GROUND PENETRATING RADAR (GPR)

To fully understand the movement and deformation patterns within the interior of a rock glacier, a fundamental (i.e., generic) description of development is required. In this study, ground penetrating radar (GPR) is being used to "look" inside a lobate rock glacier and identify its internal structure. GPR offers the sophistication of other geophysical techniques combined with portability and ease of use. It is ideally suited to applications in alpine regions, where logistics and access are generally prohibitive. This study is being conducted in an effort to understand the formation history of a lobate rock glacier (see Fig. 3.1) by identifying its internal structure and determining the origin of ridges and furrows, a characteristic feature of rock glaciers. To date, GPR has been used on only three rock glaciers (Isaksen et al., 2000; Berthling et al., 2000; Degenhardt et al., 2000).

Theoretical Background

Digital GPR profiles are generated using transient reflections of electromagnetic energy (EM) in the frequency range of 10-1000 MHz. The profiles, which are similar in appearance to standard seismic profiles (Annan and Davis, 1976), represent that portion of the transmitted EM that is reflected back to the ground surface as a result of changes in bulk electrical properties of the underlying materials (Smith and Jol, 1997). Such changes in electrical properties can be attributed to sedimentological variation (i.e., changing grain size), facies changes, differences in state of materials (i.e., water-rock or water-ice contacts), mineralogy, and density. These factors are closely linked to the water content of a material, which plays a crucial role in GPR reflections.

The Yankee Boy rock glacier contains flowing water beneath the surface and may also contain 'free' water within pore spaces or cavities. In terms of propagating radar waves, water has a direct affect on the capacity of a transmitting material to store electrical potential energy under the influence of an electric field (dielectric constant or capacitance). Since relative permittivity is high for water (81) relative to that of dry rock (< 9), even a small amount of water may increase the bulk permittivity of the rock (Reynolds, 1997).

Porosity (ϕ) must also be considered with regard to the proportions of constituents present and their respective dielectric constants. The relationship between bulk relative permittivity (ε_r) and ϕ for an external field applied perpendicular to bedding is:

$$\varepsilon_r = \varepsilon_m \varepsilon_w \Big/ \left[(1-\phi)\varepsilon_m + \phi \varepsilon_w \right] \tag{3.1}$$

Where ε_m and ε_w are the permittivities for the rock matrix and pore fluid water, respectively (Reynolds, 1997). Thus, the average radiowave velocity through rock glacier medium will be the weighted affect of the contributions from rock, granular materials, ice and water - each having significantly different propagating properties. For example, the radar velocity through fresh water is 0.033 m/ns whereas it is 0.12 m/ns through a low-porosity sandstone (McCann et al., 1988). Given this range of water-dependent velocity values, accurate analysis and interpretation of the GPR data requires that special attention be given to all of the above factors.

Equipment and Methodology

GPR data was collected at frequencies of 25 MHz and 50 MHz using a PulseEKKO™ 100A system from Sensors & Software, Inc. (Mississauga, Canada). The system was configured in perpendicular broadside reflection mode using constant source-receiver offsets. A step interval of 1 m (4 m antennae spacing) was used for the 25 MHz (center frequency) configuration, and a step interval of 0.5 m (2 m antennae spacing) was used for the 50 MHz configuration. Each collected section was edited for

noisy/corrupt traces and adjusted to time zero. On all profiles, the horizontal scale is distance in meters (m), and the vertical scale is presented as two way travel time (twt) in nanoseconds (ns) and depth in meters. Data were acquired using a 1000 V transmitter and stacked 64 times with a time sampling rate of 800 ps. The profiles were processed and plotted in standard gray-scale and wiggle-trace formats using PulseEKKO™ software. The two earliest continuous reflections in all profiles represent air-wave and ground-wave arrivals, respectively.

The locations of the GPR transects were chosen for the purpose of identifying gross internal features and to determine if links can be established between the internal structure and surface morphology. The data were collected over two summers on a section of the rock glacier where ridges and furrows are prominent (Fig. 3.3). Two 50 MHz surveys were made in July 2000 and a single 25 MHz survey was made in July 2001. The 25 MHz survey consists of a 440 m longitudinal transect line (A-A') that begins in the middle of the head area of the rock glacier and terminates at the crest of the toe. It trends in a northeast direction and is oriented approximately normal to a series of arcuate transverse ridges and furrows that extend down the central portion of the rock glacier. A bend was made at 255 meters to a more easterly direction so that the transect line would remain approximately normal to the ridges and furrows, and so that a greater profile length could be attained.

The two 50 MHz surveys were conducted along the same series of ridges and furrows as A-A’. One of these surveys was made along an 86 m linear transect (B-B') that trends to the northeast (~N45°E) and crosses A-A’ at a distance of 238 m. Transect B-B’ was offset rotationally from A-A’, so that its orientation would be perpendicular to the strike axes of ridges and furrows on that part of the rock glacier. The other transect, C-C’, follows 75 m along the top of a prominent ridge in the series. It trends in a general east-west direction and curves toward the southeast at its end. C-C’ intersects B-B’ at 38 m and provides a perspective that is normal to the ridge axis.

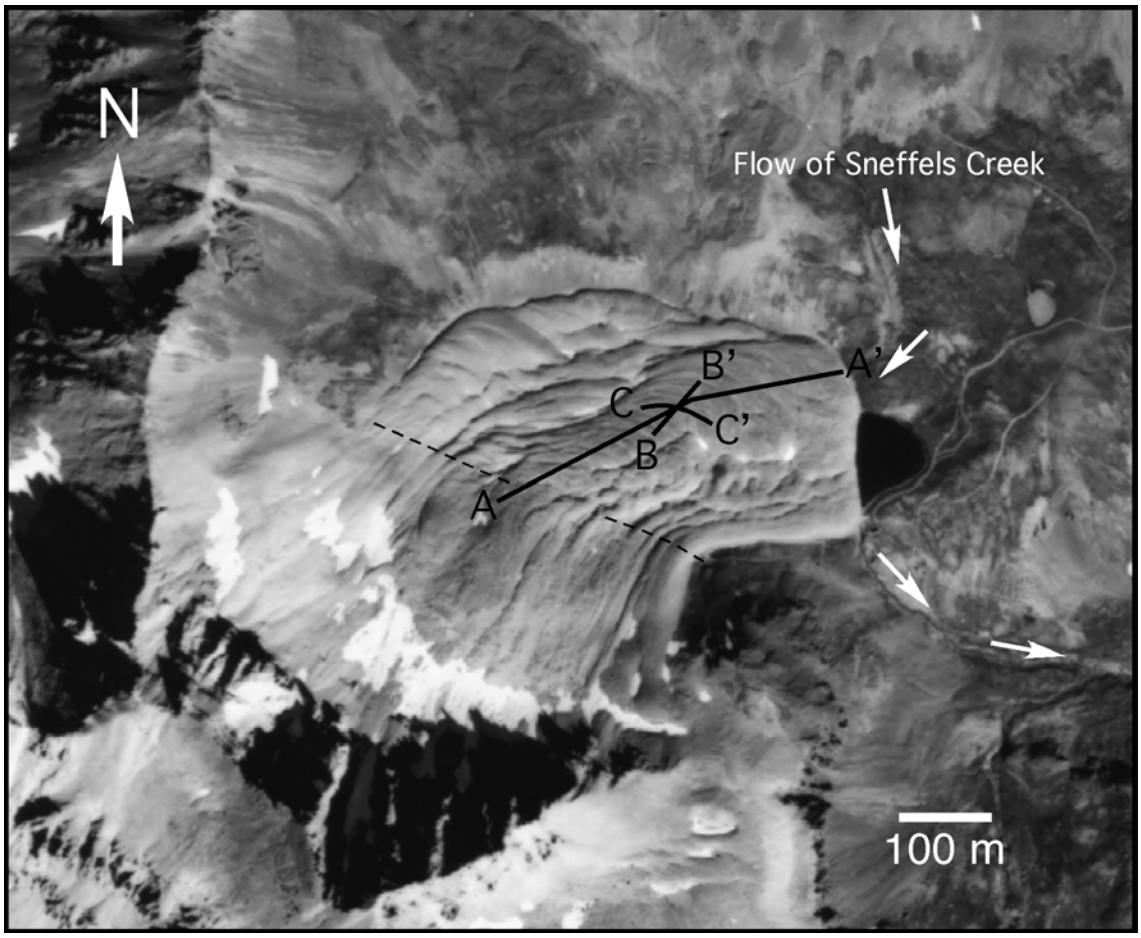

Fig. 3.3. United States Department of Agriculture (USDA) 1:20,000 scale vertical aerial photo of Yankee Boy rock glacier taken in 1979. GPR transects are indicated by solid lines. The Common mid point (CMP) survey was performed along the west end of C-C'. The dashed line indicates the inflection where slope of the rock glacier decreases sharply. Position of the line is based on topographic surveys of the rock glacier. Below the inflection line (head), the direction of rock glacier flow is toward the northeast. Above the inflection line (downvalley) the flow is to the east.

Data Processing

All processing was completed using Win_EKKO™ Pro version 1.0, a Windows®-based software package that accompanies the PulseEKKO™ GPR system. The raw reflection data were first corrected using a time filter for signal saturation (dewow). An automatic gain control (AGC) gain was applied to the dewowed data using a manual gain limit of GMAX = 500 followed by spatial low pass filtering at 20% cutoff. The 25 MHz section was migrated at a velocity of 0.15 m/ns using synthetic aperture image reconstruction (2D Kirchhoff method) and the 50 MHz sections were left unmigrated. Finally, topographic corrections were applied to the profiles using laser surveyed elevation data collected along the GPR transect lines.

RESULTS

Media Characteristics

The Common mid point (CMP) method was used to determine an average radarwave velocity value for the rock glacier medium. Two CMP surveys were conducted, one during the July 2000 field season (f = 50 MHz), and the other during the July 2001 season (f = 25 MHz). Both surveys (Fig. 3.4, top and bottom) were collected along the west portion of transect C-C' under similar weather conditions. This location was chosen because the topography along the ridge crest is relatively flat and because several strong sub-horizontal reflectors were detected within 200 ns (f = 50 MHz) of the rock glacier surface.

Two semblance analyses, performed using the Win_EKKO™ CMP Analysis Program, each yielded a best-fit velocity value of 0.12 m/ns. The solutions, which centered upon reflections at 15 ns and 70 ns in the 50 MHz and 25 MHz profiles, respectively, were based on CMP velocity values that were wide-ranging. For example, The 25 MHz velocities range from approximately 0.24 m/ns at the near surface to 0.09 m/ns at depth. The high near-surface velocities are the result of surface irregularities encountered as the antennae were moved along the boulders and large blocky clasts that

comprise the surface of the rock glacier. In addition to the gaps between the flat antennae and the rock

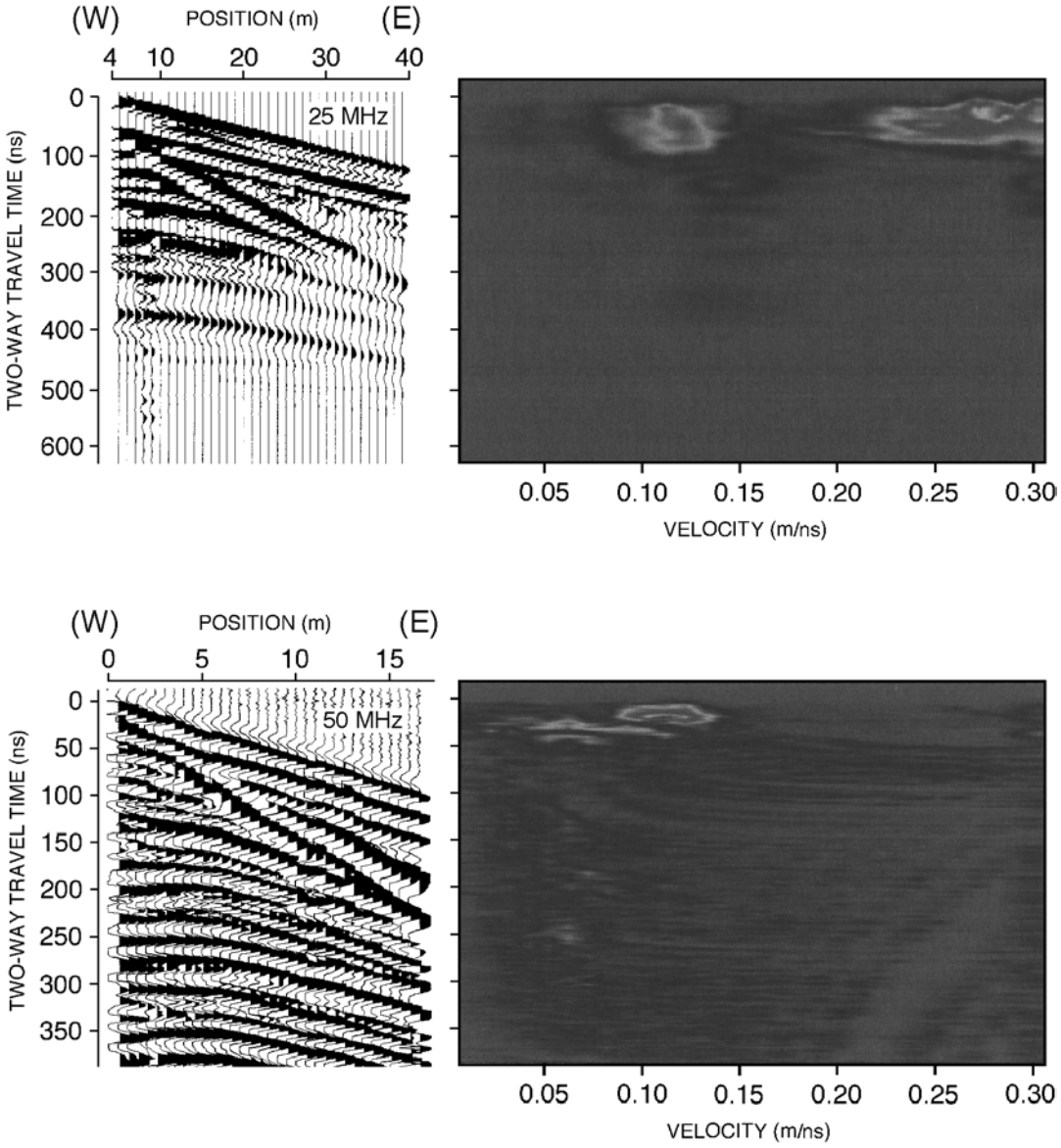

Fig. 3.4. Common mid point (CMP) surveys. Data collected at 25 MHz (top) and 50 MHz (bottom). Accompanying semblance analysis diagrams are shown to the right. A best-fit velocity value of 0.12 m/ns, obtained in both semblance solutions, was used for the average velocity of the rock glacier medium.

glacier surface, the active layer (upper 3 m) of the rock glacier also contains a significant amount of air-filled void space (i.e., cavities) which speeds up radarwave propagation. This phenomenon is apparent in the 25 MHz semblance diagram (Fig. 3.4, top), where values in the high amplitude field above 50 ns approach 0.33 m/ns (air-wave velocity). The low velocity value for the reflection located at 40 ns in the 50 MHz CMP profile (0.07 m/ns) equates to $\varepsilon_r \cong 18$, which is consistent with the relative permittivity of wet to saturated coarse-grained sands and gravels (Reynolds, 1997).

The semblance-derived velocity of 0.12 m/ns, used for the average value of the rock glacier medium, equates to an approximate relative permittivity (ε_r) of 6. This falls within the range of ε_r values for permafrost (Daniels and Roberts, 1994; Reynolds, 1997). The average velocity is slightly lower than values for rock glaciers located in continuous permafrost regions (e.g., Berthlig et al., 2000; Isaksen et al., 2000), which is consistent for a water-bearing permafrost rock glacier located in a temperate alpine region.

Resolution and Penetration

The theoretical vertical resolution of the radar signals was determined using the equation (e.g., Reynolds, 1997):

$$\lambda/4 = (V/F)/4 \qquad (3.2)$$

Where λ is the wavelength (m), V is the radarwave velocity of the medium (m/ns), and F is the centre frequency of the antenna (MHz). At 25 MHz, the calculated vertical resolution is 1.2 m. Therefore any layers visible on the 25 MHz radar profiles therefore have a thickness of greater than 1 m. The detectable limit of the radar achieved at this frequency was approximately 330 ns (~40 m). The 50 MHz antennae provided a maximum depth of penetration to 500 ns (~26 m) and resolution of at least 3/4 of a meter, given a calculated theoretical vertical resolution of 0.60 m.

The 25 MHz GPR Profile Section

The unmigrated 440 m longitudinal GPR profile (A-A') shown in the top of Fig. 3.5, effectively depicts the topographic characteristics along the center portion of the rock glacier. The steep sloping surface at the beginning of the profile marks the accumulation zone at the head of the rock glacier. Ridges and furrows, which begin at the 35 m position, are represented by undulations along the top of the section. Elevations range from 3800 m at the beginning of the profile (rock glacier head) to 3735 m at the end (beginning of the over-steepened toe) and ridge and furrow relief is from 1-5 m.

Gross structural features are defined by numerous reflections of variable coherence that are recognizable down to ~800 ns (45 m). A strongly coherent reflection along the bottom of the profile (~750 ns) represents the contact between the rock glacier and the cirque floor. It defines the complete cross-sectional shape of the rock glacier. Thickness ranges from ~15 m at the head of the rock glacier to a maximum of ~40 m at the middle and decreases to a thickness of ~18 m at the toe. The shape of this reflector is consistent with the 'scooped' contour of a glacially- scoured cirque. Along the profile, and down the flowline of the rock glacier, there is a transition in the dip of the reflection horizons. In the first 50 m, the reflection horizons slant downward, parallel to the surface. Further along the profile, from 50-125 m, the reflection horizons trend upward toward the surface at ~45° and display undulated patterns similar to that exhibited at the top of the profile (e.g., ridge and furrow topography). From 125-230 m the reflections parallel the surface and again trend upward toward the surface further down profile.

Migration revealed six moderately strong coherent reflection horizons throughout the profile, ranging in length from 75-400 m. The horizons are sub-parallel to the surface and to each other, and converge toward the beginning of the profile. In general, the reflections are approximately horizontal beyond 100 m, making them sub-parallel with the top surface of the profile. The orientations of less coherent reflections parallel these major horizons, and non-coherent reflections and diffraction events occur in the upper 5 m of the profile. Diffraction events are more prevalent throughout the section from 50-125 m. It should be noted that although migration enhanced the moderately to strongly

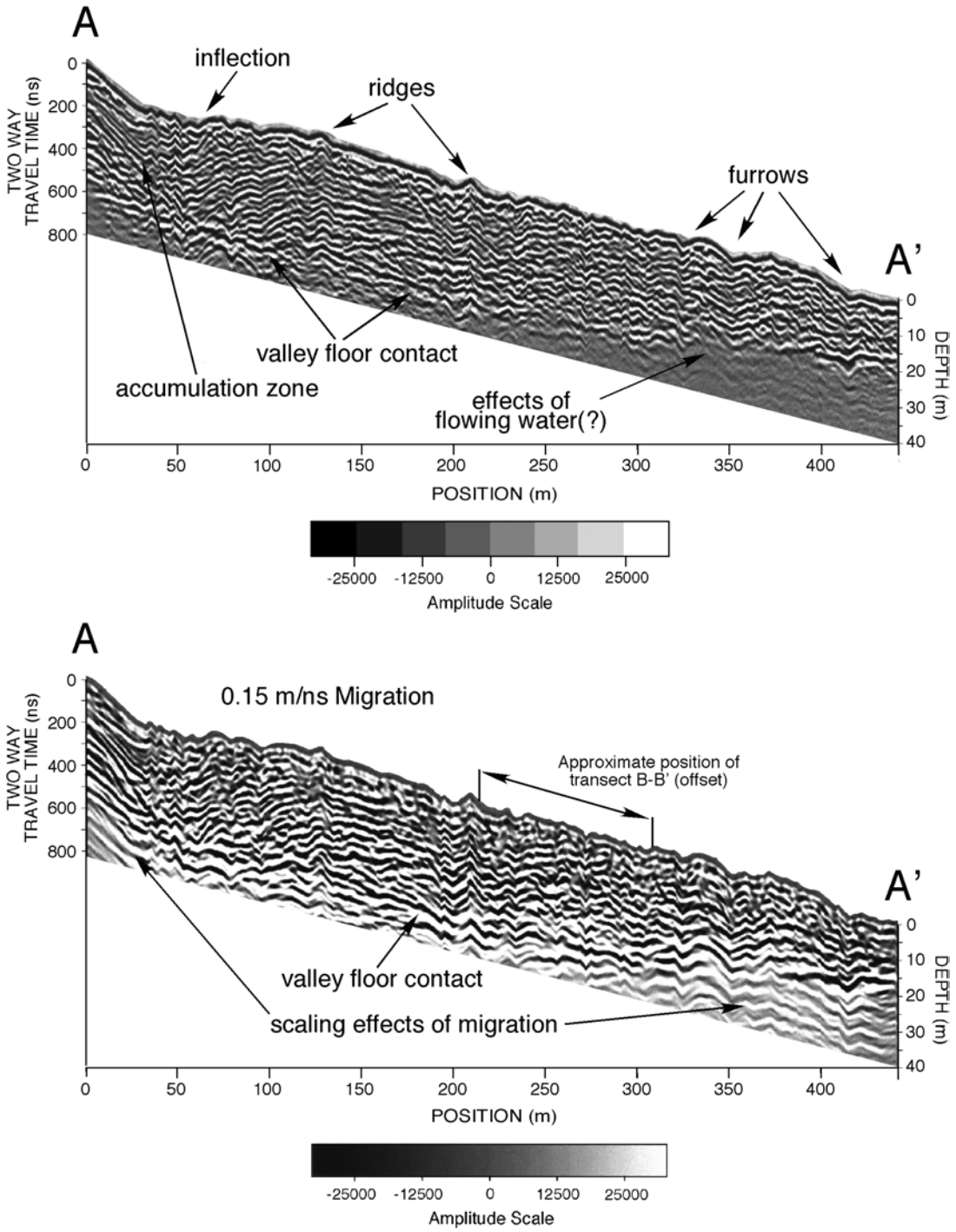

Fig. 3.5. Topographically corrected longitudinal profile collected at f = 25 MHz (velocity = 0.12 m/ns). Unmigrated section (top); Migrated section (bottom); The collected water is in hydrologic communication with Wright's Lake, which is located at the right end of the profile.

coherent reflections, the presence of interfering diffraction events generated by the coarse grained and talus-sized materials of the rock glacier make it difficult to determine the true nature of the reflection terminations in some parts of the profile.

The 50 MHz GPR Profile Sections

The two 50 MHz sections, rendered in wiggle-trace format, provide more detail about the subsurface structure in an area of the rock glacier where ridges and furrows are well developed. Profile B-B', shown in Fig. 3.6, represents an 86 m cross-sectional view in a direction normal to the ridges and furrows. Topographic relief varies from 1–2 m as measured from the bottom of the deepest furrow to the top of the highest ridge. The profile is characterized by a series of dipping reflections that downlap onto more continuous sub-horizontal reflections. The downlapping reflections, which dip in a general downslope direction, range in length from 5–7 m and terminate against the sub-horizontal reflections at angles of 10°-20° from horizontal. The sub-horizontal reflections range in length from 10–30 m and generally trend toward the top of the profile at shallow angles. A small number of toplapping reflections are also present in the central part of the profile (35-50 m). They are 3–5 m in length and are oriented at 5°–10° to the sub-horizontal reflections.

The upward trend of sub-horizontal reflections in B-B' is consistent with reflections that are identifiable on the 25 MHz longitudinal profile, A-A' (see Fig. 3.5 inset). These reflections represent segments of longer sub-horizontal reflectors that slant toward the rock glacier surface at low angles (~5°). Two of these, located at 140 ns and 490 ns, can be correlated to moderately strongly coherent reflections (major horizons) from 220-310 m on profile A-A'.

Profile C-C', shown in Fig. 3.7, was made along the crest of a prominent ridge that crosses profile B-B' at 38 m. It represents a view of the reflectors as they appear normal to the ridge axis. Continuous reflections form an undulate structure reminiscent of a gentle synclinal fold over the length of the profile. Reflections are sub-parallel with the surface from 0–15 m and dip downward at ~10° from 15–55 m. Beyond 60 m the

reflections slant upward at ~10°. Short downlapping and toplapping reflections terminate at angles of 5-10° against the more continuous sub-horizontal reflections, as observed in B-B'.

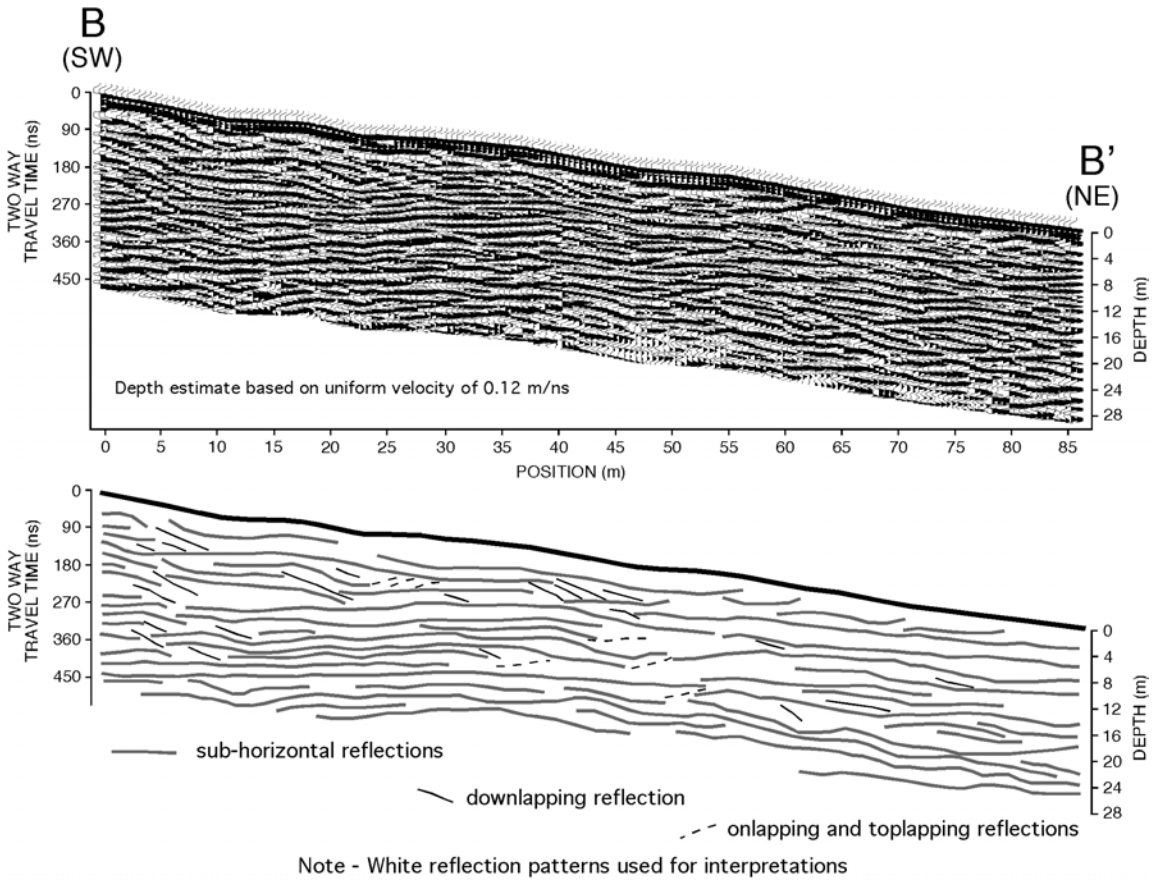

Fig. 3.6. Topographically corrected 50 MHz GPR profile B-B'. Profile is oriented normal to prominent ridges and furrows as shown in Fig. 3. Top: Processed data without interpretations; Bottom: interpretations generated from profile above. The section is characterized by many dipping reflections that terminate against more continuous sub-horizontal reflections. Data were processed using Win_EKKO™ software provided by Sensors and Software, Inc.

The intersection of profiles in Figs 3.6 and 3.7 shows that continuous reflections in B-B’ can be correlated with those in C-C’ (Fig. 3.8). Reflections at 330 ns and 480 ns are the most continuous in both profiles and can be clearly traced from one profile to the other. Almost all of the less continuous reflections can be correlated between the two profiles at the point of intersection. In addition, correlation can be made between many of the reflections at both ends of the two profiles. This indicates that some of the reflectors in this part of the rock glacier are laterally continuous (i.e., laterally continuous layers).

DISCUSSION

Composition and Inner Structure

The 50 MHz profiles indicate a complex stratigraphy for the layers that underlie prominent ridges and furrows. However, it can be seen that many of these layers are laterally continuous (e.g., Figs 3.7 and 3.8). The degree of continuity observed in the layers, and the average velocity value of the rock glacier medium, suggests that alternating ice-rich and ice-poor layers make up the bulk of the rock glacier medium to a depth of at least 20 meters. The layers are interpreted to be the result of flow, perhaps generated by seasonal snow pack covered by episodic flows or high-magnitude discharges of talus debris. This is supported by Haeberli and Vonder Mühll (1996), who argue that the ice created in the rear (accumulation zone) of the rock glacier derives mainly from snowdrifts or from water in the active layer. Isaksen et al. (2000) also concluded that large mass movement events are of great importance in the process of debris input and preservation of ice in the frozen sediments.

Unpublished descriptions of a 7.6 m length of drill core, recovered by the authors in 1997 from a position approximately 50 m east of profile B-B', confirm the presence of alternating layers of coarse ice-rich and ice-poor layers that range from 0.5-1 m in thickness. The layers are composed mainly of blocks and platy clasts that span less than 0.5 m in the largest dimension. The overall ratio of debris to ice was found to range from 60-70%, and some ice layers are comprised of up to 30% silts and fines. Lenses of clean

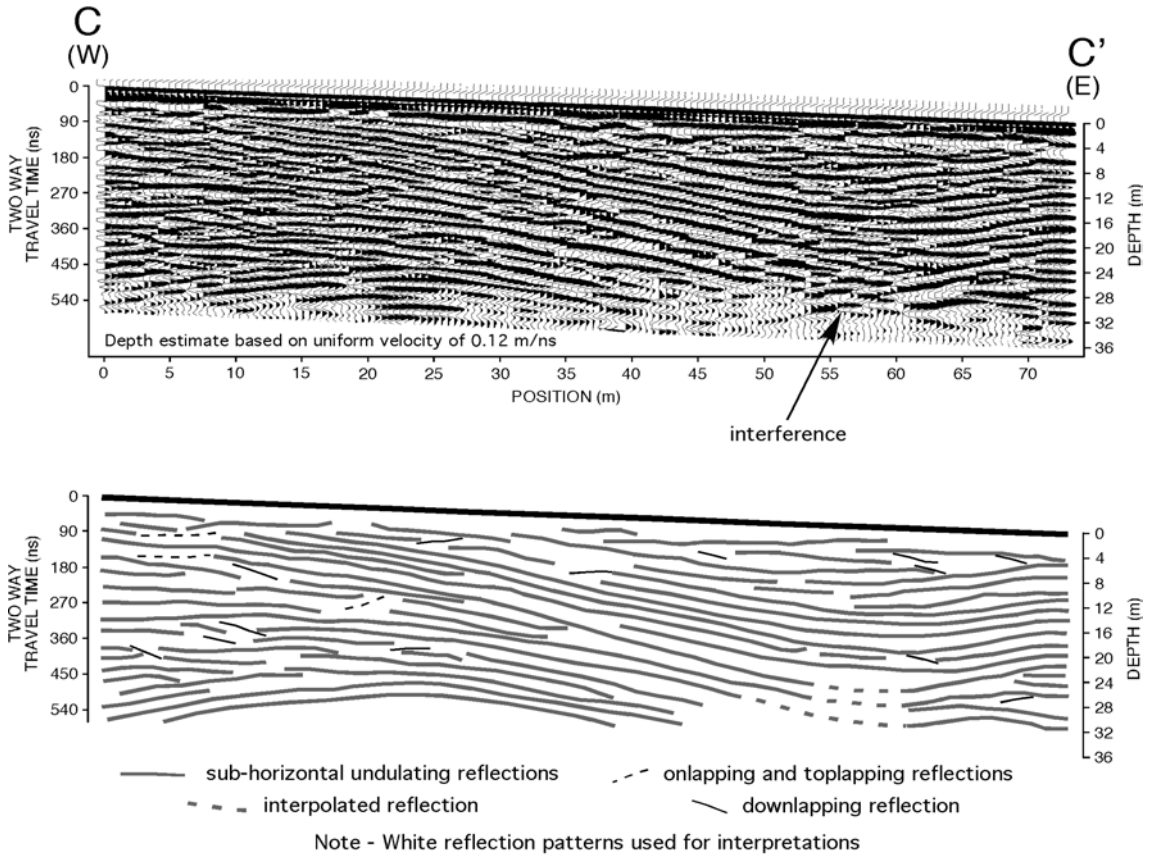

Fig. 3.7. Topographically corrected 50 MHz GPR profile C-C'. Profile is oriented along the crest of a prominent ridge in the sequence of ridges and furrows and furrows crossed by A-A' (Fig. 3.3). Top: Processed data without interpretations; Bottom: interpretations generated from profile above. The section is characterized by many undulating reflections that resemble a synclinal structure. The dip in the layers is interpreted to be a longitudinal furrow that was filled in by overriding flow lobe materials. Data were processed using Win_EKKO™ software provided by Sensors and Software, Inc.

ice were also recovered, ranging in thickness from 0.1-0.5 m. This is generally consistent with findings for drill core samples from other rock glaciers of permafrost origin (Haeberli, 1985; Barsch, 1996) and descriptions from an exposed rock glacier near Longyeardalen, Svalbard (Liestøl, 1962).

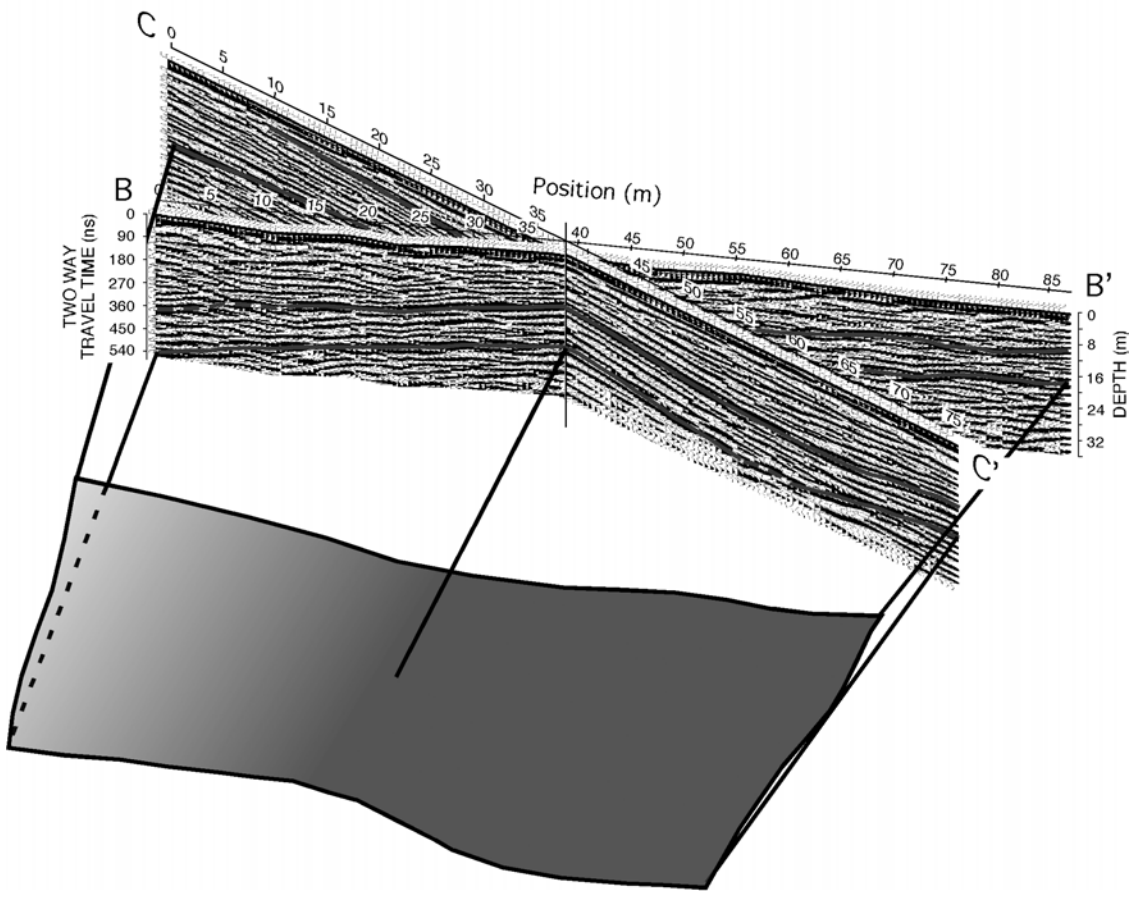

Fig. 3.8. The intersection of profiles B-B' and C-C'. Note the continuity of layers in the upper 20 m of the rock glacier. Lateral continuity is as much as 70 m.

Deformation of the layers involves minor (gentle) folding and small-scale, terminal overlap (as evidenced by downlapping reflections in profile B-B' and C-C', Figs 3.6 and 3.7). An example of larger scale adjustment is also seen in profile C-C', where continuous layers along a ridge undulate in a style similar to synclinal folding. The structure is believed to have formed when individual layers, or perhaps a unit of layers, flowed over an older deposit. The deposits filled in a longitudinal furrow, which is visible on the aerial photo. The overriding flow extended eastward and spread to the southeast.

Gross Features

The longitudinal profile and accompanying interpretation (Fig. 3.9) provides a general picture of the overall structure of the rock glacier. Six continuous horizons, defined by moderately strongly coherent reflections, divide the rock glacier into a series of distinct sub-horizontal components that are interpreted as layered depositional units. Layers within each unit are 1–3 m thick and generally conform to the orientation and character of the main horizons.

In the head portion of the rock glacier, the layers are flat and closely spaced. This type of layering is consistent with a process in which snow and talus debris, accumulated at the lower reaches of the talus slope, moves in tension down the steep gradient of the head. Below the zone of accumulation, the layers exhibit a more undulating structure and upward slant. Here, materials leaving the accumulation zone encounter a decrease in the slope of the cirque floor. The highly undulated character of the layers marks the onset of compressive stresses, which are likely to be at a maximum (Barsch, 1996). This is consistent with observations made by Giardino (1979) and Haeberli (1985), who report that ridge and furrow development is most pronounced at sites of increased compression (i.e., slope decline). It is suggested here that ridges and furrows originate as small surface irregularities just beyond the slope inflection and develop into large ridges and furrows at lower sections of the rock glacier, where slope decline results in increased compressive stresses.

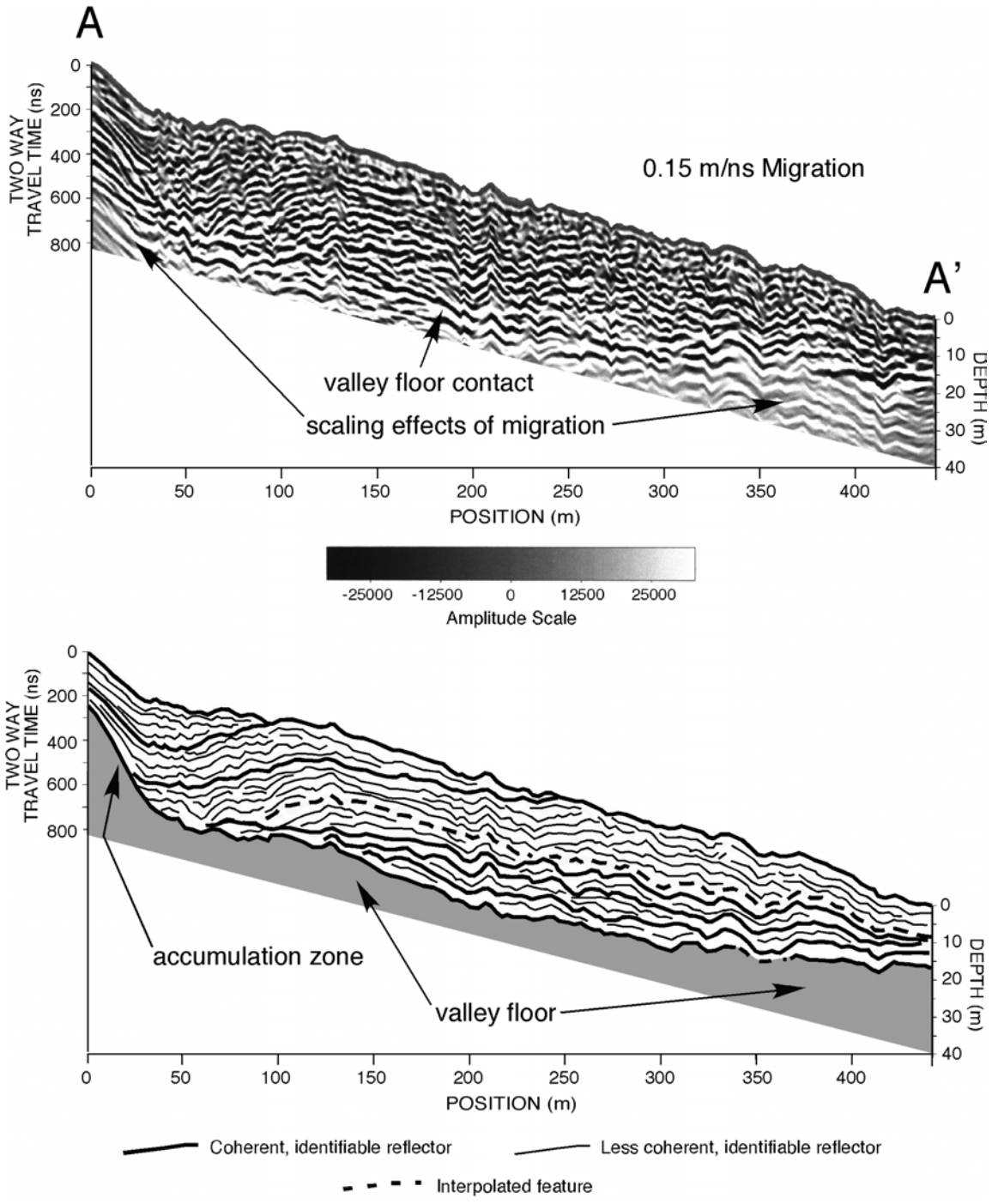

Fig. 3.9. Migrated longitudinal profile from Fig. 3.5. Accompanying interpretation is shown at bottom. Seven main depositional units can be identified and each unit is comprised of layers that are sub-parallel to the major reflection horizons.

The upward slant of the layers is similar to results for steady-state flow modeling of debris-covered glaciers (rock glaciers) by Konrad and Humphrey (2000). They showed that flow paths in the ablation area initially curve up toward the surface (where ablation rates are relatively high) but turn back to parallel the surface further down-valley (where ablation rates are lower). The structure observed in Fig. 3.9 is generally consistent with this type of behavior, which reinforces the idea that layers comprising permafrost rock glaciers deform by creep. In this regard, Barsch (1992) definitively states that the creep of supersaturated mountain permafrost is the important and decisive process in rock glacier formation.

The difference in orientation and character of layers in the upper 10–12 m of the rock glacier compared to layers in underlying units suggests that a process of material override is governing the gross structural character of the rock glacier interior. Beyond 125 m, the layers in the bottom half of the rock glacier do not deviate significantly from the horizontal, in contrast to the upper layers, which assume a variety of orientations with respect to horizontal. Such a difference in character can be attributed to changes in flow direction that result when supply of talus shifts from one location on the headwall to another. This effect can also be achieved through variable rates of talus supply along different parts of the headwall. The controlling factor for direction of flow is therefore the maximum gradient encountered by the flow given its location within the cirque. The result over time is the generation of multiple source flows leading to discrete depositional units (i.e., flow lobes).

The upward slant of reflectors from 210-320 m (along A-A') can be explained by examining the profile line shown on the aerial photo in Fig. 3.3. The flow of materials along the centre-most portion of the rock glacier appears to have been diverted by an underlying (older) depositional unit (flow lobe). The exposed portion of the underlying flow lobe stands in higher relief than the lobe that immediately overlies it, thus providing a gradient that forces flow of the overriding lobe to a more easterly direction.

Model for Rock Glacier Formation

As the aerial view in Fig. 3.3 suggests, the rock glacier can be considered in terms of a series of discrete flow lobes. Such a model is supported by the gross internal structure as interpreted from the 25 MHz longitudinal survey. Fig. 3.10 shows one interpretation for how the major depositional units of the rock glacier may be correlated with individual flow lobes as mapped on the aerial photo. The terminations of the major

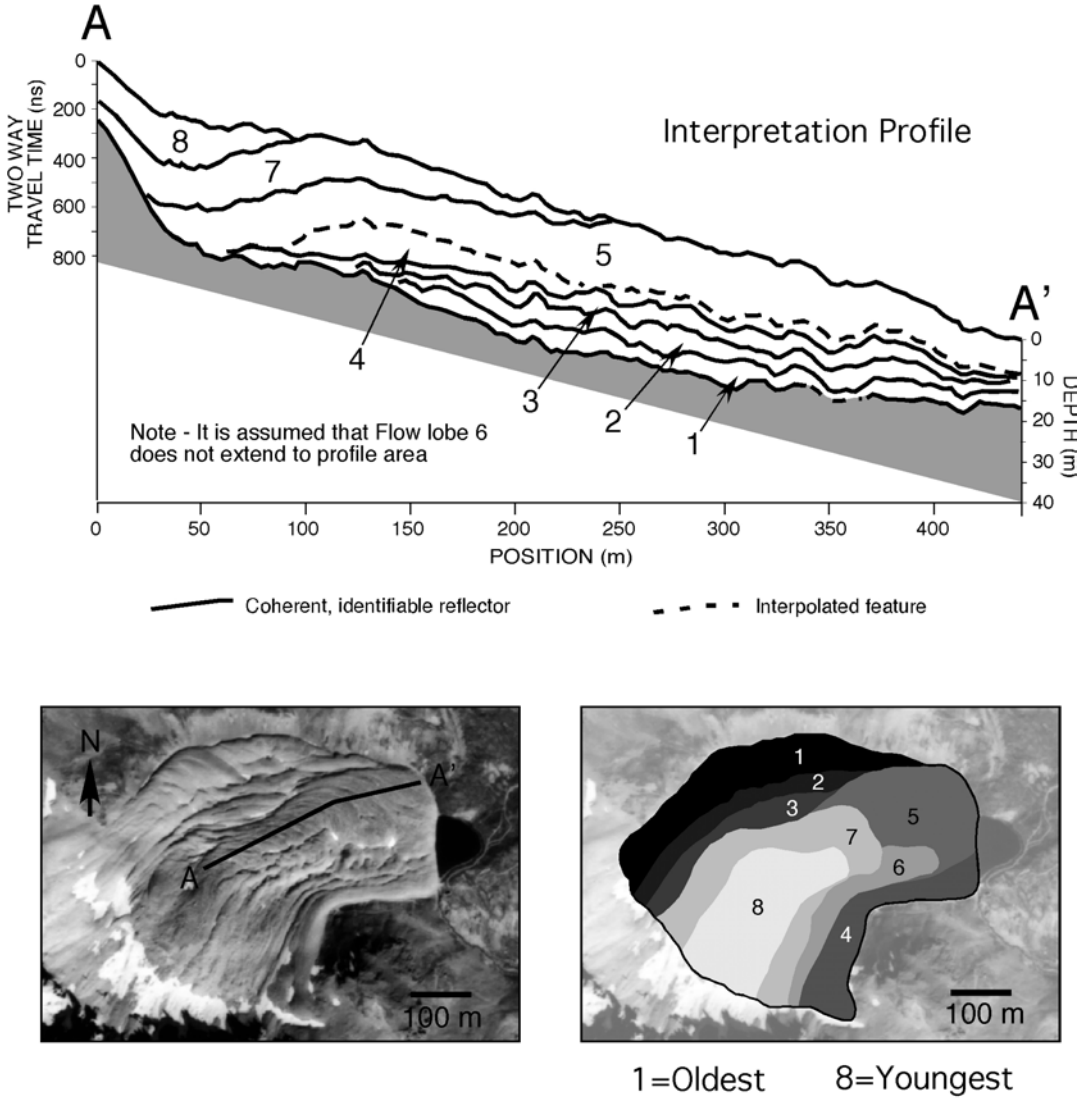

Fig. 3.10. Correlation between the main depositional units. The correlation is based on interpretation of the GPR profile shown in Fig. 3.9 and the flow lobe boundaries as mapped on the 1:20,000 scale vertical aerial photo (bottom right).

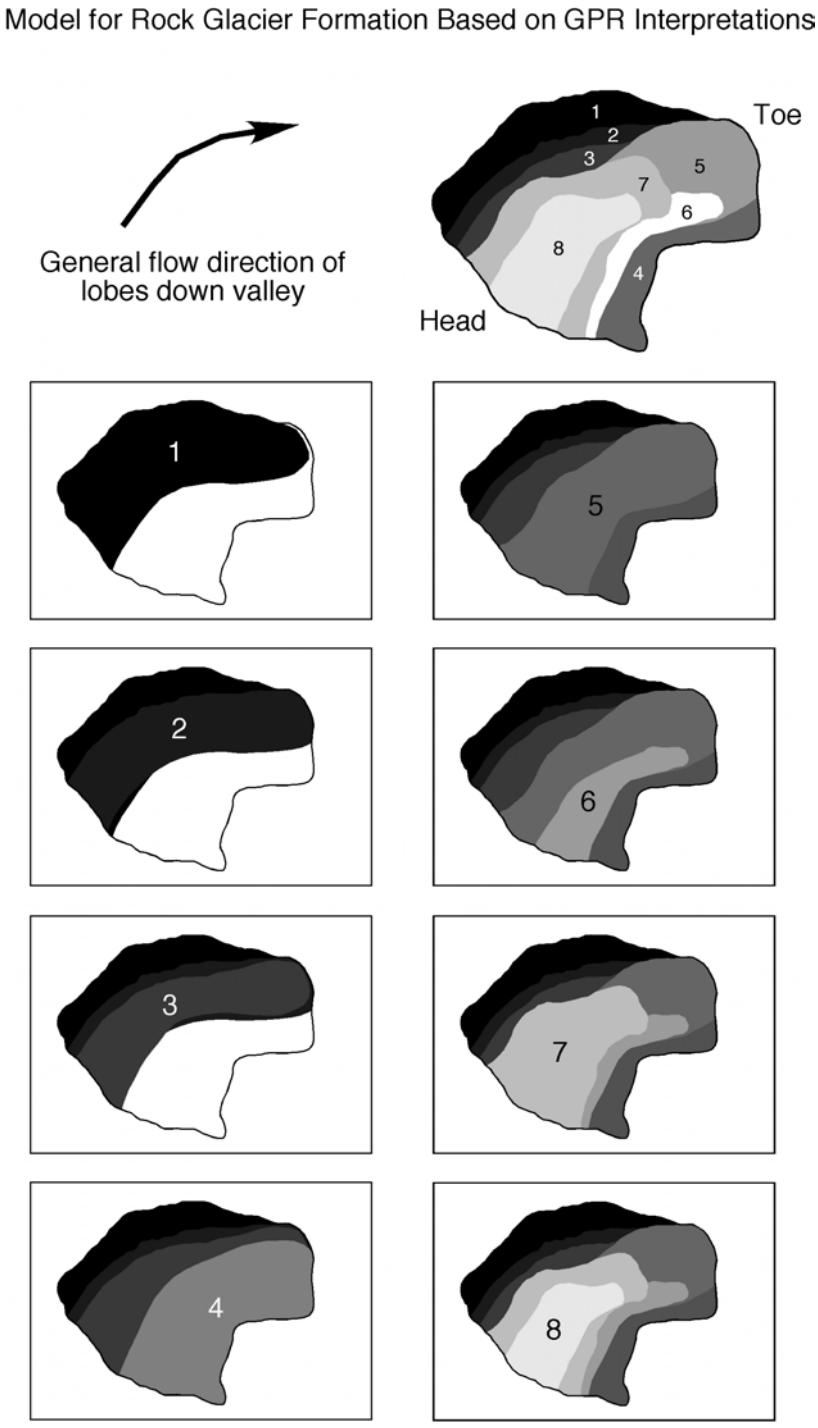

Fig. 3.11. Model for rock glacier formation. Model is based on interpretations made from the 440-m, 25 MHz longitudinal profile and the layering sequence depicted in Fig. 3.10. The location and rate of talus supply along the headwall controls the avenue (i.e., slope) and direction of flow for each lobe.

horizons in the interpreted profile match closely with the exposed and inferred boundaries of the flow lobes in plan view. Using this method, a sequence of seven discrete flow lobes is identifiable. It appears that the lobes flow down the cirque valley together as a composite geomorphological unit.

From this exercise, a model for rock glacier development can be formulated. Fig. 3.11 illustrates in plan view the proposed sequence of events involved in the formation of the Yankee Boy rock glacier. Using a fundamental system of superposition, it appears that the lower half of the rock glacier was formed by a series of five flow lobes that flowed over each other in a prograding fashion from north to south. Two younger flow lobes followed this sequence, one of which remains active today. As indicated in the profile, layers in the lower part of the rock glacier appear truncated, and are not continuous to the head area. This implies 'pinch-out' of the earliest layers by subsequent (overriding) layered units. In terms of flow lobe development, this means that the first flow lobes to form flowed along different avenues of the valley floor. Thus, the rate and position of talus production along the headwall controls the avenue and direction of flow lobes.

CONCLUSIONS

The results of this radar investigation show that the Yankee Boy rock glacier consists of horizontal to sub-horizontal layers of ice-rich and ice-poor strata. These layers, some of which are laterally continuous up to 70 m in all directions, are interpreted to be ice-supersaturated sediments and coarse blocky rockslide debris. The layers are considered to be the result of flow, perhaps generated by seasonal snow pack covered by episodic debris flows or high-magnitude discharges of talus.

Major depositional units, identifiable by prominent reflection events in the GPR profiles, are believed to be individual flow lobes that formed at different positions along the cirque headwall. On this basis, it is concluded that the formation history of the rock glacier involves incorporation of ice within talus debris to form supersaturated permafrost, and subsequent creep of this material down-valley. We interpret this rock

glacier to be a composite feature that formed by a process involving the development and overlap of discrete flow lobes. A sequence of seven discrete flow lobes is identifiable. It appears that the lobes flow down the cirque valley as a composite geomorphological unit.

CHAPTER IV

SUBSURFACE INVESTIGATION OF A ROCK GLACIER USING GROUND PENETRATING RADAR (GPR): IMPLICATIONS FOR LOCATING STORED WATER ON MARS

OVERVIEW

The discovery of rock glacier-like features on Mars suggests the presence of flowing, or once-flowing ice-rock mixtures. These landforms, which include lobate debris aprons, concentric crater fill and lineated valley fill, hold significant promise as reservoirs of stored water ice that could be used as fuel sources for human exploration of Mars and provide a frozen record of the climatic history of the planet. To understand the deformation and distribution of ice within these landforms, fundamental descriptions of their internal structure and development are required. To this end, a ground penetrating radar (GPR) investigation was initiated in the summer of 2000 using rock glaciers in the San Juan Mountains of Colorado as surrogates for similar Martian landforms. Results obtained from one of these rock glaciers show that the landform is comprised of distinct, continuous alternating ice-rich and ice-poor layers that comprise thicker depositional units formed through high-magnitude debris falls originating from the cirque headwall. Folds in the uppermost layers correspond to the surface expression of ridges and furrows, suggesting that compressive stresses originating in the accumulation zone are transmitted downslope through the rock glacier. The rock glacier interior consists of a matrix of ice, sediment and ice lenses. Rock glacier features on Mars may also consist of layered permafrost ice and ice lenses, which would suggest a history of permafrost development involving seasonal frost accumulation and/or water influx from below. Liquid water, found to be abundant in the San Juan rock glacier, occurs within a network of interconnected channels that permeate throughout the landform. In terms of water storage within Martian analogs, consideration must include the possibility that some

water ice may be stored in relatively pure form within lenses and vein networks such as observed in the surrogate rock glacier of this study.

INTRODUCTION

Rock glaciers are lobate or tongue-shaped bodies composed of mixtures of poorly sorted angular, blocky rock debris and ice. These landforms, whose wide distribution, occurrence, and significance often go unnoticed, move by slip, flow and/or creep deformation (Giardino, 1979; Haeberli, 1985; Giardino and Vitek, 1988a, 1988b) and have distinctive surface morphologies, including ridges and furrows perpendicular to flow direction. They generally occur in dry, continental areas rather than humid regions, perhaps because thin to absent snow cover and reduced glacier extension favor the existence of periglacial permafrost conditions and, hence, the preservation over long time intervals ground ice – a primary condition of rock glacier formation (Humlum, 1997). Ages of rock glaciers range from incipient forms on Pico de Orizaba volcano (Palacios and Vazquezselem, 1996) through forms associated with the Little Ice Age (Humlum, 1996), to features several thousand years old (e.g., Kaeaeb et al., 1997; Calkin et al., 1998). Relict rock glaciers that formed at the end of the last Ice Age ~18,000-10,000 years BP have also been documented (Sandeman and Ballantyne, 1996; Humlum, 1998). Direct dating of rock glaciers using pollen analysis and C^{14} ages of moss has recently been provided by Haeberli et al. (1999). The occurrence of past or present glaciers is not necessarily a prerequisite to the formation of rock glaciers because these landforms exist in both glacial and non-glacial areas (Giardino, 1979, 1983; Johnson, 1983; Haeberli, 1985).

Serious study of rock glaciers began with the seminal work by Wahrhaftig and Cox (1959), who put forth the idea that rock glaciers represent a landform continuum in the alpine environment. Barsch (1977) and Giardino (1979) later addressed the role of rock glaciers in terms of debris transport and found that rock glaciers account for approximately 60% of all mass transport in the alpine environment. Our current understanding of rock glacier deformation is outlined in the work of Haeberli (1985). It

is based on flow models adopted from studies of glaciers and limited physical data from rock glaciers around the world. Subsequent continuum-based (Giardino and Vitek, 1988b), dynamics-based (Johnson, 1978, 1983), and form-based (Corte, 1987) classification schemes have also been developed.

Although the geomorphology of lobate landforms with surficial ridges and furrows perpendicular to flow direction is well documented, our current knowledge of their movement mechanics and flow behavior is based on limited data obtained exclusively from terrestrial rock glaciers. Knowledge of the internal composition and fabric is necessary to understand the flow dynamics responsible for rock glacier deformation (Fitzgerald, 1994), but the difficulty and cost associated with direct observation of the internal characteristics make acquisition of these data problematic. For example, direct rheological measurements (i.e., flow direction, flow velocity, and stress fields) are time dependent and lengthy because rock glacier flow is not observable at human time-scales. To fully understand the movement and deformation patterns within rock glaciers, a fundamental (i.e., generic) description of their development is required. However, before the mechanics of motion can be understood, internal structure must be accurately identified.

In this study, we identify the internal structure of a lobate rock glacier with characteristic ridges and furrows using ground penetrating radar (GPR), a non-intrusive method of subsurface remote sensing. The investigation is directed at understanding the movement and deformation of ice-rich, slow mass-movement forms on Mars through the use of surrogate rock glaciers on Earth. The insights presented in this paper have been developed through a process of: (1) describing the internal structure of a lobate rock glacier, (2) developing a model for rock glacier development, (3) providing a plausible explanation for the origin of transverse ridges and furrows, and (4) mapping water pathways within a rock glacier. The methodology established here can be applied directly to investigations on Mars where information about the distribution of stored ice within landforms is paramount.

SIMILAR FEATURES ON MARS

Water Ice in Regolith

On Mars, geomorphic features resembling rock glaciers (Fig. 4.1) have been recognized as possible ice-rich bodies that have undergone viscous creep (Lucchitta, 1986, 1993). Much of this ice may consist of frozen water, perhaps formed by recent or ongoing processes. This concept is supported by theoretical arguments of Mellon and Jakosky (1995), who suggest substantial quantities of ice exist in the near-surface regolith. Generally, the thin atmosphere of Mars forces the frost point of water to remain below 200°K. Thus, at higher temperatures, ice at the surface would sublime rather than melt. The regolith covering of these landforms may, however, provide sufficient insulation for the persistence of the ice within, particularly if the water ice is sealed off from the atmosphere by a continuous layer of frozen CO_2.

The geographic distribution of viscous-creep features on Mars is consistent with the stability of ice as dictated by thermodynamic laws. Farmer and Doms (1979) provide a model for ice stability which suggests that in locations where temperatures in the top 10 meters of regolith exceed 198°K, ground ice will become unstable and can escape to the atmosphere by sublimation and diffusion. Using thermodynamic models, Clifford and Hillel (1983) and Mellon and Jakosky (1995) found that a zone of ground ice instability exists between ±30° latitude. This is consistent with mapping done by Carr (1986) that shows virtually no creep features within 30° of the equator.

Viking images of the northern plains on Mars reveal the presence of lobate features with wrinkled surfaces associated with rift valleys and the peripheral margins of splash-form craters. These landforms, which include lobate debris aprons, lineated valley fill and concentric crater fill, have been interpreted as possible viscous ice-flow features (e.g., Carr, 1987; Lucchitta, 1993) derived from materials loosened from their original locations. The materials appear to have been transported generally down gradient by mass-wasting processes followed by accumulation and subsequent creep flow (Squyres, 1978).

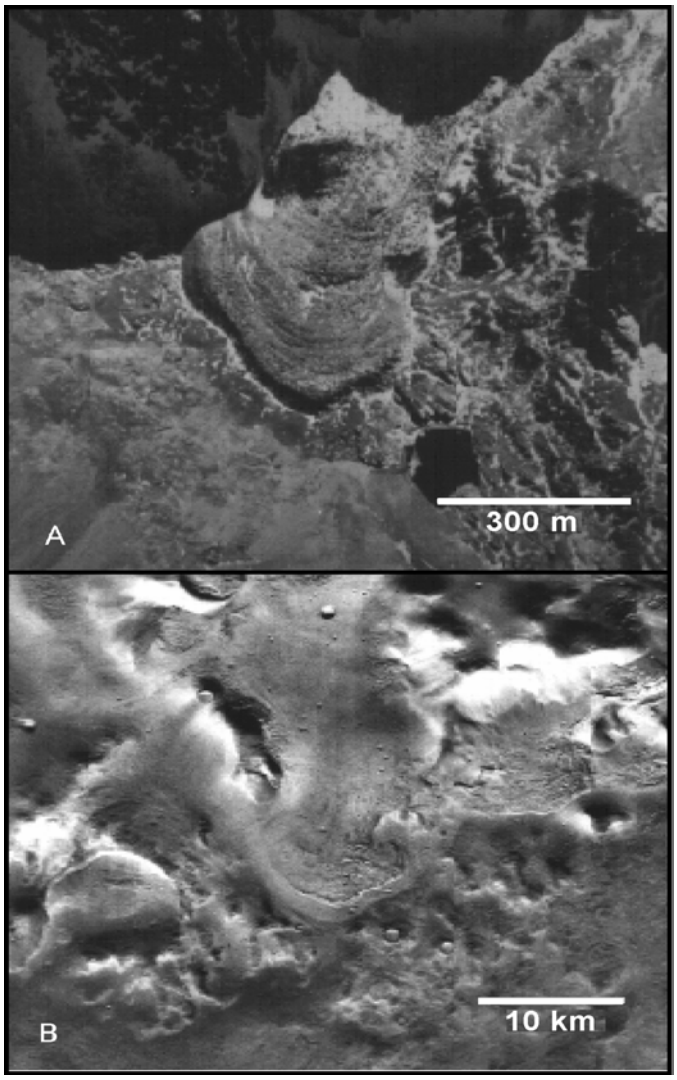

Fig. 4.1. Lobate viscous-flow features on Earth and Mars. (a) Rock glacier located in the San Juan Mountains of Southwest Colorado, USA; (b) A landform on Mars resembling terrestrial rock glaciers. This feature, a lobate debris apron, is located in the northeast portion of the Hellas Impact Basin (Viking Orbiter Image 585-B09, courtesy of the Lunar and Planetary Institute, Clear Lake, TX).

Lobate debris aprons are thick, topographically convex accumulations of debris at the base of escarpments. The surface of a debris apron slopes gently away from its source (e.g., the escarpment), and then steepens to form a distinct flow terminus analogous to the toe of a rock glacier. This morphology is a reliable indicator that

deformation and flow have taken place throughout a significant thickness of the deposit (Squyres and Carr, 1986). In terrestrial rock glaciers, a steep-crested toe indicates that the landform is currently active or was active in the recent past (Giardino et al., 1987). Some lobate debris aprons exhibit distinctive surface lineations that are both parallel and transverse to flow. These features bear striking resemblance to terrestrial rock glacier counterparts. Debris aprons that are confined in narrow valleys have been termed lineated valley fill. They appear to be composed of the same material as lobate debris aprons. Lobate debris aprons are very common in the fretted terrain separating the northern lowlands from the southern highlands between 280° and 250° longitude (Colaprete and Jakosky, 1998). Almost all of these types of features are restricted to a region between 50° and 80° latitude (Squyres, 1988).

Rock Glacier Analogs - Hellas Impact Basin and Region of Fretted Terrain

The Hellas region (27.5°–42.5°S, 260°–275°W), dominated by the Hellas impact basin, is topographically and geologically diverse. The generalized geology, recently mapped by Tanaka (1995), includes Mid- to Upper Noachian-age (~3,900-3,500 Ma) Patera material to the north of the impact basin, basin rim units of late Noachian (~3,600 Ma) to the north and west, and dissected rim units of upper Hesperian (~2,400–1,800 Ma) and late Amazonian (~300-100 Ma) to the south and east of the basin. Farther south and east of the basin are ridges plains materials of upper Noachian to late Hesperian age. The basin was formed during the early bombardment period (~3,900 Ma), but is relatively well preserved. It makes up the deepest and broadest depression on Mars (~9 km relief, ~2,000 km across). Volcanism and channel dissection have significantly modified large portions of the northeastern and southern parts of the basin rim.

Large-scale examples of rock glacier-like features have been documented in the region surrounding the Hellas Impact Basin (Figs. 4.2 and 4.3) and in areas of fretted terrain extending 25° in longitudinal width, centered on 40° N. latitude and 45° S. latitude. Concentric crater fill, observed on the floors and walls of craters, exhibit concentric patterns of ridges and roughs that result from compressional stress acting inward from the crater walls (Fig. 4.3c). The concentric ridges are especially common in

these forms, owing to the sharp transition in slope as materials flow down the walls of craters to the crater floors. The material also displays large-scale morphologic features and eolian etchings similar to those found on the other types of viscous flow bodies described in the preceding section. Some crater fill landforms appear to be “deflated”, a characteristic observed in some debris aprons. In the southern hemisphere, lobate debris aprons are restricted to the mountainous terrains of the Argyre and Hellas impact basins. In the Hellas region, debris aprons are located mainly in the mountainous terrain on the eastern side of the basin. They are most common at the bases of escarpments and are less common as concentric crater fill (Squyres and Carr, 1984).

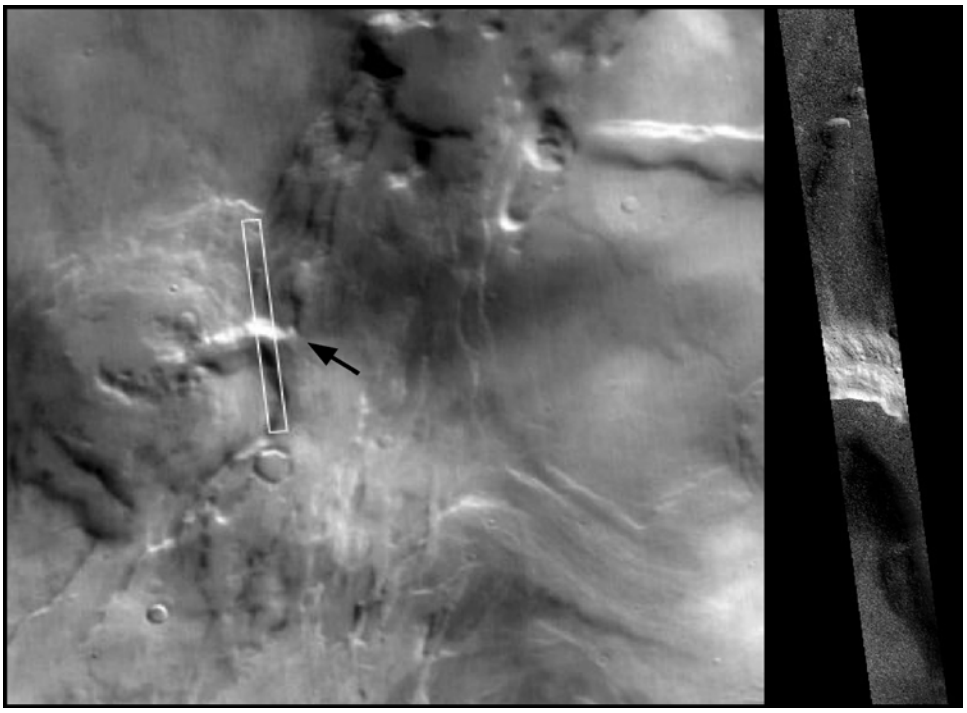

Fig. 4.2. Mars Orbiter Camera (MOC) image of a lobate debris apron. The feature is located in a valley in the Tempe Terra region on Mars (black arrow). The narrow angle image (right) traverses the valley, which appears to dissect the wall of an impact crater. Debris accumulated at the base of the wall displays a wrinkled texture resembling ridges and furrows (white arrow). The area in the context image (M07-02045) is located at 47.29˚N, 77.99˚W and the narrow angle image scale is 2.40 km x 30.57 km (image M07-02044). Images courtesy of Malin Space Systems (Malin et al., 1996).

CONVERGENCE OF INVESTIGATIVE APPROACHES

Previous Methods of Investigation

Researchers have used both direct and indirect methods in their investigations of rock glacier structure (Burger et al., 1999). Until recently, direct investigative methods included tunnels through rock glaciers (e.g., Brown, 1925), visual inspection of exposures, and shallow pits (e.g., Wahrhaftig and Cox, 1959). Potter (1972) successfully used shovel excavations to investigate Galena Creek rock glacier and Giardino (1979) used bulldozer excavations to study the structure of rock glaciers on Mount Mestas, Colorado.

Coring methods must negotiate the difficult surface debris as well as interior heterogeneity. Mechanically operated drills have proven to be effective in penetrating both rock and ice by changing drill bits to meet encountered conditions (e.g., Haeberli et al., 1988). Clark et al. (1996) used a lightweight, hand-operated auger for studies of Galena Creek rock glacier (i.e., massive ice). The tool was useful at this locality because the volcanic source rock breaks into small clasts, making hand excavation of the debris feasible. During the summer of 1997, Giardino and Degenhardt were able to extract ice cores from the Yankee Boy rock glacier in the San Juan Mountains of Colorado. Such coring is no longer permissible in this area owing to increased government restrictions on sampling, equipment use, and the addition of new areas designated as national forest. Most of the techniques outlined above are also impractical for many localities where investigation is restricted by resources and accessibility. Large clast sizes and thick debris cover on rock glaciers challenge many investigations.

Indirect methods include geophysical surveys, such as seismic refraction, gravimetry, resistivity, radio-echo surveys, and ground penetrating radar. In contrast to the labor- and time-intensive direct methods, geophysical methods allow relatively rapid and inexpensive acquisition of three-dimensional data for a rock glacier. Seismic refraction and resistivity surveys are the most commonly applied geophysical techniques. According to Haeberli and Vonder Müehll (1996), surface layer seismic velocities, typically ranging from 300 to 1,000 m/s contrast sharply with velocities from

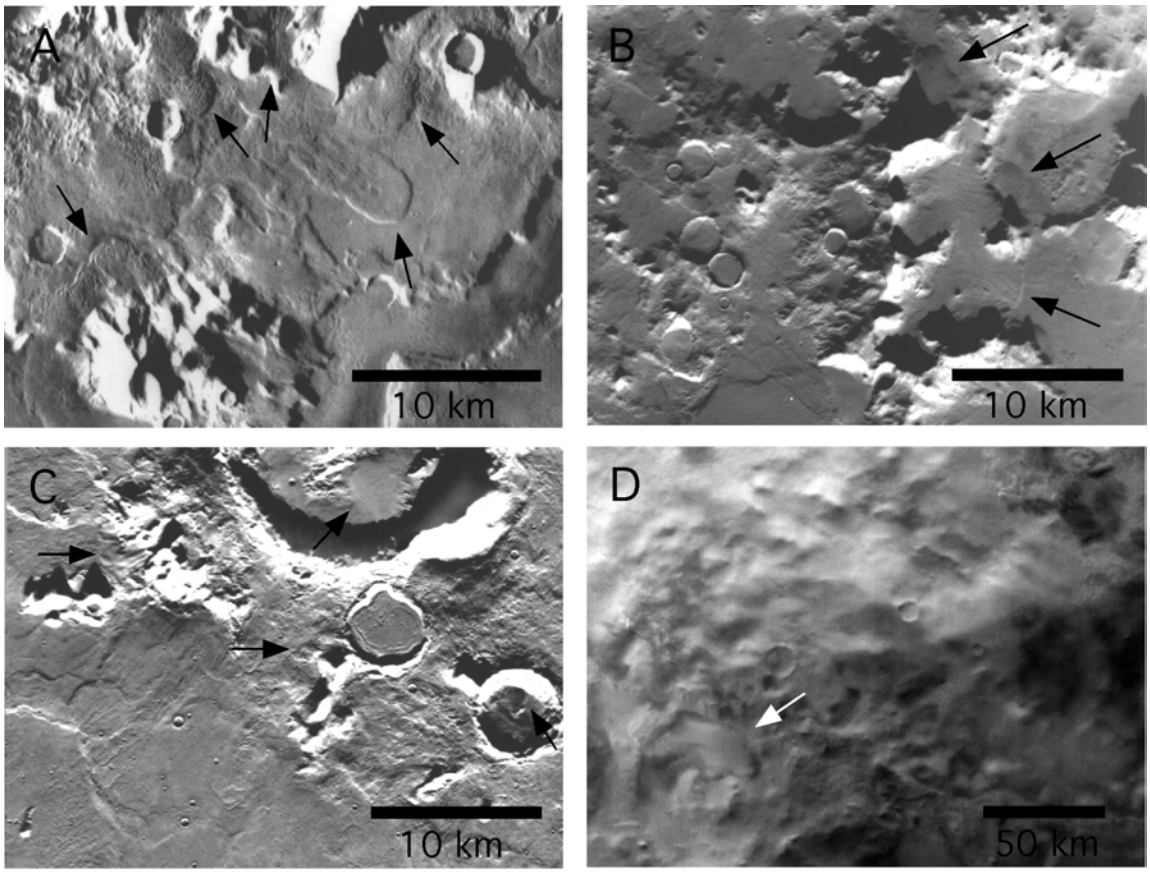

Fig. 4.3. Viscous flow features located in the East and Northeast regions of the Hellas impact basin (27.5˚-42.5˚S, 260˚-275˚W). (a and b) Viking images of the northern plains showing lobate features with wrinkled surfaces and lineated flow patterns; (c) Concentric crater fill in the peripheral margins of splash-form craters; (d) Mars Orbiter Camera (MOC) image of a viscous-flow feature resembling a rock glacier. Image numbers for (a-c) are 408S15, 412S82, and 412S16. The MOC image is M19-01420, located at 47.47˚S, 299.57˚W (Malin et al., 2001).

the top of ice-bearing layers. This contrast, which roughly parallels the surface of the rock glacier, can be traced along its length and is readily interpreted as the refractor representing the top of frozen sediment. Ice-supersaturated frozen material has an average seismic velocity of 3,500 m/s and a seismic velocity range of 2,000 to 4,000 m/s (indicating a degree of heterogeneity). Electrical resistivity, which is dependent on ice content and type, ranges from 1 to 10,000 kΩm in frozen sediments (Haeberli and

Vonder Müehll, 1996). Ice at marginal permafrost conditions has low resistivity (5-500 kΩm); massive ice has much higher resistivity (1,000-2,000 kΩm). Recent gravimetry applications at the much-studied Murtèl-Corvatsch rock glacier were successful, but required an intense modeling effort to correct for surrounding topography. Existing data were also extensively used to develop the model (Vonder Müehll and Klingelé, 1994).

Few results from the use of geophysical methods mentioned in the previous paragraphs have been verified by drilling or other methods to determine "ground truth," and few results except the depth of the boundary between an unfrozen surface layer and frozen material below are unequivocal. General limitations of these geophysical techniques sometimes include complex modeling efforts that can produce non-unique models and may require additional ground-truth data collection. Based on these limitations, a more practical method of subsurface remote sensing is needed for rock glaciers. Ground penetrating radar now provides a low-cost, accurate alternative to standard seismic techniques, without noise and disturbance to the environment.

Application of GPR to Rock Glaciers

Ground penetrating radar (GPR) is a relatively recent development (Morey, 1974; Annan and Davis, 1976; Ulriksen, 1982; Daniels et al., 1988), having reached user practicality in the mid-1980's. This technique offers the sophistication of other geophysical techniques combined with portability and ease of use. It is ideally suited to applications in the alpine, where logistics and associated expense are usually prohibitive. GPR has been used effectively in a variety of geologic and geomorphologic environments including karst, glacial, periglacial, fluvial, and wetlands (e.g., McMechan et al., 1998; Murray et al., 1997; Horvath, 1998; Roberts et al., 1997; Jol and Smith, 1995).

Digital GPR profiles are generated using transient reflections of electromagnetic energy (EM) (Daniels et al., 1988) and are similar in appearance to standard seismic profiles (Daniels, 1996). EM in the frequency range of 10-1,000 MHz is transmitted into the ground in the form of short pulses. Profiles are generated from the return of radar signals as a portion of the transmitted energy that is reflected back to the surface as a

result of changes in bulk electrical properties of the underlying materials (Smith and Jol 1997). Such changes in electrical properties can be attributed to sedimentological variation (i.e., changing grain size), facies changes, differences in state of materials (i.e., water-rock or water-ice contacts), mineralogy, and density. Resolution of GPR at 100 MHz (assuming a velocity of 0.1 m/ns) is ~0.25-0.50 m, which is ~10 times greater than conventional high-resolution shallow seismic sounding (Smith and Jol, 1995).

Investigation of a Surrogate Rock Glacier: Yankee Boy Basin, CO.

At present, indirect evaluations of landforms exhibiting viscous flow properties focus on rock glaciers with 'wrinkled' surface textures. This requires that primary consideration be given to those rock glaciers having prominent transverse ridge and furrow structure. Abundant examples of such rock glaciers can be found in the San Juan Mountains of Colorado. The rock glacier chosen for this investigation exhibits many morphologic characteristics (i.e., transverse ridges and furrows, lobate form, oversteepened toe, proximity to a headwall) that make it desirable for use as a surrogate for similar landforms on Mars. It is located in Yankee Boy Basin between Ouray and Telluride, Colorado.

Yankee Boy Basin is a series of compound cirques defined by a sharp arête extending from Gilpin Peak to Mt. Sneffels. The basin consists predominantly of Tertiary volcanics underlain by a block of Precambrian quartzite (Luedke and Burbank, 1976). Mountain peaks that flank the basin are composed of San Juan volcanics, including Gilpin Peak tephra deposits, the Picayune Formation and the San Juan Formation. The Picayune Formation consists of a series of flows, breccias and tephra layers of intermediate composition and the San Juan Formation is mainly bedded tephra deposits of felsic composition. In the area of Mt. Sneffels, and along the northern edge of the basin, the mountains also include cores composed of older granodiorite and gabbro stock containing Precambrian quartzite inclusions. Quaternary deposits comprising the San Juan Formation cover most of the basin floor with limited exposure of the granodiorite and gabbro stock. The easily eroded bedrock supplies the parent material for deposits such as rock glaciers, alluvium, glacial drift, and landslide deposits.

Holocene talus deposits occur at the base of most valley walls and rock glaciers typically occupy the heads and valleys of cirques. The rock glacier at the head of Yankee Boy Basin is shown in Fig. 4.4.

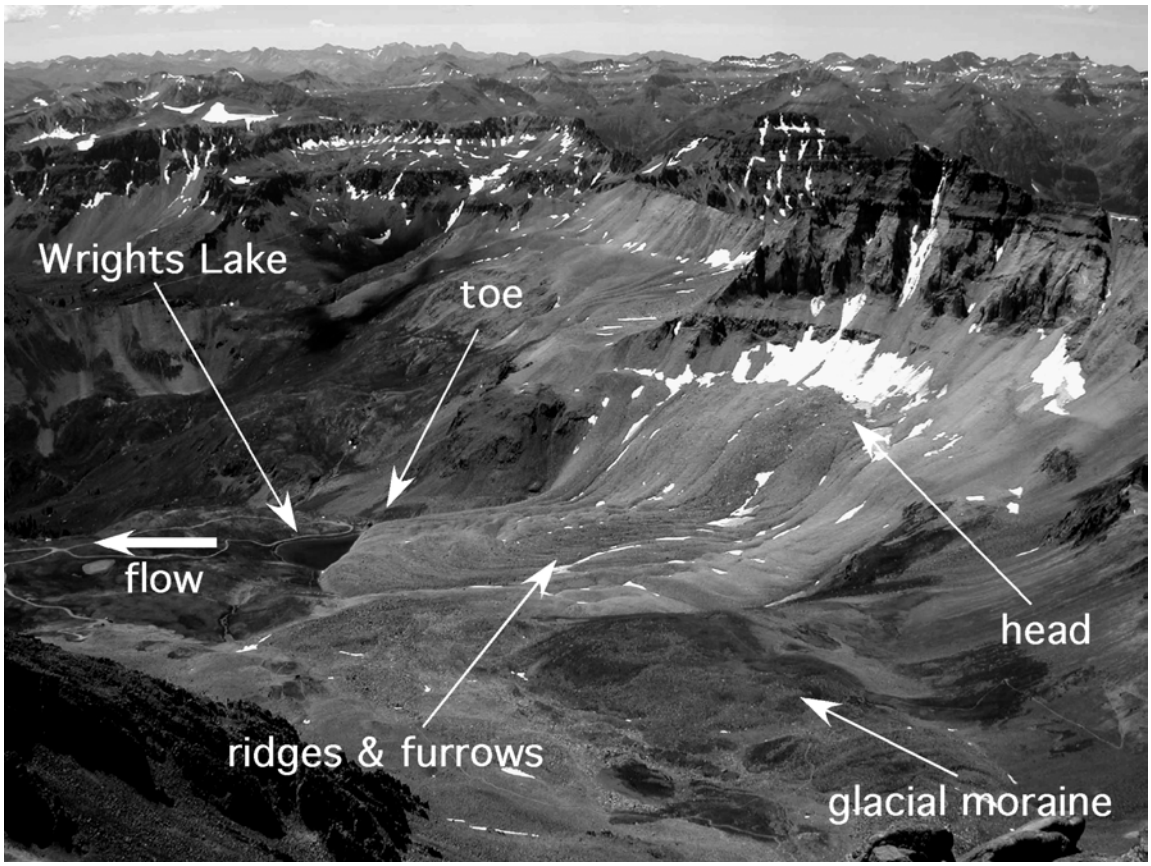

Fig. 4.4. Components of the Yankee Boy Basin rock glacier. Basin is located in the San Juan Mountains of southwest Colorado. Photo was taken from atop nearby Mount Sneffels, a 4,328 m (14,200 ft) peak. The rock glacier is approximately 500 m (1,640 ft) long from the snowline to the toe at Wright's Lake, and 300 m (984 ft) wide at the middle. The rock glacier flows down a cirque that is bounded on the southwest side by Gilpin peak ridge (4,174 m) seen in the background.

Equipment and Techniques

A PulseEKKO™ 100A radar system from Sensors & Software, Inc. (Mississauga, Canada) was used in perpendicular broadside reflection mode with a constant source-receiver offset. Data for individual transects were collected using 2-m and 4-m source-receiver offsets for 50 MHz and 25 MHz (center frequency) antennae, respectively. For these configurations, 0.5-m and 1-m step intervals were used. On all profiles, the horizontal scale is distance in meters (m), and the vertical scale is presented as two-way travel time in nanoseconds (ns; right side of profiles) and depth in meters (m; left side of profile). Profiles were acquired with a 1,000 V transmitter and stacked 64 times with a time sampling rate of 800 ps. The profiles were processed and plotted in wiggle-trace and gray scale formats using PulseEKKO™ software.

The raw 25 MHz reflection data were first processed using a correction for signal saturation (DEWOW). This correction reduces the easily diffused low frequency component of the radar signal through high-pass filtering. The DEWOWED data were then filtered using automatic gain control (AGC) at GMAX = 500, and low pass filtered at 20% for spatial correction. To accentuate amplitude variations, the processed data were bandpass filtered (1,024 PT FFT) at frequencies of 10, 20, 30 and 40 MHz to remove noise. Processing of the 50 MHz data was similar to that accomplished for the 25 MHz data with the exception that bandpass filtering was performed for frequencies of 20-50 MHz and 60-80 MHz. Laser surveying equipment was used to collect elevation data along the GPR transect lines. Topographic corrections were applied to the profiles prior to filtering.

Data and Interpretations

The locations of the GPR transects were chosen for the purpose of identifying the gross morphologic and hydrologic characteristics of the rock glacier and for determining if a link can be established between internal structure and surface morphology. To measure the thickness of the rock glacier and to identify the internal structure (i.e., the nature and distribution of ice therein), a 440 m longitudinal transect (A-A') was made parallel to the long axis of the rock glacier using the 25 MHz antennae. The transect line,

which extends from the midpoint of the head area to the end of the toe, was routed over a prominent set of well-defined ridges and furrows on the youngest of the central flow lobes (Fig. 4.5).

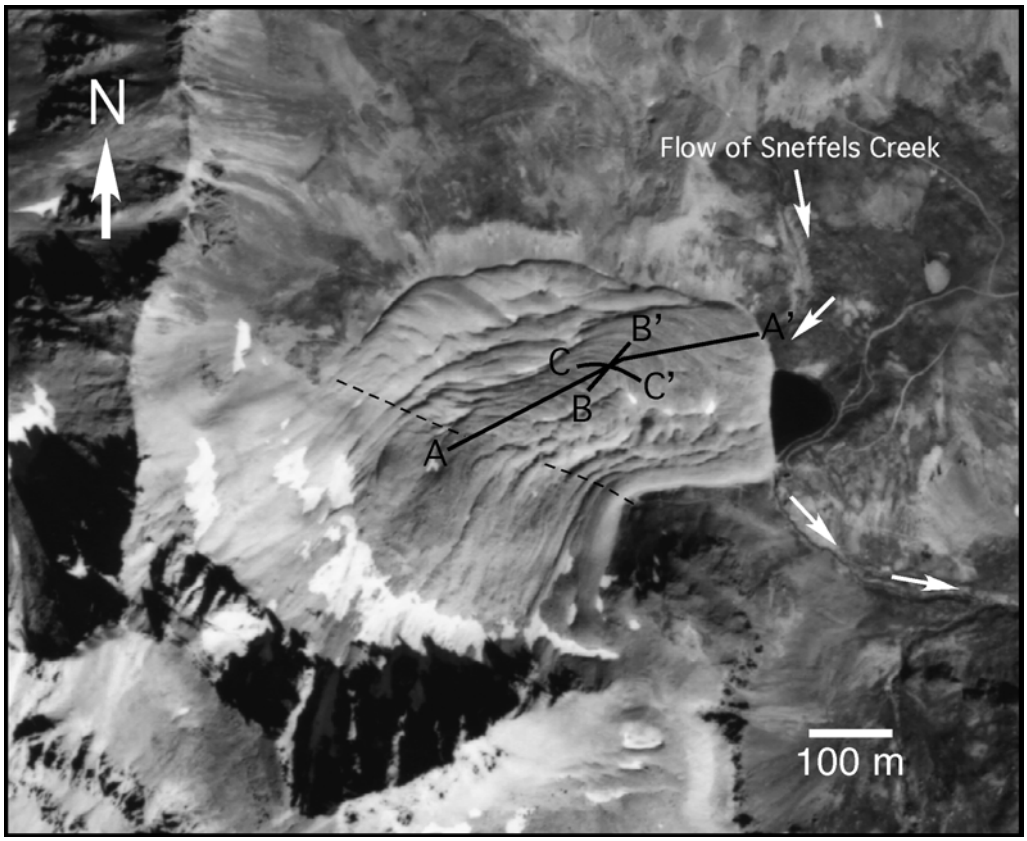

Fig. 4.5. Aerial photograph of the Yankee Boy rock glacier taken in 1979. The rock glacier is located at 37°59'N, 107°47'W. The image, cropped from a 9 x 9 inch 1:20,000 USDA photo, shows the rock glacier flowing down valley away from the headwall of the cirque. Cross section lines are shown for the radar profiles described in the text. Line A-A' is 440 m long (25 MHz), and lines B-B' and C-C' are 90 and 75 m long, respectively. The latter were collected using 50 MHz antennae. The 25 MHz CMP was made along C-C' and the dashed line marks the inflection of the rock glacier. Small arrows indicate the flow path of Sneffels Creek, which runs through the toe of the rock glacier.

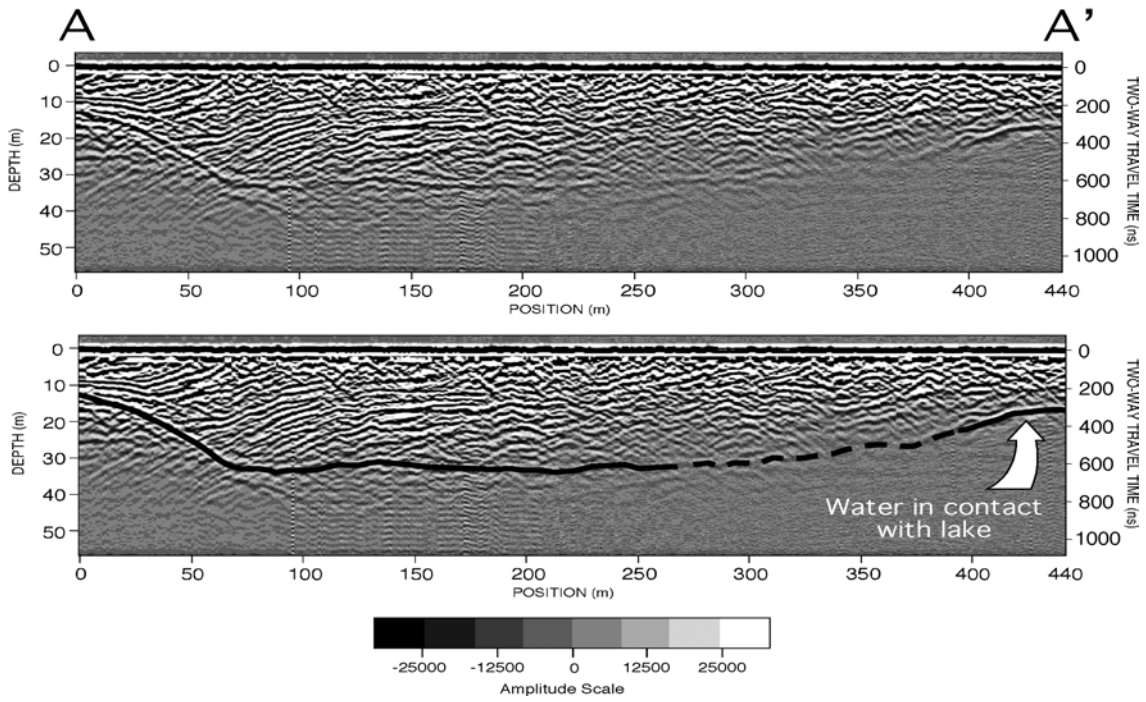

Fig. 4.6. Longitudinal profile collected using 25 MHz antennae (uncorrected for topography). Line marks the contact between the rock glacier and the cirque floor. The inferred (dashed) portion of the line indicates a zone along the bottom where the radarwaves were attenuated by (running) water. The strongly coherent reflection in the last 50 m of the profile is interpreted as collected water in contact with Wright's Lake, which is located at the right end of the profile.

Fig. 4.6 shows the longitudinal profile prior to topographic correction. The data were spatially filtered at 20% and at 15% to determine the limit of processing that could be applied. At a filtering level of 20%, the reflection horizons are sharp and continuous, but a zone of 'ringing' is noticeable at the bottom of the profile (from 95-210 m). At 15%, the ringing was effectively removed. However, the reduced variation in amplitude throughout the remaining signal eliminated much of the contrast needed to clearly resolve individual reflection horizons. Thus, 20% spatial filtering was used for interpreting the profile. The two earliest continuous reflections represent air-wave and ground-wave arrivals, respectively, and the strong continuous reflection at the bottom of the profile represents the limit of the velocity window and is not a detected feature.

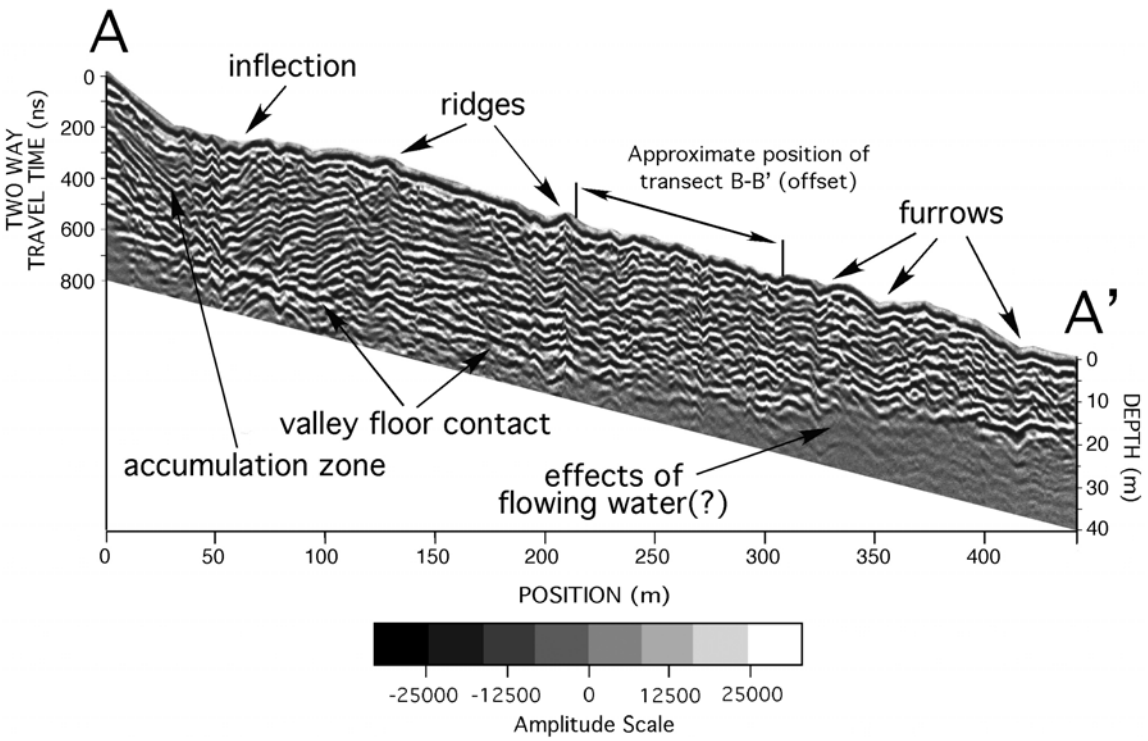

Fig. 4.7. Topographically corrected 25 MHz longitudinal profile. Corrections were made to the profile in Fig. 4.6 using laser survey data that was collected along the same transect line as the GPR survey. Note the relationship between undulations in the reflection horizons and surface topography. 20% spatial filtering was applied.

A noticeable feature of the topographically corrected profile (Fig. 4.7) is the sharp change in slope of the reflection horizons where the steep accumulation zone (0-60 m) transitions abruptly to ridges and furrows (~60 m). This inflection (see Fig. 4.5) marks a change in the slope of the cirque floor that corresponds to the onset of compression within the rock glacier. Reflection horizons in the accumulation zone are generally parallel to sub-parallel with the surface of the rock glacier. From 60–120 m (immediately beyond the inflection), the reflections are clear and continuous, and slant upward toward the surface of the rock glacier. Beyond 120 m, the reflections are generally parallel to the surface. It is significant to note that in the latter 320 m of the

longitudinal profile, bends in the reflections strongly correspond to topography of the rock glacier where ridges and furrows are well pronounced. Reflections are continuous up to 100 m.

Velocity Determinations – Common Midpoint Profile (CMP)

A radarwave velocity of 0.12 m/ns was established for the rock glacier medium using a common midpoint profile (CMP) and semblance analysis (solution at 70 ns; Fig. 4.8). The CMP, which was carried out along the first 40 m of transect C-C' using 25 MHz antennae, was used for depth conversion and processing of the raw GPR data (Fig. 4.9). The velocity value, which is slightly lower than those reported by Isaksen et al. (2000) and Berthling et al. (2000), likely represents frequency-dependent attenuation losses caused by the effect of fresh running water within the rock glacier. This reduction in velocity is expected to be greater at higher frequencies. To a lesser degree, dissipative losses by surface or volume scattering from heterogeneities on a scale close to the wavelength of propagation in the material may have been a factor. The pulse wave lengths (the product of frequency pulse period and velocity of the radarwaves) through the rock glacier medium, are 4.8 m and 1.8 m at 25 MHz and 50 MHz, respectively.

Unpublished descriptions of shallow (7.6 m) drill core recovered from the frontal area of the Yankee Boy rock glacier in 1997 confirm the presence of alternating 0.5-1 m thick layers of coarse ice-rich and ice-poor layers. The layers are composed of blocks and platy clasts that are predominantly less than 0.5 m size in the largest dimension. The overall ratio of debris to ice ranges from 60-70%, and some ice layers are comprised of up to 20-30% silts and fines. This is generally consistent with findings for drill core samples from other rock glaciers (Haeberli, 1985; Barsch, 1996).

The theoretical vertical resolution of the radar signals was calculated using the equation (e.g., Reynolds, 1997):

$$\lambda/4 = (V/F)/4 \qquad (4.1)$$

where λ is the wavelength (m), V is the radarwave velocity of the medium (m/ns), and F is the center frequency of the antenna (MHz). Using the 25 MHz antennae, the theoretical vertical resolution was calculated to be 1.2 m. Therefore, any layer visible on

the radar profile has a thickness greater than one meter. The reflection patterns are coherent down to 700 ns (~45 m), which is the detectable limit of the radar achieved at this frequency. The 50 MHz antennae provided depth of penetration to 500 ns (~32 m) and resolution of 0.75 m, given a calculated theoretical vertical resolution of 0.60 m.

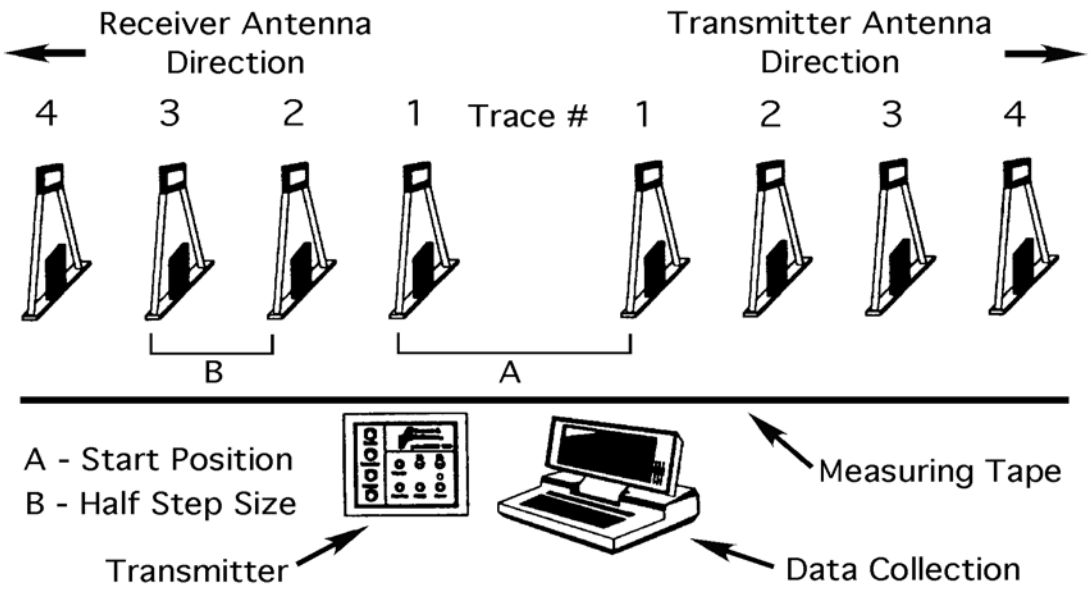

Fig. 4.8. Diagram illustrating the concept of collecting a common midpoint (CMP) profile for velocity determinations. The transmitting and receiving antennae are placed along a traverse perpendicular to the direction of movement. The antennae are moved at equal distance intervals (1/2 meter for 25 MHz antennae) from a common center point and separated until an average velocity value can be determined (using a representative, continuous reflection event in the profile), or when the maximum length of the fiber optic antenna cables is reached. The velocity value is determined by semblance analysis or by dividing the runout distance by the average two-way travel time for the given reflection horizon. This can be done by taking the inverse gradient of the reflection horizon as plotted on a T^2-X^2 graph (Reynolds, 1997). Diagram modified from Sensors & Software (1996).

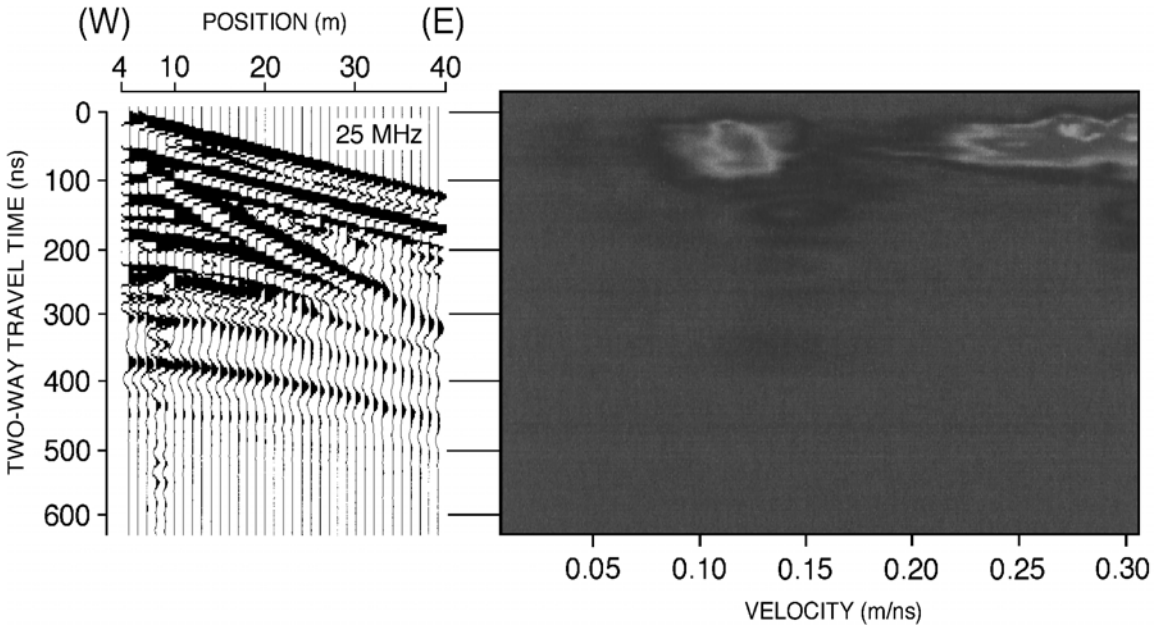

Fig. 4.9. Common midpoint profile (CMP) used for determination of the radarwave velocity through the rock glacier medium. The profile was obtained at a frequency of 25 MHz with a 1,000 V transmitter. A pulseEKKO™ 100A radar system from Sensors & Software, Inc. was used. The velocity value as determined from the semblance diagram on the right is 0.12 m/ns. The origin of the 'Position' (4 m) corresponds to the initial antennae separation at 25 MHz.

Hydrologic Character and Water Pathways

The resolution and depth of penetration at 25 MHz was sufficient to identify the contact between the rock glacier and debris-covered cirque floor, as well as materials 5-8 m below the cirque floor. The contact reflection is strongly coherent from 0-190 m along the profile, beyond which diffusion of the radar signal obscures the reflection patterns. In the last 50 m of the profile the reflections are again coherent. We interpret the zone of diffusion, which reaches at least 5 m above the contact between rock glacier and cirque floor, to be a collection area for water residing in the downvalley portion of the rock glacier. The strongly coherent reflection in the toe area is interpreted to be a water table that is in contact with Wright's Lake. This contact is supported by the observation that water from nearby Sneffels Creek enters the toe of the rock glacier on the north side and

exits the toe on the south side (see Fig. 4.5). At the end of the GPR profile (440 m), this reflection horizon is estimated to be 7-8 m above the rock glacier-cirque floor contact. This corresponds closely to the level of Wright's Lake, which was estimated to rise 8 m on the oversteepened toe of the rock glacier. Together with meteoric waters, springs, seeps, and other water input sources, the volume of water flowing in Sneffels Creek is more than sufficient to maintain a water table at the levels observed within the rock glacier during the summer months.

In addition to the stored water, a network of water pathways was detected in the headward portion of the rock glacier. These pathways are identifiable in the longitudinal profile as intermediate range amplitude signals that do not conform to the characteristic horizontal reflection horizons (Fig. 4.10). Such intermediate amplitude values are generated because the amplitude (and velocity) of radar waves are affected mainly by differences in the dielectric properties of the various phases encountered throughout the rock glacier (e.g., rock, ice and liquid water). Factors such as chemistry (i.e., salinity), state (liquid/gas/solid), distribution (pore space connectivity) and content of water also significantly affect the propagation of radar waves through the rock glacier medium. These affects are manifested in values of permittivity (the ability of a dielectric to store electrical potential energy under the influence of an electric field) for each of the phases. Fresh water (80 Farads/m) has a much higher permittivity than either freshwater ice (4 Farads/m) or granodiorite (~5 Farads/m). Thus, the observed amplitude variations can be attributed to the contrast between water and the solid phases of rock and ice.

To test the validity of this means of detection, locations were recorded along the longitudinal transect where running water was audibly detected just below the surface of the rock glacier. The locations and estimated flow directions were then plotted on an enlarged portion of the longitudinal profile. The locations of running water detected on the surface of the rock glacier correspond closely to locations along the profile where branches of the water pathway network approach the surface (see Fig. 4.10). The individual pathways, estimated to be 0.5–1.5 m in width, are in some places continuous from the surface of the rock glacier down to the cirque floor.

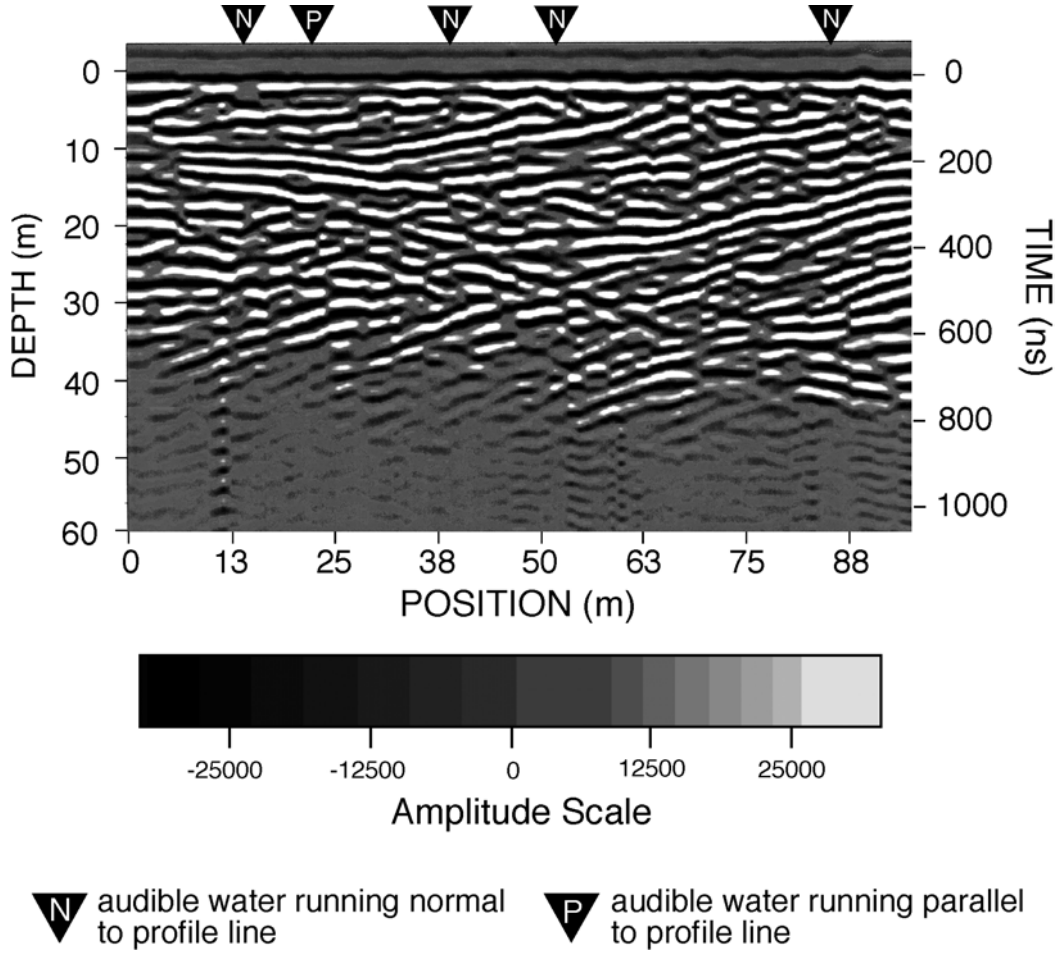

Fig. 4.10. Variations corresponding to phase differences throughout the rock glacier. Radar profile is rendered in shades of black, white and gray and includes the first 94 meters of the longitudinal profile. Alternating ice-rich and ice-poor layers are depicted in black and white. The network of gray colored lines is interpreted to represent liquid water. The recorded positions of audible running water just below the surface of the rock glacier correspond well with locations where branches of the network meet the surface.

Ridge and Furrow Morphology

To determine if ridge and furrow morphology is a manifestation of subsurface processes, two 50 MHz GPR transects were made on a section of the Yankee Boy rock glacier where ridge and furrow structure is prominent (see Fig. 4.5). By providing greater resolution, these profiles were useful for interpreting the 25 MHz longitudinal profile described above. Profile B, a 90-m transect (B-B', Fig. 4.11), was made following a line oriented normal to ridges and furrows. The transect was located in close proximity to the 440-m longitudinal transect and rotated counterclockwise approximately 15° to maximize normalcy to the transverse ridges and furrows. Profile C, also collected using 50 MHz antennae, consists of a 75-m transect (C-C', Fig. 4.12) made along the top of a prominent ridge in the sequence. It trends in a direction orthogonal to Profile A and provides a perspective that is normal to the ridge axis.

The 50 MHz radar results show that the internal structure of the rock glacier consists of parallel to sub-parallel layers of ice-rich and ice-poor strata. The laminated and overlapping character of the material is consistent throughout the sampling area and is continuous in all transect directions. This indicates that layering is continuous in the direction of ridge and furrow development as well as normal to it and implies that the layers were deposited by voluminous flows of rock debris that occasionally buried substantial amounts of snow pack on the surface of the rock glacier. The layering is deformed predominantly by folding, and fold fabric is evident throughout the entire thickness of the rock glacier. Minor faulting was also detected, mainly in the upper portions of the profiles. This aspect, however, does not appear to be the predominant mode of deformation within the rock glacier.

Contemporary Investigations

To date, limited research involving the application of GPR to rock glaciers has been carried out (e.g., Berthling et al., 2000; Degenhardt et al., 2000, 2001; Isaksen et al., 2000). In a recent study, Isaksen et al. (2000) used GPR to investigate the composition, flow and development of two tongue-shaped rock glaciers in the permafrost of Svalbard, Norway. Using 50 MHz antennae, they obtained a 303 m longitudinal profile following

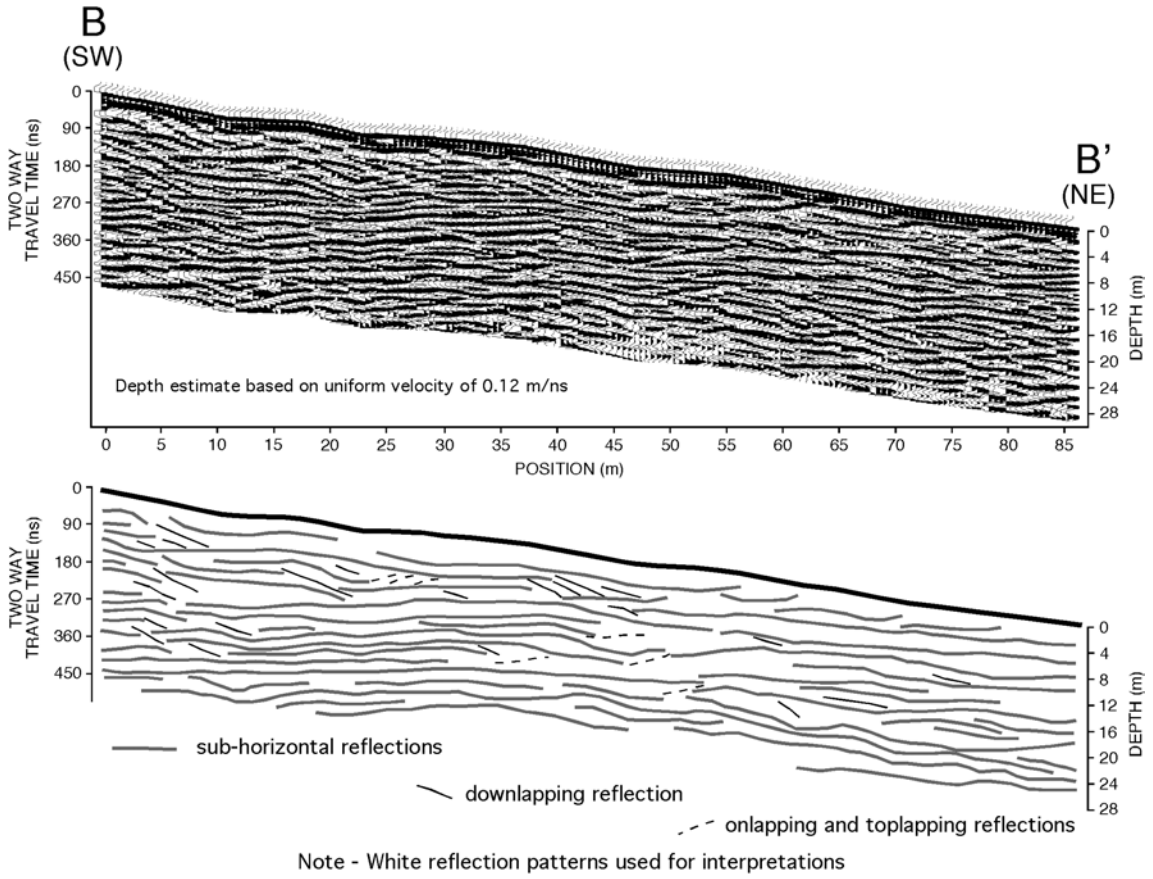

Fig. 4.11. Topographically corrected GPR profile trending southwest to northeast along transect line B-B' shown in Fig. 4.5. Top: processed data without interpretations; Bottom: processed data showing interpretations based on mappable stratigraphic reflection horizons. Data was processed using software provided by Sensors & Software, Inc. Equipment includes a 1,000 V transmitter and 50 MHz antennae. A 2-m antenna spacing was used and data was collected using 0.5-m step intervals. The two earliest continuous reflections represent air-wave and ground-wave arrivals, respectively.

the central flowline of the Hiorthfjellet rock glacier. The results show a clear reflection horizon to 15-20 m depth with reflections disappearing completely at 25 m. Along the profile line reflection horizons transition from parallel or slanting orientations relative to the surface, to horizons that dip upward in the mid-section (downslope) portions of the

profile. These reflection horizons were interpreted to represent the end of a steep talus cone that marks a transition between the accumulation zone and the lower part of the rock glacier (Isaksen et al., 2000). Based on exposures in a lobate rock glacier near Longyeardalen, Norway, reflection horizons from the Hiorthfjellet rock glacier are believed to be caused by layers of ice alternating with layers comprised of fine material and blocks.

In another study, Berthling et al. (2000) used GPR to investigate internal structures in four rock glaciers located in the continuous permafrost zone on Prins Karls Forland, western Svalbard. The longitudinal profiles obtained in that study revealed a system of reflectors that was comparable between the different rock glaciers. As observed in the Hiorthfjellet rock glacier, a layering structure parallel with the surface is visible in the upper parts of the profiles where the talus cones above the rock glaciers are located. Farther down profile, towards the rock glaciers, these reflectors are oriented at a slant against the surface slope. It was concluded that the layering formed by mass movements of higher magnitude that covered snow patches or the active layers above supersaturated permafrost.

CMP velocities at Yankee Boy rock glacier are significantly lower than the 50 MHz values in the studies above. A velocity of 0.15 m/ns was obtained for the Murtèl-Corvatsch rock glacier (Lehmann et al., 1998) and the Brøggerbreen rock glacier near Svalbard yielded a value of 0.14 m/ns (Isaksen et al., 2000). The low velocity values obtained in this study can be attributed to the presence of running (liquid) water throughout the Yankee Boy rock glacier, and to a lesser degree, by high attenuation in the conductive sand- and silt-rich ice layers that comprise the upper portions of the rock glacier.

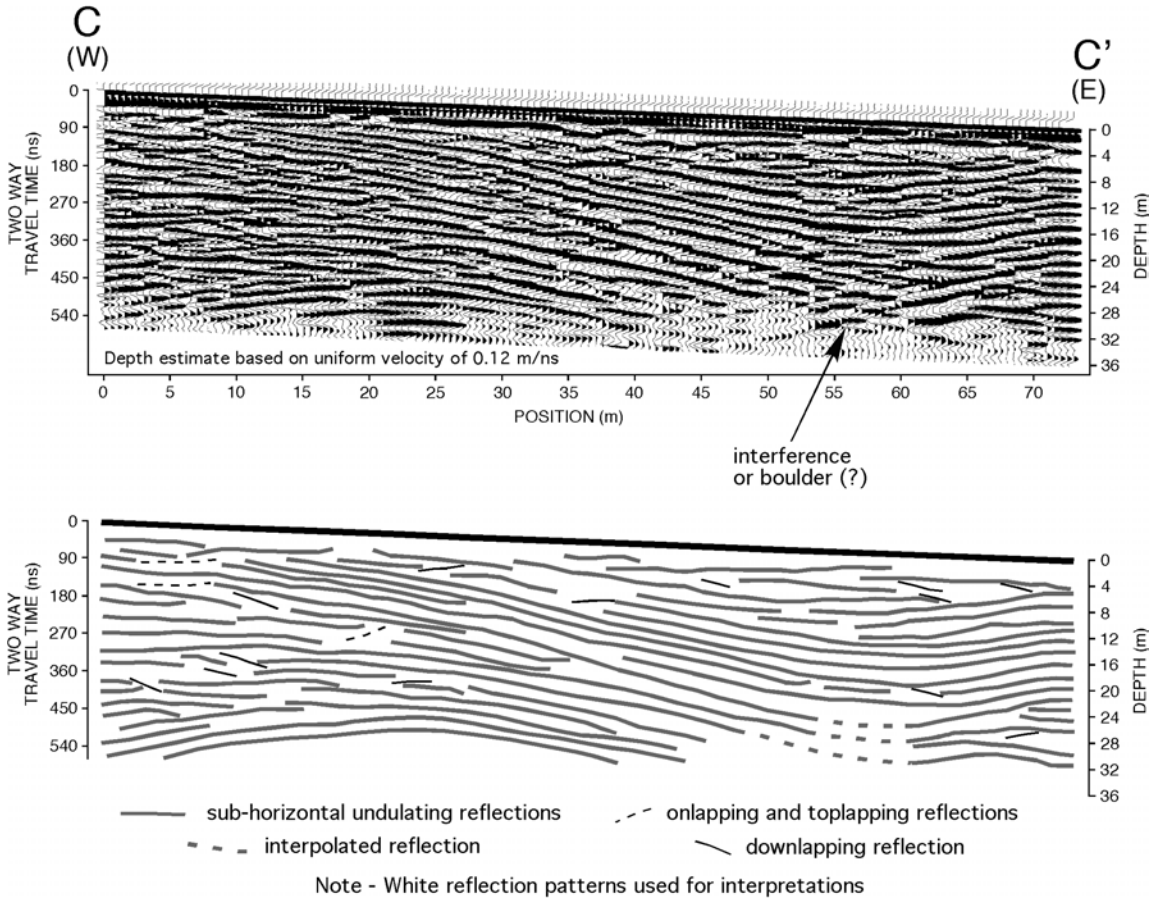

Fig. 4.12. Topographically corrected GPR profile trending west to east along transect line C-C'. The transect runs along a single prominent ridge (see Fig. 4.5). Top: processed data without interpretations; (Bottom: processed data showing interpretations based on mappable stratigraphic reflection horizons. The concave folding in the right half of the profile is interpreted to represent infilling of a longitudinal furrow by overriding flow lobe materials. Equipment included a 1,000 V transmitter and 50 MHz antennae. A 2-m antenna spacing was used and data was collected using 0.5-m step intervals. The two earliest continuous reflections represent air-wave and ground-wave arrivals, respectively.

RESULTS – IMPLICATIONS FOR LANDFORMS ON MARS

Rock Glacier Development

The pioneering work of Wahrhaftig and Cox (1959) suggested that rock glaciers formed by permafrost processes to create a frozen mixture of rock debris and ice within talus or morainal deposits. Since then, it has been found that rock glaciers occur as a physical response to three types of geomorphic processes: (1) glacial, (2) periglacial [Johnson, 1984], or (3) talus (as illustrated by Shakesby et al., 1987). They often represent transitional forms in the landscape continuum, a geomorphologic concept developed by Giardino and Vitek (1988b) (Fig. 4.13). With the advent of new technology and increased interest in recognizing and studying rock glaciers, these ideas have been affirmed and expanded through subsequent studies. A few of these studies provide evidence of thick massive ice in the rock glacier interior and suggest that these forms are debris-covered glaciers (Potter, 1972; Whalley, 1974; Clark et al., 1994; Whalley et al., 1994; Potter et al., 1998) or forms that originated as perennial snowbanks or glacierets Haeberli (2000).

Terrestrial rock glaciers are generally situated at the bases of massive, homogeneous and fractured cliffs and are rarely found where debris is finely crushed or where headwall fractures are excessively large (Wahrhaftig and Cox, 1959; Evin, 1987). Source material is loosened by freeze-thaw action and transported by gravity downvalley or down escarpment, where it accumulates in locations of gradient decline (White, 1971).

The general conditions for the formation of rock glaciers have been reviewed by Corte (1987):

(a) relatively young mountain ranges having bedrock with rock mass properties (e.g., joint spacing, weathering characteristics, etc.) favoring the formation of blocky debris;

(b) microclimate conducive to daily freeze-thaw cycles or frost weathering, sufficient ground moisture for periglacial processes, low to moderate snowfall sufficient for production of debris and avalanche, and low insulating snow cover;

(c) a combination of geographic position (e.g., latitude, elevation) and climate conditions (e.g., temperature, aspect) that promote periglacial processes and sustained subzero ground temperatures; and

(d) talus supply promoted by steep, rough terrain, perhaps by debris from a previous glaciation, frequent freeze/thaw cycles, and rock mass properties.

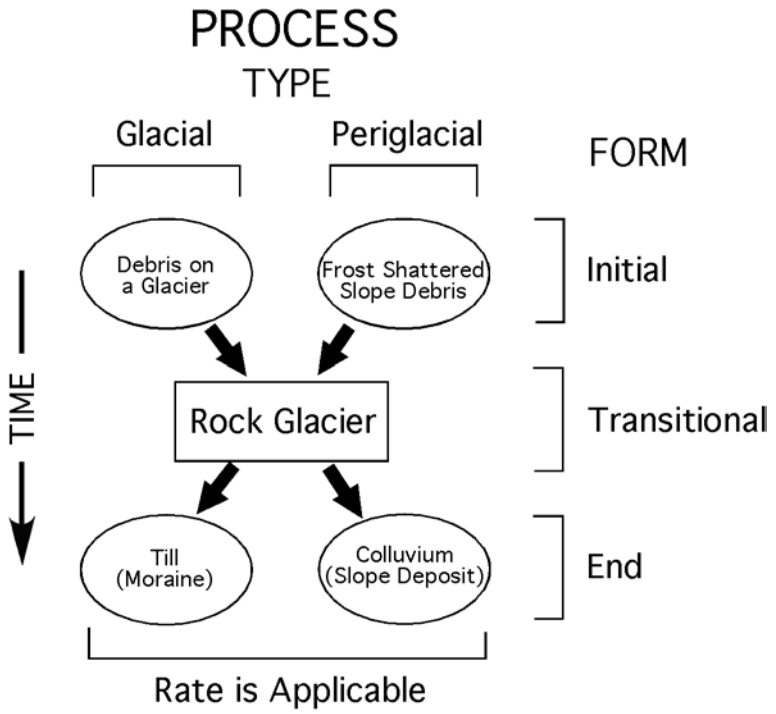

Fig. 4.13. Diagram illustrating the alpine landscape continuum. Rock glaciers are transitional forms that can develop from two distinct processes and can progress to two distinct end-members. Rate of movement is related to process, not form (modified from Giardino and Vitek, 1988b).

On Mars, the material that comprises the insulative cover for lobate debris aprons and valley fill is also thought to be the product of rockfall processes (Lucchitta, 1984; Squyres, 1988; Carr, 1995). The production of regolith materials suitable for

development of viscous flow features is largely attributed to meteorite impact, a process that played a major role in the structural evolution of the Martian crust (Soderblom et al., 1974).

Results of this GPR investigation show that the internal structure of the Yankee Boy rock glacier was formed by permafrost processes rather than by covering of remnant glacial ice. The distinct reflection horizons of the GPR profiles are discernable from the surface of the rock glacier to the bottom contact with the valley floor. These horizons depict the accumulation of snow/ice layers toward the upper reaches of the rock glacier and creeping permafrost where the valley slope declines. We interpret these horizons to represent units of alternating layers of talus or rockslide debris and ice lenses and/or ice supersaturated sediments. The ice-rich layers are most likely formed by accumulation of seasonal snow, which, upon burial by pulses of headwall debris (i.e., via large mass movement events), are buried and compacted. This mechanism of ice formation is believed to be the most important accumulation process for the rock glaciers investigated in Svalbard, Norway (Isaksen et al., 2000; Berthling et al., 2000). Based on observations from limited amounts of recovered drill core and from GPR profiles generated in this study, the overall percentage of ice comprising the Yankee Boy rock glacier is estimated to be 30-40%.

Ice Sustainability and Flow

For ice to be sustained within a dynamic (creeping) landform, minimizing the amount of insulation is required to reduce ablation of the permafrost (cryolithospheric ice). Haeberli et al (1998) found that the temperature beneath the 3-m thick active layer of the Murtèl rock glacier remains negative throughout the year. For example, temperatures recorded in a 11.6-m borehole at the Murtèl/Corvatsch rock glacier showed that the mean annual ground temperature generally increased from –2.3°C in 1987 to –1.4°C in 1994 with intermittent cooling during the interim years of 1994 to 1996 (Vonder Mühll et al., 1998). Permafrost in alpine rock glaciers, however, is relatively warm and typically tens of meters thick with temperatures commonly vary around 0°C at depth. Considering the thermal inertia of ice-rich permafrost it is reasonable to assume that, in

general, permafrost conditions have existed within alpine rock glaciers since the end of the last ice age (Lunardini, 1996). The effects of snow cover may play an important role in regulating ground temperature and may likely influence the relations between the atmosphere and permafrost. To some degree, ventilation and cold air circulation within the blocky active layer also regulates the coupling between atmosphere and permafrost on mountain slopes and rock glacier surfaces (Bernhard et al., 1998). Vonder Mühll et al. (1998) attribute the variability of observed permafrost temperatures to summer radiation and air temperature influences on the active layer, snow cover history, and shortened periods of negative temperatures during autumn months. Although the contribution and magnitude of these effects are likely to be significantly different on Mars, it is expected that they do play an important role in the preservation and location of water within viscous flow features there.

A model of ice stability formulated by Farmer and Doms (1979) suggests that anywhere temperatures in the top 10 m of the Mars regolith exceed 198°K, ground ice will become unstable and can sublime and diffuse into the atmosphere. Thermodynamic models by Clifford and Hillel (1983) and Mellon and Jakosky (1995) produced similar results suggesting an ice-free region between ±30° latitude. Our study shows that a blocky debris mantle 1–5 m thick insulates the Yankee Boy rock glacier during summer months. The mantle also serves as an interchange for compacting snow that accumulates in the winter months (Fig. 4.14).

In cases where appreciable amounts of rock detach from a headwall or escarpment, a much thicker debris cover could be attained. For example, terrestrial rock glacier mantles of 1–10 m are not uncommon (Clark et al., 1994). Martian analogs, which are generally an order of magnitude larger than terrestrial rock glaciers, may have debris mantles that are considerably thicker. Using shadow lengths, Squyres (1988) estimated thicknesses between 500 and 900 m for debris aprons ranging in radial length from several kilometers to >15 km. A mantle of such thickness may be sufficient to preserve interstitial water ice or ice lenses long enough to achieve the type of flow length observed in landforms situated poleward of ±30° latitude on Mars.

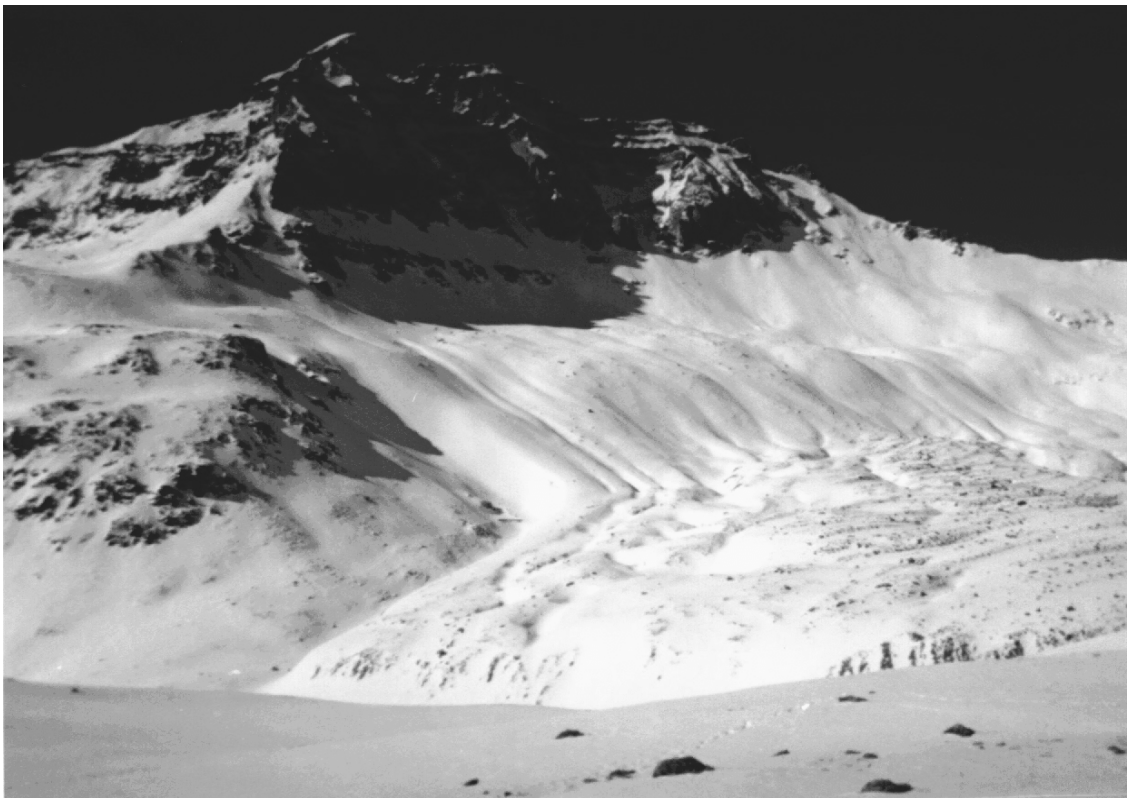

Fig. 4.14. Snow-covered rock glacier at Yankee Boy Basin. Seasonal layers of snow are most persistent in the accumulation zone. Permafrost is generated by a process of compaction and accumulation in the active layer.

In a study of ice flow characteristics on Mars, Colaprete and Jakosky (1998) used a simple model based on Glen's flow law to demonstrate the effects of ice temperature, accumulation rate, and purity on ice flow velocities in viscous flowing landforms:

$$\sigma_{xy} = A\tau_{xy}^{n} \tag{4.2}$$

$$A(T) = A_0\left(-\frac{Q}{RT}\right) \tag{4.3}$$

$$A(T) = 2.207 \times 10^{-5}\left[\frac{3155}{T} - \frac{0.16612}{(273.39 - T)^{1.17}}\right]^{n} \qquad (4.4)$$

where: equation (4.2) represents the relation between shear strain rate (σ) and shear stress (τ). The coefficient *A* and exponent *n* represent the dependence on ice temperature, crystal orientation, impurity and other factors. *A(T)* is the variation of coefficient *A* with respect to temperature (measured in Kelvins) according to the Arrhenius relation, where A_o is the temperature independent constant, *R* is the universal gas constant, and *Q* is the activation energy for creep (Paterson, 1994). Equation (4.4) is an empirical relation developed by Hooke et al. (1972) for *A(T)* across all temperatures below freezing.

Results by Colaprete and Jakosky (1998) suggest that ice temperatures must be greater than 220°K, and the net ice accumulation rate >1 cm/yr to produce the smallest observed rock glaciers. They calculated that at this temperature and accumulation rate it would take ~10^6 years to produce a 15-km flow, which is the average size flow observed on Mars. It was further concluded that formation times greater than 10^6 years are unlikely based on the climate fluctuations caused by variations in planetary obliquity and inclination (Mellon and Jakosky, 1995). Ice held only in debris voids (i.e., at saturation or below) will have high yield strength and creep rates will be very low, if it occurs. Thus, ice within a body of debris will contribute to movement only when contained in lenses or similar masses. Furthermore, creep will only occur when these lenses or masses are interconnected or highly contiguous.

If it is accepted that lobate debris aprons are commonly comprised of ice-cemented soils or ice-debris mixtures (e.g., Squyres, 1988; Carr, 1995), then consideration must be given to the condition that small concentrations of solid impurities in interstitial ice (at temperatures below 220°K) would reduce the flow velocities of Martian rock glaciers by an order of magnitude. For ice impurities of 30% or greater, flow velocities are so low that the time required for ice to reach the length of the features observed would exceed

10 Myrs (Colaprete and Jakosky, 1998). Considering this discrepancy in flow rate versus landform size, a less viscous (i.e., soluble) component may be strongly affecting the rheology of the ice. Such a component is needed to generate large viscous flow features such as those observed under current Martian conditions (surface temperatures around 200°K for frost and accumulation rates of ~1 cm/yr). Under certain climatic and cryolithospheric conditions, liquid water may be a sustainable component that contributes significantly to the overall deformation.

Role of Water

Numerous major geologic features on Mars appear to have formed by the release of large volumes of water from beneath the surface. Based on our current state of knowledge about the history of the planet in terms of water and ice, there is no obvious way that such a volume of water could have been lost from the planet since the development of these features (Squyres et al., 1992). Outflow channels, however, provide persuasive evidence that a large reservoir of groundwater was stored in the Martian crust throughout its first billion years of geologic history (Baker, 1982; Carr, 1986).

Under the influence of gravity, groundwater will drain to saturate the lowest porous regions of the crust. A subpermafrost groundwater system is viable if the present inventory of H_2O on Mars exceeds the quantity required to saturate the pore volume of the cryolithosphere. Once the pore volume of the cryolithosphere has been saturated with ice, any additional subsurface H_2O will inevitably be stored as groundwater (Squyres et al., 1992). Estimates by Clifford (1993) and Clifford and Parker (2001) indicate that a planetary inventory of H_2O equivalent to a several hundred meter-deep global ocean may satisfy this condition. Given an exponential decline in crustal porosity with depth, a groundwater inventory equivalent to a 100-m global ocean would then be sufficient to create a global aquifer nearly 4.3 km deep, assuming reasonable values of surface porosity (20-50%) and an exponential decay constant of 2.82 km (Clifford, 1993). This range of porosity values is consistent with estimates of the bulk porosity of Martian soil as analyzed by the Viking Landers (Clark et al., 1976).

The hydrologic characteristics of the Yankee Boy rock glacier substantiate the presence of a water table and networks of interconnected water pathways throughout the layers of permafrost within (Fig. 4.15a). The input sources for these water systems include streams, meteoric water/snow/ice, valley side runoff, lake water, springs, and frost. In light of the evidence provided for outflow channels on Mars, and the close proximity with which lobate debris aprons and other viscous flow bodies occur to them, it is possible that a number of these water sources have contributed to the development of ice-rich landforms. Channels or tables of liquid water and pure water ice residing within the permafrost (i.e., cryolithospheric material) for finite periods of time may be capable of initiating or sustaining the rates of deformation demonstrated by the lobate debris aprons and rock glaciers on Mars. It may even be possible that the dominant source of ice within these landforms originated from the subsurface as liquid water. Ice formed by the recharge of liquid water originating at depth (e.g., from outflow channels) could conceivably compensate for the volumes of ice lost to ablation in latitudes between 30° and 60°. Current models of rock glacier formation do not account for such a process. Fig. 4.15b provides a conceptualized model for the internal structure of a Martian rock glacier and possible sources of water ice based upon findings from the surrogate rock glacier at Yankee Boy Basin.

Flow Dynamics and Kinematic Properties

Kinematic properties have been used to describe a variety of geomorphic systems including pool and riffle development, ice glacier surge, distributed stream flow, and slow mass movement (Langbein and Leopold, 1968; Gerber and Scheidegger, 1979). Kinematic wave theory, as applied to glaciers (Lighthill and Whitman, 1955) and rock glaciers (Olyphant, 1987), requires that a wave of increased discharge (kinematic wave) travels down the rock glacier at a speed greater than the mean velocity of the surface (Nye, 1960). The propagation of a kinematic wave can explain the discrepancies observed in rock glacier movement (rate and distance) as compared to talus supply rate

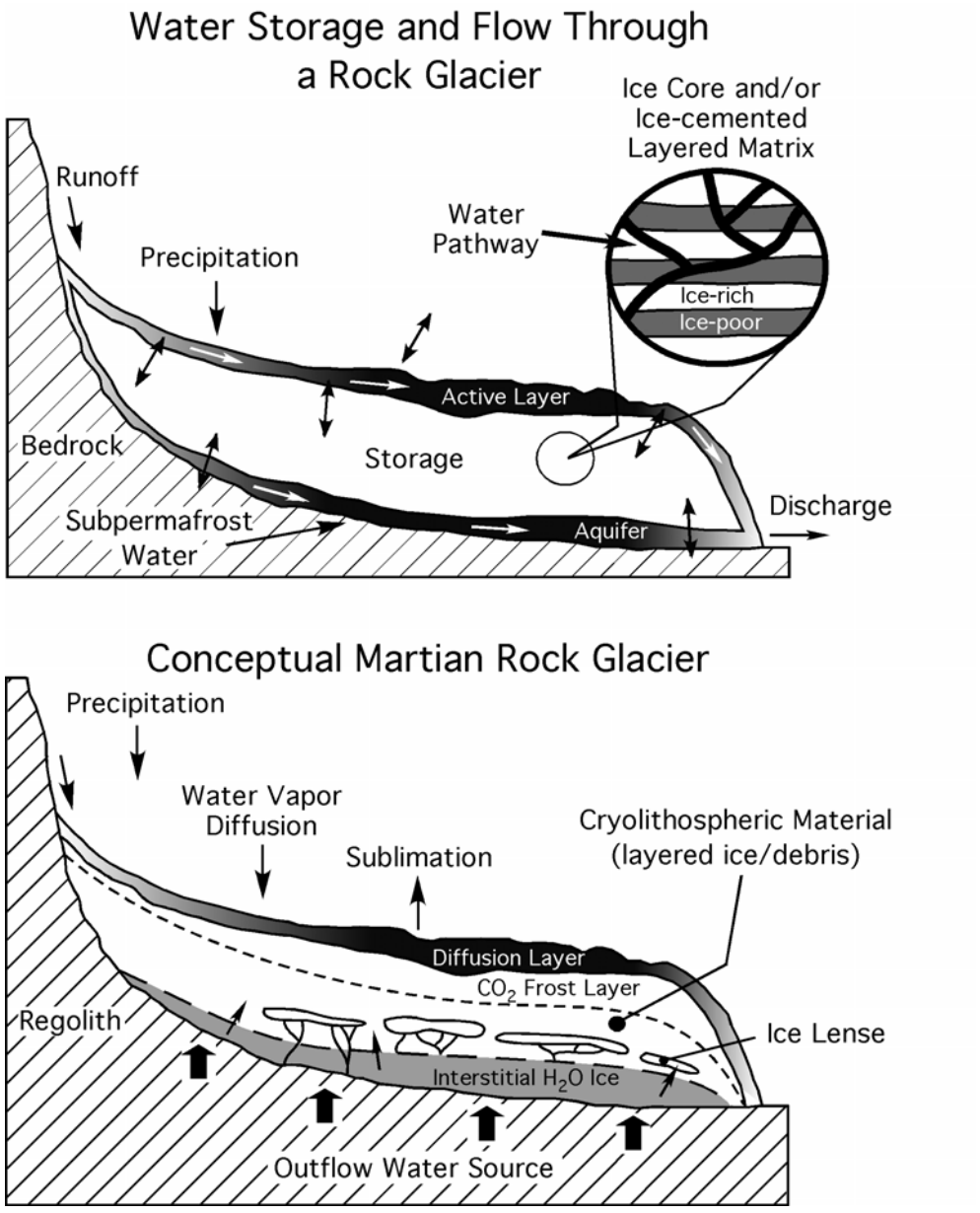

Fig. 4.15. Diagrams illustrating water storage and flow through a terrestrial rock glacier and a conceptual Martian rock glacier based upon information obtained from terrestrial rock glaciers. Water entering the rock glacier system from outflow channel sources is transmitted upward through pore spaces, fractures, and zones of weakness. A network of water pathways is formed when the (warmer) water exploits pore spaces and melts through areas of weakness within the cryolithospheric material. The pathways terminate in lense-shaped pockets, with the remainder forming a water ice table at the base. Top diagram modified from Giardino et al., (1992).

(Birkeland, 1973; Miller, 1973; White, 1987). Such a mechanism also allows for a disproportionally high rate of movement in the toe of a rock glacier with little or no increase in talus supply rate at the head. Thus, rheologic properties that govern movement may not control morphological development of the landform (i.e., kinematic wave motion may control form development even though mass and force control movement potential). Further, such development may be independent of variations in the driving forces responsible for the overall rheological properties (Giardino and Vitek, 1988).

The layering exhibited in the Yankee Boy rock glacier is not consistent with glacial and periglacial models that call for deformation exclusively by faulting or surface-relegated (skin) folding (e.g., Whalley et al., 1983; Johnson, 1984). The depth of folding within the rock glacier indicates that energy is being transmitted through the major depositional units comprising the landform (i.e., through a succession of flow lobes), and not preferentially along the upper or lower portions. Haeberli (1985) notes that the surface of a rock glacier will deform into sequences of folds when: (1) compression develops parallel to the flow direction and (2) viscosity decreases downward from the surface of the rock glacier to the interior of the mass. The geometry of distinctive ridges and furrows and the internal structure observed at Yankee Boy suggests that folding is linked to propagation of the rock glacier. It also appears that the major units depicted in the longitudinal GPR profile represent distinct depositional episodes or overriding flow lobes. Currently, the most accepted model for the deformation of a rock glacier (i.e., Glen's Flow Law creep), does not take into account this type of folding or composite depositional effect. Efforts to refine the flow model must account for this internal structure, and considerations involving the movement of viscous-flow features on Mars should also include this phenomenon (Degenhardt et al., 1999a, 1999b).

SUMMARY AND CONCLUSIONS

Rock glacier-like features on Mars suggest the presence of flowing, or once-flowing ice-rock mixtures. These landforms, which include lobate debris aprons, concentric crater fill and lineated valley fill, hold significant promise as reservoirs of stored water ice that could be useful for human exploration of Mars. They may also contain frozen records of the climatic history of the planet. As such, it is important to understand the deformation and distribution of ice within these landforms. Using terrestrial rock glaciers as surrogates, we can apply the knowledge gained about internal structure, landform morphology, viscous flow properties, and the role of water to learn about the formation, internal character and deformation processes of Martian analogs.

Results obtained from the rock glacier at Yankee Boy Basin show that the landform is comprised of distinct, continuous alternating ice-rich and ice-poor layers. Folds in the layers correspond to the surface expression of ridges and furrows, indicating that compressive stresses originating in the accumulation zone are transmitted downslope through the rock glacier. Thus, ridge-furrow topography is interpreted to be a surface manifestation of this process. Rock glacier features on Mars may also consist of layered permafrost ice and ice lenses, which would suggest a history of permafrost development involving seasonal frost accumulation and/or water influx from below the surface. Based on estimated thickness of lobate debris aprons and valley fill, and given the current climate and atmospheric conditions on Mars, mantle insulation may be sufficient to preserve water ice within these landforms.

Liquid water, found to be abundant in the Yankee Boy rock glacier, occurs as a network of interconnected channels that permeate throughout the landform. In terms of water storage within Martian analogs, considerations must include the possibility that some water ice may be stored in relatively pure form within lenses and vein networks such as observed in the Yankee Boy rock glacier. Proximity of viscous-flow features to outflow channels indicates that a plentiful supply of water once flowed on the surface of Mars. If the total water budget of Mars exceeds the amount of ice stored within the Martian regolith, then the presence of liquid water beneath the surface is probable.

Subterranean water could serve to replenish or to maintain the content of ice within Martian rock glaciers, thus providing a mechanism to perpetuate their flow for periods of time necessary to account for their size given current temperatures. Such water ice could be preserved within debris mantles of sufficient thickness, particularly if the mantles contain an insulating layer of frozen CO_2.

Results of this work are also being used to test the concept of kinematic wave theory as applied to the dynamics of rock glacier movement. A kinematic wave model is appropriate because it considers motion and does not rely on the influences of mass and force, parameters that are poorly understood given the current knowledge of rock glaciers. Such evidence provides a better foundation for the use of rheological models that are required if rock glaciers are to be used as surrogates for evaluating water sources on Mars.

This work is an important step toward understanding the fundamental development processes for rock glaciers. The flow dynamics of these and similar landforms can be understood only with knowledge of internal structure and composition. The results obtained in this study point toward the need for developing lighter and smaller remotely operated robotic GPR systems that can be sent to Mars. Development of lighter, more compact wireless systems should also be pursued for the eventual presence of human visitors to the planet.

CHAPTER V

INTERPRETATION OF A BLOCK STREAM IN TOM MAYS CANYON, FRANKLIN MOUNTAINS, TX

OVERVIEW

The origin of the block stream in Tom Mays Canyon is reconsidered in light of new data on surface fabric, longitudinal profile shape, topographic cross-sections, and local geologic factors. Eigenvector analysis of fabric data from six transects along the block stream shows a close association with lowland tills of glacial origin and talus slopes, but no similarity to trends for ridge and furrow structures associated with rock glaciers. The absence of segments above and below the regression least-squares line (LSL) for surface roughness indicates a single episode of deposition that resulted in a coherent morphological unit. Hummocky surfaces and lobate portions of the block stream, whose origins have been a source of controversy in previous investigations, are interpreted to be the result of sudden braking of material that underwent rapid transport via grain flow and/or acoustic fluidization. High-speed emplacement is supported by the observation that the block stream is detached from its point of origin at the cliff face and superelevated along steep walls of the canyon downvalley. Considering the nature of the fabric data, and based on the relationships between estimated volume and mean gradient (H/L), it is suggested that the Tom Mays feature is a small sturzstrom.

INTRODUCTION

The geomorphic implications of the block stream at Tom Mays Canyon have been addressed principally through the works of Lovejoy (1972, 1973) and Shroder (1973b). Lovejoy (1972) argued that the feature formed in a manner similar to that of a debris flow containing large clasts. He concluded in particular that the flow formed via

“boulder-charged surges” as a result of flash flood waters that liberated stream-clogging accumulations of rhyolite boulders formed during cold Pleistocene climates. Although Lovejoy discounted rubble streams and rock glaciers as applicable to the Tom Mays deposit, he believed these surges were responsible for topographic forms on the block stream that are similar to those of rock glaciers and certain alpine felsenmeers (i.e., lobate form and transverse ridges that are convex downstream). He further concluded that the surface form most nearly resembles the "frost lag rubble streams" described by Richmond (1962), but did not form in situ in the same way.

Shroder (1973b) suggested that Lovejoy’s model for flash-flood deposition of the block stream should be considered one of several working hypotheses based on the premise that it is not always possible to distinguish between inactive landforms produced by different flow processes (equifinality). He emphasized four possible mechanisms that could have produced such a landform through a complex combination of some or all of the following processes: (1) washing out of fines after deposition of debris; (2) frost-induced, rock-stream, or rubble-stream deposition; (3) rubble flow and sieve deposition; and (4) landslip deposition. For example, evidence for landslip in boulder deposits around the Aquarius and Table Cliffs plateaus in Utah prompted Shroder (1972) to suggest that surficial and topographic elements of the Tom Mays block stream may be attributable to landslip, and that landslip should be considered as a plausible mechanism of movement. Through the course of exchange between Lovejoy and Shroder, the question was raised as to whether the deposit is partly the result of rapid or slow debris flow(s) subsequently flushed clean of fines, or if it is partly the result of movement of a blocky veneer over fine clastic rocks. To date, a satisfactory explanation for the origin of the block stream at Tom Mays Canyon has not been established.

In this study we refine the interpretation for the formation of the Tom Mays block stream through the introduction of new fabric data, volume estimates, aerial photo analysis, and topographic cross-sections. The purpose is to reduce the number of plausible interpretations for the formation of this feature and ideally to settle on the most plausible mechanism of deposition.

MORPHOLOGY OF THE TOM MAYS BLOCK STREAM

The Tom Mays block stream has been characterized by Shroder (1973b, p.3745) as "…an unusual boulder deposit" following the thalweg of Tom Mays Canyon in the Franklin Mountains of West Texas (Fig. 5.1). It is situated 0.5 km to the northwest of North Franklin Mountain, which is located just outside of Tom Mays Park (Fig. 5.2). The head of the canyon forms the north face of North Franklin Mountain, which is a component of a tilted fault block. With a total elevation of 2132 m, it is the highest peak in the Franklin Mountains. Precambrian and Paleozoic strata strike north to northwest and Precambrian igneous rocks dip west at angles between 25° and 45°, and at steeper angles along the western range front (Figs. 5.3a, b).

The block stream is composed of coarsely elongate angular clasts of rhyolite commonly measuring 30-50 cm in the longest dimension. It is approximately 378 m (1,240 ft) long and 31 m (100 ft) to 91 m (300 ft) wide with an average thickness of about 3 m (Figs. 5.4a, b). Maximum relief is estimated to be 3 m (~10 ft) above the valley sides and between 2 and 3 m (~7-10 ft.) on average. The surface is hummocky along the widest portions of the block stream and a small number of transverse ridges are present toward the downvalley end of the deposit. Several scars are also evident along the east wall of the canyon, immediately upstream from the location where the deposit begins (see Fig. 5.4a). The scars originate just below rhyolite outcrops near the ridgeline and extend down to the thalweg of the canyon. The bulk of the block stream material appears to have been supplied and transported along the northernmost scar, which terminates directly at the head of the block stream deposit. According to Lovejoy (1972), the block stream deposits probably began to form in the early Pleistocene, subsequently clogging stream channels and gulleys as talus was detached from the rhyolite canyon walls during episodes of colder climate.

Topography

Cross-sectional topographic profiles made at five locations along the block stream show distinct changes in the distribution of material across the canyon (Fig. 5.5). It is

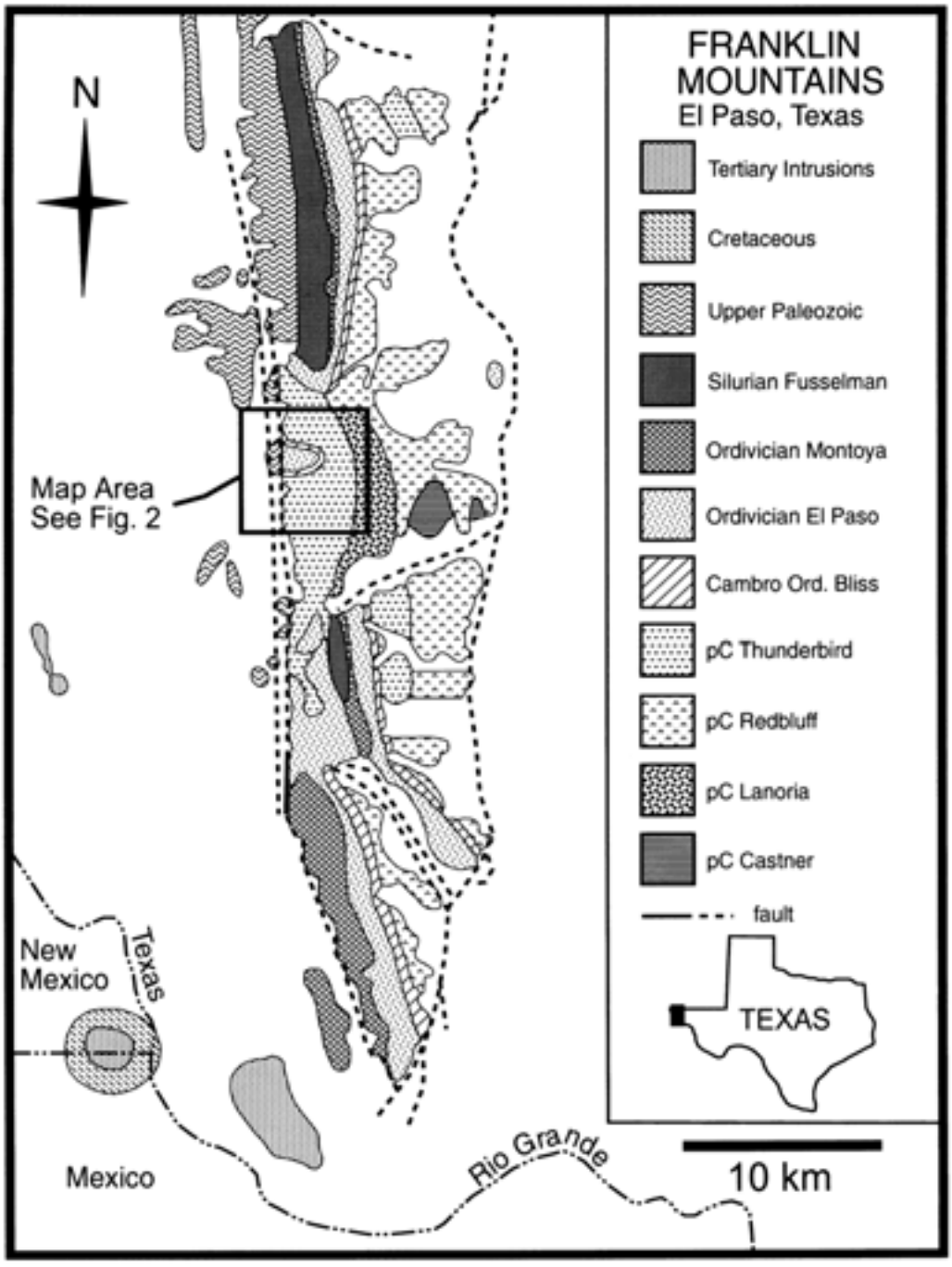

Fig. 5.1. General geology of the Franklin Mountains, West Texas; (Map modified from The University of Texas at El Paso web page, http://www.geo.utep.edu/loca/, 1999).

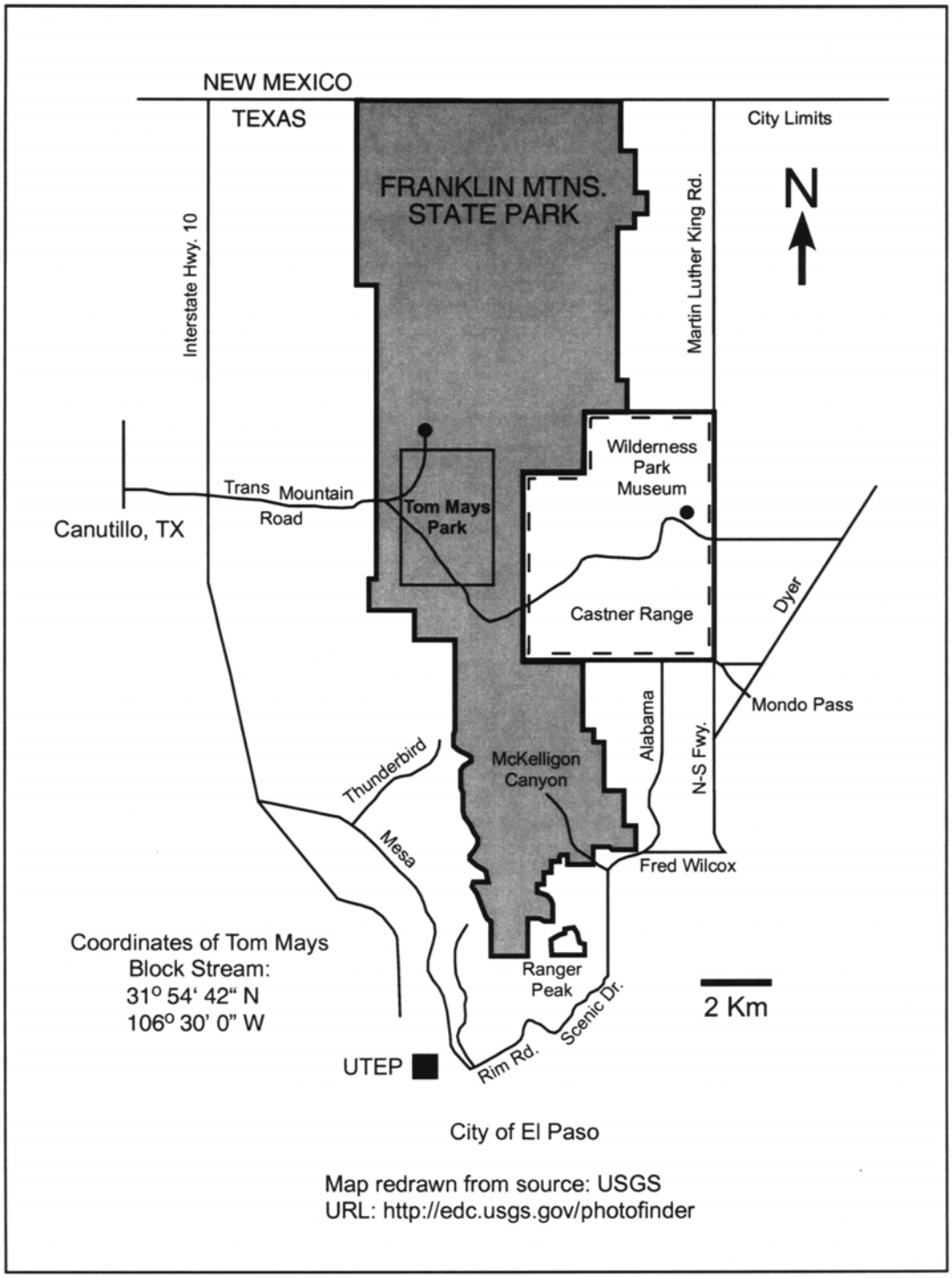

Fig. 5.2. Area map of Franklin Mountains State Park. The location of Tom Mays Park and major roadways are shown. The block stream is located in the northeast portion of Tom Mays Park.

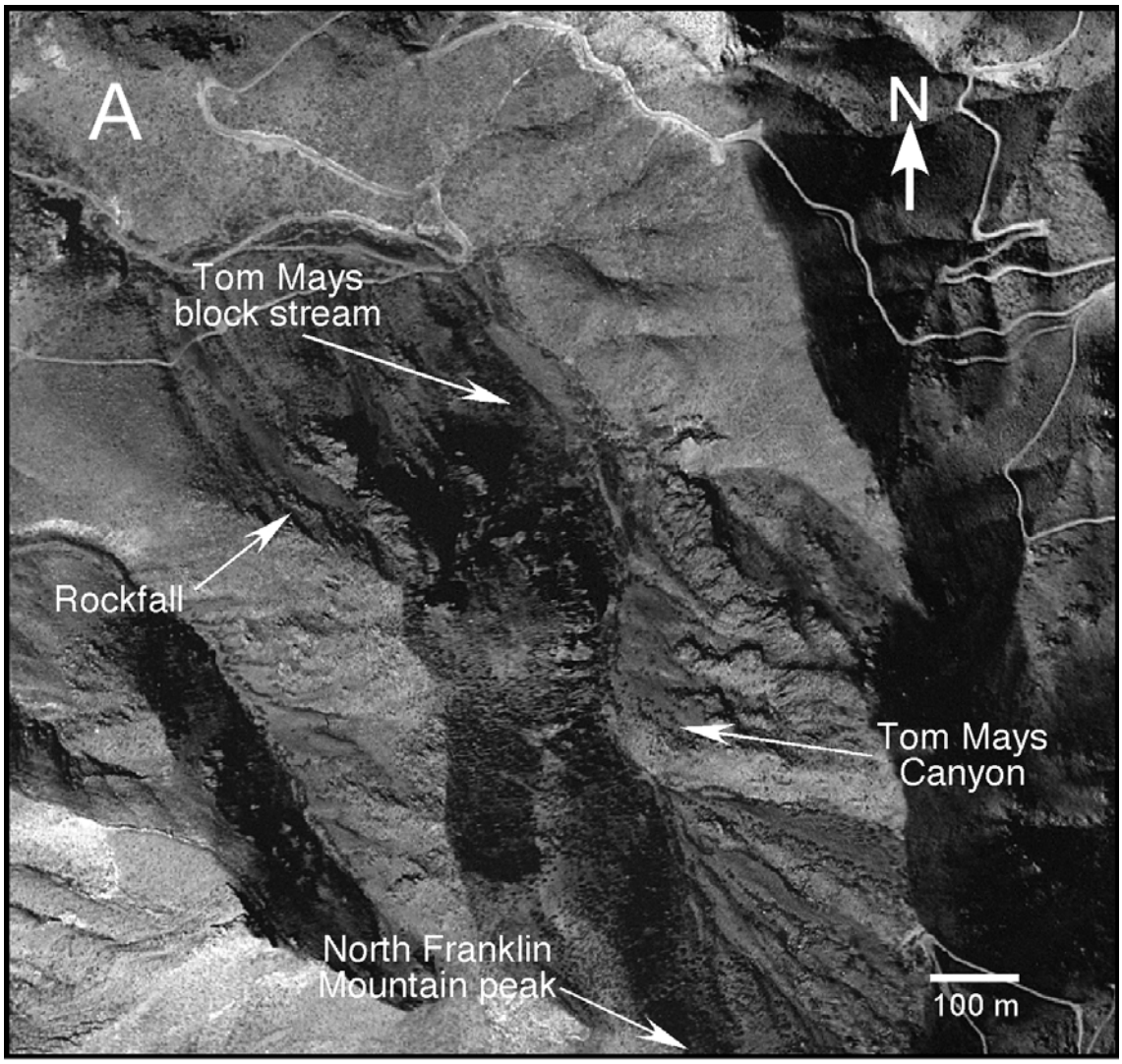

Fig. 5.3a. 1-m resolution digital orthophoto quarter quadrangle (DOQQ) image (Canutillo SE quadrangle) of Tom Mays Canyon. The head of the canyon forms the north face of North Franklin Mountain. The block stream, which is located in the thalweg of the canyon, is easily distinguished from talus slopes and rockfalls in the area.

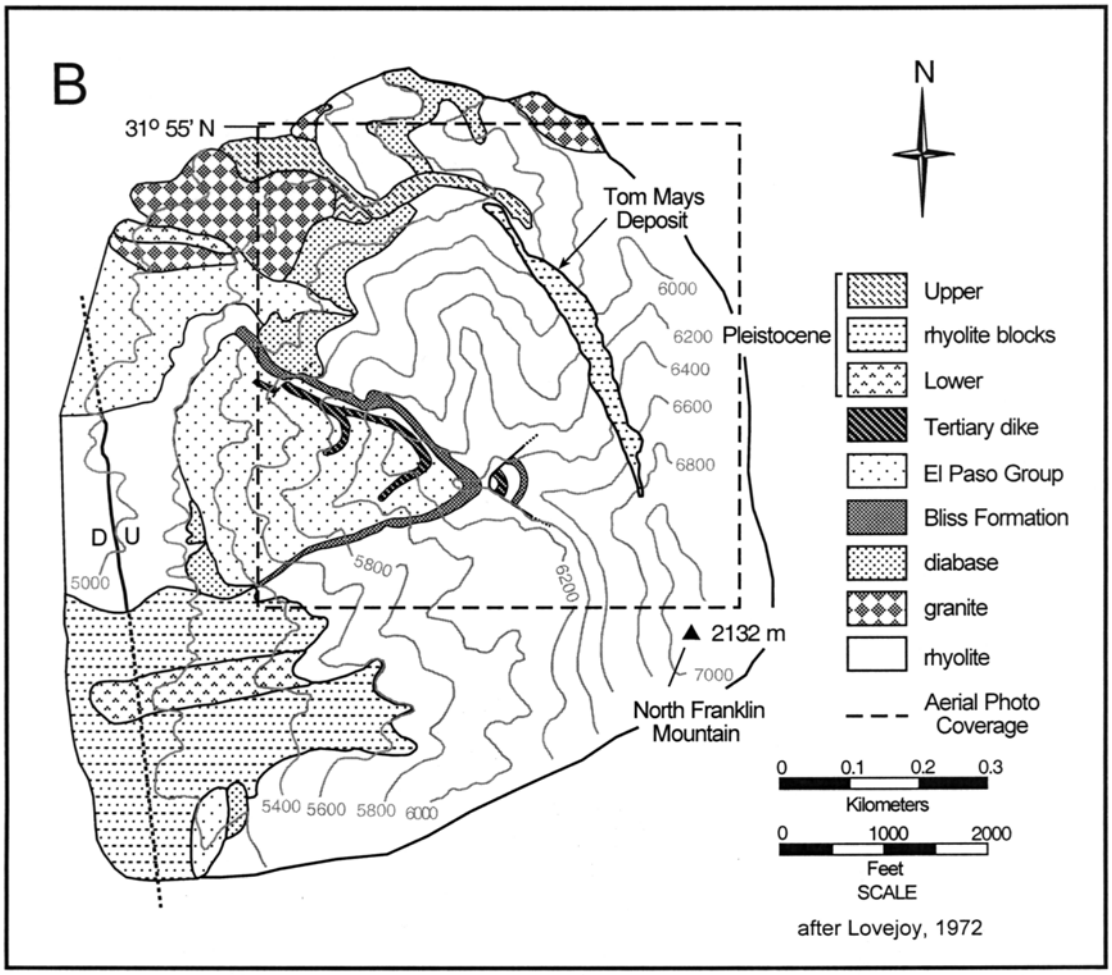

Fig. 5.3b. Geologic map of the area around Tom Mays Park. Map includes block stream. Depiction of block stream is modified from Lovejoy (1972).

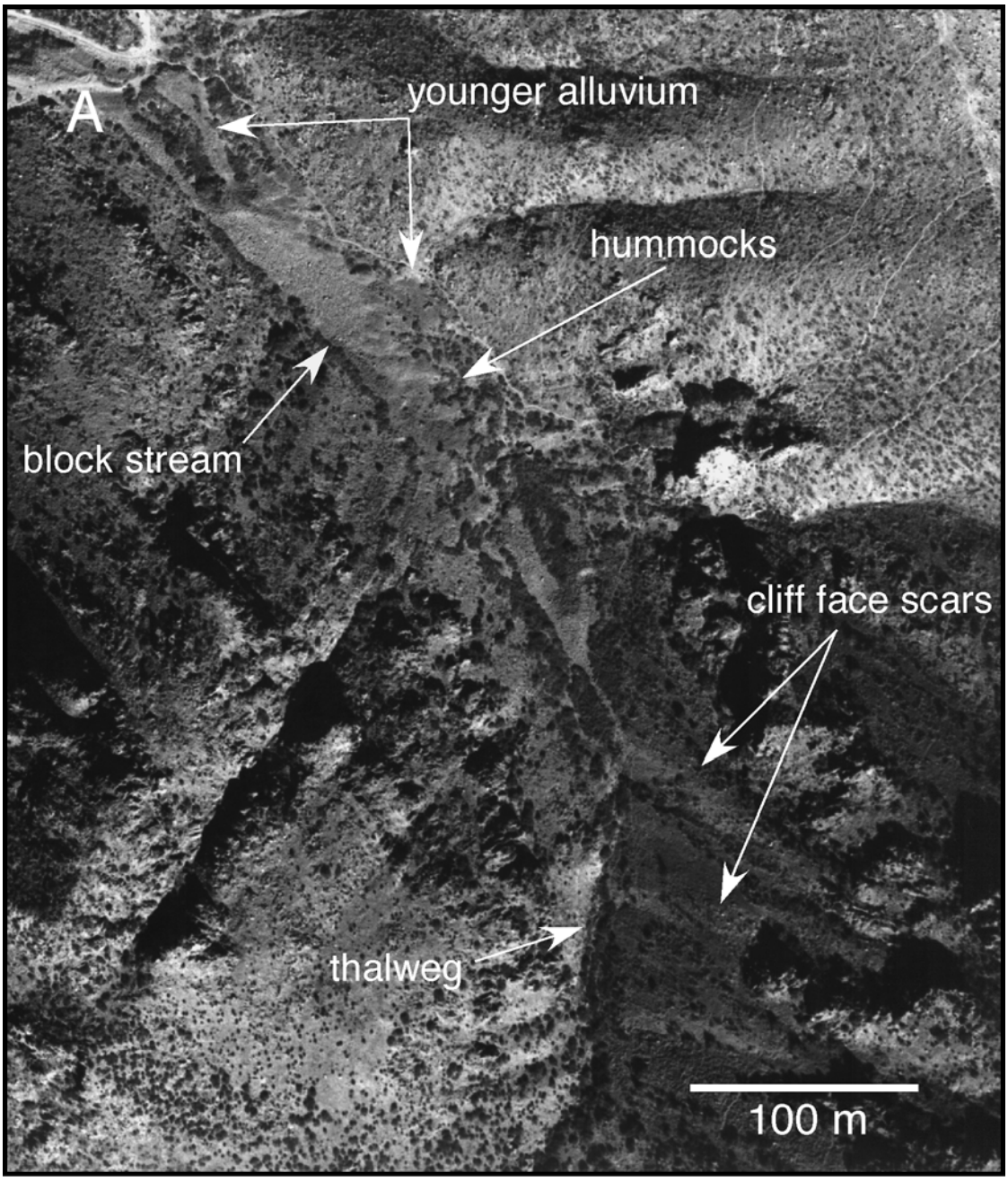

Fig. 5.4a. Enlarged aerial photograph of the Tom Mays block stream. Photo illustrates notable geomorphic features. The 10X enlargement was made from a 1"=2,000' standard aerial photo provided by the Texas Department of Transportation.

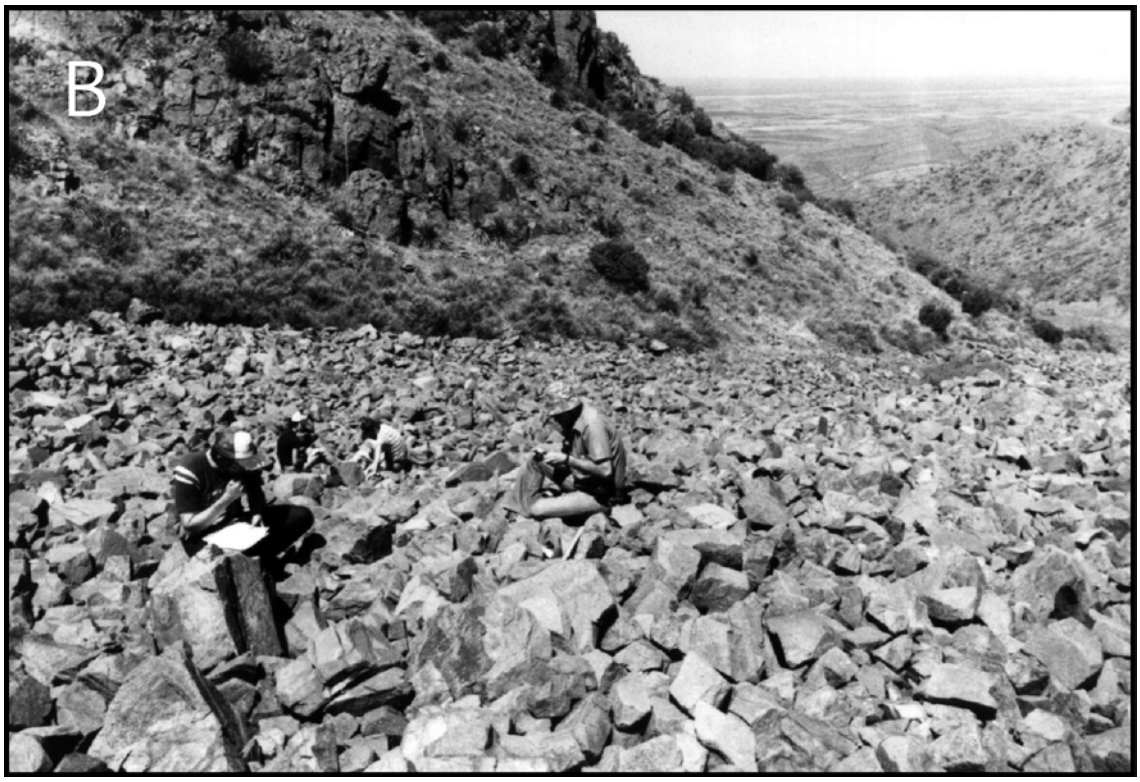

Fig. 5.4b. Downvalley view atop the block stream illustrating the character of individual blocks. The largest blocks encountered were sporadic boulder-sized clasts approximately 1 m in the longest dimension.

significant to note that the boundaries of the block stream are well defined and the estimated center of mass in profiles 2-4 is offset from the thalweg of the canyon. This observation suggests that the block stream moved rapidly enough to climb centrifugally up the walls of the canyon before coming to rest. The volume of rock contained in the Tom Mays block stream is approximately 7,386 m^3 (estimated error ± 10%) based on the surface area as measured from aerial photos (6,155 m^3), an estimated thickness of 3 m, and an assumed void space value of 40% (Wahrhaftig and Cox, 1959).

The estimated runout distance, defined by Pariseau and Voight (1978) as the distance from top of headwall to the toe of the landform, is 0.43 km. This places the Tom Mays block stream outside of Kilburn and Sørensen's (1998) field of sturzstroms based on

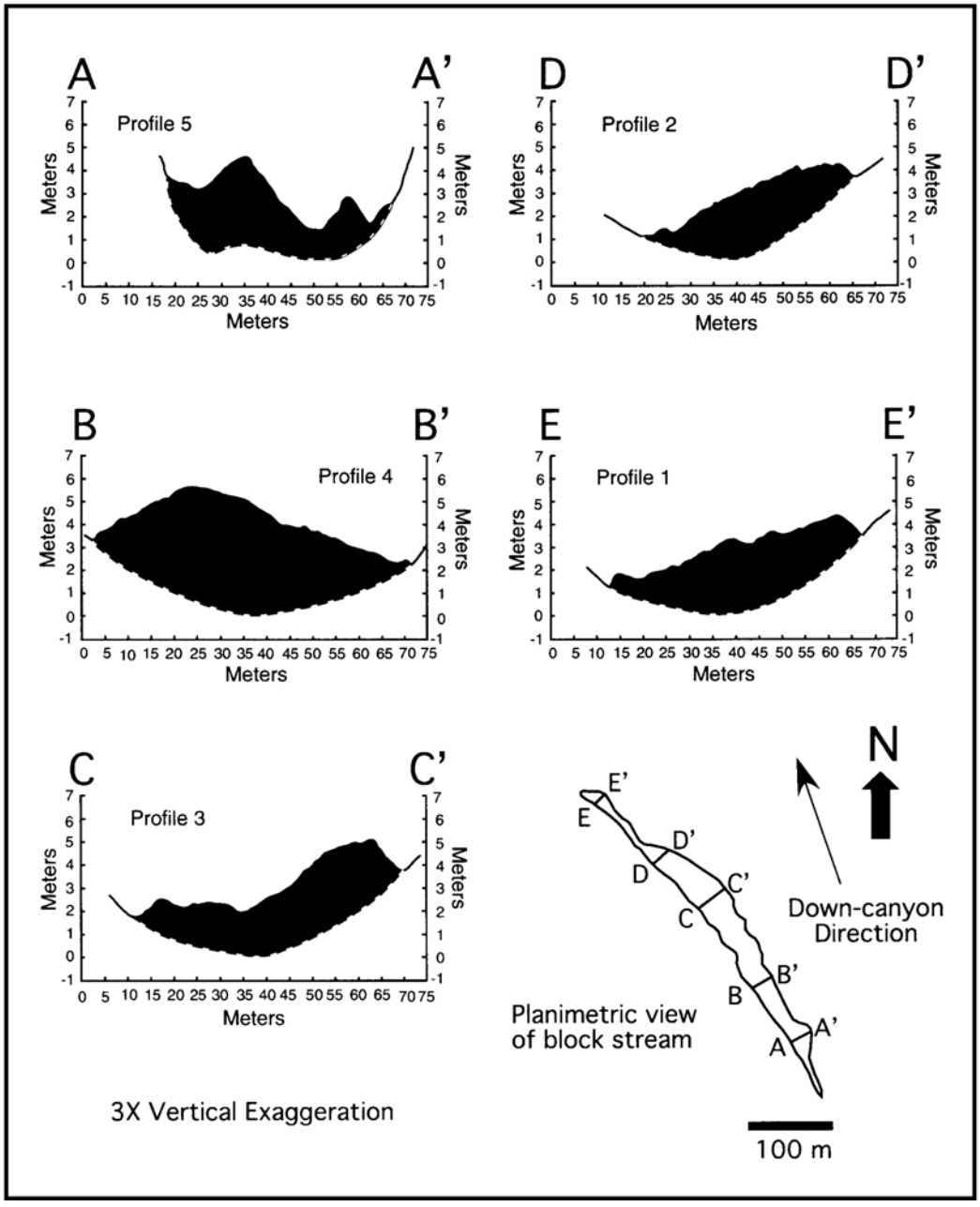

Fig. 5.5. Topographic cross-sections made at five positions along the block stream illustrating the lack of symmetry in cross-canyon directions. The assymetry is interpreted to be the result of centrifugal forces associated with a catastrophic avalanche mechanism. Topographic measurements were made using a pantometer device which was moved along lines oriented normal to the center of Tom Mays Canyon (see planimetric inset). Dashed lines at bottom of profiles indicate inferred boundaries between canyon bedrock and the material comprising the block stream.

distance traveled versus volume of deposit (Fig. 5.6a). However, a value of 0.91 for H/L (the ratio of height of fall over runout distance) places it remotely along the trend within the field for sturzstroms (Fig. 5.6b). The Tom Mays block stream conforms more with the trend for dry-rock avalanches of non-volcanic origin (Scheidegger, 1973; Hsü, 1975; Fig. 5.6c).

Surface Slope and Ground Surface Roughness

Appropriate classification of the Tom Mays block stream depends upon the proper selection of a scale of inquiry that will reveal features significant to the origin of the deposit. Under this premise, the block stream was examined in terms its longitudinal profile, surface roughness, and clast fabric for the purpose of characterizing the manner of emplacement. For the latter determinations, the elongate blocky nature of the talus necessitates the use of caution when selecting a sampling scheme and choosing which talus blocks to measure.

The longitudinal profile was constructed in 1-m steps along a 290 m length of the block stream (Fig. 5.7) using a visual level and staff. The 1-meter measuring interval was chosen because it provides sufficient detail to accommodate the surface roughness while giving an accurate impression of the overall shape of the landform surface in the longitudinal direction. The profile, which encompasses the bulk of deposited material, indicates that the surface of the block stream is slightly concave with a zone of higher relief (~1-2 m) from 225-260 m. The general trend of the slope is ~17° in the downvalley direction.

In conjunction with the longitudinal profile, a measure of ground surface roughness was used to reveal depositional characteristics that would provide some clue as to the mode of emplacement of the block stream deposit. Surface roughness values were obtained using a series of individual slope angle measurements along the surface of the block stream. Measurements were collected in 1-m steps along a 204-m downvalley stretch (from 80 m to 284 m) of the 290-m longitudinal transect using the slope pantometer method developed by Pitty (1968). The data were then smoothed by applying

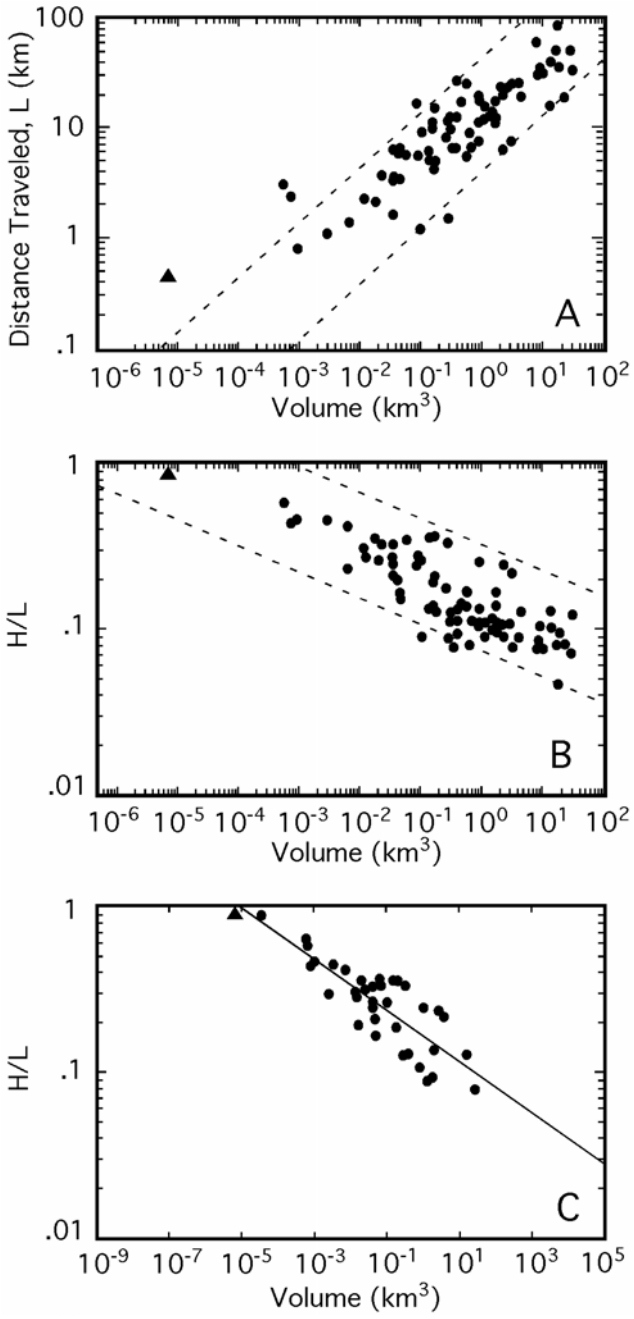

Fig. 5.6. The volumetric dependence of effective travel distance (L) and mean drop gradient (H/L) among sturzstroms on Earth. (a and b) Data for the Tom Mays block stream (triangle) is compared to sturzstrom data from Hayashi and Self (1992) (circles). Dashed lines show the empirical limits established by Kilburn and Sorensen (1998). (c) Tom Mays block stream data compared to terrestrial data for sturzstroms and dry-rock avalanches of non-volcanic origin (solid circles; Scheidegger, 1973; Hsu, 1975). Line indicates least-squares fit.

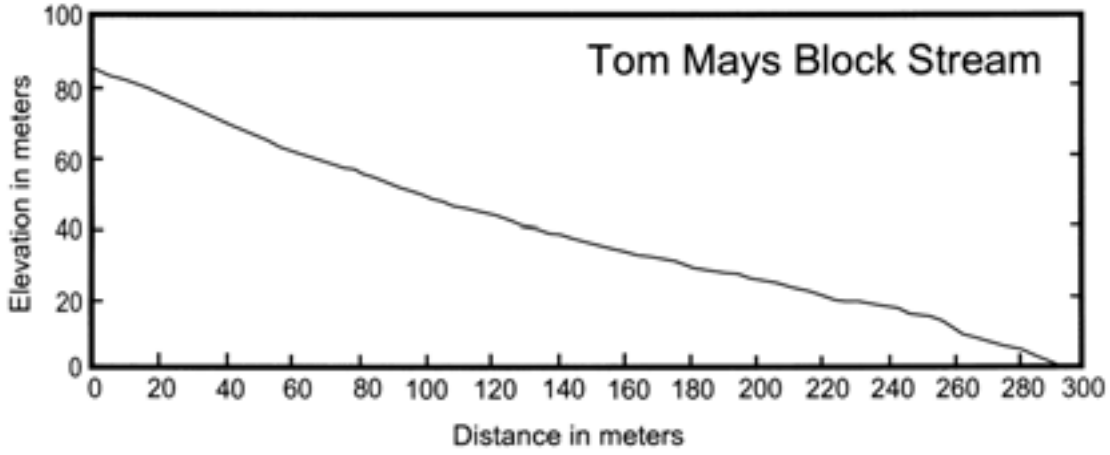

Fig. 5.7. Longitudinal profile covering 290 m of the 378 m-long Tom Mays block stream. The block stream was surveyed at 1-m intervals using a visual level and staff.

Hart's (1942) mean square of successive differences (MSSD), adapted here as an index for ground surface roughness (R_I):

$$R_I = \sqrt{MSSD} \tag{5.1}$$

where:

$$MSSD = \frac{1}{N-1}\sum_{i=1}^{N-1}(X_{i+1} - X_i)^2 \tag{5.2}$$

and N is the total number of measurements in the sample population, and X_i is the ith slope value. This index has been widely used, for example, with reference to rugged karst terrain in the north of Western Australia (Pitty, 1982, pp. 46-48).

Figs. 5.8a and 5.8b represent respectively the slope angle line graph for unit lengths of 1-meter and a plot of the accompanying ground surface roughness indices that were calculated using equation (5.1). The line graph shows a high degree of oscillation as the

amount of variation between measurements generally increases with decreasing slope angle and in the downvalley direction. The highest magnitude oscillations are the result of measurements that were made between blocks and off the edges of larger blocks. Although the trend of roughness indices also shows an increase in roughness with decreasing slope angle (N = 5, mean R_I = 12.4), a simple correlation between slope angle and R_I values (r = -0.56, 50 groups) is not entirely appropriate because statistical bias (skewness) is imparted by a few very steep angles.

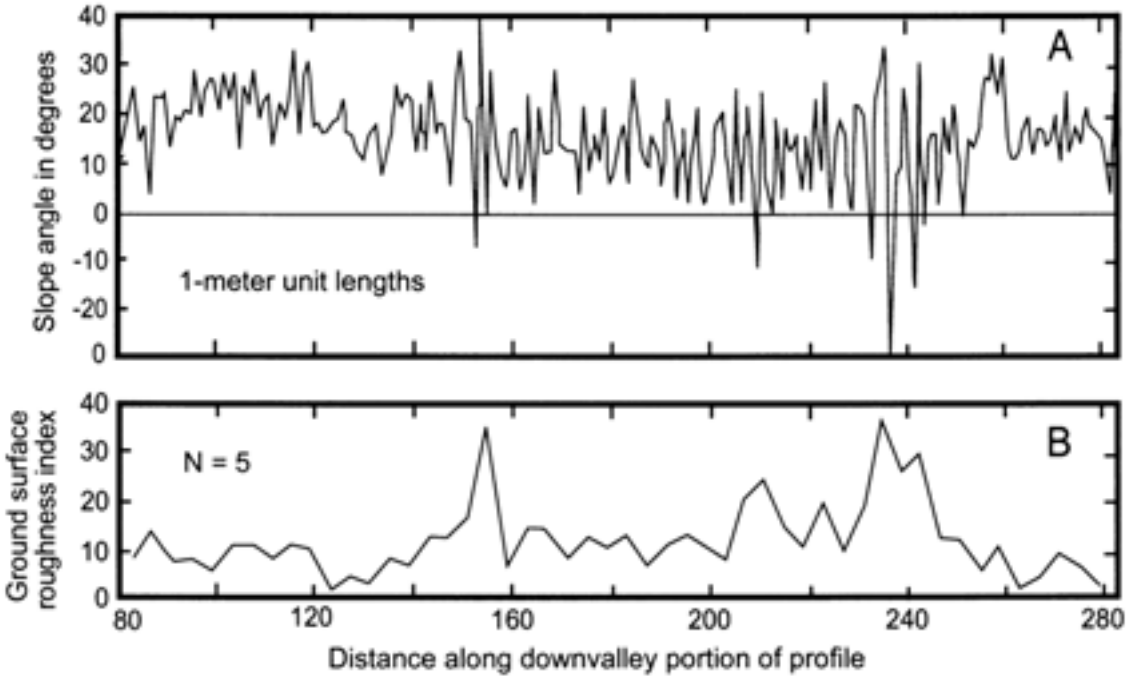

Fig. 5.8. Slope-angle line graph (a) using 1-m unit-length measurements on the Tom Mays block stream, and corresponding sequence of ground-surface roughness indices (b). The graphs, which represent a 200-m portion (from 80 to 280 m) of the longitudinal profile (Fig. 5.7), show an increase in roughness with decreasing slope and with distance downvalley.

The skewness was accommodated by using averaged 4-m spans of slope angle measurements in the line graph plot. This reduced the inverse association between slope angle and roughness and provided a more generalized description of the surface shape of the block stream. When the downvalley progression of 4-m average lengths was plotted (37 groups), the level of 'noise' inherent in the 1-m plots was reduced, thereby producing a distinctive and consistent trend of decline in slope angle (Fig. 5.9a). The corresponding plot of roughness indices (Fig. 5.9b) reflects the reduced trend of roughness at 4-m resolution.

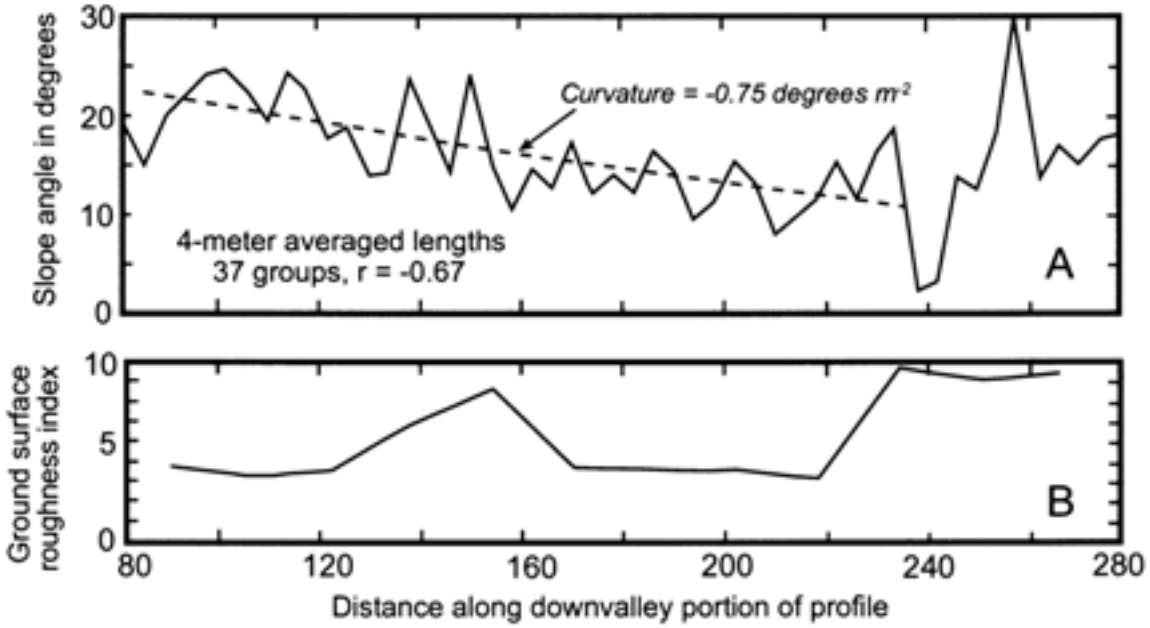

Fig. 5.9. Slope-angle line graph (a) using 4-m averaged lengths on the Tom Mays block stream and corresponding sequence of ground-surface roughness indices (b) showing elimination of trend in roughness at 4-m resolution. The graphs represent a 200-m portion (from 80 to 280 m) of the longitudinal profile (Fig. 7). Note the horizontal trend of roughness indices indicates that the gradient of the slope angle graph is not an artifact.

FABRIC ANALYSIS

Fabric data have historically been assessed in tills, gravels and sedimentary environments (Mark, 1974; Potter and Pettijohn, 1977; Mills, 1977) for the purpose of developing an understanding about the mechanics of movement of these types of deposits. For example, Caine (1968) observed two types of fabric in the surface block layers on block streams in Tasmania. One fabric was associated with upslope imbrication in response to solifluction-generated stress, and the other fabric (i.e., isotropic orientation) occurred in the upper reach of the block stream where movement was insufficient to produce preferred orientation. Caine's analysis demonstrated that the orientation and strength of fabric increased downslope, thereby suggesting a response to movement within the lower reaches of the landform.

In a similar fashion, fabric analysis was applied to the study of the Tom Mays feature to differentiate its depositional character from landforms having similar morphology and to understand the mechanics of movement involved in its transport. The eigenvalue method was used to analyze the fabric data based on its effective application to similar features by other workers (Mark, 1973, 1974; Mills, 1983; Pèrez, 1984, 1989, 1992; Bertran et al., 1997) This technique involves approximating the orientation and shape of clasts using ellipsoids (Nielsen, 1983). Analytical procedures and the application of eigenvector analysis to the study of clastic materials can be reviewed in Fara and Scheidegger (1963) and Gould (1967). Mardia (1972) also provides a summary of the categories used for comparing eigenvalues.

Fabric data were obtained along six transect lines oriented normal to the longitudinal axis of the block stream (Fig. 5.10). Clast selection was based on the following criteria: (1) a/c>2 (a = long axis of clast; c = short axis of clast); (2) minimum length of 10 cm along length a; (3) 1m x 2m x 1m spacing area between samples; (4) 100 clast measurements per site. Measurements consisted of trend and plunge of the long axis (a-axis) of each clast and a series of rose diagram polar coordinate plots were constructed to represent these measurements for groups of clasts taken along the six transects. Rose plots for left, center and right portions along each transect line are included in Fig. 5.10.

The rose diagrams are plotted as poles to planes with the center point of the stereogram representing a plunge of 0°. Long-axis directions are measured in azimuth form with 0° located at the top of the stereogram. Raw data for clasts (i.e., orientation and plunge) were plotted on Schmidt equal area nets and contoured by the method outlined in Kamb (1959) using Allmendinger's (1989) stereo plotting program. Data were plotted so that 'north' represents the azimuth downslope along the center axis of the landform.

Using the method of Woodcock (1977), normalized eigenvalues (generated using Allmendinger's (1989) stereo plotting program) were plotted on a two-axis ratio diagram for the purpose of assessing fabric shape (Fig. 5.11). These data, contained in Table 5.1, include samples collected from the six profile lines on the block stream. The diagrams show that most sample populations, independent of transect, contain wide-ranging distributions for trend and plunge. In a few instances, bimodal distributions are indicated (e.g., transects 1, 3 and 6). The most consistent fabric is obtained from transect 6 (see Fig. 5.10), located at the farthest position downvalley. Such a preferred orientation on this part of the block stream may be the result of movement of materials from the toe of the block stream following the initial deposition (i.e., a secondary fabric).

The eigenvalue plot in Fig. 5.11 characterizes the orientation fabric such that, in general, samples having strong preferred orientations plot further from the origin of the graph than samples with weak orientations. Random distributions plot near the origin, the origin itself representing a uniform distribution. Values plotting near the x-axis represent uniaxial stereographic distributions, and those that plot near the y-axis approach uniaxial clusters. The transition between girdles and clusters is denoted by a line at $K = 1$, where $K = \ln(S_1/S_2)/\ln(S_2/S_3)$. Girdles are represented by K values between 0 and 1, and clusters by values of K between 1 and ∞ (Woodcock, 1977).

The fabric shape for the block stream (Fig. 5.11) shows that the data are randomly distributed ($C \leq 2.5$). Most of the points in the scatter have K values greater than 0, signifying a predominance of cluster patterns. Comparison of the eigenvalue sets to the case criteria Mardia (1972) demonstrates that none of the sample sites fall into the Case IV category (i.e., signifying a uniform distribution). Five data points, however, cross the

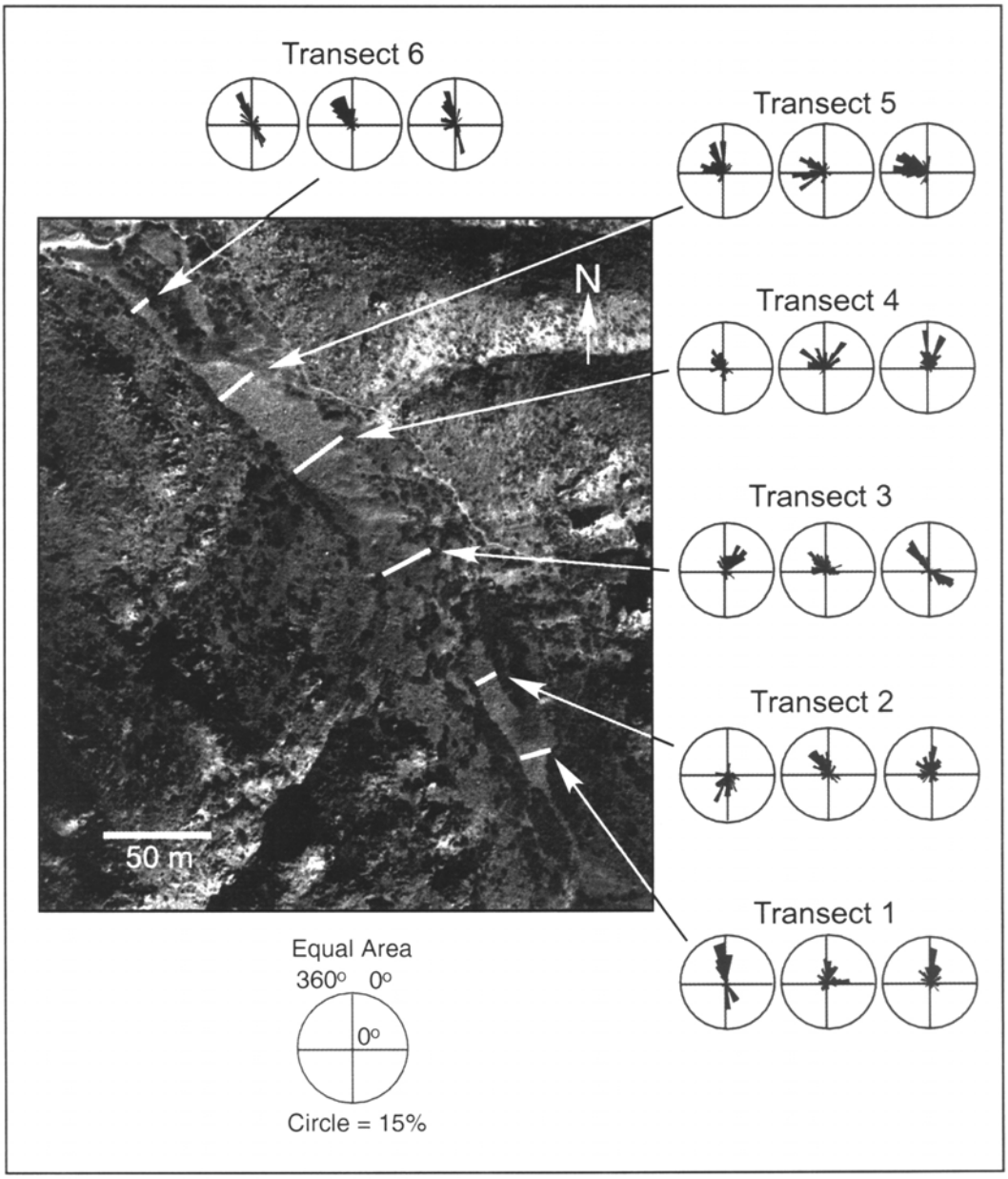

Fig. 5.10. Fabric data for several positions along six transects across the Tom Mays block stream. Rose diagrams are polar coordinate plots of fabric data for the left, middle, and right portions of each transect, respectively. The plots, representing the long axis (*a*-axis) plunge and orientation, are plotted as poles to planes with the center point of the stereogram representing a plunge of 0°. Long-axis directions are measured in azimuth form with 0° located at the top of the stereogram.

$K = 0$ transition line indicating a moderate degree of variation in the overall character of the fabric. This variation is not systematic, as data points from four sites are included within the girdle field (i.e., two points from site 6). The Tom Mays data are best classified as Case II, with a scatter that is transitional between girdle and cluster patterns.

Fabric shapes were also compared using a method of normalized eigenvalues plotted on a triangular graph (Mark, 1974; Mills, 1977; Woodcock, 1977). This procedure allows for comparison of various depositional processes and environments. Fig. 5.12 is a partial ternary plot of normalized eigenvalue data for the Tom Mays block stream compared to rock glacier data from a Mount Mestas rock glacier (Giardino and Vitek, 1985; Giardino et al., 1987) and two additional sites on avalanche debris and talus (Giardino and Vitek, 1988). A field for lowland till deposited by continental glaciers (Mark, 1974) is also included. The block stream data scatter again indicates a random distribution, plotting throughout the lowland till field and distinct from ridge and furrow data for the rock glacier. The uniform spread of data within the ternary diagram also reflects the intermediate range of values for S_1 ($0.47 \leq S_1 \leq 0.68$) and consistent variation between S_1 and S_2 values.

Various fabric studies (Caine, 1967; Nelson, 1982; Innes, 1983; Mills, 1983; Giardino and Vitek, 1985) have shown that orientation of the long axis (*a*-axis) of a clast is determined by its response to the mechanics of motion at work during formation of the landform. Pèrez (1998) reported a noticeable gradient in particle size across the slopes of talus aprons located in Chaos Crags, CA. This gradient was found to be related to the height of cliffs above the talus. It was suggested that the larger and more abundant clasts found below areas of rockfalls were the result of control exerted by present debris supply on talus morphology. Van Steijn et al. (1995) observed that the upper talus, comprised ofrelatively few small clasts scattered over fine gravel, was affected mainly by dry grain flows, which allowed particles to creep and to slide downhill with their a-axes roughly parallel to the slope plane. In contrast, the large blocks that cover the lower talus were mainly deposited by rockfall. Previously, Caine (1967) explained that the tendency of

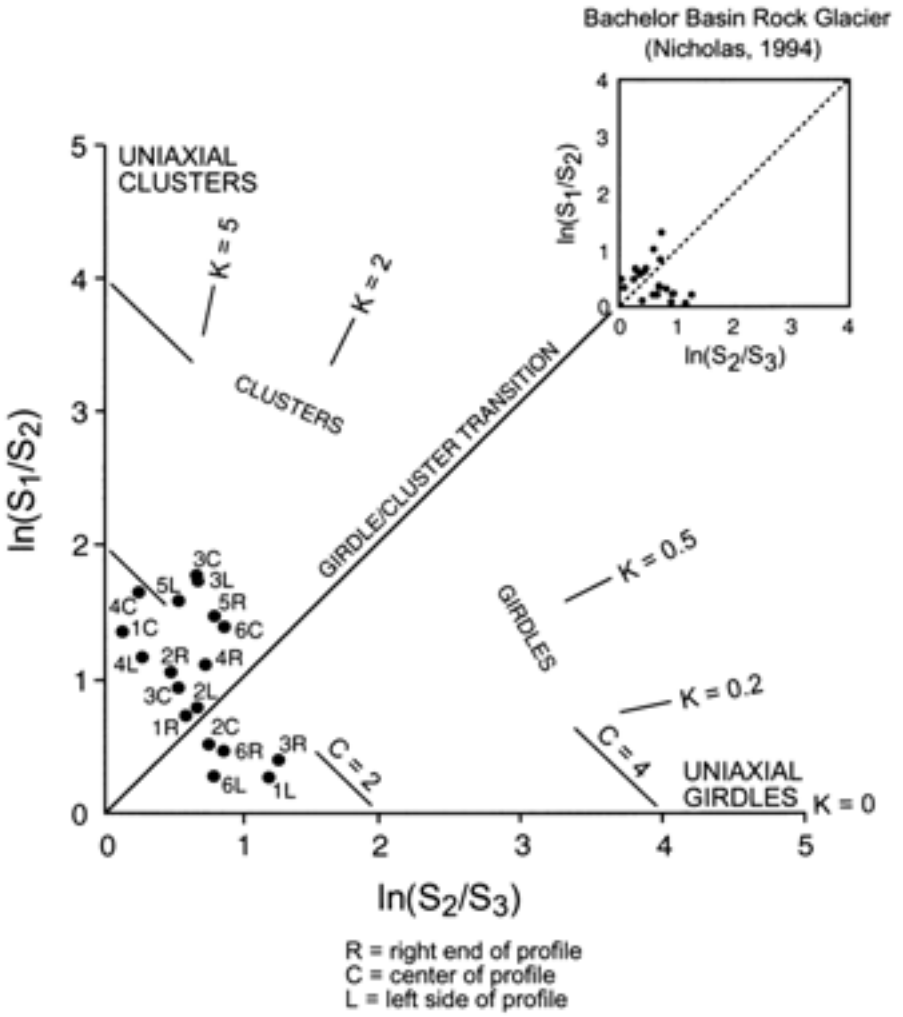

Fig. 5.11. Graph of normalized eigenvalues plotted on a two-axis ratio diagram showing fabric shape. Data includes samples collected from the six profile lines on the block stream as shown in Fig. 5.10. The eigenvalue plot characterizes the orientation fabric in terms of patterns defined by stereographic distributions of the data. The inset graph shows rock glacier surface data from Nicholas (1994) for the Bachelor Basin rock glacier, La Sal Mountains, Utah.

Table 5.1. Eigenvalues for the Tom Mays block stream with ratios used in the two-axis ratio diagram (Fig. 5.11).

Site	S_1	S_2	S_3	$\ln(S_1/S_2)$	$\ln(S_2/S_3)$
1 L	0.6494	0.2004	0.1502	1.18	0.29
1 C	0.4698	0.4230	0.1072	0.10	1.37
1 R	0.5468	0.3074	0.1458	0.58	0.75
2 L	0.5691	0.2971	0.1338	0.65	0.80
2 C	0.5676	0.2720	0.1604	0.74	0.53
2 R	0.5418	0.3404	0.1178	0.46	1.06
3 L	0.6214	0.3213	0.0573	0.66	1.72
3 C	0.5469	0.3264	0.1266	0.52	0.95
3 R	0.6772	0.1946	0.1281	1.25	0.42
4 L	0.4971	0.3837	0.1192	0.26	1.17
4 C	0.5119	0.4095	0.0786	0.22	1.65
4 R	0.6072	0.2965	0.0963	0.72	1.12
5 L	0.5832	0.3472	0.0696	0.52	1.61
5 C	0.6206	0.3229	0.0565	0.65	1.74
5 R	0.6395	0.2934	0.0671	0.78	1.48
6 L	0.5538	0.2556	0.1907	0.77	0.29
6 C	0.6528	0.2791	0.0681	0.85	1.41
6 R	0.5908	0.2533	0.1559	0.85	0.49

Where: L = sample taken from left side of sample profile line, observer facing upslope.
C = sample taken from center of sample profile line, observer facing upslope.
R = sample taken from right side of sample profile line, observer facing upslope.

big stones is to rotate about their long axes while rolling and bouncing downslope. The axes subsequently become aligned with the contours of the prevailing slope. However, after colliding with other blocks on the talus slope, this orientation may not be preserved, and most clasts attain an isotropic fabric (Pèrez, 1998).

To test the strength of this association (i.e., the *a*-axis orientation of a clast versus its response to the mechanics of motion) as it applies to measurements made on the Tom Mays block stream, the chi-square method was employed. Three tests were performed, one for each position (left, center and right) along the six sample profile lines. The observed clast direction, V_1, was compared to the directional tendency of the surface

(i.e., expected trend) upon which the sample orientation was measured (Table 5.2). Observed mean directions were calculated in the eigenvalue analysis for V_1. The null hypothesis used for the chi-square test, “no significant difference between the mean direction of V_1 and surface lineations”, was rejected in each test (Table 5.3). Deviation between observed and expected values was sufficiently great to neglect the probability that random occurrence contributed significantly to the scatter in the data. Thus, no clear relationship exists between observed clast orientation and prevailing slope direction at the sample sites.

DISCUSSION

Lovejoy (1972) originally interpreted the Tom Mays block stream to be a boulder flow that probably formed as a debris flow containing large clasts. The term "boulder flow" was used to denote the lack of fines material that would be necessary to qualify the deposit as a debris flow. He further concluded that the flow formed via “boulder-charged surges” as a result of flash flood waters and noted that the hummocky surface was more reminiscent of rock glaciers than alluvial deposits. These interpretations were undoubtedly influenced by early workers (Cross and Howe, 1905; Howe, 1909; Capps, 1910) who interpreted rock glaciers as landslides, noting superficial relationships to the Elm and Frank sturzstrom features (Nicholas and Garcia, 1997). Unified block movement and morphological similarities with glaciers are characteristics noted by the first recorders of catastrophic debris streams generated by rockfalls. Hsü (1975) retains the German expression “sturzstrom” as the most appropriate term for this type of mass wasting deposit.

Landform Mobility

Mobility in a sturzstrom is attributed to the stress transmitted by clasts as a result of their collisions. This motion of colliding clasts has been termed “grain flow” by Bagnold (1954, 1956) in which kinetic energy is transferred through collisions and dissipated by friction during these collisions. The dispersion of clasts during grain flow explains why

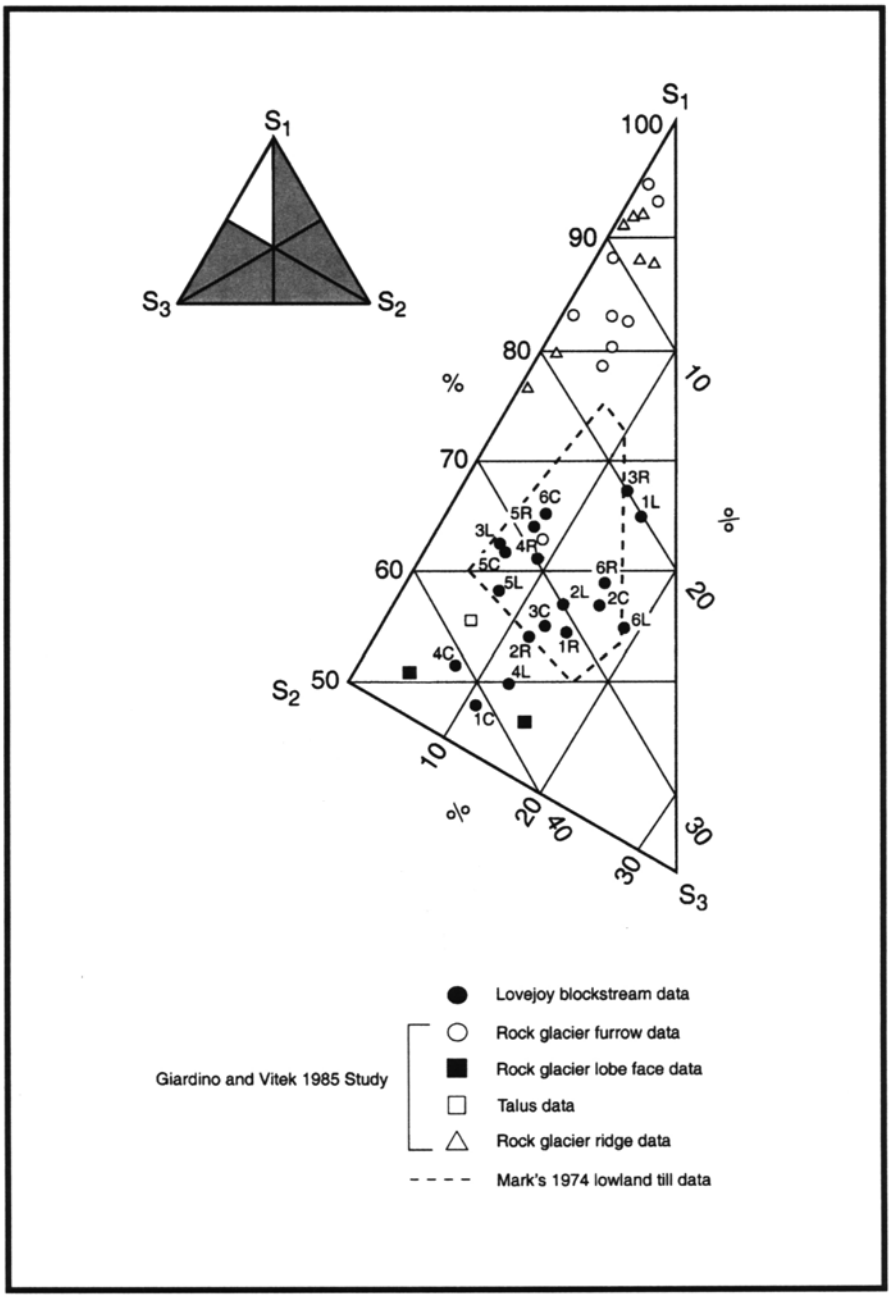

Fig. 5.12. Partial ternary plot of normalized eigenvalue data for the Tom Mays block stream. Tom Mays data is compared to rock glacier data from Mount Mestas rock glacier (Giardino and Vitek, 1985) and two additional sites on avalanche debris and talus. A field for lowland till (Mark, 1974) is also included. The gray area on the inset triangle indicates values that cannot occur because $\lambda_1 \geq \lambda_2 \geq \lambda_3$ by definition.

Table 5.2. List of observed clast direction (V_1) compared to the directional tendency of the surface (expected trend). Sample orientation was measured for each position (left, center and right) along the six sample profile lines. Observed mean directions were calculated in the eigenvalue analysis for V_1.

	Slope ∠ (deg.)	**Slope Aspect (deg.)**	**V_1 (trend, deg.)**	**V_1 (plunge, deg.)**	**S_1**	**V_3 (trend, deg.)**	**V_3 (plunge, deg.)**	**S_3**	**Clast/Surface Angle**
1 L	15	0	343	15	0.649	76	13	0.150	30
1 C	12	0	56	8	0.470	172	71	0.423	20
1 R	20	315	2	20	0.547	193	70	0.307	40
2 L	14	20	180	19	0.569	12	71	0.297	33
2 C	13	315	318	21	0.568	181	32	0.272	34
2 R	13	300	348	27	0.542	142	60	0.340	40
3 L	21	240	10	12	0.621	211	77	0.321	33
3 C	26	310	302	20	0.547	160	65	0.326	46
3 R	15	60	314	1	0.677	219	75	0.195	16
4 L	18	285	314	19	0.497	108	69	0.384	37
4 C	21	295	329	23	0.512	161	67	0.410	44
4 R	23	30	9	14	0.607	161	75	0.297	37
5 L	15	285	316	26	0.583	128	64	0.347	41
5 C	15	295	262	16	0.621	86	74	0.323	31
5 R	22	220	282	25	0.640	102	65	0.293	47
6 L	14	280	325	13	0.554	157	77	0.256	27
6 C	14	295	320	21	0.653	140	69	0.279	35
6 R	18	40	339	6	0.591	86	70	0.253	24

Table 5.3. The null hypothesis used for the chi-squared test. Hypothesis states "no significant difference between the mean direction of V_1 and surface lineations." The hypothesis was rejected in each test.

Samples from the Left Side of Sample Profile Line, Observer Facing Upslope						
Site Number	1	2	3	4	5	6
Observed direction	343°	180°	10°	314°	316°	325°
Expected trend	360°	200°	60°	285°	285°	280°
$\chi^2 = 58.02$ with DF = 5 $\chi^2_{0.05} = 11.07$; null hypothesis rejected						

Samples from the Center of the Sample Profile Line, Observer Facing Upslope						
Site Number	1	2	3	4	5	6
Observed direction	236°	318°	302°	329°	262°	320°
Expected trend	360°	315°	310°	295°	295°	295°
$\chi^2 = 52.67$ with DF = 5 $\chi^2_{0.05} = 11.07$; null hypothesis rejected						

Samples from the Right Side of Sample Profile Line, Observer Facing Upslope						
Site Number	1	2	3	4	5	6
Observed direction	182°	348°	314°	9°	282°	339°
Expected trend	315°	300°	240°	30°	220°	220°
$\chi^2 = 183.19$ with DF = 5 $\chi^2_{0.05} = 11.07$; null hypothesis rejected						

the fahrböschung, or dependence of horizontal travel distance on height of fall (Hsü, 1975), of a sturzstrom is considerably smaller than the angle of repose of cohesionless debris. Empirical tests performed by Lowe (1976) suggest that a gradient of 17° to 22° is needed for sturzstroms; the fahrböschung for the classic 1881 sturzstrom at Elm, Switzerland is 17° (Hsü, 1975). These values compare favorably with the measured mean angle of 17° for the Tom Mays block stream.

There are two elements of significance regarding the gradient of the Tom Mays block stream. First, the slight concavity describes the arc of a circle (Fig. 5.7). This observation is also represented by the trend in the slope-angle line graph (Fig. 5.8a). If the rate of landform profile curvature changes, as in decline of gradient with distance, curved trends would be evident in the slope-angle line graph. Second, microfeatures are not present on the block stream surface, other than a small number of transverse ridges and conical pits (also referred to as ellutriation orifices) Lovejoy (1972). Otherwise, the

slope-angle line graph would display runs of residuals above or below the least-squares line. The absence of local steepening or flattening of the gradient suggests that the block stream is a single morphological unit and not a succession of advancing material overriding earlier deposits.

The random clast fabric for the block stream deposit points toward a mode of deposition that is remotely related to the formation of talus slopes. There is no systematic or consistent trend to the fabric on one part of the block stream as compared to another part. The lack of correlation between the observed and expected clast orientations and range of orientations illustrated in the rose plots of Fig. 5.10 argues against slower systematic mass-movement processes such as those responsible for talus accumulation and rock glacier movement (e.g., solid-state creep or solifluction). Features in the block stream are instead interpreted to be the result of catastrophic mass movement and associated rapid dissipation of energy, perhaps resulting from a powerful triggering mechanism caused by one or more catastrophic events (i.e., such as an earthquake or a series of tremors). A formation mechanism involving episodic mass-movement of blocky material is supported by the observation that the block stream is superelevated along steep continuous portions of the canyon walls (see Figs. 5.5 and 5.10). It is plausible that this lack of symmetry in the cross-valley deposits was caused by centrifugal forces associated with a catastrophic avalanche. Near-preferred orientations at the outer portions of transects 1 and 6 likely represent younger alluvium deposited locally from the canyon walls following block stream emplacement.

Mobility of the block stream can also be demonstrated by comparison with published values for H/L and runout length for large rock avalanches (McEwen, 1989) and sturzstroms (Kilburn and Sørensen, 1998). When plotted on a graph of travel distance versus rockfall volume for sturzstroms generated by rockfalls (see Hsü, 1975, Fig. 8), the Tom Mays feature could be characterized as a ‘small rockfall’ and is in accord with other rockfall deposits with volumes on the order of 10^6 m^3. However, the feature is unlike rockfalls of the Tom Mays Park area in several fundamental ways. For example, the rockfalls lack sharply defined boundaries, and do not appear to have traveled far

from their sources as is the case for the Tom Mays feature (Fig. 5.3a). The rockfalls also differ morphometrically from the Tom Mays deposit in that they do not exhibit the irregular hummocky surfaces that are characteristic of sturzstroms.

The relationship of volume versus H/L for the Tom Mays block stream compared to values for terrestrial sturzstroms of non-volcanic origin (Fig. 5.6b; Schiedegger, 1973; Hsü, 1975) suggests a formation mechanism such as grain flow, which does not require a liquid component. The fact that the deposit is comprised of blocky rhyolite in contact with rhyolite bedrock or colluvium along almost its entire length does not, however, preclude the formation of a substantial amount of fine clastic rock material that would be needed for landslip to occur. Shroder (1973b) acknowledged the absence of fine-grained clastic bedrock and the apparent lack of significant fine-grained clastic materials beneath the Tom Mays block and noted that it is probably unlike examples of rock glaciers and related boulder deposits affected by landslip in the Aquarius and Table Cliffs plateaus in Utah (Shroder, 1971, 1972, 1987). The position of the block stream datum in relation to the trend for dry-rock avalanches of non-volcanic origin (Fig. 5.6c) demonstrates a consistency with the systematic trends between volume of deposit and effective travel distance that have been shown by Hsü (1975) and Melosh (1987).

Based on the apparent lack of appreciable amounts of fine-grained material, it is not unreasonable to consider the possibility that fines were removed by wash-out (e.g., by moving water) from an initial deposition of debris as Shroder (1973b) offers. This mechanism does not, however, account for the gross morphologic characteristics observed in the cross-sectional topographic profiles of the block stream. If the Tom Mays block stream was a pre-existing debris deposit that was subsequently flushed of its fines, a mechanism for rapid emplacement is still required to account for the observed superelevation.

Other Considerations

Unlike wash-out, sieve deposition (Hooke, 1967, p. 456; Shroder, 1973b, p. 3747) involves the depletion of fines during formation of coarse, blocky alluvial fans or flow lobes that are composed of pebble- to boulder-size material. Some sieve deposits display

hummocky topography similar to that observed on the Tom Mays block stream (e.g., Hooke, 1967). The block stream, which is contained almost entirely within a canyon, does not display any notable gradation in clast size (i.e., fining upvalley/downvalley sequences), making it difficult to substantiate an alluvial fan process. Discounting "ellutriation orifices" as evidence for a flash-flood origin based on the argument that such features could have been man-made (Shroder, 1973b, p. 3746; Shroder, 2000, personal communication), it is unlikely that sieve deposition alone could have been responsible for such a high degree of sorting within the range of clast sizes involved. More significantly, the clast size range, setting and morphology of this feature does not resemble alluvial fan/debris flow deposits.

Similarly, for frost-induced rock stream deposition to be considered as a primary mode of emplacement, the cross-sectional characteristics of the block stream must correlate strongly with talus runs that are produced in response to freeze-thaw acting upon the strongly jointed rhyolite in the area of Tom Mays Park. Small-scale rockfall and talus movement have been recorded in the "lower tributary rubble streams" of the Tom Mays block stream (Shroder, 1973b, p. 3747), which indicates that some material is being supplied to this portion of the block stream through freeze-thaw generation of talus. However, the accumulation of materials owing to these tributaries is not substantial enough to explain the superelevated character observed in the cross-sectional topographic profiles of the block stream.

An alternative mechanism of grain flow for sturzstrom formation was proposed by Melosh (1979) to explain such mobility and rapid movement of large blocky deposits. He postulated that intense noise may produce sufficiently strong acoustic wave fields to fluidize a rock mass. Compared with the fall, leap, and surge of the rock mass at Elm, Switzerland, acoustic fluidization would depend initially on high-angle landslides building up an acoustic field of the required strength. Either the dispersive pressure in grain flow or the longer acoustic waves which "…'tunnel' through the overburden" (Melosh 1979, p. 7515) could account for the increasing surface roughness toward the base of the block stream.

Three local factors support the interpretation of the Tom Mays block stream as a sturzstrom. First, the rhyolite cliffs on the shoulder of Tom Mays Park Canyon (see Fig. 5.4a) are often greatly weakened by joints that are widely open for the full height of the free faces. Second, being extensively fractured by thermal contraction joints, rhyolite shatters readily on impact into blocks of a size proportional to the fracture density. Third, Tom Mays Park Canyon is only 2 km to the east of a major active fault. Earthquakes associated with fault movement could readily provide the triggering mechanism for mass movements of unstable rock masses. Thus, a catastrophic run-out of blocky material down the canyon of Tom Mays Park remains the most plausible mechanism of emplacement for the Tom Mays block stream. Although other modes of emplacement (e.g., landslip deposition or frost-induced rock stream deposition) warrant consideration, the fabric and field data presented in this study do not favor these as primary emplacement mechanisms.

CONCLUSIONS

We interpret the Tom Mays block stream to be a sturzstrom based on the combination of fabric data, morphological features, cliff face scarring, and run-out characteristics. The very distinctive combination of local geologic factors are sufficient to promote such an event. The surface fabric of the block stream compares well with that for lowland tills, and the profile concavity is indicative of a single morphological unit resulting from rapid transport. Rapid emplacement is supported by the superelevation of the blockstream along the steep canyon walls. Microfeatures of the block stream are also consistent with characteristic mechanics of sturzstroms, including sudden braking power, grain flow and/or acoustic fluidization. Compared with the volume and length of documented sturzstroms, the Tom Mays block stream must be considered small, but based on morphologic character and relationships between estimated volume and mean drop gradient (H/L), the feature does exhibit characteristics of sturzstroms and much larger rockfalls.

CHAPTER VI

SUMMARY

INTRODUCTION

This dissertation attempted to provide a more accurate model for the formation and development of lobate rock glaciers such as the one at Yankee Boy Basin. This was accomplished through a detailed description of the internal structure using the non-intrusive means of ground penetrating radar (GPR). The GPR method has been applied effectively in many different geomorphic environments over the last twenty years, but has only recently been applied to the study of rock glaciers (Isaksen et al., 2000; Berthling et al., 2000; Degenhardt et al., 2000).

The following sections contain a generalized summary of the results as discussed in Chapters II through V. The work contained in these chapters represent accomplishment of the following objectives:

(1) identify the internal structure of an active lobate rock glacier with characteristic ridge and furrow surface structure using GPR, a non-intrusive method;
(2) analyze rock glacier surface morphology in relation to its subsurface characteristics;
(3) develop a model that describes the movement mechanics and development of the rock glacier; and
(4) apply the model to Martian analogues using the terrestrial rock glacier as a surrogate. The model was developed for the purpose of evaluating Martian landforms for potential stores of water.

ENGINEERING ASPECTS: ROCK GLACIER GEOMORPHOLOGY

Rock glaciers, which are distinctive landforms occurring in alpine environments, provide locations for urban water sources, construction borrow sources, drill sites, shaft and tunnel portals, ski tower supports, and dam abutments. The growing number of

mountain subdivisions constructed in alpine regions necessitates an understanding of potential hazards that are created because of the interplay between humans and rock glaciers and the geologic processes associated with their formation and movement.

Rock glaciers are temporary forms that mark the transition from glacial or periglacial processes to current geomorphic processes. In spite of their dynamic nature, many engineers and engineering geologists incorrectly regard rock glaciers as static forms. Instead, geologists and engineers must be aware of and understand the formation and dynamics of rock glaciers before establishing human developments on or adjacent to them. It is therefore important that the current status (i.e., active or inactive) of a rock glacier be determined so that the proper engineering approaches can be employed. Placing structures on, in, or adjacent to rock glaciers also requires an appreciation and understanding of the temporal stability of these forms.

From an engineering perspective, the internal structure of a rock glacier is significant because it provides important evidence on how the rock glacier deforms as well as how the rock glacier settles during periods of melting. Rock glaciers cause three primary types of damage to engineered works: damage from gross active movement; damage from other deformational processes; and damage from settlement and sloughing. Even the most slow-moving active rock glacier will damage or destroy structures built directly on or through it. When inactive rock glaciers are considered, the consequences of structural failure and the availability of alternative sites are the primary considerations.

In addition to their role as debris transport phenomena, rock glaciers serve as alpine aquifers. However, these aquifers have limited spatial extent and the structures of most rock glaciers are conducive to the production of steady, continuous meltwater only during the summer months. In addition, the hydrologic cycle of a rock glacier is influenced slowly by long-term climate change. The long-term impact of climate change on the temporal nature of a rock glacier must be evaluated when considering a rock glacier for its aquifer potential.

In an attempt to address the serious lack of knowledge and understanding of the important role that rock glaciers play in alpine environments, this chapter provided a

discussion of the morphologic and dynamic aspects of rock glaciers. In addition, a discussion and guidelines for engineering evaluation and use of rock glaciers was developed. The intent was to provide concise background and a set of practical tables to help engineers, engineering geologists, and geomorphologists deal competently with rock glaciers. Although the chapter addresses the potential problems that must be considered and overcome to build on a rock glacier, the general recommendation is that rock glaciers must be avoided for essentially all structures.

MODEL BASED ON YANKEE BOY ROCK GLACIER

The results of the GPR investigation show that the Yankee Boy rock glacier consists of horizontal to sub-horizontal layers of ice-rich and ice-poor strata. These layers, some of which are laterally continuous up to 70 m in all directions, are interpreted to be ice-supersaturated sediments and coarse blocky rockslide debris. The layers are considered to be the result of flow, perhaps generated by seasonal snow pack covered by episodic debris flows or high-magnitude discharges of talus.

Major depositional units, identifiable by prominent reflection events in the GPR profiles, are believed to be individual flow lobes that formed at different positions along the cirque headwall. The formation history of the rock glacier involves incorporation of ice within talus debris to form supersaturated permafrost, and subsequent creep of this material to form discrete flow lobes. The rate and position of talus production along the headwall controls the avenue and direction of individual flow lobes. It appears that once formed, the lobes flow down the cirque valley as a coherent geomorphological unit (i.e., a rock glacier). The Yankee Boy rock glacier is interpreted to be a composite feature that formed by a process involving the development and overlap of discrete flow lobes. A sequence of seven discrete flow lobes is identifiable.

A SURROGATE FOR LANDFORMS ON MARS

Rock glacier-like features on Mars suggest the presence of flowing, or once-flowing ice-rock mixtures. These landforms, which include lobate debris aprons, concentric

crater fill and lineated valley fill, hold significant promise as reservoirs of stored water ice that could be useful for human exploration of Mars. They may also contain frozen records of the climatic history of the planet. Using terrestrial rock glaciers as surrogates, we can apply the knowledge gained about internal structure, landform morphology, viscous flow properties, and the role of water to learn about the formation, internal character and deformation processes of Martian analogues.

Results obtained from the rock glacier at Yankee Boy Basin show that the landform is comprised of distinct, continuous alternating ice-rich and ice-poor layers. Folds in the layers correspond to the surface expression of ridges and furrows, indicating that compressive stresses originating in the accumulation zone are transmitted down slope. Thus, ridge-furrow topography is interpreted to be a surface manifestation of this process. Rock glacier features on Mars may also consist of layered permafrost ice and ice lenses, which would suggest a history of permafrost development involving seasonal frost accumulation and/or water influx from below the surface. Based on estimated thickness of lobate debris aprons and valley fill, and given the current climate and atmospheric conditions on Mars, mantle insulation may be sufficient to preserve water ice within these landforms.

Liquid water, found to be abundant in the Yankee Boy rock glacier, occurs as a network of interconnected channels that permeate throughout the landform. In terms of water storage within Martian analogs, considerations must include the possibility that some water ice may be stored in relatively pure form within lenses and vein networks such as observed here. Proximity of viscous-flow features to outflow channels indicates that a plentiful supply of water once flowed on the surface of Mars. If present, subterranean water could serve to replenish or to maintain the content of ice within Martian rock glaciers, thus providing a mechanism to perpetuate their flow for periods of time necessary to account for their size given current temperatures. Water ice could be preserved within debris mantles of sufficient thickness, particularly if the mantles contain an insulating layer of frozen CO_2.

CONVERGENCE OF LANDFORM MORPHOLOGY

The distinctive “wrinkled” surface morphology of ridges and furrows has long been used as a criterion to identify rock glaciers. This approach has resulted in the mis-identification of features such as block streams, block runs, boulder flows and sturzstroms as rock glaciers. Consequently, the equifinality of the Tom Mays block stream was called into question. The origin of the block stream has been reconsidered in light of new data on ground surface roughness, clast fabric, longitudinal and cross-sectional topographic profiles, and local geologic factors. The surface fabric of numerous features were examined, including lowland tills, talus slopes, and ridge and furrow structures associated with rock glaciers. This complementary approach was effective in differentiating the Tom Mays block stream landforms that are morphologically similar (e.g., rock glaciers and landslip boulder deposits).

In general, Chapter V dealt with building a case for interpreting the Tom Mays block stream as a sturzstrom based on the combination of fabric data, morphological features, cliff face scarring, and run-out characteristics. The surface fabric of the block stream compares well with that for lowland tills, and the profile concavity is indicative of a single morphological unit resulting from rapid transport. Rapid emplacement is supported by the superelevation of the blockstream along the steep canyon walls. Microfeatures of the block stream are also consistent with characteristic mechanics of sturzstroms, including sudden braking power, grain flow and/or acoustic fluidization. Compared with the volume and length of documented sturzstroms, the Tom Mays block stream must be considered small, but it does exhibit scarring, superelevation, detachment from point of origin, and topographic features (e.g., hummocky surface and transverse ridges) that are characteristics of sturzstroms and much larger rockfalls. The results of this study suggest that the Tom Mays feature is a small sturzstrom.

CLOSING REMARKS AND FUTURE RESEARCH

As mentioned previously, the application of GPR to the study of rock glaciers is in its infancy. There are a number of benefits that would result from a more detailed

understanding about the internal structure of rock glaciers. Because many researchers are interested in the paleoclimate records that are contained in the ice of rock glaciers, it is important to determine whether a rock glacier is ice-cored or ice-cemented. This would allow the formation process (i.e., glacial versus permafrost origin) and deformation history to be accounted for when attempting to reconstruct past climate. Detailed information provided by GPR about internal structure is therefore essential for understanding these issues. In terms of the implications for Yankee Boy Basin and the San Juan Mountain region, the results presented in this dissertation provide a basis for which to examine glacial and depositional history by correlating episodes of rock glacier flow lobe generation with cliff face degradation and moraine deposits throughout cirques and valleys. Techniques such as lichenometry, remote sensing and geomorphic mapping hold much promise for developing such an understanding.

Future studies on rock glaciers should attempt to answer fundamental questions about hydrologic balance, kinematics, and thermodynamics. One basic piece of information needed for modeling these parameters is the ice/debris ratio within the rock glacier. To this end, GPR field methods should be developed in conjunction with other sensing techniques (i.e., in-situ temperature measurements) and include provision for three-dimensional description. Greater resolution of the interior of rock glaciers can also provide a basis upon which to refine values for shear stress in creeping ice-rich landforms. Along these lines, an important goal of rheological modeling should be to identify the ice accumulation processes in rock glaciers and to quantify the rates at which they operate during various climate conditions. Temporal monitoring with GPR and sustained climatological data collection would facilitate this type of effort. From such data, inferences can be made of the distribution and characteristics of active and extinct rock glaciers, and help in the interpretation of suspect landforms such as the Tom Mays block stream. The author’s hope for the future is that the application of GPR will continue to a variety of rock glaciers of different size and classification (e.g., lobate, tongue-shaped, valley side, ice-cored, ice-cemented) for the purpose of correlating

internal structure with environment, geology, and position within the landform continuum.

REFERENCES

Allmendinger, R.W., 1989. Stereonet v. 4.25, © 1988, 1989. – Computer graphing program for personal computers.

Andersland, O. and Anderson, D. (Eds.) 1978, Geotechnical Engineering for Cold Regions. McGraw-Hill, New York, 566 pp.

Annan, A. P., Davis, J. L., 1976. Impulse radar sounding in permafrost, Radio Science 11, 383-394.

Assier, A., Fabre, D., Evin, M., 1996. Prospection èlectrique sur les glaciers rocheux du cirque de Sainte-Anne (Queyras, Alpes du Sud, France). Permafrost and Periglacial Processes 7, 53-67.

Bagnold, R. A., 1954. Experiments on a gravity-free dispersion of large solid spheres in a Newton fluid under shear. Proceedings of the Royal Society of London Series A 225, 49-63.

Bagnold, R. A., 1956. The flow of cohesionless grains in fluids. Proceedings of the Royal Society of London Series A 235-297.

Bajewski, I., Gardner, J. S. 1989. Discharge and sediment-load characteristics of the Hilda rock-glacier stream, Canadian Rocky Mountains, Alberta. Physical Geography 10, 295-306.

Baker, V. R. 1982. The Channels of Mars. University of Texas Press, Austin, 198 pp.

Ballantyne, C. K., Kirkbride, M. P. 1987. Rockfall activity in upland Britain during the Loch Lomond stadial. Geography Journal 153, 86-92.

Barsch, D. 1969. Studien und messungen an blockgletschern in Macun, Unterengadin, Zeitschrift für Gletschkunde und Glazialgeologie 8, 11-30.

Barsch, D. 1977. Nature and importance of mass-wasting by rock glaciers in alpine permafrost environments. Earth Surface Processes 2, 231-245.

Barsch, D. 1988. Rockglaciers. In: Clark, M. J., (Ed.), Advances in Periglacial Geomorphology. Wiley, Chichester, West Sussex, 69-90.

Barsch, D. 1996. Rock Glaciers – Indicators for the Present and Former Geoecology in High Mountain Environments. Springer-Verlag, Berlin, 331 pp.

Barsch, D., Fierz, H., Haeberli, W., 1979. Shallow core drilling and bore-hole measurements in permafrost of an active rock glacier near the Grubengletscher, Wallis, Swiss Alps. Arctic and Alpine Research 11, 215-228.

Barsch, D., Jakob, M., 1993. Active rockglaciers and the lower limit of discontinuous alpine permafrost in the Khumbu Himalaya, Nepal. Proceedings of the Sixth International Conference on Permafrost, Beijing, China. 1 South China. University of Technology Press, Wushan, China.

Bell, R. A., Rahn, P. H., 1972. Rock glaciers in the Rocky Mountains of Wyoming and Colorado. Geological Society of America Abstracts with Programs 4 (6), 365.

Benedict, J. B., Benedict, R. J., Sanville, D., 1986. Arapaho rock glacier, Front Range, Colorado, U.S.A.: A 25-year resurvey. Arctic and Alpine Research 18 (3), 349-352.

Bernhard, L., Sutter, F., Haeberli, W., Keller, F., 1998. Processes of snow/permafrost-interactions at a high-mountain site, Murtèl/Corvatsch, Eastern Swiss Alps. Proceedings of the Seventh International Conference on Permafrost. Yellowknife, Canada, Collection Nordicana 57, 35-41.

Berthling, I., Etzemueller, B., Eiken, T., Sollid, J. L., 1998. Rock glaciers on Prins Karls Forland, Svalbard. I: Internal structure, flow velocity and morphology. Permafrost and Periglacial Processes 9, 135-145.

Berthling, I., B. Elzelmuller, K. Isaksen, J. L., 2000. Sollid, Rock Glaciers on Prins Karls Forland II: GPR Soundings and the Development of Internal Structures. Permafrost and Periglacial Processes 11, 357-369.

Bertran, P., Hètu, B., Texier, J. P., Van Steijn, H., 1997. Fabric characteristics of subaerial slope deposits. Sedimentology 44, 1-16.

Birkeland, P. W., 1973. Use of relative age dating methods in a stratigraphic study of rock glacier deposits, Mt. Sopris, Colorado. Arctic and Alpine Research 5 (4), 401-416.

Blumstengel, W. K., 1988. Studies of an active rock glacier, Slims River Valley, Kluane National Park, Yukon Territory; unpublished M.Sc. thesis, Department of Geography, University of Calgary, Calgary, Alberta, 207 pp.

Brown, W. H., 1925. A probable fossil glacier. Journal of Geology 33, 464-66.

Burger, K. C., Degenhardt, J. J. Jr., Giardino, J. R., 1999. Engineering geomorphology of rock glaciers. In: Giardino, J. R., Marston, R. A., Morisawa, M. (Eds.), Engineering Geology – Changing the Face of Earth. 28th Binghamton Symposium Special Volume, Elsevier, Amsterdam, pp. 93-132.

Burger, K. C., Giardino, J. R., Ridenour G., Vitek J. D., 1997. A thermodynamic approach to rock glacier development. In: Abstracts and Program, Annual Meeting, The Geological Society of America, Salt Lake City, Utah., 32-33.

Caine, N., 1967. The texture of talus in Tasmania. Journal of Sedimentary Petrology 37, 796-803.

Caine, N., 1968. Air photo analysis of blockfield fabrics in Talus Valley, Tasmania. Journal of Sedimentary Petrology 42, 33-48.

Calkin, P. E., Haworth, L. A., Ellis, J. M., 1987. Rock glaciers of central Brooks Range, Alaska, U.S.A. In: Giardino, J. R., Shroder, J. F. Jr., Vitek, J. D. (Eds.), Rock Glaciers. Allen and Unwin, London, pp. 65-82.

Calkin, P. E., Kaufman, D. S., Przybyl, B. J., Whitford, W. B., Peck, B. J., 1998. Glacier regimes, periglacial landforms, and holocene climate change in the Kigluaik Mountains, Seward Peninsula, Alaska, U.S.A. Arctic and Alpine Research 30 (2), 154-165.

Capps, S. R., 1910. Rock glaciers in Alaska. Journal of Geology 18, 359-375.

Carr M. H., 1986. Mars a water-rich planet? Icarus 68, 187-216.

Carr M. H., 1987. Mars: A water-rich planet. In: Baker, V., Carr, M. H., Fanale, F. P., Greeley, R. M., Haeberli, W., Leovy, C., Maxwell, T. A. (Eds.), MECA Symposium on Mars: Evolution of its Climate and Atmosphere. pp. 23-25.

Carr M. H., 1995. The Martian drainage system and the origin of valley networks and fretted channels. Journal of Geophysical Research 100, 7,479-7,507.

Chaix, A., 1919. Coulées de blocs (rock glaciers, rock streams) dans le Parc National Suisse de la Basse-Engadine. C.R. Seances Societé Physique et d'Histoire Naturelle de Genève 36, 12-15.

Chaix, A., 1923. Les coulées des blocs du Parc National Suisse d'Engadine (note prelimminaire), Le Globe (Organe de la Societé de Géog. de Genève). Journal of Géography 62, (Memoires), 34 pp.

Chaix, A., 1943. Les coulées des blocs du Parc National Suisse: Nouvelles mesures et comparison avec les "rock streams" de la Sierra Nevade de Californie. Le Globe 82, 121-128.

Chuang, F. C., Greeley, R., Moore, J. M., The Galileo SSI Team, 1999. Large-scale mass movements observed from the Galileo Nominal Mission. Lunar and Planetary Science Conference Abstracts, 86.

Clark, M. J., 1988. Advances in Periglacial Geomorphology. Wiley, Chichester, West Sussex, 481 pp.

Clark, D. H., Clark, M. M., Gillespie, A. R., 1994a. Debris-covered glaciers in the Sierra Nevada, California, and their implications for snowline reconstructions. Quaternary Research 41, 139-153.

Clark, D. H., Clark, M. M., Gillespie, A. R., 1994b. Reply to comment by M. Jakob on debris-covered glaciers in the Sierra Nevada, California, and their implications for snowline reconstruction. Quaternary Research 42, 359-362.

Clark, B. C., A. K. Baird, H. J. Rose, P. Toulmin III, K. Keil, A. J. Castro, W. C. Kelliher, C. D. Rowe, P. H. Evans, 1976. Inorganic analysis of Martian surface samples at the Viking landing sites. Science 194, 1,283-1,288.

Clark, D. H., Steig, E. J., Potter, N. Jr., Fitzpatrick, J., Updike, A. B., Clark, G. M., 1996. Old ice in rock glaciers may provide long-term climatic records. EOS, Transactions, American Geophysical Union 77 (23) 217, 221-222.

Clifford, S. M., 1984. A Model for the Climatic Behavior of Water on Mars. Ph.D. Dissertation, University of Massachusetts. Amherst, Massachussetts, 275 pp.

Clifford, S. M., 1993. A Model for the hydrologic and climatic behavior of water on Mars. Journal of Geophysical Research 98, 10,973-11,016.

Clifford, S. M., 1987. Mars: Crustal pore volume, cryospheric depth, and the global occurrence of groundwater. In: Baker, V., Carr, M. H., Fanale, F. P., Greeley, R. M., Haeberli, W., Leovy, C., Maxwell, T. A. (Eds.), MECA Symposium on Mars: Evolution of its Climate and Atmosphere, LPI Technical Report 87-01, abstract, 32.

Clifford, S. M., Hillel, D., 1983. The stability of ground ice in the equatorial regions of Mars. Journal of Geophysical Research 88, 2,456-2,474.

Clifford, S. M., Parker T. J., 2001. The evolution of the Martian hydrosphere: implications for the fate of a primordial ocean and the current state of the northern plains. Icarus 154, 40-79.

Colprete, A., Jakosky, B. M., 1998. Ice flow and rock glaciers on Mars. Journal of Geophysical Research 103 (E3), 5,897-5,909.

Corte, A. E., 1976a. Rock glaciers. Biuletyn Peryglacjalny 26, 175-197.

Corte, A. E., 1976b. The hydrological significance of rock glaciers. Journal of Glaciology 17 (75), 157-158.

Corte, A. E., 1978. Rock glaciers as permafrost bodies with debris cover as an active layer. A hydrological approach. Andes of Mendoza, Argentina. In: Proceedings of the Third International Conference on Permafrost, Edmonton, Alberta, Canada 1 National Research Council of Canada, Ottawa, pp. 262-269.

Corte, A. E., 1987a. Rock Glacier Taxonomy. In: Giardino, J. R., Shroder, J. F. Jr., Vitek, J. D. (Eds.), Rock Glaciers. Allen and Unwin, London, pp. 27-39.

Corte, A. E., 1987b. Central Andes rock glaciers: Applied aspects. In: Giardino, J. R., Shroder, J. F. Jr., Vitek, J. D. (Eds.), Rock Glaciers. Allen and Unwin, London, pp. 289-304.

Cross, C. W., Howe, E., 1905. Geography and general geology of the quadrangle in Silverton folio. U. S. Geological Survey Folio 120, 1-25.

Cui, Z., Zhu, C., 1989. The structural type of temperature and mechanism of movement of rock glacier at the head of Ürümqi River, Tianshan Mountains. Chinese Science Bulletin 34 (15), 1,286-1,291.

Daniels, D. J., 1996. Surface penetrating radar. In: IEEE Radar, Sonar, Navigation and Avionics 6, 300 pp.

Daniels, D. J., Gunton, D. J., Scott, H. F., 1988. Introduction to subsurface radar. Institute of Electrical and Electronic Engineers Proceedings 135 (Part F, No. 4), 277-320.

Degenhardt, J. J. Jr., Giardino, J. R., in review. GPR survey of a lobate rock glacier in Yankee Boy Basin, Colorado, USA. In: Bristow, C., Jol, H. (Eds.), Ground Penetrating Radar (GPR) in Sediments: Applications and Interpretation. Geological Society of London.

Degenhardt, J. J. Jr., Giardino, J. R., 1999a. Kinematic wave models for Martian landforms based on rock glacier analogs. Meteoritics and Planetary Science 34 (4) Supplement, A31.

Degenhardt, J. J. Jr., Giardino J. R., 1999b. Describing lobate Martian landforms using a terrestrial rock glacier kinematic wave model. Geological Society of America Abstracts with Program, Denver, Colorado, A175.

Degenhardt, J. J. Jr., Giardino, J. R., Junck, M. B., Quintana, M. P., Marston, R. A., 2000. Evaluating the internal structure of a rock glacier using ground penetrating radar (GPR): Yankee Boy Basin, Colorado, U.S.A. Geological Society of America Abstracts with Program, Reno, Nevada 32 (7), A516.

Degenhardt, J. J. Jr., Giardino, J. R., Pierce, C., 2001. Longitudinal survey of a lobate rock glacier using ground penetrating radar (GPR), Yankee Boy Basin, Colorado, U.S.A. Geological Society of America Abstracts with Program, Boston, Massachussetts 33 (6), A65.

Domaradzki, J., 1951. Blockströme im Kanton Graubünden. Ergebnisse Wiss Untersuchtungen Schweiz Nationalparks 3 (23), 173-235.

Elconin, R. F., Lachapelle, E. R., 1997. Flow and internal structure of a rock glacier. Journal of Glaciology 43 (144), 238-244.

Evin, M., 1983. Structure et mouvement des glaciers rocheux des Alpes du Sud, Université de Grenoble I, Institut de Géographie Alpine, Thèse de 3^{e} cycle, 343 pp.

Evin, M., 1984. Glaciers rocheux actuels et limites du périgelisol alpin: L'exemple des Alpes du Sud, Communication a la commission pour l'etude des phénomènes périglaciaires, Fountainebleau-Avon, 14-15 Janvier, 1984.

Evin, M., 1987. Lithology and fracturing control of rock glaciers in southwestern Alps of France and Italy. In: Giardino, J. R., Shroder, J. F. Jr., Vitek, J. D. (Eds.), Rock Glaciers. Allen and Unwin, London, pp. 83-106.

Evin, M., Fabre, D., Johnson, P. G., 1997. Electrical resistivity measurements on the rock glaciers of Grizzly Creek, St. Elias Mountains, Yukon. Permafrost and Periglacial Processes 8, 179-189.

Fara, H. D., Scheidegger, A. E., 1963. An eigenvalue method for the statistical evaluation of fault plane solutions of earthquakes. Seismological Society of America Bulletin 53, 811-816.

Farmer, C. B., P. E. Doms, P. E., 1979. Global and seasonal variation of water vapor on Mars and the implications for permafrost. Journal of Geophysical Research 84, 2,881-2,888.

Fisch, W. Sr., Fisch W. Jr., Haeberli, W. 1977, Electrical D.C. resistivity soundings with long profiles on rock glaciers and moraines in the Alps of Switzerland. Zeitschrift für Gletschkunde und Glazialgeologie 13, 239-260.

Fitzgerald, J. W., 1994. Morpho-dynamic Modeling of Rock Glaciers: San Juan Mountains, Colorado, USA, unpublished Ph.D. dissertation, Texas A&M University, College Station, Texas, 202 pp.

Fitzgerald, J. W., Giardino, J. R., Maggio, R. C., Vitek, J D., 1988. Mapping and evaluating geomorphic engineering aspects of high mountain terrain using a geographic information system, Sangre de Cristo Mountains, Colorado. Geological Society of America Centennial Celebration 20 (7), 64-65.

Fitzgerald, J. W., Giardino, J. R., Vitek, J. D., 1993. Computer simulation and visualization for validating geomorphic models of the alpine environment; Yankee Boy Basin, San Juan Mountains, Colorado. Annual Meeting of the Association of American Geographers, Southeastern Division, abstracts 89, 70.

Foster, H. F., Holmes, G. W., 1965. A large transitional rock glacier in the Johnson Area, Alaska Range, U. S. Geological Survey Professional Paper 525-B, B112-B116.

Francou, B., Reynaud, L., 1992. Ten years of surficial velocities on a rock glacier (Laurichard, French Alps). Permafrost and Periglacial Processes 3 (2), 209-213.

Gardner, J. S., Bajewsky, I., 1987. Hilda rock glacier stream discharge and sediment load characteristics, Sunwapta Pass area, Canadian Rocky Mountains. In: Giardino, J. R., Shroder, J. F. Jr., Vitek, J. D. (Eds.), Rock Glaciers. Allen and Unwin, London, pp. 161-174.

Gerber, E. K., Scheidegger, A. E., 1979. Systematics of Geomorphic Surfaces and Kinematics of Movements Thereon. Zeitschrift für Geomorphologie. N. F. 23 (1), 1-12.

Giardino, J. R., 1979. Rock glacier mechanics and chronologies: Mount Mestas, Colorado, unpublished Ph.D. dissertation, University of Nebraska, Lincoln, Nebraska, 244 pp.

Giardino, J. R., 1980. Rock glacier mechanics. American Quaternary Association, abstract 83.

Giardino, J. R., 1983. Movement of ice-cemented rock glaciers by hydrostatic pressure: An example from Mt. Mestas, Colorado. Zeitschrift für Geomorphologie 27, 297-310.

Giardino, J. R., Shroder, J. F. Jr., Lawson, M. P., 1984. Tree-ring analysis of movement of a rock-glacier complex on Mt. Mestas, Colorado, U.S.A. Arctic and Alpine Research 16 (3), 299-309.

Giardino, J. R., Shroder, J. F. Jr., Vitek, J. D., 1987. Rock Glaciers. Allen & Unwin, London, 355 pp.

Giardino, J. R., Vick, S. G., 1985. Engineering hazards of rock glaciers. Bulletin of the Association of Engineering Geologists 22 (2), 201-216.

Giardino, J. R., Vick, S. G., 1987. Geologic engineering aspects of rock glaciers. In: Giardino, J. R., Shroder, J. F. Jr., Vitek, J. D. (Eds.), Rock Glaciers. Allen and Unwin, London, pp. 265-287.

Giardino, J. R., Vitek, J. D., 1985. A statistical study of the fabric of a rock glacier. Arctic and Alpine Research 17, 165-177.

Giardino, J. R., Vitek, J. D., 1988a. Rock glacier rheology: A preliminary assessment. In: Senneset, K. (Ed.), Proceedings of the Fifth International Conference on Permafrost. Trondheim, Norway, pp. 744-748.

Giardino, J. R., Vitek, J. D., 1988b. The significance of rock glaciers in the glacial-periglacial landscape continuum. Journal of Quaternary Science 3 (1), 97-103.

Giardino, J. R., Vitek, J. D., Demorett, J. L., 1992. A model of water movement in rock glaciers and associated water characteristics. In: Dixon, J. C., Abrahams, A. D. (Eds.), Periglacial Geomorphology. Wiley, Chichester, West Sussex, pp. 159-184.

Giardino, J. R., Marston, R. A., Degenhardt, J. J. Jr., Pitty, A., Vitek, J. D., 1999. Rock glacier vs. sturzstrom; A convergence of processes and landform morphology: Fabric data from the Franklin Mountains, TX, and the San Juan Mountains, Colorado, U.S.A. Geological Society of America Abstracts with Program, Denver, Colorado 31 (7), 52.

Gorbunov, A. P., 1983. Rock glaciers of the mountains of Middle Asia. In: Proceedings of the Fourth International Conference on Permafrost. National Academy Press, Washington, D.C., pp. 359-362.

Gorbunov, A. P., Polyakov, S. N., 1992. Dynamics of rock glaciers of the Northern Tien Shan and the Djungar Ala Tau, Kazahkstan. Permafrost and Periglacial Processes 3, 29-39.

Gould, P. R., 1967. On the geographical interpretation of eigenvalues. Transactions of the Institute of British Geography 42, 53-86.

Grab, S. W., 1996. The occurrence of a Holocene rock glacier on Mount Kenya: Some observations and comments. Permafrost and Periglacial Processes 7, 381-389.

Griffiths, T., 1976. Personal communication. Professor, Department of Geography, University of Denver, Denver, Colorado 80210.

Guglielmin, M., Lozej, A., Tellini, C., 1994. Permafrost distribution and rock glaciers in the Livigno area (northern Italy). Permafrost and Periglacial Processes 5, 25-36.

Guglielmin, M., Claudio, S., Cannone, N., 1997. The rock glaciers of the Lombardy Alps (Italy) as indicators of mountain permafrost. Fourth International Conference on Geomorphology, The International Association of Geomorphologists Bologna, Italy (Supplement 3), 193.

Haeberli, W., 1985. Creep of mountain permafrost: Internal structure and flow of alpine rock glaciers: Mitteilungen der Versuchsanstalt fur Wasserbau, Hydrologie und Glaziologie Nr. 77, Zurich, 142 pp.

Haeberli, W., 1998. Personal communication. Professor, Department of Geography, University of Zurich, Winterthurerstrasse 190, CH-8057 Zurich.

Haeberli, W., 2000. Modern research perspectives relating to permafrost creep and rock glaciers. Permafrost and Periglacial Processes 11, 290-293.

Haeberli, W., Keusen, H. R., 1983. Site investigation and foundation design aspects of cable car construction in alpine permafrost at the “Chli Matterhorn,” Wallis, Swiss Alps. In: Proceedings of the Fourth International Conference on Permafrost. National Academy Press, Washington, D.C., pp. 601-605.

Haeberli, W., Schmid, W., 1988. Aerophotogrammetrical monitoring of rock glaciers. In: Proceedings of the Fifth International Conference on Permafrost 1 Tapir Publishers, Trondheim, Norway, pp. 764-769.

Haeberli, W., Vonder Müehll, D., 1996. On the characteristics and possible origins of ice in rock glacier permafrost. Zeitschrift für Geomorphologie (Supplement 104), 43-57.

Haeberli, W., King, L., Flotron, A., 1979. Surface movement and lichen-cover studies at the active rock glacier near the Grubengletscher, Wallis, Swiss Alps. Arctic and Alpine Research 11, 421-41.

Haeberli, W., Huder, J., Keusen, H., Pika, J., Röthlisberger, H., 1988. Core drilling through rock glacier-permafrost. Proceedings of the Fifth International Conference on Permafrost 2, Trondheim, Norway, 937-942.

Haeberli, W., Hoelze, M., Kääb, A., Keller, F., Vonder Müehll, D., Wagner, S., 1998. Ten years after drilling through the permafrost of the active rock glacier Murtel, Eastern Swiss Alps: Answered questions and new perspectives. Proceedings of the Seventh International Conference on Permafrost. Yellowknife, Canada, Collection Nordicana 57, 403-410.

Haeberli, W., Kääb, A., Wagner, S., Vonder Müehll, D., Geissler, P., Haas, J. N., Glatzel-Mattheier, H., Wagenbach, D., 1999. Pollen analysis and C14 age of moss remains in a permafrost core recovered from the active rock glacier Murtel-Corvatsch, Swiss Alps: geomorphological and glaciological implications. Journal of Glaciology 45 (149), 1-8.

Hamilton, S. J., Whalley, B. W., 1995. Rock glacier nomenclature: a re-assessment. Geomorphology 14, 73-80.

Hart, B. I., 1942. Tabulation of the probabilities for the ratio of the mean square of successive differences of the variance. Annals of Mathematical Statistics 13, 207-214.

Hayashi, J. N., Self, S., 1992. A comparison of pyroclastic flow and debris avalanche mobility. Journal of Geophysical Research, B, Solid Earth and Planets 97 (6), 9,063-9,071.

Höllerman, P., 1983. Blockgletscher als mesoformen der Periglaziastufe - Studien aus europaischen und nordamerikanischen Hochgebirgen. Bonner Geografische Abhandlungen 67, 83 pp.

Hooke, R. LeB., 1967. Processes on arid-region alluvial fans. Journal of Geology 75, 438-460.

Hooke R. LeB., Dalin, B. B., Kauper, M. T., 1972. Creep of ice containing dispersed fine sand. Journal of Glaciology 11, 327-336.

Horvath, C. L., 1998. An evaluation of ground penetrating radar for investigation of palsa evolution, Macmillan Pass, NWT, Canada. In: Lewkowicz, A. G., Allard, M. (Eds.), Proceedings of the Seventh International Conference on Permafrost, Yellowknife, Canada, pp. 473-478.

Howe, E., 1909. Landslides in the San Juan Mountains, Colorado, including a consideration of their causes and their classification. U. S. Geological Survey Professional Paper 67, 31-40.

Hsü, K. J., 1975. Catastrophic debris streams (sturzstroms) generated by rockfalls. Geological Society of America Bulletin 86, 129-140.

Humlum, O., 1996. Origin of rock glaciers from Mellemfjord, Disko Island, Central West Greenland. Permafrost and Periglacial Processes 7, 361-380.

Humlum, O., 1997a. Active layer thermal regime at three rock glaciers in Greenland. Permafrost and Periglacial Processes 8, 383-408.

Humlum, O., 1997b. Rock glacier observations in Greenland. In: Fourth International Conference on Geomorphology (Supplement 3) International Association of Geomorphologists, Bologna, Italy, p. 210.

Humlum, O., 1998. Rock glaciers on the Faeroe Islands, the north Atlantic. Journal of Quaternary Science 13 (4), 293-307.

Imhof, M., 1996. Modelling and verification of the permafrost distribution in the Bernese Alps (Western Switzerland). Permafrost and Periglacial Processes 7, 267-280.

Innes, J., 1983. Debris flows. Progress in Physical Geography 7, 469-501.

Isaksen, K., Odegard, R. S., Eiken, T., Sollid J. L., 2000. Composition, flow and development of two tongue-shaped rock glaciers in the permafrost of Svalbard. Permafrost and Periglacial Processes 11 (3), 241-257.

Ives, R. L., 1940. Rock glaciers in the Colorado Front Range. Geological Society of America Bulletin 51, 1,271-1,294.

Jackson, L. E., Macdonald, G. M., 1980. Movement of an ice-cored rock glacier, Tungsten, N. W. T., Canada, 1963-1980. Arctic 33 (4), 842-847.

Johnson, P. G., 1978. Rock glacier types and their drainage systems, Grizzly Creek, Yukon Territory. Canadian Journal of Earth Science 15, 1,496-1,507.

Johnson, P. G., 1981. The structure of a talus-derived rock glacier as deduced from its hydrology. Canadian Journal of Earth Science 18 (9), 1,422-1,430.

Johnson, P. G., 1983. Rock glaciers: a case for a change in nomenclature. Geografiska Annaler 65A, 27-34.

Johnson, P. G., 1984. Rock glacier formation by high-magnitude low-frequency slope processes in the southwest Yukon. Annals of the Association of American Geographers 74 (3), 408-419.

Johnson, P. G., 1987. Rock glaciers; glacier debris systems or high magnitude low-frequency flows. In: Giardino, J. R., Shroder, J. F. Jr., Vitek, J. D. (Eds.), Rock Glaciers. Allen and Unwin, London, pp. 175-192.

Johnson, P. G., 1992. Microrelief on a rock glacier, Dalton Range, Yukon, Canada. Permafrost and Periglacial Processes 3, 41-47.

Jol, H.M., 1995. Ground penetrating radar antennae frequencies and transmitter powers compared for penetration depth, resolution and reflection continuity. Geophysical Prospecting 43, 693-709.

Jol, H. M., Smith, D. G., 1995. Ground penetrating radar surveys of peatlands for oilfield pipelines in Canada, Journal of Applied Geophysics 34 (2), 109-123.

Kaeaeb, A., Haeberli W., Gundmundsson, G. H., 1997. Analysing the creep of mountain permafrost using high precision aerial photogrammetry: 25 years of monitoring Gruben rock glacier, Swiss Alps. Permafrost and Periglacial Processes 8, 408-426.

Kamb, W. B., 1959. Ice petrofabric observations from Blue Glacier, Washington, in relation to theory and experiment. Journal of Geophysical Research 64, 1,891-1,909.

Kilburn, C. R. J., Sørensen, S. A., 1998. Runout lengths of sturzstroms: the control of initial conditions and of fragment dynamics. Journal of Geophysical Research 103, 17,877-17,884.

King, L., Fisch, W. W., Haeberli, W., Waechter, H. P., 1987. Comparison of resistivity and radio-echo soundings on rock glacier permafrost. Zeitschrift für Gletscherkunde und Glazialgeologie 23 (1), 77-97.

Konrad, S. K., Humphrey, N. F., 2000. Steady-state flow model of debris-covered glaciers (rock glaciers). In: Nakawo, M., Raymond, C. F., Fountain, A. (Eds.), Debris-Covered Glaciers, Proceedings of a workshop held at Seattle, Washington, International Association of Hydrological Sciences Publication no. 264, Wallingford, United Kingdom, pp. 255-263.

Langbein W. B., Leopold, L. B., 1968. River channels, bars and dunes – theory of kinematic waves. U. S. Geological Survey Professional Paper 122L, L1-20.

Lehmann, F., D. Vonder Mühll, M. van der Veen, P. Wild, A. Green, 1998. True topographic 2-D migration of geo-radar data. In: Bell, R. S., Powers, M. H., Larson, T. (Eds.), Proceedings of the Symposium on the Application of Geophysics to Environmental and Engineering Problems (SAGEEP), Chicago, pp. 107-114.

Lighthill, M. J., Whitman, G. B., 1955. On kinematic waves I. Flood movement in long rivers (281-316). II. A theory of traffic flow on long crowded roads (317-345). Proceedings of the Royal Society of London Serial A 222, 281-345.

Lovejoy, E. M. P., 1972. Wisconsin boulder flow and its geomorphic implications, Franklin Mountains, El Paso County, Texas. Geological Society of America Bulletin 83, 3,501-3,508.

Lovejoy, E. M. P., 1973. Wisconsin boulder flow and its geomorphic implications, Franklin Mountains, El Paso County, Texas: Reply. Geological Society of America Bulletin 84, 3,751-3,754.

Lowe, D. R., 1976. Grain flow and grain flow deposits. Journal of Sedimentary Petrology 46, 188-199.

Lucchitta, B. K., 1984. Ice and debris in the fretted terrain, Mars. Proceedings of the 14th Lunar and Planetary Science Conference Part 2, Journal of Geophysical Research 89 (Supplement), B409-B418.

Lucchitta, B. K., 1986. Water and ice on Mars: Evidence from Valles Marineris. In: MECA: Papers Presented to the Symposium on Mars: Evolution of Its Climate and Atmosphere. Lunar and Planetary Institute Contribution 599, pp. 59-61.

Lucchitta, B. K., 1993. Mars: Periglacial and glacial forms of relief. In: Kartashov, I. P., Nikiforova, K. V. (Eds.), Studies of the Quaternary Period: Selected papers from the XI INQUA congress. Izd. Nauka, Moscow, pp. 183-193.

Luedke, R. G., Burbank, W. S., 1976. Map showing types of bedrock and surficial deposits in the Telluride Quadrangle, San Miguel, Ouray, and San Juan counties, Colorado. Miscellaneous Investigations Series, U. S. Geological Survey, Reston, Virginia.

Malin, M. C., Edgett, K. S., Davis, S. D., Caplinger, M. A., Jensen, E., Supulver, K. D., Sandoval, J., Posiolova, L., Zimdar, R., (Image M19-01420), Malin Space Science Systems Mars Orbiter Camera Image Gallery (http://www.msss.com/moc_gallery/), (Released October 8, 2001).

Mardia, K. V., 1972. Statistics of Directional Data. Academic Press, New York, 357 pp.

Mark, D. M., 1973. Analysis of axial orientation data, including till fabrics. Geological Society of America Bulletin 84, 1,396-1,374.

Mark, D. M., 1974. On the interpretation of till fabrics. Geology 2, 101-104.

Martin, H. E., Whalley, W. B., 1987. Rock glaciers part I: rock glacier morphology, classification and distribution. Progress in Physical Geography 11 (2), 260-282.

McEwen, A. S., 1989. Mobility of large rock avalanches: evidence from Valles Marineris, Mars. Geology 17, 1,111-1,114.

McMechan, G. A., Loucks, R. G., Xiaoxian, Z., Mescher, P., 1998. Ground penetrating radar imaging of a collapsed paleocave system in the Ellenburger dolomite, central Texas. Journal of Applied Geophysics 39 (1), 1-10.

Mellon M. T., Jakosky, B. M., 1995. The distribution and behavior of Martian ground ice during past and present epochs. Journal of Geophysical Research 100, 11,781-11,799.

Melosh, H. J., 1979. Acoustic fluidization, a new geologic process? Journal of Geophysical Research 84 (B13), 7,513-7,520.

Melosh, H. J., 1987. The mechanics of large rock avalanches. In: Costa, J. E. Wiczorek, G. F. (Eds.), Debris Flows/Avalanches: Process, Recognition, and Mitigation. Geological Society of America Reviews in Engineering Geology 7, pp. 41-49.

Miller, C. D., 1973. Chronology of neoglacial deposits in the Northern Sawatch Range, Colorado, Arctic and Alpine Research 5, 385-400.

Mills, H. H., 1977. Basal till fabrics of modern alpine glaciers. Geological Society of America Bulletin 88, 824-828.

Mills, H. H., 1983. Clast-fabric strength in hillslope colluvium as a function of slope angle. Geografiska Annaler 65A, 255-262.

Morey, R. M., 1974. Detection of subsurface cavities by ground penetrating radar. Proceedings of the Highway Geological Symposium 27, 28-30.

Morris, S. E., 1987. Regional and topography implications of rock glacier stratigraphy: Blanca Massif, Colorado, U.S.A. In: Giardino, J. R., Shroder, J. F. Jr., Vitek, J. D. (Eds.), Rock Glaciers. Allen and Unwin, London, pp. 107-126.

Murray, T., Gooch, D. L., Stuart, G. W., 1997. Structures within the surge front at Bakaninbreen, Svalbard, using ground-penetrating radar. Annals of Glaciology 24, 122-129.

Nelson, F. E., 1982. Sorted stripe microfabrics. Geografiska Annaler 64A, 25-33.

Nicholas, J. W., 1994. Fabric analysis of rock glacier debris mantles, La Sal Mountains, Utah. Permafrost and Periglacial Processes 5, 33-66.

Nicholas J. W., Butler D. R., 1996. Application of relative age-dating techniques on rock glaciers of the La Sal Mountains, Utah - an interpretation of Holocene paleoclimates. Geografiska Annaler Series A - Physical Geography 78A (1), 1-18.

Nicholas, J. W., Garcia, J. E., 1997. Origin of fossil rock glaciers, La Sal Mountains, Utah. Physical Geography 18(2), 160-175.

Nielsen, K. C., 1983. Pebble population ellipsoid; a three-dimensional algebraic description of sedimentary fabric. Journal of Geology 91(1), 103-112.

Nye, J. F., 1960. The Response of glaciers and ice sheets to seasonal and climatic changes. Proceedings of the Royal Society of London Serial A 256, 559-584.

Olyphant, G. A., 1987. Rock glacier response to abrupt changes in talus production. In: Giardino, J. R., Shroder, J. F. Jr., Vitek, J. D. (Eds.), Rock Glaciers. Allen and Unwin, London, pp. 55-64.

Outcalt, S. E., Benedict, J. B., 1965. Photointerpretation of two types of rock glaciers in the Colorado Front Range, U.S.A. Journal of Glaciology 5 (42), 849-856.

Palacios, D., Vazquezselem L., 1996. Geomorphic effects of the retreat of Jamapa glacier, Pico de Orizaba volcano (Mexico). Geografiska Annaler Series A - Physical Geography 78A (1), 19-34.

Palmentola, G., Baboçi, Gruda Gj., Zito G., 1995. A note on rock glaciers in the Albanian Alps. Permafrost and Periglacial Processes 6, 251-257.

Pancza, A., 1998. Les bourrelets-protalus: Liens entre les eboulis et les glaciers rocheux. Permafrost and Periglacial Processes 9, 167-175.

Pariseau, W. G., Voight, 1978. Rockslides and avalanches: Basic principles and perspectives in the realm of civil and mining operations. In: Voight, B. (Ed.), Rockslides and Avalanches, vol. 1. Elsevier, New York, pp. 5-30.

Parker, M. A., Giardino, J. R., and Coulson, R. N., 1999. Landscape ecology: An innovative approach to drainage basin-scale engineering geology; a study of the upper San Miguel River, Colorado. Geological Society of America Abstracts with Program, Denver, Colorado, 31 (7), 33.

Parson, C. G., 1987. Rock glaciers and site characteristics on the Blanca Massif, Colorado, U.S.A. In: Giardino, J. R., Shroder, J. F. Jr., Vitek, J. D. (Eds.), Rock Glaciers. Allen and Unwin, London, pp. 127-144.

Paterson, W. S. B., 1994. The Physics of Glaciers, 3rd Ed., Elsevier Sci., New York.

Pèrez, F. L., 1984. Striated soil in an Andean paramo of Venezuela: it's origin and orientation. Arctic and Alpine Research 16, 277-289.

Pèrez, F. L., 1989. Talus fabric and particle morphometry on Lassen Peak, California. Geografiska Annaler 71A, 43-57.

Pèrez, F. L., 1992. Miniature sorted stripes in the Páramo de Piedras Blancas (Venezuelan Andes). In: Dixon, J. C., Abrahams, A. D. (Eds.), Periglacial Geomorphology, Wiley, New York, pp. 125-157.

Pèrez, F. L., 1998. Talus fabric, clast morphology, and botanical indicators of slope processes on the Chaos Crags (California Cascades), U.S.A. Gèographie Physique et Quaternaire 52 (1), 47-68.

Pitty, A. F., 1968. A simple device for the field measurement of hillslopes. Journal of Geology 76, 717-720.

Pitty, A. F., 1982. The Nature of Geomorphology. Methuen, London, 161 pp.

Potter, N., Jr., 1972. Ice-cored rock glacier, Galena Creek, northern Absaroka Mountains, Wyoming. Geological Society of America Bulletin 83 (10), 3,025-3,057.

Potter, P. E., Pettijohn, F. J., 1977. Paleocurrents and Basin Analysis. Springer Verlag, Berlin, 425 pp.

Potter, N. Jr., Steig, E. J., Clark, D. H., Speece, M. A., Clark, G. M., Updike, A. B., 1998. Galena Creek Rock Glacier revisited - New observations on an old controversy, Geografiska Annaler 80A, 251-266.

Reynolds, J. M., 1997. An Introduction to Applied and Environmental Geophysics. Wiley, Chichester, West Sussex, 796 pp.

Richmond, G. M., 1962. Quaternary stratigraphy in the La Sal Mountains, Utah, United States Geological Survey Professional Paper 324, 131.

Roberts, M. C., Bravard, J. P., Jol, H. M., 1997. Radar signatures and structure of an avulsed channel: Rhone River, Aoste, France. Journal of Quaternary Science 12 (1), 35-42.

Sandeman A. F., Ballantyne C. K., 1996. Talus rock glaciers in Scotland - characteristics and controls on formation. Scottish Geographical Magazine 112 (3), 138-146.

Sayles, F. H., Haynes, D., 1974. Creep of frozen silt and clay, Cold Regions Research and Engineering Laboratory (CRREL) Technical Report 252, Hanover, New Hampshire.

Scheidegger, A. E., 1973. On the prediction of the reach and velocity of catastrophic landslides. Rock Mechanics 5, 231-236.

Schrott, L., 1996. Some geomorphological-hydrological aspects of rock glaciers in the Andes (San Juan, Argentina). Zeitschrift für Geomorphologie Supplement 104, 161-173.

Schweizer, G., 1968. Der formenschatz des spät- und postglazials in den höhen Seealpen. Zeitschrift für Geomorphologie 6, 167 pp.

Scott, D. K., Cheverst, W., 1968. The Midlands Hindu Kush Expedition Report, 1967. Dividend Token Press, London, England, pg. 62.

Sensors & Software, PulseEKKO™ 100 Run Users Guide ver. 1.2, Technical Manual 25, Sensors & Software, 1996.

Shakesby, R. A., Dawson, A. G., Matthews, J. A., 1987. Rock glaciers, protalus ramparts and related phenomena, Rondane, Norway: a continuum of large-scale talus-derived landforms. Boreas 16, 305-317.

Shroder, J. F., Jr., 1971. Landslides of Utah. Utah Geological and Mineralogical Survey Bulletin 90, 51 pp.

Shroder, J. F., Jr., 1972. Rock glaciers on Aquarius Plateau, Utah. In: Adams, W. P., Helleiner, F. M. (Eds.), International Geography 1972. 22nd International Geographical Congress, Montreal, 1972, pp. 63-65.

Shroder, J. F. Jr., 1973a. Movement of boulder deposits, Table Cliffs Plateau, Utah. Geological Society of America Abstracts with Program, Rocky Mountain Section 5, 511-512.

Shroder, J. F. Jr., 1973b. Wisconsin boulder flow and its geomorphic implications, Franklin Mountains, El Paso County, Texas. Discussion. Geological Society of America Bulletin 84, 3,745-3,750.

Shroder, J. F. Jr., 1978. Dendrogeomorphic analysis of mass movement of Table Cliffs Plateau, Utah. Quaternary Research 9, 168-185.

Shroder, J. F., Jr., 1987. Rock glaciers and slope failures: High Plateaus and La Sal Mountains, Colorado Plateau, Utah, U.S.A. In: Giardino, J. R., Shroder, J. F. Jr., Vitek, J. D. (Eds.), Rock Glaciers. Allen & Unwin, London, pp. 193-238.

Sloan, V. F., Dyke, L. D., 1998. Decadal and millennial velocities of rock glaciers, Selwyn Mountains, Canada. In: Steig, E. J., Clark, D. H., Potter, N. Jr., Gillespie, A. R. (Eds.), The Geomorphic and Climatic Significance of Rock Glaciers. Geografiska Annaler Series A: Physical Geography 80 (3-4), pp. 237-249.

Smiraglia, C., 1992. Observations on the rock glaciers of Monte Emilius (Valle d'Aosta, Italy). Permafrost and Periglacial Processes 3 (2), 163-168.

Smith, D. G., Jol, H. M., 1997. Radar Structure of a Gilbert-Type Delta, Peyto Lake, Banff National Park, Canada. Sedimentary Geology 113 (3-4), 195-209.

Smith, H. T. U., 1973. Photogeologic study of periglacial talus glaciers in northwestern Canada, Geografiska Annaler 55A, 69-84.

Soderblom L. A., Condit, C. D., West, R. A., Herman, B. M., Kriedler, T. J., 1974. Martian planetwide crater distributions: implications for geologic history and surface processes. Icarus 22, 239-263.

Squyres, S. W., 1978. Martian fretted terrain: Flow of erosional debris. Icarus 34, 600-613.

Squyres S. W., 1988. Urey Prize Lecture: water on Mars, Icarus 79, 229-288.

Squyres, S. W., Carr, M. H., 1984. The distribution of ground ice on Mars. EOS, Transactions, American Geophysical Union 65 (45), 979.

Squyres, S. W., Carr, M. H., 1986. Geomorphic evidence for the distribution of ground ice on Mars. Science 231, 249-253.

Squyres, S. W., Clifford, S. M., Kuzmin, R. O. Zimbelman, J. R., Costard, F. M., 1992. Ice in the Martian regolith. In: Kieffer, H. H., Jakosky, B. M., Snyder, C. W., Matthews, M. S. (Eds.), Mars. University of Arizona Press, Tucson, pp. 523-554.

Steepstrup, K. J. V., 1883. Bidrag til Kjendskab til Braeerne og Brae-isen I Nord-Grönland. Meddeleser om Grönland 4 (2), 69-112.

Tanaka, K. L., 1995. Geologic/geomorphologic map of the Chryse Planitia Region of Mars, U. S. Geological Survey Atlas of Mars. 1:5,000,000 Geologic Series, Miscellaneous Investigations Map I-2, 441.

Terzaghi, K., Peck, R. B., 1948. Soil Mechanics in Engineering Practice, Wiley, New York, 51-55.

Titkov, S. N., 1988. Rock glaciers and glaciation of the central Asia Mountains, In: Senneset, K. (Ed.), Proceedings of the Fifth International Conference on Permafrost 1 Tapir Press, Trondheim, Norway, pp. 259-262.

Ulriksen, C. P. V., 1982. Application of impulse radar to civil engineering, unpublished Ph.D. dissertation, Lund University of Technology, Lund, Sweden, (republished by Geophysical Survey Systems Inc., Hudson, New Hampshire), 175 pp.

Van Steijn, H., Bertran, P., Francou, B., Hètu, B., Texier, J. P., 1995. Models for the genetic and environmental interpretation of stratified slope deposits: a review. Permafrost and Periglacial Processes 6, 125-146.

Vick, S. G., 1981. Morphology and the role of landsliding in formation of some rock glaciers in the Mosquito Range, Colorado. Geological Society of America Bulletin 92 (2), 75-84.

Vick, S. G., 1987. Significance of landsliding in rock glacier formation and movement. In: Giardino, J. R., Shroder, J. F. Jr., Vitek, J. D. (Eds.), Rock Glaciers. Allen & Unwin, London, pp. 239-263.

Vietoris, L., 1972. Über den Blockgletscher des Äusseren Hochebenkares. Zeitschrift für Gletschkunde und Glazialgeologie 8, 169-88.

Vitek, J. D., Deutch, A. L., Parson, C. G., 1981. Summer measurements of dissolved ion concentrations in alpine streams, Blanca Peak Region, Colorado. Professional Geographer 33, 436-444.

Vonder Müehll, D., Haeberli W., 1990. Thermal characteristics of permafrost within an active rock glacier (Murtèl/Corvatsch, Grison, Swiss Alps). Journal of Glaciology 36, 151-158.

Vonder Müehll, D., Klingelé E. E., 1994. Gravimetrical Investigation of ice-rich permafrost within the rock glacier Murtèl-Corvatsch (Upper Engadin, Swiss Alps). Permafrost and Periglacial Processes 5, 13-24.

Vonder Müehll, D., Stucki, T., Haeberli, W., 1998. Borehole temperatures in Alpine permafrost. Proceedings of the Seventh International Conference on Permafrost, Yellowknife, Canada, Collection Nordicana 57, 35-41.

Wagner, S., 1996. DC resistivity and seismic refraction soundings on rock glacier permafrost in northwestern Svalbard. Norsk Geografisk Tidsskrift 50, 25-36.

Wahrhaftig C., Cox, A., 1959. Rock glaciers in the Alaska Range. Geological Society of America Bulletin 70, 383-436.

Whalley, W. B., 1974. Rock glaciers and their formation as part of a glacier debris-transport system, Geographic Papers, No. 27, University Reading, England, 48 pp.

Whalley, W. B., 1983. Rock glaciers-permafrost features or glacial relics? In: Proceedings of the Fourth International Conference on Permafrost. National Academy Press, Washington, D.C., pp. 1,396-1,401.

Whalley, W. B., Douglas, G. R., Jonsson, A., 1983. The magnitude and frequency of large rockslides in Iceland in the postglacial. Geografiska Annaler Series A 65 (1-2), 99-110.

Whalley, W. B., Palmer, C. F., Hamilton, S. J., and Gordon, J. E., 1994. Ice exposures in rock glaciers. Journal of Glaciology 40, 427.

White, S. E., 1971. Debris falls at the front of Arapaho rock glacier, Colorado Front Range, U.S.A. Geografiska Annaler 53A (2), 86-91.

White, S. E., 1976. Rock glaciers and rock fields, review and new data. Quaternary Research 6 (1), 77-97.

White, S. E., 1987. Differential movement across transverse ridges on Arapaho rock glacier, Colorado, Front Range, USA. In: Giardino, J. R., Shroder, J. F. Jr., Vitek, J. D. (Eds.), Rock Glaciers. Allen & Unwin, London, pp. 145-149.

Woodcock, N H., 1977. Specification of fabric shapes using an eigenvalue method. Geological Society of America Bulletin 88, 1,231-1,236.

VITA

John Jerome Degenhardt

Research Associate, Office of Graduate Studies
Texas A&M University
College Station, Texas 77843-1113

Personal Data

Birth Date and Place:
December 01, 1962, Houston, Texas

Home Address:
103 South Park Drive
Montgomery, Texas 77356

Marital Status:
Single

Education

Doctor of Philosophy, Geography with emphasis in planetary geomorphology and geophysics, Texas A&M University, College Station, Texas. August, 2002.

Master of Science, Planetary geology, University of Houston, Houston, Texas. December, 1994.

Bachelor of Science, Geology, minor petroleum engineering, Texas A&M University, College Station, Texas. December, 1987.